universität
wien

DISSERTATION

Titel der Dissertation

Functional Proteomics of Bcr-Abl Signaling

angestrebter akademischer Grad

Doktor der Naturwissenschaften (Dr. rer.nat.)

Verfasserin / Verfasser:	Marc Jochen Brehme, M.Sc.
Matrikel-Nummer:	0605249
Dissertationsgebiet (lt. Studienblatt):	490 Molekulare Biologie
Betreuerin / Betreuer:	Prof. Dr. Giulio Superti-Furga
	CeMM – Research Center for Molecular Medicine Austrian Academy of Sciences

Wien, im Februar 2009

"In any case: The future looks bright, but let's talk about it!"

Giulio Superti-Furga (July 2005)

Major parts of the results presented in this thesis are submitted for publication and currently under revision in the following manuscript:

Brehme, M. *, Hantschel, O. *, Colinge, J., Kaupe, I., Planyavsky, M., Köcher, T., Mechtler, K., Bennett, K.L., Superti-Furga, G., "Charting the molecular network of the drug target Bcr-Abl", <u>PNAS</u>, *under revision*

* Equal contributions of Brehme, M. and Hantschel, O.

SUMMARY

The constitutively active oncogenic fusion tyrosine kinase Bcr-Abl is the product of a reciprocal chromosomal translocation (t(9;22), 'Philadelphia Chromosome'). The constitutive tyrosine kinase activity is central to Bcr-Abl's ability to cause chronic myeloid leukemia (CML) and is the target of tyrosine kinase inhibitors like imatinib (Gleevec®, Novartis). Despite the success of imatinib, many patients either develop resistance to the drugs and eventually relapse or they do not respond, when the treatment is initiated in advanced stages of the disease. However, the actual molecular setup of the endogenous drug target Bcr-Abl is still unknown. We have therefore charted the protein-protein interaction network of Bcr-Abl by a systematic two-pronged proteomics approach:

Using a monoclonal antibody we have first purified endogenous Bcr-Abl protein complexes from the CML cell line K562 and characterized a set of eighteen most tightly associated interactors by mass spectrometry. Nine interactors were subsequently subjected to tandem affinity purification/mass spectrometry analysis to obtain a molecular interaction network. The resulting network revealed a high degree of interconnection of seven 'core' components around Bcr-Abl (Ship2, c-Cbl, p85, Sts-1, Shc1, Grb2 and Crk-I), as well as their links to the AP2 adaptor protein complex and different signaling pathways. Quantitative analysis of these Bcr-Abl 'core' complex components showed that the absolute protein copy numbers range within one order of magnitude consistent with a stoichiometric complex of around 200,000 to 300,000 copies per cell and revealed the highest interaction stoichiometry for the 5-inositol phosphatase Ship2. Quantitative proteomics analysis showed that tyrosine kinase inhibitors disrupt this complex, while certain components still appear to interact with Bcr-Abl in a phospho-tyrosine-independent manner.

The results of this study therefore motivate us to propose that Bcr-Abl and other drug targets, rather than being considered as single polypeptides, can be considered as complex protein assemblies that are disrupted or re-modeled upon drug action.

ZUSAMMENFASSUNG

Die konstitutiv aktive onkogene Fusions-Tyrosin-Kinase Bcr-Abl resultiert aus einer reziproken chromosomalen Translokation (t(9;22), ‚Philadelphia Chromosom'). Die konstitutive Tyrosin-Kinaseaktivität von Bcr-Abl ist Auslöser der Chronisch Myeloischen Leukämie (CML) und das Ziel von Tyrosin-Kinaseinhibitoren wie Imatinib (Gleevec®, Novartis). Trotz des Erfolges von Imatinib entwickeln Patienten Resistenzen und werden rückfällig oder sprechen nicht auf die Therapie an, wenn diese erst in fortgeschrittenen Krankheitsstadien initiiert wird. Dennoch ist die genaue Beschaffenheit des endogenen Arzneistoffziels Bcr-Abl noch unbekannt. Daher haben wir das Protein-Interaktionsnetzwerk um Bcr-Abl mit einer doppelten proteomischen Herangehensweise systematisch kartiert:

Anhand eines monoklonalen Antikörpers haben wir zunächst endogene Bcr-Abl - Proteinkomplexe aus der CML-Zelllinie K562 gewonnen und massenspektrometrisch die achtzehn engsten Interaktoren charakterisiert. Nach ‚Tandem-Affinitätsreinigung' von neun dieser Kandidaten und massenspektrometrischer Analyse haben wir ein Interaktionsnetzwerk erstellt, das eine intensive Vernetzung der sieben ‚Kernkomponenten' (Ship2, c-Cbl, p85, Sts-1, Shc1, Grb2 und Crk-I) mit Bcr-Abl und deren Verknüpfung mit dem AP2-Adapterproteinkomplex und verschiedenen Signaltransduktionswegen offenbarte. Quantitative Analysen dieser sieben Komponenten zeigten, dass sich deren absolute Kopienzahl innerhalb einer Größenordnung bewegt und auf 200,000 - 300,000 stöchiometrische Komplexe pro Zelle schließen lässt, wobei die 5-Inositol-Phosphatase Ship2 die höchste Interaktionsstöchiometrie aufweist. Massenspektrometrische Quantifizierungen zeigten, dass Tyrosin-Kinaseinhibitoren den Bcr-Abl-'Kernkomplex' zerstören, einige Komponenten aber in Phospho-Tyrosin-unabhängiger Weise mit Bcr-Abl verbunden bleiben.

Wir kommen daher zu der Hypothese, dass Bcr-Abl und auch andere Arzneistoffziele nicht nur als einzelne Polypeptide, sondern vielmehr als komplexe Proteinverbände zu betrachten sind, die durch Arzneistoffe zerstört oder verändert werden.

TABLE OF CONTENTS

INTRODUCTION

1   INTRODUCTION

1.1   Chronic myeloid leukemia (CML)

Chronic myeloid leukemia (CML) is a clonal myeloproliferative disorder of a pluripotent hematopoietic stem cell that was first described in 1845 (Bennett 1845; Craigie 1845; Virchow 1845). In patients, CML displays three major characteristic clinical phases (Figure 1.1). In most patients, CML is manifested as a longer chronic phase (CP) disease that is identifiable by an initial leukocytosis with an increased count of peripheral blood myeloid progenitor cells often remaining undiscovered for years, as mature granulocytes are still produced (Melo and Barnes 2007). However, most patients are diagnosed at chronic phase, where the first symptoms include splenomegaly, fatigue and weight loss (Melo and Barnes 2007). Upon disease progression, patients enter an intermediate stage of CML development, the so-called accelerated phase (AP), usually characterized by aggravating splenomegaly and leukocytosis, increasing numbers of blast cells and additional cytogenetic abnormalities that lead to therapy failure (Figure 1.1) (Melo and Barnes 2007). Finally patients succumb to the blast crisis (BC) phase, where the haematopoietic differentiation process is fully arrested while immature blasts continue accumulating in the bone marrow and the blood circulation to 20% or more in the peripheral blood or bone marrow (Melo and Barnes 2007). Secondary cytogenetic and molecular changes associated with progression into BC usually directly or indirectly affect p53 and/or Rb gene activity, which further drive proliferation of blast crisis cells in addition to secondary effects such as differentiation arrest (Figure 1.1) (Calabretta and Perrotti 2004). Most cancerous malignancies are the consequence of a sequel of mutagenic events (Hanahan and Weinberg 2000). However, as CML was the first human cancer that was found associated with only a single consistent and causative chromosomal abnormality, the Philadelphia (Ph) chromosome (Nowell and Hungerford, 1960), diagnosis of CML was significantly improved and it has become one of the most comprehensively studied human malignancies and a breakthrough story in cancer biology (Deininger, Goldman et al. 2000; Melo and Barnes 2007).
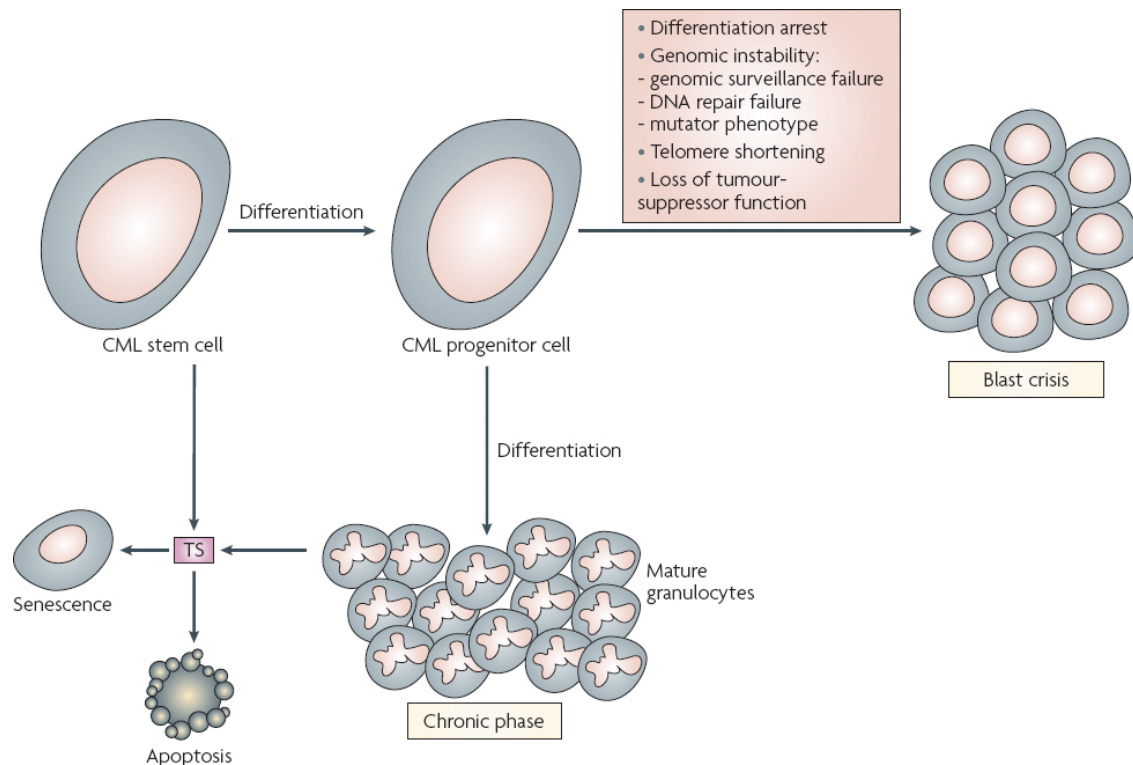
Figure 1.1 Multi-step disease progression and major disease stages in chronic myeloid leukemia (CML)
During chronic phase (CP) of CML leukemic stem cells differentiate into progenitor cells and lead to the accumulation of mature granulocytes. As tumour-suppressors (TS) are still functional in these granulocytes, they undergo either senescence or apoptosis. However, acquisition of a series of additional genomic alterations during the accelerated phase (AP) of the disease leads to differentiation arrest and excessive proliferation of immature blasts finally leading to blast crisis (BC)(Figure taken from (Melo and Barnes 2007)).

CML and a subset of acute lymphocytic leukaemia (ALL) are caused by the expression of the fusion protein Bcr-Abl (Advani and Pendergast 2002; Druker, Sawyers, Capdeville et al. 2001; Goldman and Melo 2003; Sattler and Griffin 2003) and serve as a paradigmatic example for the development of target tyrosine kinase inhibitor cancer treatment. Prior to the advent of targeted molecular Bcr-Abl therapy, most CML treatments aimed at the destruction of actively proliferating cells. Typical cytostatic chemotherapeutic agents were busulfan and hydroxyurea, which were effective in the generation of hematological responses in chronic phase CML patients. However, due to the lack of specificity of these therapies, they were unable to selectively clear Ph[+] - positive cells or to inhibit Bcr-Abl activity, therefore never achieved cytogenetic

remissions and could at most delay the onset of blast crisis (Sawyers 1999). Therapy with Interferon-α (IFN-α), however, lead to both complete hematological (CHR) and cytogenetic (CCR) responses in chronic phase patients who consequently showed excellent long-term prognosis and survived for more than ten years upon IFN-α treatment (Kantarjian, O'Brien et al. 2003). Combination therapy with IFN-α and cytosine arabinoside (Ara-C), however, showed even better efficacy and was therefore established as standard therapy before the advent of imatinib (Ezaki 2000; Ferrajoli, Liberati et al. 1995). For all these therapies, early diagnosis and therapy are crucial as diagnosis of CML at accelerated or blast crisis stage is almost inevitably associated with poor survival prognosis, as more and more cytogenetic abnormalities, such as trisomy 8 (Jennings and Mills 1998), are likely to be acquired during the course of the disease (Mitelman 1993). Until today, the only curative CML therapies consist in the combination of chemotherapy with irradiation therapy followed by bone marrow transplantation (BMT), if compatible healthy bone marrow cells are available (Druker, Sawyers, Capdeville et al. 2001).

With the discovery of the constitutively active oncogenic fusion tyrosine kinase Bcr-Abl as the cause of CML (Bartram, de Klein et al. 1983; Ben-Neriah, Daley et al. 1986; de Klein, van Kessel et al. 1982; Konopka, Watanabe et al. 1984) almost 26 years after the discovery of the Philadelphia chromosome and its link to CML (Nowell and Hungerford 1960), the first successful targeted cancer drug imatinib mesylate initiated a new era of CML treatment with CCR rates of > 90% in chronic phase CML patients (Buchdunger, Zimmermann et al. 1996; Druker, Tamura et al. 1996). This key discovery was followed by detailed structural and functional characterization of the Abl kinase domain in complex with imatinib (Nagar, Bornmann et al. 2002) and elucidation of the mechanism of action of imatinib. However, treatment with imatinib mesylate and the following second (Lombardo, Lee et al. 2004; Shah, Tran et al. 2004; Weisberg, Manley et al. 2005) and third generation (Golas, Arndt et al. 2003; Yokota, Kimura et al. 2007) inhibitors turned out not to be the curative end of the story, as drug resistances and disease relapses persist.

1.2 Expression of Bcr-Abl from the Philadelphia chromosome is sufficient to cause CML

Bcr-Abl is a constitutively active tyrosine kinase and its expression is the result of a reciprocal chromosomal translocation event between chromosomes 22 and 9 (t9;22; Philadelphia Chromosome) (Rowley 1973) that leads to the fusion of the breakpoint cluster region (BCR) gene and the Abelson tyrosine kinase (ABL1) and sequences from the first exon of the ABL1 tyrosine kinase are replaced by sequences from the BCR (breakpoint cluster region) gene, thereby generating a de-regulated, constitutively activated tyrosine kinase (Figure 1.2) (de Klein, van Kessel et al. 1982), (Wong and Witte 2004). Despite of evidence for remaining functional autoinhibitory mechanisms of c-Abl in Bcr-Abl, such as SH3 domain binding to P242 (c-Abl-1b) within the SH2-CD linker (Barilá and Superti-Furga 1998; Smith, Yacobi et al. 2003), fusion-dependent aberrations such as loss of the c-Abl N-terminal myristate (Hantschel, Nagar et al. 2003) as well as oligomerisation via the amino-terminal Bcr-coiled-coil domain (Figure 1.2) (McWhirter, Galasso et al. 1993; Tauchi, Miyazawa et al. 1997; Taylor and Keating 2005; Zhao, Ghaffari et al. 2002) lead to an open and active enzyme conformation, intermolecular autophosphorylation of the Bcr-Abl catalytic domain on Y412 within the activation loop and consequently on Y245 within the SH2-CD linker finally resulting in constitutive activity of the c-Abl tyrosine kinase. Depending on the particular cell type, Bcr-Abl expression either results in enhanced cell proliferation, morphological transformation or abrogation of growth factor/adhesion dependence (Daley, Van Etten et al. 1990; Raitano, Whang et al. 1997). Most importantly, however, expression of Bcr-Abl alone is sufficient for the transformation of hematopoietic stem cells leading to chronic myeloid leukemia (CML) in humans and a CML-like myeloproliferative disorder in mice (Daley, Van Etten et al. 1990; Li, Ilaria et al. 1999; Van Etten 2007). Also, a transgenic B-ALL mouse model demonstrated that continued expression of tetracycline-regulatable Bcr-Abl is required for the initiation and maintenance of leukemia (Huettner, Zhang et al. 2000).
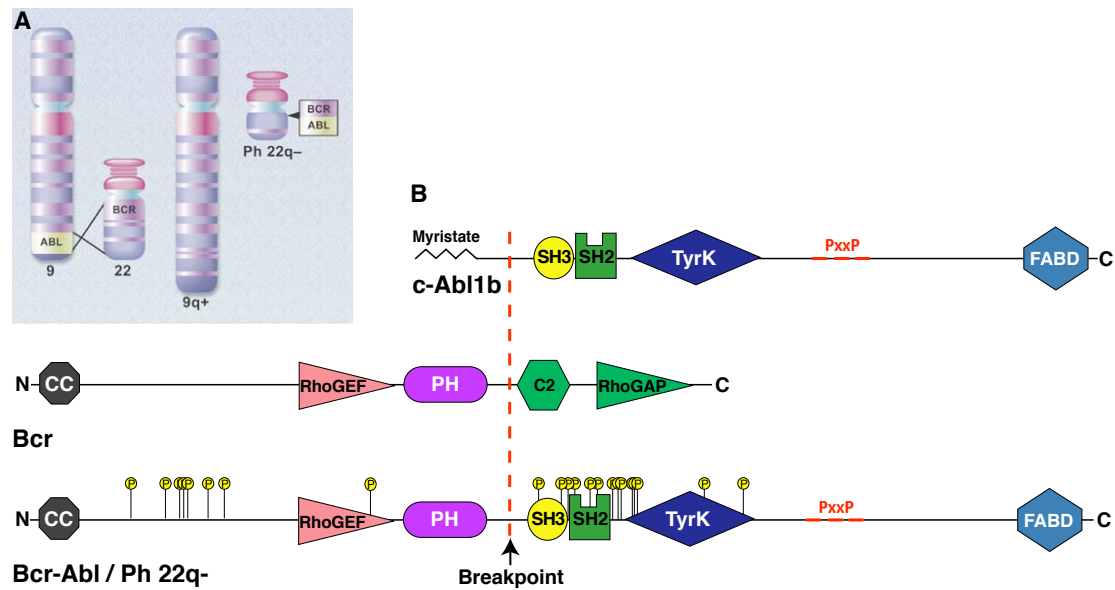
Figure 1.2 The Philadelphia chromosome translates into the oncogenic fusion tyrosine kinase Bcr-Abl
(A) The reciprocal chromosomal translocation between chromosomes 9 and 22 (t9;22) leads to formation of the Philadelphia chromosome (Ph 22q-) (Figure adapted from (Druker 2008)).
(B) Domain model representation of the consequences of the (t9;22) chromosomal translocation. Exon 1 of c-Abl (including the myristate of c-Abl1b) and the C-terminal C2- and RhoGAP-domains of Bcr are lost in the Bcr-Abl fusion protein. Phosphorylation sites on Bcr-Abl are shown.

Two major p210 Bcr-Abl fusion protein types are found in CML, b2a2 (e13a2) and b3a2 (e14a2) (Deininger, Goldman et al. 2000). The e1a2 p190 Bcr-Abl fusion protein is only rarely found in CML but represents the major fusion type in Ph[+] cases of B-cell acute lymphoblastic leukemia (ALL) (Melo, Gordon, Tuszynski et al. 1993; Melo, Myint et al. 1994). Besides the Bcr-Abl hybrid gene, also its counterpart chimeric gene Abl-Bcr was found to be expressed by reverse transcription polymerase chain reaction amplification of mRNA in Ph[+] positive CML patients (31/44) (Melo, Gordon, Cross et al. 1993), in patients with Ph[+] positive acute lymphoblastic leukemia (ALL) (Zheng, Guller et al. 2006) as well as in three out of five Bcr-Abl positive cell lines, where the K562 cell line was negative for Abl-Bcr probably due to transcriptional inactivity (Melo, Gordon, Cross et al. 1993). As the Abl-Bcr fusion transcript is not consistently expressed in Ph[+] positive leukemias, its differential expression was hypothesized to represent a determinant of the heterogenic character of CML

6

(Melo, Gordon, Tuszynski et al. 1993). However, a recent study showed that there is no correlation between Abl-Bcr expression and response to IFN-α therapy in CML.

1.3   Bcr-Abl protein architecture, domain structures and regulation

The two genes involved in the t(9;22) translocation constituting the Philadelphia chromosome and its translation Bcr-Abl are the proto-oncogene Abelson non-receptor tyrosine kinase *ABL1* (chromosome 9), the human homologue of the *v-Abl* oncogene encoded by the Abelson murine leukemia virus (A-MuLV) (de Klein, van Kessel et al. 1982) and the breakpoint cluster region gene *BCR* (chromosome 22) (Groffen, Stephenson et al. 1984), both ubiquitously expressed genes (Laneuville 1995). Human c-Abl is a 145kDa protein expressed as two isoforms upon alternative splicing of its first exon, c-Abl-1a and c-Abl-1b. The c-Abl-1b isoform, which is slightly longer than isoform c-Abl-1a, carries a myristate group attached to the glycine residue at position two (Figure 1.2B) (Hantschel, Nagar et al. 2003). This myristate group was shown to be crucially involved in the intra-molecular regulation of c-Abl and maintenance of c-Abl in an inactive state following a "latching" mechanisms induced by binding of the myristate into a deep hydrophobic pocket within the C-lobe of the kinase that leads to close "clamping" of the structure with the SH2-SH3 domains attached to the backside of the kinase (Figure 1.3B) (Hantschel, Nagar et al. 2003; Nagar, Hantschel et al. 2003). The importance of this "clamping" mechanism is confirmed by directed mutational disruption of SH2 and SH3 domain residues that lead to activation of the kinase (Barilá and Superti-Furga 1998; Hantschel, Nagar et al. 2003; Nagar, Hantschel et al. 2003). Equally, loss of the myristate upon mutation of the glycine residue to alanine led to dramatic increase in c-Abl tyrosine kinase activity compared to wild-type c-Abl (Hantschel, Nagar et al. 2003). The myristoylation consensus site is absent in c-Abl-1a and all Bcr-Abl fusion proteins and although hydrophobic residues in the Abl cap-domain were proposed to replace the missing myristate (Hantschel, Nagar et al. 2003; Nagar, Hantschel et al. 2003) it

is still unknown how c-Abl-1a compensates for the missing myristate in terms of intra-molecular auto-inhibitory regulation. Additionally, c-Abl features numerous domains and motifs critical for its enzymatic and signaling activity, most of whose structures have been solved in detail. The N-terminal Src homology 2 (SH2) and 3 domains (SH3) mediate protein-protein interactions with other proteins via binding of phospho-tyrosine or proline-rich sequences (PXXP-motifs), respectively (Cicchetti, Mayer et al. 1992; Mayer, Jackson et al. 1991). After its discovery by Tony Pawson as a stretch of 100 residues conserved in v-Src and other non-receptor tyrosine kinases (Sadowski, Stone et al. 1986), the structure of the SH2 domain of v-Src tyrosine kinase has been solved in 1992 in complex with phosphotyrosyl peptides using X-ray crystallography (Waksman, Kominos et al. 1992; Waksman, Shoelson et al. 1993) showing that the domain features a central antiparallel beta-sheet flanked by two alpha-helices, where the peptide is bound by the beta-sheet, intervening loops and one of the alpha-helices. In addition to hydrogen-bond formation and ionic interactions with the phosphate-group, specific recognition of the phosphotyrosine peptide by the v-Src SH2 domain was shown to involve two specificity pockets often compared to a "two-pronged plug engaging a two-holed socket" involving a phospho-tyrosine binding pocket and amino-aromatic interactions between lysine and arginine side-chains with the "+3 specificity determining region". The structure without bound peptide was also determined and displayed only small local changes (Waksman, Kominos et al. 1992; Waksman, Shoelson et al. 1993). Additionally, the in solution structure of the SH2 domain of the p85α subunit of PI3-kinase had been solved by nuclear magnetic resonance spectroscopy (NMR) and confirmed the basic structure determined by X-ray diffraction before (Booker, Breeze et al. 1992). These results on the structure and specificity of the SH2 domain (Waksman and Kuriyan 2004) initiated a line of discoveries that ultimately led to the elucidation of the regulatory mechanisms in both c-Src and c-Abl that were decisive for explaining the specificity of imatinib for c-Abl (Nagar, Hantschel et al. 2003). While in c-Src, the SH2 domain binds the tyrosine-phosphorylated C-terminal tail, in c-Abl the SH2 domain is positioned closely to the kinase domain (Hantschel and Superti-Furga 2004) where access

to the SH2 ligand-binding site is blocked by the kinase domain (Figure 1.3B) (Nagar, Hantschel et al. 2003). The SH2 domain of Bcr-Abl/c-Abl is crucially involved in leukemogenesis via complex formation with other tyrosine-phosphorylated signaling proteins, as inactivation by mutation of the arginine residue within the conserved FLVRES motif (R171K, mAbl-1b and hAbl-1b; R152K, hAbl-1a) renders the SH2 domain unable to bind phosphotyrosine-containing proteins, which correlates with reduced *in vitro* phosphotyrosine binding and transforming ability (Mayer, Jackson et al. 1992). The structure of the SH3 domain of spectrin was solved at 1.8 Å resolution (Musacchio, Noble et al. 1992) and revealed a compact beta-barrel consisting of five antiparallel beta-strands, with a region consisting of conserved aromatic and acidic amino acids on one side of the molecule that was assumed to mediate ligand binding. The elucidation of the function of the SH3 domain and structures of Abl and Fyn tyrosine kinase SH3 domains in complex with proline-rich peptide showed that proline-rich peptides (PXXP-ligands), whose majority forms a left-handed polyproline type II-helix, are bound over their entire length (about 10 residues) via hydrogen-bonding and van-der-Waals contacts (Musacchio, Saraste et al. 1994; Musacchio, Wilmanns et al. 1994). As for the regulation of c-Abl (Barilá and Superti-Furga 1998), the SH3 domain is also implicated in the negative regulation of Bcr-Abl by binding to P1124 in the linker between the SH2 and catalytic domains (SH2-CD linker) in the monomeric and unphosphorylated state of Bcr-Abl (Smith, Yacobi et al. 2003). Oligomerization of Bcr-Abl via its coiled-coil domain (Figure 1.2), however, disrupts the autoinhibited conformation by inducing intramolecular autophosphorylation of tyrosine residues in the activation loop of the catalytic domain (CD) and the SH2-CD linker and is required for leukemogenesis (Hantschel and Superti-Furga 2004; Smith, Yacobi et al. 2003). The tyrosine kinase domain of c-Abl carries tyrosine kinase activity and structural studies of the kinase domain (Nagar, Bornmann et al. 2002; Schindler, Bornmann et al. 2000) and in consequence of the kinase domain together with the SH2-SH3-unit (Nagar, Hantschel et al. 2006; Nagar, Hantschel et al. 2003) showed that the outward orientation of the activation loop away from the kinase domain in combination with activatory phosphorylation on

Y412 represents another crucial mechanism involved in regulation of c-Abl activity. Upon "unclamping" of the kinase other protein ligands to the SH2 and SH3 domains further open up the kinase followed by further Y412 phosphorylation and full kinase activation (Hantschel and Superti-Furga 2004). Overall, these mechanisms show how similar the regulatory mechanisms of c-Abl are to Src kinases (Harrison 2003). Besides these functional protein domains that enable enzymatic activity and binding of other proteins, c-Abl also harbors C-terminal proline-rich sequences that mediate binding of other SH3 domains as well as three C-terminal nuclear localization signals (NLS), DNA-binding (Kipreos and Wang 1992) and an F-actin binding domain (FABD) at the very C-terminus (McWhirter and Wang 1993) (Figure 1.2). The NLS and DNA-binding domains are located in the so-called 'last exon region' of c-Abl. It was shown that this 'last exon region' is not required for autoinhibition of c-Abl and its functional role is still unclear (Pluk, Dorey et al. 2002). The NMR structure of the FABD of Bcr-Abl/c-Abl revealed a compact left-handed four-helix bundle and provided first insight into the mechanism of cytoskeletal association and localization of Bcr-Abl/c-Abl (Figure 3.1C) (Hantschel, Wiesner et al. 2005; Wiesner, Hantschel et al. 2005). Importantly this study identified that a nuclear export signal (NES) reported within the FABD (Taagepera, McDonald et al. 1998) is 'burried' inside the hydrophobic core and nonfunctional while residues within helix alpha-III were identified to be crucial for F-actin binding and association with the cytoskeleton (Hantschel, Wiesner et al. 2005). c-Abl has recently been implicated in regulation of actin remodeling at the immune synapse during T-cell activation (Huang, Comiskey et al. 2008). Generally, c-Abl presumably controls various cellular signaling processes as Abl knockout mice show a variety of phenotypes from splenic/lymphic atrophy and lymphopenia (Zipfel, Grove et al. 2000) to osteoporosis (Li, Boast et al. 2000).

The 160kDa Bcr protein also features several structural protein domains, including a N-terminal coiled-coil domain (McWhirter, Galasso et al. 1993), a central region with homology to Rho guanine nucleotide exchange factors (Rho-GEF) and pleckstrin-homology (PH) domains (Sahay, Pannucci et al. 2007) and a C-terminal Rac-GAP (Diekmann, Brill et al. 1991). The N-

terminal coiled-coil domain (residues 1-72) was shown to mediate homotetramerization of Bcr-Abl correlating with activation of c-Abl tyrosine kinase and F-acting-binding activity as well as Bcr-Abl transforming potential *in vitro* (McWhirter, Galasso et al. 1993). The structure revealed a new mechanism of oligomer formation by dimerization of two N-shaped monomers followed by tetramerization of two dimers (Zhao, Ghaffari et al. 2002). The Rho-GEF domain, autoinhibited in Bcr, is activated in Bcr-Abl, activates RhoA and is required for full transforming activity by Bcr-Abl (Sahay, Pannucci et al. 2007). Accordingly, RhoA, Rac1 and Cdc42 interact with p210Bcr-Abl *in vivo*, but not with p190Bcr-Abl, which does not harbor the Rho-GEF domain, and p210Bcr-Abl but not p190Bcr-Abl was able to activate RhoA *in vitro* and *in vivo* (Harnois, Constantin et al. 2003) further underlining the importance of the Rho-GEF domain together with its target RhoA for transforming potential of Bcr-Abl. Bcr also encodes a Rac-GAP domain (residues 1065-1249), with GTPase activating protein (GAP) function for p21Rac, a Ras superfamily small GTPase known to regulate actin polymerization (Diekmann, Brill et al. 1991; Thomas, Cancelas et al. 2008). Small G proteins such as Rac are crucial molecular switches involved in cytoskeleton dynamics, cell proliferation and JNK signaling (Diekmann, Brill et al. 1991). GAPs interactwith small G proteins and serve as catalyzing enhancers of small G protein function by increasing GTP hydrolysis (Rittinger, Walker et al. 1997). A structure of the small Rho family G protein Cdc42Hs in complex with the GAP domain of p50rhoGAP has been solved at 2.7 Å resolution (Peck, Douglas et al. 2002; Rittinger, Walker et al. 1997). While the Rac-GAP domain is absent in the Bcr-Abl fusion proteins, overexpression of Bcr in p190Bcr-Abl expressing fibroblasts reduced the transforming potential of p190Bcr-Abl (Wu, Ma et al. 1999), which supports a potential regulatory role of the Rac-GAP domain of Bcr in light of its absence in constitutively active Bcr-Abl. While Bcr serine-threonine kinase activity seems to target only itself (Laneuville 1995) and the 14-3-3 protein Bap-1 (Reuther, Fu et al. 1994), serine-phosphorylated Bcr within Bcr-Abl, featuring serine 354, was shown to bind the SH2 domain of Bcr-Abl and to consequently inhibit the oncogenic activity of Bcr-Abl (Arlinghaus 2002). As for c-Abl, however, also the biological

function of endogenous Bcr is still controversial such as the function of its serine-threonine kinase domain (Maru and Witte 1991) is. *BCR* knockout mice are viable and only few subtle defects were recognized, probably hinting towards signaling redundancy in the context of Bcr (Voncken, van Schaick et al. 1995).

1.4   The Bcr-Abl phospho-tyrosine profile

The major feature of the oncogenic fusion tyrosine kinase Bcr-Abl is its constitutive tyrosine kinase activity, which is central to Bcr-Abl's ability to transform haematopoietic cells (Daley, Van Etten et al. 1990; Konopka, Watanabe et al. 1984). Expression of constitutively active Bcr-Abl leads to the phosphorylation of a large number of proteins in the cell causing activation of a large number of key signaling components (Sattler and Griffin 2003; Steelman, Pohnert et al. 2004). Furthermore, Bcr-Abl, which is itself phosphorylated on numerous tyrosine residues upon autophosphorylation, recruits a set of proteins containing SH2 and/or PTB domains and also binds to tyrosine-phosphorylated proteins via its own SH2 domain. These signaling effects were shown to be responsible for the oncogenic effect of Bcr-Abl and are the major rationale for targeted therapy using Bcr-Abl tyrosine kinase inhibitors. Bcr-Abl autophosphorylation is the consequence and a major driver of its constitutive activity alike. While the autoinhibited form of c-Abl is not tyrosine phosphorylated in unstimulated cells (Brasher and Van Etten 2000; Hantschel and Superti-Furga 2004), c-Abl acquires tyrosine phosphorylation at several residues upon activation of the kinase (Van Etten, Debnath et al. 1995). Tyrosine phosphorylated c-Abl residues include Y412 in the activation loop and Y245 in the SH2-CD linker (Figure 1.3). Phosphorylation of Y412 was shown to affect the positioning of the activation loop in a way that favors kinase activation and to positively correlate with catalytic activity of c-Abl (Figure 1.3B) (Brasher and Van Etten 2000; Dorey, Engen et al. 2001). In addition, phosphorylation of Y245 is required for full activation of c-Abl (Brasher and Van Etten 2000). Further tyrosine phosphorylation sites in c-Abl were determined from cells co-

transfected with constitutively active Src (Plattner, Kadlec et al. 1999) (Superti-Furga lab, unpublished observations) and Bcr-Abl tyrosine phosphorylation sites have been systematically mapped by mass spectrometry (Salomon, Ficarro et al. 2003; Steen, Fernandez et al. 2003). Besides Y245 and Y412 (see above), these include the c-Abl tyrosine residues Y134 (SH3-domain, ligand-binding surface), Y204 (SH2 domain 'south face'), Y251 (SH2-CD linker), Y272 (CD/P-loop), Y276 (CD/N-lobe), Y283 (CD/N-lobe-SH3 interface) and Y488 (CD/C-lobe 'south face') (Figure 1.3B) (Hantschel and Superti-Furga 2004). Two of these, Y272 and Y276, are particularly interesting, as they confer resistance to imatinib *in vitro* (Azam, Latek et al. 2003; Pendergast, Quilliam et al. 1993) and Y272 could accordingly be identified in imatinib - resistant patients (Roumiantsev, Shah et al. 2002). Also, Y134 is interesting, as it is conserved in SH3 domains and crucially involved in PXXP ligand binding (Musacchio, Wilmanns et al. 1994). Phosphorylation of Y134 potentially clashes with the SH3-linker-CD interface and disturbs kinase autoinhibition (Figure 1.3) (Hantschel and Superti-Furga 2004). Tyrosine phosphorylation of Bcr-Abl by Src family kinases such as Hck, Lyn and Fyn was assessed in more detail and shown to affect residues Y89 and Y134 (Abl SH3 domain), Y147 (SH3-SH2 connector) and Y158, Y191, Y204 and Y234 in the SH2 domain and phenylalanine substitution of the SH2-SH3 domain phospho - tyrosine residues confirmed their influence on Bcr-Abl transforming potential (Figure 1.3) (Meyn, Wilson et al. 2006).

Also Bcr was shown to be phosphorylated on several tyrosine residues, most importantly on Y177 within the first exon of Bcr, which is the crucial event for binding of the small adaptor protein Grb2 and a link to the Ras-pathway, activated by Bcr-Abl and crucial for Bcr-Abl - mediated leukemogenesis (Pendergast, Quilliam et al. 1993; Zhang, Subrahmanyam et al. 2001). Besides Y177, Bcr is also phosphorylated on Y283, Y328 and Y360 and tyrosine-phosphorylated Bcr, phosphorylated by Bcr-Abl, has reduced serine-threonine kinase activity (Liu, Wu et al. 1996; Wu, Liu et al. 1998). The first exon of p160Bcr is predominantly tyrosine phosphorylated in *trans* by Bcr-Abl or autophosphorylated within Bcr-Abl as was shown by p160Bcr / p185Bcr-Abl and p210Bcr-Abl co-precipitation studies (Liu, Campbell et al. 1993). Another study

reported phosphorylation of the Bcr-Abl kinase on tyrosine Y644 using metabolic labeling with light or heavy tyrosine (SILAC) and detection by quantitative mass spectrometry (Liang, Hajivandi et al. 2006).
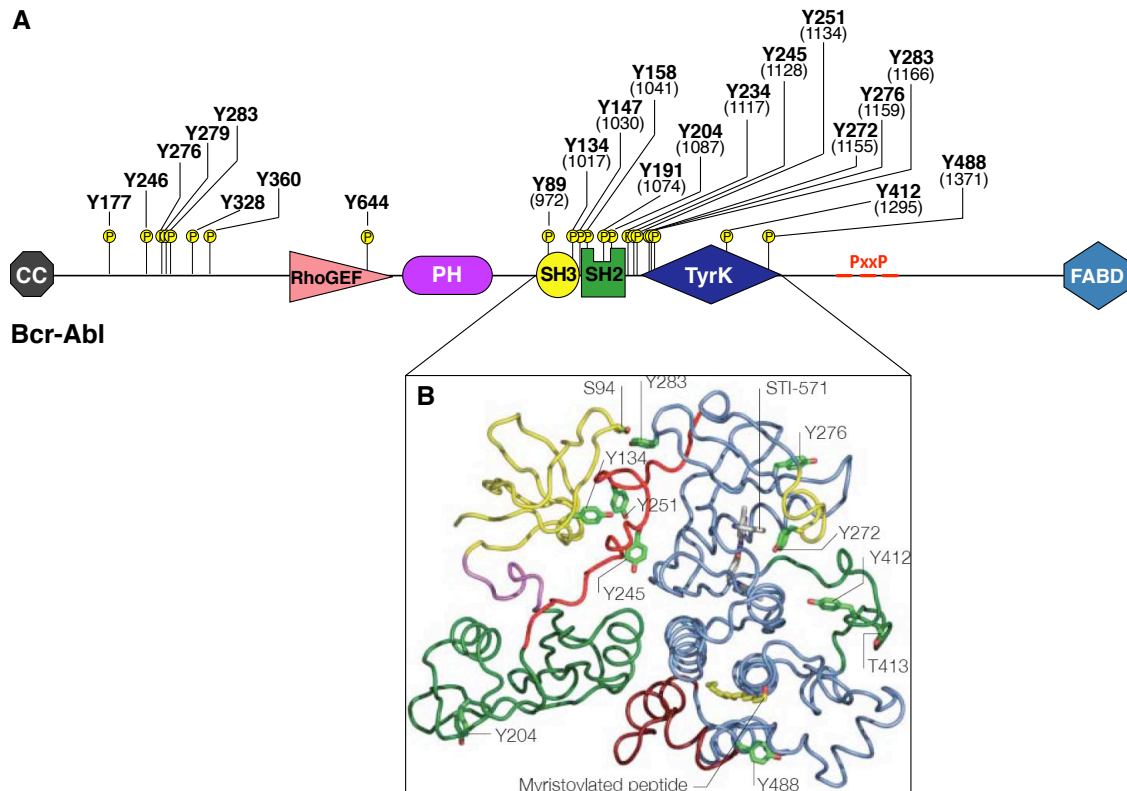
Figure 1.3 The Bcr-Abl phospho-tyrosine profile
(A) Location of known phospho-tyrosine residues mapped onto the domain-structure representation of Bcr-Abl. Domains and location of phospho-tyrosine residues shown in scale (mapped using Prosite MyDomains - Image Creator (http://www.expasy.ch/cgi-bin/prosite/mydomains/)).
(B) Inlet showing phosphorylation sites within the SH3-SH2-Kinase-domain unit of Bcr-Abl mapped onto the regulated Abl structure (PDB entry 1OPK) and shown as green sticks (SH3 domain (yellow), SH2 domain (green) and kinase domain (blue)). Some phospho-serine and -threonine residues as well as bound imatinib (STI-571) and a myristoylated peptide are shown (Figure adapted from Hantschel and Superti-Furga 2004).

Besides tyrosine phosphorylation of Bcr-Abl itself, also numerous tyrosine-phosphorylation sites on other signaling proteins associated with Bcr-Abl activity have been mapped and recent phospho-proteomics approaches in combination with mass spectrometric detection have led to an enlarged global profile of tyrosine-phosphorylation sites in Bcr-Abl expressing cells (Goss, Lee, Moritz, Nardone, Spek, MacNeill et al. 2006). The p210 Bcr-Abl expressing cell

line K562, for instance, is now known to harbor about 89 Bcr-Abl associated tyrosine-phosphorylation sites (Goss, Lee, Moritz, Nardone, Spek, MacNeill et al. 2006). Several tyrosine phosphorylation targets of Bcr-Abl, for instance in K562 cells, are kinases themselves, such as PI3K, c-Abl, Bcr, Btk, Cdc2, Cdk2, DYRK1A, Erk1/2, Fyn, GSK3-β, HIPK1, Lck, Lyn, p38-α, PRP4 (Goss, Lee, Moritz, Nardone, Spek, MacNeill et al. 2006; Hornbeck, Chabra et al. 2004). The overall 'phospho-tyrosine signature' varies for the different Bcr-Abl expressing cell-lines and Bcr-Abl fusion types expressed (b2a2/e13a2; b3a2/e14a2 for p210 Bcr-Abl and e1a2 for p190 Bcr-Abl). However, a defined common signature of the tyrosine-phosphorylated proteins Bcr, c-Abl, VASP, Ship2, Shc1, c-Cbl, CD2AP (novel) and GRF1 (novel) could be concluded for Bcr-Abl positive cell lines (Goss, Lee, Moritz, Nardone, Spek, MacNeill et al. 2006). Ship2 tyrosine phosphorylation by Bcr-Abl (Y1135) was confirmed by an independent quantitative proteomics study (tyrosine SILAC) that additionally identified Dok-2 (Y299) as tyrosine phosphorylation target of Bcr-Abl, both of which were reduced by about 90% following imatinib treatment (Liang, Hajivandi et al. 2006). These proteins could therefore represent a 'consensus' target set of Bcr-Abl tyrosine kinase activity irrespective of cellular background or fusion type and could therefore serve as candidate Bcr-Abl therapy response biomarkers (Goss, Lee, Moritz, Nardone, Spek, MacNeill et al. 2006).

1.5   Bcr-Abl, its interactors and affected signaling pathways

As a consequence of the constitutive tyrosine kinase activity of Bcr-Abl, tyrosine phosphorylation sites on Bcr-Abl and its substrates act as docking sites thereby initiating and modifying protein-protein interactions via SH2 and PTB domains (Mayer, Jackson et al. 1991). Thereby, Bcr-Abl is thought to serve as a large docking framework assembled in a multi-protein complex, which is itself in the centre of a protein-protein interaction network (Hantschel and Superti-Furga 2004; Ren 2005; Salomon, Ficarro et al. 2003; Steen, Fernandez et al. 2003). Numerous individual interactions with Bcr-Abl have been described in the past so that it seems hard to picture an overview of Bcr-Abl signaling. These include

the well-described "canonical" interactors of Bcr-Abl Grb2 (Patel, Marley et al. 2006; Pendergast, Quilliam et al. 1993), Grb4 (Coutinho, Jahn et al. 2000), Grb10 (Bai, Jahn et al. 1998), Cbl (Gaston, Johnson et al. 2004; Patel, Marley et al. 2006), Syp (Tauchi, Feng et al. 1994), Gab2 (Sattler, Mohi et al. 2002), Shc1 (Tauchi, Boswell et al. 1994), Nck1 (Miyoshi-Akiyama, Aleman et al. 2001; Smith, Katz et al. 1999), SHP-2 (Tauchi, Miyazawa et al. 1997), Ship2 (Wisniewski, Strife et al. 1999), Abl-interacting protein 1 and 2 (Abi-1/2) (Dai and Pendergast 1995; Fan, Cong et al. 2003; Shi, Alin et al. 1995), 14-3-3 family proteins such as Bcr-associated protein (Bap-1) (Reuther, Fu et al. 1994) and CrkL (Patel, Marley et al. 2006; Sattler and Salgia 1998). Many of these interactors are phosphorylated by Bcr-Abl, such as CrkL, Crk, Shc1 (Goga, McLaughlin et al. 1995), Dok-1, Gab2, Cbl, p130Cas (Salgia, Pisick et al. 1996), Stat5, PI3KR2 (p85β), Vav1 (Bassermann, Jahn et al. 2002), Fes, Paxillin or PLCγ (Ren 2005). Besides CrkL, also c-Crk (Crk-I/II) was found interacting with Bcr-Abl (Feller, Knudsen et al. 1994). Of the three Crk isoforms expressed in hematopoietic cells (CrkL, Crk-I and Crk-II), however, CrkL is considered the most prominent substrate of Bcr-Abl and often used as readout for Bcr-Abl activity (Feller, Posern et al. 1998) and it was shown to be in a complex with Bcr-Abl, Cbl and Grb2 (Patel, Marley et al. 2006). Also, the Src kinase Hck has been reported to directly interact with Bcr-Abl via its SH2 and/or SH3 domain (Stanglmaier, Warmuth et al. 2003).

Via some of these interactors, Bcr-Abl manages to harness important proliferative and anti-apoptotic signaling pathways, including the Ras-MAPK/JNK, PI3K-Akt and Jak/STAT pathways, which were shown to be activated in Bcr-Abl expressing cells and to contribute to transformation of haematopoietic cells (Mahlmann, McLaughlin et al. 1998; Raitano, Halpern et al. 1995; Steelman, Pohnert et al. 2004). Grb2, Gab2, Shc1 and Crk are involved in the activation of the Ras-MAPK pathway (Pendergast, Quilliam et al. 1993; Tanaka, Gupta et al. 1995; Tauchi, Boswell et al. 1994). As Grb2 binds the Bcr-Abl autophosphorylation site Y177 it co-recruits Gab2, which is crucial for activation of the Ras-MAPK pathway via Sos-1, the guanine-nucleotide exchange factor for Ras (Puil, Liu et al. 1994). The interaction between Grb2

and Bcr-Abl seems to be counteracted by expression of the phosphatase PTP1B (LaMontagne, Flint et al. 1998; LaMontagne, Hannon et al. 1998). Furthermore, binding of Grb2/Gab2 to Y177 leads to binding of Shp2 and phosphatidylinositol 3-kinase (PI3K) via Gab2 and activation of the PI3K-Akt pathway (Sattler, Mohi et al. 2002). The resistance of Gab2 knockout mice to Bcr-Abl mediated transformation confirmed the importance of Bcr-Abl, Gab2 and these two pathways in Ph$^+$ leukemia (Sattler, Mohi et al. 2002). Shc1 is also involved in Grb2-mediated activation of the Ras-MAPK pathway, as it binds the SH2 domain of Abl and, following tyrosine phosphorylation, recruits Grb2 (Goga, McLaughlin et al. 1995). Next, in v-Abl and Bcr-Abl transformed cells, the oncogenes have been shown to activate Janus kinase (JAK) tyrosine kinases consequently leading to constitutive phosphorylation of signal transducer and activator of transcription 5 (Stat5), independently of cytokines such as GM-CSF (granulocyte-macrophage colony stimulating factor) (Danial, Pernis et al. 1995; Danial and Rothman 2000; Shuai, Halpern et al. 1996). Regarding Stat5 there is evidence that, in addition to its activity as signal transducer and activator of transcription, it can serve as cytoplasmic signalling effector in a complex with Gab2 and the p85 subunit of PI3K (Harir, Pecquet et al. 2007). Apart from the activation of proliferative pathways also apoptosis signalling is influenced in Bcr-Abl expressing cells. For instance, Bcr-Abl's inhibitory effect on Ship1 phosphatase leads to decreased apoptotic signalling (Sattler, Verma et al. 1999). Furthermore, Stat transcription factors, which are activated by Bcr-Abl (Shuai, Halpern et al. 1996), induce expression of anti-apoptotic genes, such as Bcl-X$_L$ (Danial and Rothman 2000). In line with these insights, various downstream activation markers have been described for Bcr-Abl expressing cells such as total phosphotyrosine, phospho-Stat5 (Frank and Varticovski 1996; Shuai, Halpern et al. 1996), phospho-Akt (Chu, Li et al. 2007), phospho-Erk1/2 and total Erk1/2 levels (Mizuchi, Kurosu et al. 2005; Steelman, Pohnert et al. 2004).

Despite this wealth of protein interactors and downstream signaling pathways described, however, the precise molecular setup of the endogenous Bcr-Abl protein and the molecular mechanism of downstream signaling pathway

regulation is still unknown (Deininger, Buchdunger et al. 2005; Wong and Witte 2004). At this point it has to be stated that the majority of the past studies on Bcr-Abl signaling have been performed mostly on individual protein associations that were characterized in different cell types by different methods and investigators. Therefore, there is a lack of a systematic, standardized and comprehensive approach to map the Bcr-Abl signaling network that would allow a unifying view on the identity of the Bcr-Abl binding partners in a qualitative and quantitative sense.

1.6   The human leukemia model cell line K562

The human leukemia model cell line K562 was derived from leukemic cells from a pleural effusion of a 53 year old patient suffering from chronic myeloid leukemia at terminal blast crisis stage in 1970, reported as Ph^+ cell line in 1975 (Lozzio and Lozzio 1975) and characterized in further detail already about 32 years ago (Klein, Ben-Bassat et al. 1976). The K562 cell line is, by far, the most widely used Ph^+ model cell line in CML research with more than 10,000 PubMed entries to date. While a good proportion of data on Bcr-Abl signaling was accumulated using K562 cells as a leukemia model, this cell line represents numerous other key advantages that justify its use for a systematic Bcr-Abl signaling pathway mapping approach, as described in this thesis:

- ease of culture (standard media) and rapid division ensure production of sufficient amounts of cells (from 1x108), typically needed for the TAP-LC-MSMS procedure
- well-characterized prototypic CML cell line ((Hantschel, Gstoettenbauer et al. 2008; Klein, Ben-Bassat et al. 1976))
- expression of endogenous p210Bcr-Abl present in the majority of CML patients from the Bcr promoter
- no need to co-infect with Bcr-Abl
- pathways activated by Bcr-Abl are already switched-on
- cells respond to tyrosine kinase inhibitor treatment (imatinib, dasatinib, nilotinib)

- Bcr-Abl has "normal" expression level, close to c-Abl from non-translocated allele

- high transduction rates (up to 95%) can be achieved routinely with a single infection (Superti-Furga lab observation)

Besides this line of advantages, K562 cells suffer from the fact that they do not allow for an easy Bcr-Abl - dependent readout assay as they endogenously express constitutively active Bcr-Abl. Furthermore, as the K562 cell line was derived from a CML patient in blast crisis and given that it is now established in cell culture for almost four decades (Lozzio and Lozzio 1975), it has undergone numerous additional karyotypic changes, featuring gains and losses of chromosomal material, that may underlie unpredictable biological alterations as compared to a clinical CML setting. Karyotypic analysis of long-term culture K562 cell lines have found varying manifestations from Ph$^+$ hyperdiploid (Collins and Groudine 1983) to hypotriploid karyotypes (Dimery, Ross et al. 1983). In addition to the Philadelphia chromosome (t9;22), a more recent complete karyotypic characterization has corroborated previous findings and identified a hypotriploid karyotype with a modal chromosome number of 67 and 21 unique marker chromosomes, including five entirely novel karyotypic markers (Naumann, Reutzel et al. 2001). Overall, these studies show that the K562 karyotype has undergone numerous changes but, at the same time, remained relatively stable over about three decades of sub-culture (Naumann, Reutzel et al. 2001). Nevertheless, several sub-lines of K562 might exist displaying distinct marker sets (Dimery, Ross et al. 1983).

1.7 "Oncogene addiction"

The phenomenon "oncogene addiction" describes the dependency of cancer cells on an oncogene and its associated signaling pathway for survival or proliferation (Weinstein and Joe 2008). This hitherto unexplained phenomenon has been documented in a series of tumor models and cancer cell lines, such as the Ph$^+$ K562 cell line expressing the oncogenic fusion tyrosine kinase Bcr-Abl (Sharma, Gajowniczek et al. 2006). 'Addiction' to the respective

oncogene can be so strong, that even transient inactivation of the oncogene can result in reduced transforming activity, as was shown in cell culture models. For instance, in a conditional transgenic mouse model for Myc-induced tumorigenesis (Felsher and Bishop 1999), brief inactivation of Myc by doxycycline durg treatment resulted in the sustained loss of the neoplastic phenotype, regression of tumors and differentiation of osteogenic sarcoma cells into mature osteocytes (Jain, Arvanitis et al. 2002). Even subsequent reactivation of the oncogene Myc was unable to restore the cells' neoplastic phenotype and induced apoptosis instead, probably as a consequence of durable epigenetic changes that render the cells insensitive to Myc-induced tumorigenesis. This shows, at hands of the example oncogene Myc, that brief inactivation of an oncogene might represent effective cancer therapy in relevant cases and clearly classifies oncogenes as the 'Achilles' heel' of the cancer they cause (Jain, Arvanitis et al. 2002; Weinstein 2002). As regards the underlying molecular mechanism, evidence points towards a possible therapeutic strategy that could harness a signaling cascade common to several oncogenes such as Src, Bcr-Abl or EGF receptor in order efficiently target the 'addicted' cells into remission. Following inactivation of these three oncogenes in cell culture models, all shared a similar ensuing profile of signal attenuation represented by diminution of phospho-ERK, -Akt and -STAT3/5 levels accompanied by a delayed increase in the proapoptotic effector phospho-p38MAPK (Bandyopadhyay, Biswas et al. 2004). In the TonB210.1 conditional Bcr-Abl expressing cell line, for instance, decrease in the survival effectors Akt, STAT5 and ERK1/2 phosphorylation coincided with Bcr-Abl inactivation following doxycycling treatment for about 8hrs as did the increase of the levels of the phosphorylated proapoptotic Bcr-Abl downstream target p38 MAP kinase (Bandyopadhyay, Biswas et al. 2004) at 24hrs of doxycycline treatment (Sharma, Gajowniczek et al. 2006). Harnessing this transient imbalance between rather short-lived survival versus longer persisting apoptotic oncogenic outputs upon oncogene inactivation by using targeted kinase inhibitor treatment in a discontinuous cyclic fashion rather than continuously could be a more effective therapeutic option (Sharma, Gajowniczek et al. 2006). 'Addiction' of

K562 cells to their oncogenic 'Achilles heel' Bcr-Abl may explain the dramatic success of targeted Bcr-Abl tyrosine kinase inhibitors such as imatinib and excellent clinical response rates in CML patients treated with these inhibitors, providing a paradigmatic rationale for targeted molecular therapy (Druker 2004; Weinstein and Joe 2008). Similarly, RNA interference (RNAi) mediated inactivation of Bcr-Abl with a Bcr-Abl breakpoint-specific short-interfering RNA (siRNA) was shown to efficiently inhibit Bcr-Abl dependent cell growth (Wohlbold, van der Kuip et al. 2003). In the case of drug resistances, however, alternative strategies such as synergistic combination therapy might be required to overcome oncogene addiction (Chen, Gandhi et al. 2006; Weinstein and Joe 2008; Weinstein and Joe 2006).

1.8 Targeted therapy by imatinib: the current front-line therapy for Ph-positive CML and ALL

For a long time, kinases were considered 'undruggable', as it seemed basically impossible to achieve the required specificity, a debate that is having its revival when it comes to the 'druggability' of protein-protein interactions (Mayer and Dimarchi 2005). However, as tyrosine kinases represent a major fraction of known oncogenes, they were destined the prime target for development of targeted small molecule inhibitors and the strategy 'drugging the cancer kinome' lead to the development of successful drugs like trastuzumab (Herceptin) targeting ERBB2/HER2 (Workman 2005; Workman, Clarke et al. 2006). Also, the central role of the oncogenic Bcr-Abl kinase in the pathophysiology of CML represented a paradigmatic chance for molecular targeted therapy and ultimately lead to the development of the highly specific Bcr-Abl tyrosine kinase inhibitor imatinib (imatinib mesylate, Gleevec[®], Novartis) that is now the frontline therapy for CML in all disease stages (Deininger, Buchdunger et al. 2005). A screening of inhibitors against protein kinase C-α (PKC-α) at Ciby-Geigy (now Novartis) identified phenylaminopyrimidines as selective ATP competitive inhibitors against PKC-α, although the IC50 values were not satisfactory (Traxler, Bold et al. 2001). Upon modification of the

candidate compound, CGP53,716 was shown to be effective against PDGF-R (Traxler, Bold et al. 2001), but surprisingly also quantitatively inhibited Gag-Abl tyrosine kinase (Buchdunger, Zimmermann et al. 1995). Upon further optimization for v-Abl inhibition imatinib mesylate (Gleevec, STI571 or CGP57148B), a 2-phenylaminopyrimidine derivative with very high affinity and specificity for the tyrosine kinases PDGF-R, c-KIT (Buchdunger, Cioffi et al. 2000), c-Abl (Buchdunger, Zimmermann et al. 1996) and Arg (Okuda, Weisberg et al. 2001), was engineered (Figure 1.4A) (Traxler, Bold et al. 2001).
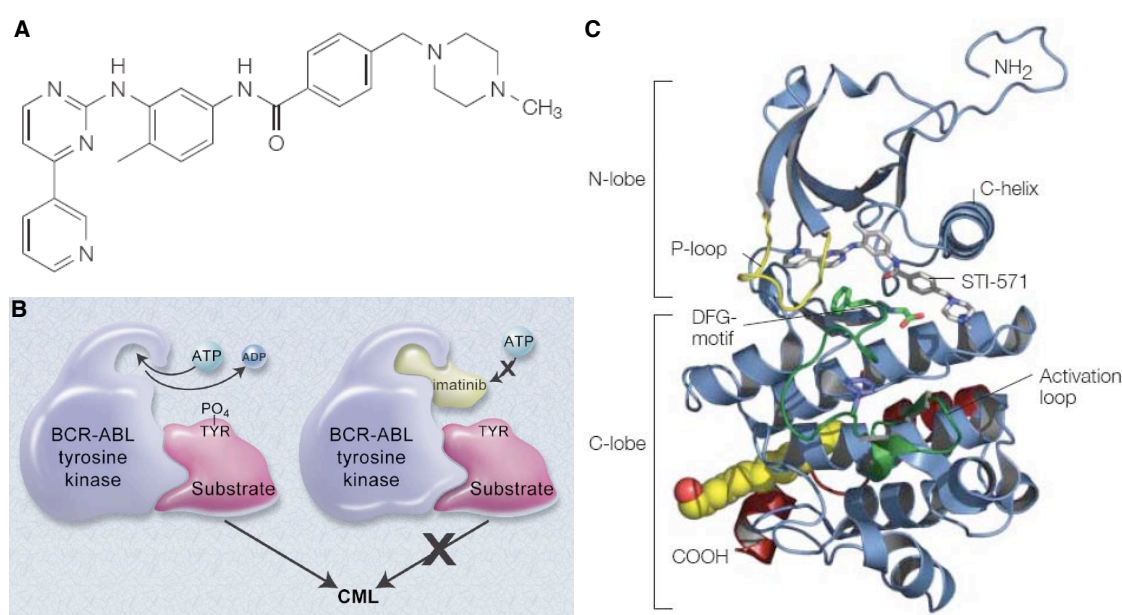
Figure 1.4 Targeted therapy by the small-molecule tyrosine kinase inhibitor imatinib
(A) Structural formula of imatinib mesylate (STI-571, Gleevec), a 2-phenylaminopyrimidine derivative with very high affinity and specificity for the ATP binding pocket of the Abl tyrosine kinase domain active site (Buchdunger, Zimmermann et al. 1996).
(B) Cartoon outlining the mechanism of action of imatinib. Binding of ATP and phosphate transfer from ATP onto substrates by the constitutively active tyrosine kinase Bcr-Abl is inhibited by the action of imatinib. This leads to inhibition of Bcr-Abl kinase activity and suppression of myeloid cell proliferation (Figure adapted from (Druker 2008)).
(C) Structural representation of the Abl kinase domain (PDB entry 1OPJ, (Nagar, Hantschel et al. 2003)) with imatinib (STI-571) complexed in the ATP binding pocket. The activation loop (shown in green) is forced into an inactive conformation (Figure adapted from (Hantschel and Superti-Furga 2004)).

Imatinib is now a clinically highly successful small-molecule inhibitor that binds to and inhibits the kinase domain of Bcr-Abl by competing with ATP (Figure 1.4B,C) (Nagar, Bornmann et al. 2002; Schindler, Bornmann et al. 2000), thereby effectively abrogating signaling by Bcr-Abl and selectively inhibiting growth of Ph$^+$ cells *in vitro* and tumor formation in mice *in vivo* (Deininger, Goldman et al. 1997; Druker, Tamura et al. 1996). The antileukemic response is believed to be due to activation of the p38 mitogen-activated protein (MAP) kinase signaling pathway upon imatinib treatment of Bcr-Abl positive cells, corroborating the possibility that Bcr-Abl, besides activating mitogenic pathways, also promotes CML by suppression of apoptotic pathways (Bandyopadhyay, Biswas et al. 2004; Parmar, Katsoulidis et al. 2004). The high selectivity and promising pharmacological properties of imatinib led to a dose-escalation clinical phase I trial in CML patients refractory, resistant or intolerant to standard therapy (e.g. IFN-α) that concluded with successful outcome, good tolerability of the drug, normalization of blood cell counts and 98% (53/54 patients) of complete hematologic response (CHR) and within one year follow-up only one patient relapsed (Druker, Talpaz et al. 2001). Even 55% (21/38 patients) of patients in myeloid blast crisis responded (Druker, Sawyers, Kantarjian et al. 2001). Following phase II and III trials, about 95% of IFN-α refractory patients responded with CHR of which 89% remained free of disease progression (Kantarjian, Sawyers et al. 2002) and only 1.5% of patients, not previously treated with IFN-α, had disease progression (Druker, O'Brien et al. 2002). 60% of the patients achieved a major cytogenetic response (defined as reduction in the percentage of Ph chromosome-positive metaphases to less then 35 (Druker 2008)) (Kantarjian, Sawyers et al. 2002). These clinical success rates led to quick approval of the drug less than three years after the first clinical trials in May 2001 (Arnold 2001). However, chronic phase patients frequently relapse due to drug resistance despite of promising initial response and a significant proportion of accelerated and blast phase CML patients does not respond to imatinib at all or not well enough, or relapses despite of the treatment (Deininger, Buchdunger et al. 2005; Druker, Sawyers, Kantarjian et al. 2001).

1.9   Molecular determinants of CML patients relapse

Targeted treatment with imatinib is a success story with an overall six-year progression-free survival of about 90%. However, despite this success, many patients develop resistance mutations and eventually relapse or do not respond to the drug when treatment starts in accelerated phase or blast crisis (REFs) (Capdeville, Buchdunger et al. 2002; Wong and Witte 2004). Different hallmarks can lead to drug resistance, most importantly point mutations in the drug target Bcr-Abl, but also gene amplifications (including Bcr-Abl) (Gorre, Mohammed et al. 2001) and chromosomal aberrations. During accelerated phase and blast crisis, other secondary chromosomal aberrations and duplication of the Ph chromosome have been reported, suggesting that imatinib resistance might also be caused by oncogenic events other than point mutations (Figure 1.1) (Mitelman 1993; Wong and Witte 2004). This increase of chromosomal aberrations in advanced stage CML may be due to increased levels of Bcr-Abl expression and the downregulation of one of the major DNA repair protein DNA-PK by Bcr-Abl (Deutsch, Dugray et al. 2001). Indeed, studies in CD34$^+$ cells indicated that Bcr-Abl-overexpression levels directly influence response or resistance to imatinib (Barnes, Palaiologou et al. 2005). This obstacle was partly successfully addressed by administration of an increased dose of imatinib (600 vs 400mg daily), however, toxicity effects at high imatinib dose, such as frequent pancytopenia at 800mg daily, limits the applicability of the dose escalation concept (Kantarjian, Talpaz et al. 2003; Talpaz, Silver et al. 2002). Also, Bcr-Abl independent overexpression of Lyn tyrosine kinase was shown to be associated with imatinib resistance in cell culture and resistant patients cells by influencing phosphorylation levels of Bcr-Abl and some of its targets (Donato, Wu et al. 2003) (Wu, Meng et al. 2008). However, mutations within the Abl kinase domain that prevent imatinib from binding have been found to be by far the most common mechanism of resistance to Imatinib (Deininger, Buchdunger et al. 2005; Griswold, MacPartlin et al. 2006; Leguay, Desplat et al. 2005; Shah, Nicoll et al. 2002), eventually leading to relapse and disease progression (Shah and Sawyers 2003). Following identification of several kinase domain mutations in imatinib -

resistant patients, an *in vitro* screen of randomly mutated Bcr-Abl recovered all of these plus many additional mutations (Azam, Latek et al. 2003). This study provided many insights on allosteric regulation of the Bcr-Abl kinase and has clinically predictive potential (Azam, Latek et al. 2003; Azam, Raz et al. 2003). Other screens followed, also to predict the resistance profiles for other inhibitors (von Bubnoff, Barwisch et al. 2005; von Bubnoff, Veach et al. 2005). Of all these mutations, the 'gatekeeper' residue mutation T315I, which is critically involved in hydrogen bond formation with imatinib but also with nilotinib and dasatinib (Tokarski, Newitt et al. 2006; Weisberg, Manley et al. 2005), and E255K turned out to be the most problematic mutations in terms of disease prognosis, as they not only confer drug resistance but also increased activity of Bcr-Abl kinase (Gorre, Mohammed et al. 2001; Yamamoto, Kurosu et al. 2004). As E255K mutants were found to respond well to 'second generation' inhibitors such as dasatinib, which inhibits all imatinib-resistant mutants except T315I (Shah, Tran et al. 2004), the T315I mutations remains the major problem in terms of tyrosine kinase inhibitor resistance (Druker 2008). Some mutations were reported to occur before inhibitor treatment indicating a gain of fitness of Bcr-Abl kinase domain mutations and indeed, mutation of the gatekeeper residue T315, that confers resistance to all current inhibitors of Bcr-Abl, was shown to positively influence ATP binding loop (P-loop) phosphorylation (Y253 and Y257) and Bcr-Abl activity levels (Skaggs, Gorre et al. 2006).

1.10 Second generation tyrosine kinase inhibitors

The occurrence of secondary imatinib resistance leading to patient relapse and disease progression lead to the development and approval of 'second-generation' inhibitors such as the highly specific nilotinib (AMN107, Tasigna®, Novartis) (Weisberg, Manley et al. 2005) and the potent dual Src/Abl kinase inhibitor dasatinib (BMS-354825, Sprycel®, Bristol-Myers Squibb) (Lombardo, Lee et al. 2004; Shah, Tran et al. 2004) that target most imatinib resistant Bcr-Abl point mutated variants (O'Hare, Walters, Stoffregen, Jia et al. 2005; Quintas-Cardama, Kantarjian et al. 2007). Despite of 20- and 325-fold

higher activity against wild-type Bcr-Abl for nilotinib and dasatinib, respectively, and activity against > 90% of clinically isolated mutants *in vitro,* these new inhibitors still fail to target the most common imatinib-resistance mutation, T315I (O'Hare, Walters, Stoffregen, Jia et al. 2005; Weisberg, Manley et al. 2006). As for imatinib, clinical trials are promising at all CML disease stages (Guilhot, Apperley et al. 2007), even in imatinib resistant patients (Kantarjian, Giles et al. 2006; le Coutre, Ottmann et al. 2007), but it seems likely that similar clinical resistances might develop even with these second generation drugs. Besides dasatinib and nilotinib, some newer 'third generation' compounds are also active against imatinib-resistant forms of Bcr-Abl, such as INNO-406, a novel Bcr-Abl / Lyn dual tyrosine kinase inhibitor (Tanaka and Kimura 2008; Yokota, Kimura et al. 2007). Bosutinib (SKI-606), a novel dual Src / Abl tyrosine kinase inhibitor, is active against Bcr-Abl at low nanomolar range and is equally effective against the majority of imatinib resistant mutations (Golas, Arndt et al. 2003; Redaelli, Piazza et al. 2008). Although inactive against T315I *in vivo*, bosutinib was found to inhibit this mutant weakly *in vitro* (Remsing Rix, Rix et al. 2008). INNO-406, bosutinib and dasatinib also target Lyn tyrosine kinase (Rix, Hantschel et al. 2007; Weinstein and Joe 2006; Yokota, Kimura et al. 2007), thereby simultaneously addressing the problem of frequent Lyn overexpression (Donato, Wu et al. 2003; Wu, Meng et al. 2008). The differential profiles of activity of dasatinib, nilotinib, INNO-406 and bosutinib against imatinib-resistant kinase domain mutations raises the possibility of case-dependent combination of these drugs upon resistance mutation related imatinib failure (Redaelli, Piazza et al. 2008). Furthermore, as the global target profiles of these inhibitors are known in more and more detail, their use might be rationalized dependent on the molecular disease background and side effect occurrences in individual patients (Rix, Hantschel et al. 2007). After all, the clinically effective T315I inhibitor still remains to be identified (O'Hare and Druker 2005; Tanaka and Kimura 2008) and the general shortcomings of primary and secondary resistance, especially in advanced disease stages (Tanaka and Kimura 2008), and issues with long-term tolerability of Bcr-Abl inhibitors remain a major clinical problem (Schiffer 2007).

1.11   Combination-therapies and alternative approaches

Despite of further attempts to develop even more powerful 'third generation' Bcr-Abl kinase inhibitors and attempts to even target different regulatory mechanisms of Bcr-Abl, using drugs like ON012380 that bind non-ATP competitively (Gumireddy, Baker et al. 2005) or GNF-2 that binds the myristate binding pocket (Adrian, Ding et al. 2006; Hantschel, Nagar et al. 2003; Ohren and Sebolt-Leopold 2006) or targeting the coiled-coil domain (Beissert, Puccetti et al. 2003), different therapeutic options than targeting Bcr-Abl alone are clearly needed to overcome resistance (Weinstein and Joe 2006). Already during early phase II clinical trials of imatinib, the advent of resistance mutations to a single inhibitory agent was foreseen and combinations with conventional chemotherapeutic agents such as IFN-α, hydroxyurea (HU), daunorubicin (DNR) and cytosine arabinoside (Ara-C) were tested *in vitro* and showed overall synergism in combination with imatinib, motivating clinical trials with these drug combinations (Thiesing, Ohno-Jones et al. 2000). Resistance problems together with the inability of current Bcr-Abl inhibitors to target leukemia stem cells require additional targets that are critical for Bcr-Abl action to be identified and exploited for pathway specific combination therapy in order to ultimately result in a curative strategy for CML rather than maintaining patients in remission with conventional chemotherapy (O'Hare, Corbin et al. 2006; O'Hare, Eide et al. 2007). Some approaches have already tried to exploit this strategy by combining imatinib with drugs that act on potentially critical components of the Bcr-Abl signaling pathway such as mTOR (rapamycin) (Mayerhofer, Aichberger et al. 2005; Mohi, Boulton et al. 2004), PI3-kinase (wortmannin and LY294002) (Chu, Holtz et al. 2004; Klejman, Rushen et al. 2002), cyclin-dependent kinases (flavopiridol) (Yu, Krystal et al. 2002), MEK-1 (Chu, Holtz et al. 2004), Raf-1 (Neshat, Raitano et al. 2000) and farnesyl transferase (SCH66336) (Hoover, Mahon et al. 2002; Nakajima, Tauchi et al. 2003), showing promising results *in vitro*. Also, chlorogenic acid (Chl) and sodium chlorogenate (NaChl) alone were shown to inhibit Bcr-Abl, which led to activation of p38 MAPK and apoptosis in K562 cells (Bandyopadhyay, Biswas et al. 2004). Simultanous targeting of Src family kinases Src / Abl inhibitors such as dasatinib together with imatinib

showed promising compatibility *in vitro* and might indeed be a promising therapeutic option (O'Hare, Walters, Stoffregen, Sherbenou et al. 2005). Lyn tyrosine kinase, shown to be involved in imatinib resistance upon overexpression, is being targeted by the inhibitors INNO-406, bosutinib and dasatinib (Donato, Wu et al. 2003; Wu, Meng et al. 2008; Yokota, Kimura et al. 2007). Furthermore, targeted knock-down of Bcr-Abl using breakpoint-specific short-interfering RNA (siRNA) represents another approach taken and confirmed that reduction of Bcr-Abl protein levels by siRNA is able to sensitize for imatinib in Bcr-Abl over-expressing cells and even in a cell line carrying the imatinib resistant mutant H396P (Wohlbold, van der Kuip et al. 2003).

Despite these largely successful and promising efforts to approach the suppression of CML by targeted tyrosine kinase inhibitor therapy and alternative approaches, Ph^+ CML stem cells are left unaffected, because they are residing in a dormant state, while the inhibitors are only effectively targeting proliferating cells (Clarkson, Strife et al. 2003; Goldman 2004). Therefore, the Ph^+ stem cells represent an unaffected pool of cells that are able, at any time, to lead to disease relapse, especially upon the advent of resistance mutations (O'Hare, Corbin et al. 2006). Such resistance mutations are likely to persist in CML stem cells throughout long-term tyrosine kinase inhibitor therapy, later leading to resistance when these stem cells exit their dormant state and start proliferating. For this process, precise mathematical kinetics models have already been generated (Michor, Hughes et al. 2005). Therefore, the ultimate goal of curative CML therapy must be the inhibition and elimination of Ph^+ CML stem cells (Shteper and Ben-Yehuda 2001). Besides the only curative strategy so far, consisting of bone marrow ablation by chemotherapy or irradiation followed by syngeneic or allogeneic bone marrow transplantation (Clarkson, Strife et al. 2003), alternative stem cell targeting strategies, such as the use of differentiating agents like retinoic acid or bryostatin (Lilly, Tompkins et al. 1990), need to be identified and applied in addition to prior therapy with conventional and targeted therapeutic approaches in a step-wise patient-specific regimen (Clarkson, Strife et al. 2003).

1.12 Signaling pathway mapping by Tandem Affinity Purification coupled to liquid chromatography and tandem mass spectrometry (TAP-LC-MSMS)

Protein – protein signal transduction networks can be mapped using an integrated approach comprised of tandem affinity purification (TAP), liquid chromatography coupled to tandem mass spectrometry (LC-MSMS) and bioinformatic network analysis (Figure 1.5). The TAP procedure is a sensitive and highly selective method of purifying, under close-to-physiological conditions (Rigaut, Shevchenko et al. 1999), multi-protein complexes formed *in vivo* by two consecutive affinity purification steps (Gavin, Bosche et al. 2002) for subsequent analysis by mass spectrometry and was successfully applied to map the yeast cellular machinery (Gavin, Bosche et al. 2002). Proteins of interest ('entry points'), such as known and candidate interaction partners or substrates implicated in the protein complex or signaling pathway under investigation are cloned into retroviral transduction vectors using the Gateway[®] technology (Invitrogen) enabling expression of N- or C-terminal TAP-tag fusion proteins. The Gateway[®] cloning technology is convenient for the cloning of large numbers of pathway 'entry points', as it circumvents limitations often encountered in restriction enzyme based cloning (Walhout, Temple et al. 2000). The TAP-tag consists of a tandem immunoglobulin G (IgG)-binding unit of protein A from *Staphylococcus aureus* and a calmodulin binding domain (CBP) with a tobacco etch virus (TEV) protease cleavage site between the two affinity tags (Rigaut, Shevchenko et al. 1999). Virus stocks containing the coding sequences of the N- or C-terminal TAP-tag fusion proteins are generated in a HEK293 Gag-Pol packaging cell line (Somia, Miyoshi et al. 2000). Viruses obtained from the supernatant of this packaging cell line are then used to infect the model expression cell line of choice as target cells, the human leukemia cell line K562 in this study (Klein, Ben-Bassat et al. 1976). Upon infection of the expression cell line K562 with the "entry point" bait construct, cells are cultured and assessed for infection efficiency by FACS, measuring the proportion of GFP-positive cells. GFP-positive cells are then FACS-sorted in order to establish homogenous cell lines stably expressing the TAP-tagged bait protein.

For tandem affinity purification of protein complexes of interest, cells are grown to about $2\text{-}5 \times 10^8$ cells and lysed in TAP buffer (see Materials and Methods). The purification of the TAP-tagged protein and bound interaction partners consists of two sequential high-affinity binding and two mild elution steps (Figure 1.5A). Using the conventional Gateway® system the protein A moiety is first bound to IgG beads and protein complexes are released upon TEV protease cleavage. Then, in the second affinity-binding step the Calmodulin binding domain (CaM BD) is bound to CaM beads and subsequently eluted with EGTA (Ca^{2+} chelation) (Rigaut, Shevchenko et al. 1999).
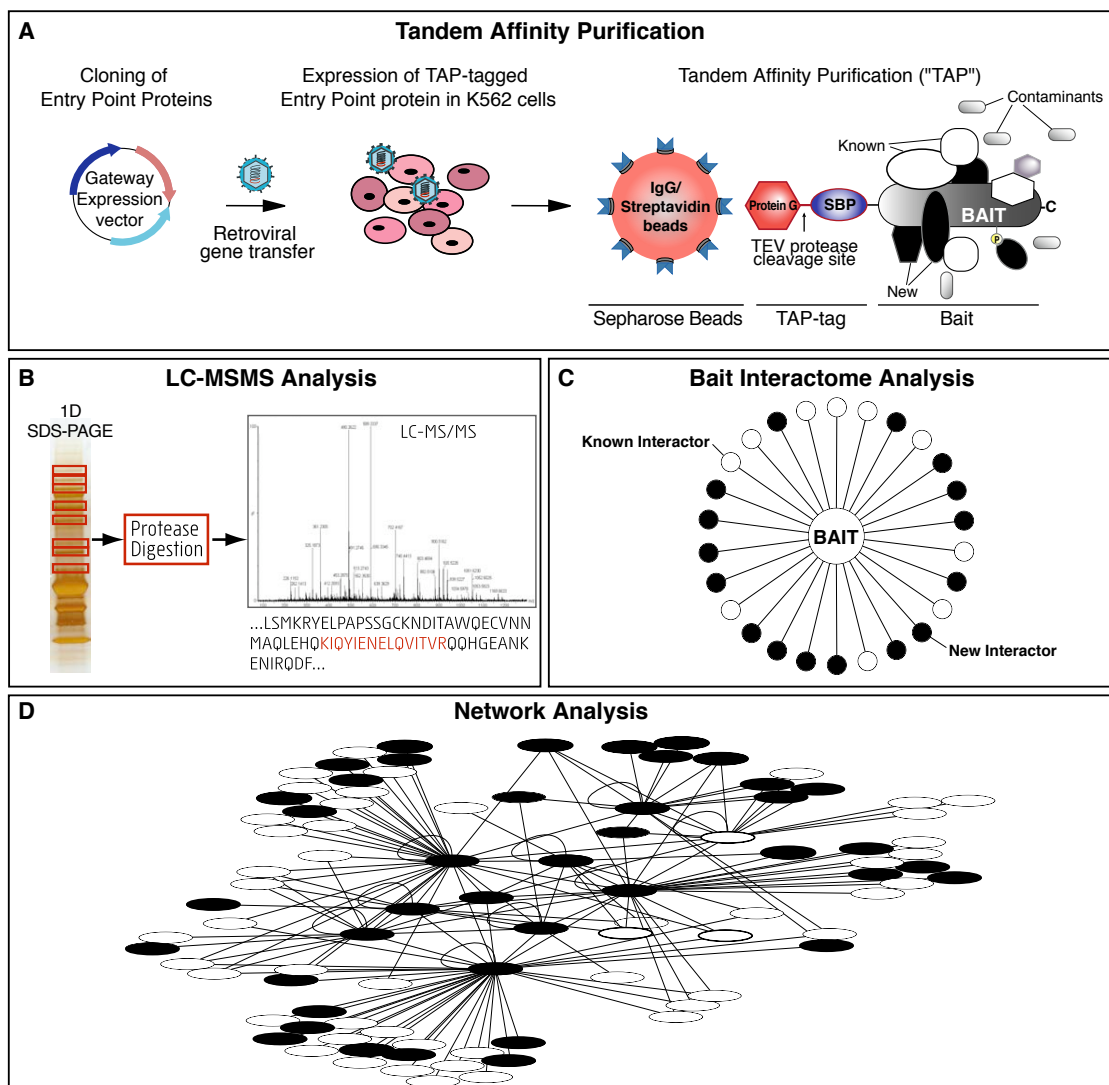
Figure 1.5 Signaling pathway mapping by Tandem Affinity Purification coupled to liquid chromatography and tandem mass spectrometry (TAP-LC-MSMS)
(A) Proteins of interest ('entry points') are cloned into retroviral transduction vectors using the Gateway® technology (Invitrogen) as N- or C-terminal TAP-tag fusion

proteins. Virus stocks containing the coding sequences are generated in a packaging cell line and used to infect the target expression cell line of choice. TAP-tagged bait protein and bound interaction partners are purified by two sequential high-affinity binding and two mild elution steps. Upon binding of the protein G moiety of the tag to IgG beads, protein complexes are released by TEV protease cleavage, then the SBP moiety is bound to streptavidin beads and protein complexes are either eluted with biotin or by boiling in SDS sample buffer (Burckstummer, Bennett et al. 2006).

(B) A fraction of each TAP sample is separated by 1D-SDS-PAGE and silver stained. Entire gel lanes are sliced into a defined number of equal pieces, digested with trypsin and analyzed by LC-MSMS.

(C) Statistically significant bait interactors identified by LC-MSMS, here represented as 'star'-diagram, are compared to human protein-protein interaction databases (e.g. HPRD, IntAct). Annotated interactions are shown as white circles, whereas black circles represent novel interactions.

(D) Computational combination of several TAP purification datasets results in a single protein-protein interaction network.

As the yield represented one of the crucial shortcoming of this method in mammalian cells, work in our laboratory resulted in an optimization of the TAP procedure following optimization of the TAP-tag composition and sequence (codon usage) for use in mammalian cells, which resulted in an approximately 10-fold overall yield increase compared to the conventional TAP system (Burckstummer, Bennett et al. 2006). The optimized TAP protocol for use in mammalian cells (Burckstummer, Bennett et al. 2006) instead uses a tag based on protein G and the streptavidin-binding-peptide (SBP) (GS-TAP). Here upon binding of the protein G moiety to IgG beads, protein complexes are released upon TEV protease cleavage, then the SBP is bound to streptavidin beads and protein complexes are either eluted with biotin or by boiling in SDS sample buffer.

Following TAP, eluted protein complexes are separated by 1D-SDS-PAGE, the entire gel lane is sliced into sections, *in situ* - digested with trypsin and analyzed by data-dependent nanocapillary reversed-phase LC-MSMS (Figure 1.5B). Proteins are identified by automated searching of the human IPI protein database (Kersey, Duarte et al. 2004) and, following at least two technical repeats of the TAP purification, identified proteins are analyzed for their statistical consistency and significance (Figure 1.5C). Finally, the data sets of multiple TAP purifications are combined in the bioinformatic analysis of the interaction network (Figure 1.5D) (as described in (Bouwmeester, Bauch et al.

2004) (for details see Materials and Methods). The raw data set of interactions can be filtered either against reference TAP purifications or a 'core proteome' (Schirle, Heurtier et al. 2003) of the cell line used, representing a defined list of the most prevalent proteins in the cell line, usually representing cytoskeletal proteins and proteins of general housekeeping function. This allows for the identification of proteins specifically enriched in the TAP-purifications by comparing TAP versus 'core proteome' datasets applying SAM statistical tests (Tusher, Tibshirani et al. 2001). In the past, the TAP procedure has been successfully used for small- and large-scale purification of protein complexes in bacteria and eukaryotic cells (Rigaut, Shevchenko et al. 1999) (Puig, Caspary et al. 2001) (Westermarck, Weiss et al. 2002) (Veraksa, Bauer et al. 2005). The TAP-LC-MSMS pathway mapping approach therefore enables the fast mapping of protein - protein interaction networks in eukaryotic cells (Brajenovic, Joberty et al. 2004; Drewes and Bouwmeester 2003; Gavin, Aloy et al. 2006; Gavin, Bosche et al. 2002) and has been successfully used in human cell lines before, for instance, to map the TNF-α signaling pathway that results in activation of the NF-κB family of transcription factors (Bouwmeester, Bauch et al. 2004).

1.13   Quantitative proteomics

As biological processes are exerted by proteins complexed in protein machines (Gavin, Bosche et al. 2002), quantitative proteomics analysis of the abundance of an entire proteome or at least of the proteins involved in the biological process under investigation represents a crucial layer of information to understand those processes. While DNA chip based quantitative transcriptomics studies are powerful in quantifying mRNA levels, quantitative proteomics methods provide a more direct measure of the quantities and characteristics of proteins (Ong and Mann 2005). When it comes to the understanding of the "logic" of a signal transduction pathway, quantitative parameters, like cellular protein copy number and protein complex stoichiometry, represent advantageous information in addition to the qualitative (physical and functional) description of participating proteins and their interactions and enrich the predictive value of the analysis for the development

of pharmacological intervention strategies (Kolch, Calder et al. 2005; Papin, Hunter et al. 2005). Quantitative protein chip technology suffers from the limitations of antibody availability and specificity, whereas MS-based approaches are thought to be the most powerful approach to quantitative proteomics (Ong and Mann 2005). Several MS-based experimental tools have been developed in order to facilitate this transition towards more quantitative proteomics (Ong and Mann 2005). These can be divided into into (i) absolute quantification methods that measure the absolute amount of protein in the sample, whereas (ii) relative quantification strategies focus on the relative change in protein amounts between two states (e.g. time points).

A straightforward absolute quantification method named XIC (extracted ion chromatogram) allows extracting quantitative information directly from mass spectra. Here, the signal intensity of a peptide eluting from a chromatographic column is plotted over time and the area under the curve (XIC) is linearly related to the amount of the peptide. While this approach suffers from various limitations related to the differing physico-chemical properties of individual proteins or peptides, more accurate 'protein abundance indices' (PAI) have been developed to normalize the XICs for the individual protein's characteristics (Andersen, Wilkinson et al. 2003). Overall however, MS-based quantification strategies using stable isotope labeling turned out to be advantageous. Here, labeling of peptides with stable isotopes (preferably ^{13}C and ^{15}N) introduces a defined mass difference between the heavy versus the unlabeled peptide from two experimental conditions (Zhang and Regnier 2002). A straightforward absolute quantification technique (AQUA) uses known quantities of chemically synthesized stable isotope-labeled peptides spiked into samples as internal standards (Kusmierz, Sumrada et al. 1990). Although AQUA suffers from the limitation that suitable peptide markers have to be identified, it can be successfully used at small or medium scale to quantify proteins and phosphoproteins from cells lysates (Gerber, Rush et al. 2003) and is applicable to identify biomarkers in body-fluids (Kuhn, Wu et al. 2004).

Relative protein quantification can be accomplished by stable isotope labeling by amino acids in cell culture (SILAC), a simple and powerful protocol

33

for metabolic incorporation of stable isotopes (Amanchy, Kalume et al. 2005), where an essential stable isotope labeled amino acid is supplied in the growth media upon which it is introduced into each newly synthesized protein of the proteome (Ross, Huang et al. 2004). Upon comparison of the labeled to the unlabeled reference sample, each peptide pair of the entire proteome is separated by the mass difference corresponding to the introduced labeled amino acid (Ong, Blagoev et al. 2002). This technique increases the feasibility of large-scale quantifications (entire proteomes) (Aebersold 2003; Aebersold and Mann 2003; Beynon, Doherty et al. 2005). Chemical tagging-based approaches like 'isotope-coded affinity tag' (ICAT) (Gygi, Rist et al. 1999), where stable isotope-carrying chemical reagents are targeted towards a reactive functional group of a peptide, are an attractive alternative. The ICAT reagent contains a reactive group targeting cysteins specifically and a biotin group for purification of labeled peptides via an avidin column. The heavy ICAT reagent features a polyether linker region containing eight deuteriums and allows quantification next to the 'light' reference sample. However, as only cysteine containing peptides are labeled and isolated, the lack of cysteine in proteins and peptides represents a major limitation.

Another approach to relative protein quantification, 'isobaric tag for relative and absolute quantitation' (iTRAQ), uses four tags that generate specific reporter ions of 114, 115, 116 and 117Da mass in their respective fragmentation spectra but, via a carbonyl balance group, finally add up to the same mass (Ross, Huang et al. 2004; Wiese, Reidegeld et al. 2007). Upon proteolytical digest, peptides are labeled with either one of the four isobaric isotope-coded tags via their lysine side chains, the four samples are combined, peptides are separated by liquid chromatography coupled to mass spectrometry (LC-MSMS) and peptides are detected, distinguishable by the tag-specific mass reporter ion. Relative quantification is then accomplished by calculation of the ratios of the four reporter signal intensities (Unwin, Pierce et al. 2005). This multiplexing strategy allows analysis of four separately labeled protein samples within one single analysis, thereby helping to increase analytical throughput (Bantscheff, Eberhard et al. 2007; Unwin, Pierce et al. 2005). The method has

been further expanded to 8-plex relative quantification proteomics and was, as an example, successfully applied to compare the activities of six leukemogenic tyrosine kinases, including Bcr-Abl, as regards their effect on the proteome (Pierce, Unwin et al. 2008). The complexity of the proteome including splice isoforms and post-translational modifications (PTMs) in concordance with the complex functional implication of proteins in biological processes calls for the use of these accurate and multiplexed quantitative proteomics tools in order to update a protein's function and position within a physical interaction network with quantitative information about its interaction partners, ideally in a temporal dimension (Ong and Mann 2005).

1.14 Aim of the thesis

Despite decades of work on the oncogenic Bcr-Abl protein and its signaling properties, the following fundamental questions on the cellular mechanism of action of the endogenous drug target Bcr-Abl are still open:

- What are the critical effectors of Bcr-Abl?
- Is it possible to derive a comprehensive and coherent map of Bcr-Abl signaling in a defined, standardized cellular setting?
- In the light of resistance problems with current small-molecule inhibitors, is it possible to identify pivotal elements in the Bcr-Abl pathway that could represent potential targets for alternative or combination therapy?

Aware of these unresolved fundamental questions and the existing extensive, but heterogeneous data on Bcr-Abl interacting proteins, substrates and downstream signaling components, the aim of this study was to

- undertake a systematic and unbiased approach to study Bcr-Abl signaling with the aim to
- complement the diverse existing data and provide a more consolidated view on actual set-up of the endogenous drug-target Bcr-Abl in a defined cellular setting, within the long-term interest to

- identify signatures of molecular endpoints of Bcr-Abl signaling useful to address unresolved resistance problems to first and second-generation anti-Bcr-Abl tyrosine kinase inhibitors, to monitor drug effectiveness and disease progression and to provide a rationale for combination therapy.

We decided to use K562 cells as a defined cellular setting for purification of protein complexes by large-scale immunoprecipitation and TAP-LC-MSMS (Bouwmeester, Bauch et al. 2004) in order to generate a physical map of the Bcr-Abl signaling pathway upon statistical analysis of significantly interacting proteins and bioinformatic network modeling. Herein, we planned to concentrate on the immediate interactors of Bcr-Abl in order to define the Bcr-Abl 'core' complex (Gavin, Aloy et al. 2006), (Tong, Drees et al. 2002), which is thought to consist of Bcr-Abl itself and its most intimately associated stoichiometric protein binders. For Bcr-Abl and its 'core' interactors, we furthermore planned to introduce quantitative parameters by determining the absolute cellular copy numbers and the 'core' complex interaction stoichiometry in order to enable the development of an interaction model and to set the foundation for a quantitative analysis of Bcr-Abl signaling. Finally, we decided to characterize the Bcr-Abl 'core' complex further by studying the effects of siRNA knock-down of its components on the proliferative potential of K562 cells and by monitoring the consequences of tyrosine kinase inhibitor perturbation on the composition of the Bcr-Abl 'core' complex.

MATERIALS AND METHODS

2 MATERIALS AND METHODS

2.1 DNA constructs

cDNAs were obtained from RZPD (Crk-I, Grb2, Sts-1, Eps15, AP2μ1), OriGene Technologies (Shc-1, p85β) or kindly provided by S. Decker (SHIP-2) and B. Mayer (c-Cbl). p210Bcr-Abl was a kind gift from Owen Witte and pSGT-Abl and -Bcr-Abl constructs were generated in our lab using standard molecular cloning techniques and described before (Barilá and Superti-Furga 1998; Pluk, Dorey et al. 2002).

The cDNAs were amplified by PCR and cloned into the respective destination vectors for expression as N-or C-terminal fusions to the tandem affinity purification cassette using the Gateway cloning system (Invitrogen, Carlsbad, CA) (Burckstummer, Bennett et al. 2006). pETM30 and pETM41 vectors were used for expression of recombinant epitope standard proteins as His-GST or His-MBP fusion proteins, respectively, using standard molecular biology techniques. The pETM30 vector was a kind gift of Gunther Stier (EMBL Heidelberg) and the pETM41 vector was obtained from the EMBL Protein Expression and Purification Facility. Constructs cloned as His-GST-fusion proteins in pETM30 were Crk-I (full-length, residues 1-204), Grb2 (full-length, residues 1-217), p85β RhoGAP-domain (residues 102-307), Shc1 SH2-domain (residues 358-474) and the Sts-1 C-terminus (residues 636-649). Constructs cloned as His-MBP-fusion proteins in pETM41 were the c-Cbl UBA-domain (residues 853-906) and the Ship2 SAM-domain (residues 1184-1258). Point mutations were obtained using the quick-change site directed mutagenesis kit (Stratagene). All cloned vectors and mutations were confirmed by sequencing.

The table below gives and overview of the constructs I generated during the time of my thesis:

Maxi #	Vector	Insert	Comments
2254	pDONRT201	p210 Bcr-Abl	Gateway, TAP entry vector, CTAP
2255	pDONRT201	p210 Bcr-Abl	Gateway, TAP entry vector, NTAP
2256	pRVCTAP-CZ69	p210 Bcr-Abl	Gateway, TAP destination vector, CTAP, clone #3.1
2257	pRVCTAP-CZ69	p210 Bcr-Abl	Gateway, TAP destination vector, CTAP, clone #3.2
2297	pPinco-Tet	p210 Bcr-Abl	Tet-inducible
2303	pRVNTAP-GS	p210 Bcr-Abl	Gateway TAP destination vector, NTAP-GS

2325	pRVNTAP-GS	Pxn	Gateway, TAP destination vector, NTAP-GS
2326	pRVCTAP-SG	Akt1	Gateway, TAP destination vector, CTAP-SG
2335	pRVCTAP-SG	Dok2	Gateway, TAP destination vector, CTAP-SG
2336	pRVCTAP-SG	Fes	Gateway, TAP destination vector, CTAP-SG
2337	pRVCTAP-GS	Hck	Gateway, TAP destination vector, CTAP-GS, GSGS linker
2338	pRVNTAP-GS	Shp2	Gateway, TAP destination vector, NTAP-GS
2353	pDONRT201	Akt1	Gateway, TAP entry vector, CTAP
2354	pDONRT201	Dok2	Gateway, TAP entry vector, CTAP
2355	pDONRT201	Fak	Gateway, TAP entry vector, CTAP
2356	pDONRT201	Fes	Gateway, TAP entry vector, CTAP
2357	pDONRT201	Hck	Gateway, TAP entry vector, CTAP
2358	pDONRT201	Myc	Gateway, TAP entry vector, NTAP
2359	pDONRT201	Pxn	Gateway, TAP entry vector, NTAP
2360	pDONRT201	Shp2	Gateway, TAP entry vector, NTAP
2361	pDONRT201	p210 Bcr-Abl	Gateway, TAP entry vector, with start and stop codons
2421	pETM-30	Grb2_1-217	N-6His-GST-Grb2 recombinant epitope standard, full length
2422	pETM-30	c-Cbl_853-906	N-6His-GST-c-Cbl recombinant epitope standard, C' UBA
2423	pETM-30	c-Cbl_721-906	N-6His-GST-c-Cbl recombinant epitope standard, C' UBA
2428	pRVNTAP-GS	Myc	Gateway, TAP destination vector, NTAP-GS
2429	pRVCTAP-SG	Fak	Gateway, TAP destination vector, CTAP-SG
2430	pRVNTAP-GS	Nck	Gateway, TAP destination vector, NTAP-GS
2432	pRVCTAP-SG	Crk-II	Gateway, TAP destination vector, CTAP-SG
2457	pRVNTAP-GS	c-Cbl	Gateway, TAP destination vector, NTAP-GS
2458	pRVNTAP-GS	Sts-1	Gateway, TAP destination vector, NTAP-GS
2459	pDONRT201	c-Cbl	Gateway, TAP entry vector
2460	pDONRT201	Crk-II	Gateway, TAP entry vector, CTAP
2461	pDONRT201	Sts-1	Gateway, TAP entry vector
2466	pETM-30-XhoI	-	N-6His-GST, TEV, NcoI mutagenized to XhoI
2470	pRVNTAP-GS	p85β	Gateway, TAP destination vector, NTAP-GS
2471	pRVNTAP-GS	Shc1	Gateway, TAP destination vector, NTAP-GS
2472	pRVNTAP-GS	PSTPIP1	Gateway, TAP destination vector, NTAP-GS
2473	pRVCTAP-SG	PKCδ	Gateway, TAP destination vector, CTAP-SG
2489	pETM-30-XhoI	Shc1_358-474	N-6His-GST-Shc1 recombinant epitope protein standard
2497	pRVNTAP-GS/2xT	Ship2	Gateway, TAP destination vector, NTAP-GS, 2xTEV
2498	pRVCTAP-SG/2xT	Ship2	Gateway, TAP destination vector, CTAP-SG, 2xTEV
2500	pDONRT201	Ship2	Gateway, TAP entry vector, NTAP
2501	pDONRT201	Ship2	Gateway, TAP entry vector, CTAP
2502	pDONRT201	p85β	Gateway, TAP entry vector, NTAP
2518	pETM-30	Ship2_2-108	N-6His-GST-Ship2 recombinant epitope standard, N' SH2
2688	pETM-30	p85β_619-728	N-6His-GST-p85β recombinant epitope standard, C' SH2
2689	pETM-30	Sts-1_254-322	N-6His-GST-Sts-1 recombinant epitope standard, SH3
2690	pETM-30	Crk-II_1-304	N-6His-GST-Crk-II recombinant epitope standard, full

			length
2718	pETM-30	Ship2_1193-1258	N-6His-GST-Ship2 recombinant epitope standard, C'SAM
2719	pETM-30	Ship2_1190-1258	N-6His-GST-Ship2 recombinant epitope standard, C'SAM
2720	pETM-30	Ship2_1184-1258	N-6His-GST-Ship2 recombinant epitope standard, C'SAM
2722	pRVCTAP-SG/2xT	Bcr-Abl-TEV	Gateway, TAP destination vector, CTAP-SG, 2xTEV, p210 Bcr-Abl C' TEV - FABD
2723	pRVCTAP-SG/2xT	ΔCC-Bcr-Abl-TEV	Gateway, TAP destination vector, CTAP-SG, 2xTEV, Δcoiled-coil p210 Bcr-Abl, C' TEV - FABD
2738	pDONRT201	Bcr-Abl-TEV	Gateway, TAP entry vector, CTAP, p210 Bcr-Abl
2739	pDONRT201	ΔCC-Bcr-Abl-TEV	Gateway, TAP entry vector, CTAP, Δcoiled-coil p210 Bcr-Abl, C' TEV - FABD
2791	pDONRT201	Shc1	Gateway, TAP entry vector, NTAP
2804	pETM-30	p85β_1-154	N-6His-GST-p85β recombinant epitope standard, N' SH3
2828	pDONRT201	AP2μ1	Gateway, TAP entry vector, NTAP
2829	pRVNTAP-GS/2xT	AP2μ1	Gateway, TAP destination vector, NTAP-GS, 2xTEV
2830	pDONRT201	Eps15	Gateway, TAP entry vector, NTAP
2831	pRVNTAP-GS/2xT	Eps15	Gateway, TAP destination vector, NTAP-GS, 2xTEV
2832	pDONRT201	Eps15	Gateway, TAP entry vector, CTAP
2833	pRVCTAP-SG/2xT	Eps15	Gateway, TAP destination vector, CTAP-SG, 2xTEV
2860	pMSCV-GW	Bcr-Abl-TEV	Gateway, p210 Bcr-Abl, C' TEV - FABD
2861	pMSCV-GW	ΔCC-Bcr-Abl-TEV	Gateway, Δcoiled-coil p210 Bcr-Abl, C' TEV - FABD
2874	pETM-30	Sts1_636-649	N-6His-GST-Sts-1 recombinant epitope standard, C' peptide
3049	pETM-41	Crk-L_1-303	N-6His-MBP-Crk-L recombinant epitope standard, full length
3205	pRVCTAP-SG/2xT	Crk-I	Gateway, TAP destination vector, CTAP-SG, 2xTEV
3275	pETM-41	Ship2_1184-1258	N-6His-MBP-Ship2 recombinant epitope standard, C' SAM
3279	pDONRT201	Crk-I	Gateway, TAP entry vector, CTAP
3782	pETM-30	p85β_102-310	N-6His-GST-p85β recombinant epitope standard, RhoGAP
3783	pETM-41	c-Cbl_853-906	N-6His-MBP-c-Cbl recombinant epitope standard, C' UBA
3784	pETM-30	Crk-I_1-204	N-6His-GST-Crk-I recombinant epitope standard, full length

2.2　Antibodies and epitopes

Antibodies used included: Abl (mouse monoclonal 24-21, Ab-3, Calbiochem), Abl (rabbit polyclonal, K-12, Santa Cruz), Ship2 (rabbit polyclonal, kind gift by D. Wisniewski), c-Cbl (rabbit polyclonal, produced in-house against recombinant c-Cbl UBA domain), Grb2 (rabbit polyclonal, C-23, Santa Cruz) and Grb2 (mouse monoclonal, clone 81, BD), c-Crk (mouse monoclonal, clone 22, BD), CrkL (mouse monoclonal, #05-414, Millipore), Shc-1 (mouse monoclonal, clone 30, BD), Sts-1 (rabbit polyclonal, Rockland Inc.), p85β (mouse monoclonal, clone T15, AbD-Serotec), Sos 1 (mouse monoclonal, A-9,

Santa Cruz) and GST antiserum (rabbit polyclonal, Z-5, Santa Cruz). The table below indicates the detailed conditions the antibodies were used with during this study.

Antibody (Ab)	Supplier	ID	Species	Dilution	Blocking & 1st Ab	2nd Ab (AlexaFluor-680/-800) (1:7000, 0.1% Tween in 1x PBS)
Bcr-Abl/c-Abl	Calbiochem	Ab-3 (21-24)	mouse	1:2000	3% BSA, 0.1% Tween in 1x PBS	goat anti-mouse
Bcr-Abl/c-Abl	Santa Cruz	K-12	rabbit	1:500	5% Milk, 0.1% Tween in 1x PBS	goat anti-rabbit
Ship2	*D. Wisniewski*	-	rabbit	1:2500	Odyssey blocking buffer (Li-Cor)	goat anti-rabbit
c-Cbl	*this study*	*#3377/#3378*	rabbit	1:1000	Odyssey blocking buffer (Li-Cor)	goat anti-rabbit
p85β	AbD-Serotec	T15	mouse	1:1000	5% Milk, 0.1% Tween in 1x PBS	goat anti-mouse
Sts-1	Rockland Inc.	600-401-870	rabbit	1:1000	5% Milk, 0.1% Tween in 1x PBS	goat anti-rabbit
Sts-1-IRDye-800	*this study*	600-401-870	rabbit	1:1000	5% Milk, 0.1% Tween in 1x PBS	-
Shc1	BD	30	mouse	1:1000	5% Milk, 0.1% Tween in 1x PBS	goat anti-mouse
Shc1-IRDye-800	*this study*	30	mouse	1:500	5% Milk, 0.1% Tween in 1x PBS	-
Grb2	BD	81	mouse	1:1000	Odyssey blocking buffer (Li-Cor)	goat anti-mouse
Grb2-IRDye-800	*this study*	81	mouse	1:250	Odyssey blocking buffer (Li-Cor)	-
Grb2	BD	C-23	rabbit	1:500	5% Milk, 0.1% Tween in 1x PBS	goat anti-rabbit
Crk-I/II	BD	22	mouse	1:500	Odyssey blocking buffer (Li-Cor)	goat anti-mouse
Crk-I/II-IRDye-800	*this study*	22	mouse	1:250	Odyssey blocking buffer (Li-Cor)	-
CrkL	Millipore	#05-414	mouse	1:5000	Odyssey blocking buffer (Li-Cor)	goat anti-mouse
Sos 1	Santa Cruz	A-9	mouse	1:500	Odyssey blocking buffer (Li-Cor)	goat anti-mouse
GST	Santa Cruz	Z-5	rabbit	1:2000	5% Milk, 0.1% Tween in 1x PBS	goat anti-rabbit

The epitope of the 24-21 antibody directed against the C-terminal F-actin binding domain of Bcr-Abl / c-Abl and used for large-scale immunoprecipitation of Bcr-Abl / c-Abl complexes was mapped by generating a series of mutants covering most surface exposed residues of the Abl F-actin binding domain (1026-1149) (Hantschel, Wiesner et al. 2005). The mutants were expressed in E. coli as recombinant GST-fusion proteins, purified to homogeneity and 5μg of each mutant recombinant fusion protein were immunoblotted against Abl FABD (24-21) and GST. Protein levels were quantified and protein recognition was monitored as ratio of 24-21- over GST-signal. Only mutation of residues Q1094, Q1095 and M1096 showed reduced binding of 24-21 of about 50%.

The table below summarizes the details of the antibodies used for quantifications and co-immunoprecipitation studies and indicates the regions of the protein within which the antibody epitope resides.

Antibody	ID	Supplier	Species	IgG type	Epitope region
c-Abl / Bcr-Abl	Ab-3 (21-24)	Calbiochem	mouse	monoclonal IgG	FABD residues Q1094,Q1095,M1096
c-Abl / Bcr-Abl	K-12	Santa Cruz	rabbit	polyclonal IgG	kinase - domain
Ship2	-	*D. Wisniewski*	rabbit	polyclonal IgG	SAM - domain, residues D1230 - K1247
c-Cbl	*#3377/#3378*	*this study*	rabbit	polyclonal IgG	UBA - domain, residues A853 - T906
p85β	T15	AbD-Serotec	mouse	monoclonal IgG1	RhoGAP - domain, residues D122 - L292
Sts-1	600-401-870	Rockland Inc.	rabbit	polyclonal IgG	C' peptide, residues P636 - E649
Shc1	30	BD	mouse	monoclonal IgG1	SH2 - domain, residues L359 - K473
Grb2	81	BD	mouse	monoclonal IgG1	full length protein
Grb2	C-23	Santa Cruz	rabbit	polyclonal IgG	C-terminal peptide
Crk-I	22	BD	mouse	monoclonal IgG2a	residues E102 - N204 (- S304 of Crk-II)
Sos 1	A-9	Santa Cruz	mouse	monoclonal IgG2b	residues Q1057 - S1178

Primary antibodies were detected with AlexaFluor-680 labeled goat anti-mouse or goat anti-rabbit secondary antibodies, detected using the Odyssey imaging system (Li-Cor Biosciences, Lincoln, NE, USA). Primary Antibodies used for detection of Grb2 and Crk-I, that migrate at the apparent molecular weight (MW) of IgG-light chain and antibodies against Shc1 and Sts-1, migrating within the MW - range of IgG-heavy chain, were directly labeled with the IRDye® 800CW microscale protein labeling kit (Li-Cor® Biosciences) in order to avoid cross-reaction of fluorescent secondary antibodies with IgG-light and -heavy chains. Grb2, c-Crk and Shc1 antisera (BD Biosciences) were depleted from BSA that would compete with antibody primary amine groups and lead to reduced labeling efficiency. For BSA removal, 400μl of antibody (100μg) were incubated with 50μl bed-volume proteinG-sepharose, pre-washed in 'binding buffer' (20mM Na_2PO_4 pH 7.0), for 2hrs at 4°C. The beads were transferred to MoBiCon columns and washed with 'binding buffer'. Antibodies were then eluted in 100μl 'elution buffer' (0.1M glycine-HCl pH 2.7) and neutralized with 10μl 'neutralization buffer' (1M Tris pH 10.0), yielding a final antibody concentration of 1μg/μl, depleted of BSA. BSA-free Grb2, c-Crk, Shc and Sts-1 antisera were dialyzed in Na_2PO_4 pH 8.5 and fluorescently labeled with IRDye® 800CW by addition of 0.8μl of reconstituted dye to 100μg (100μl) of antibody. Following incubation in the dark at room temperature for 2hrs, dye-conjugated antibody was separated from free dye by passing the sample through 0.5ml Zeba™ desalting spin columns (Pierce, Rockford, IL).

2.3 Cell culture, tyrosine kinase inhibitor treatment, immuno - precipitation and immunoblot assays

K562 (DSMZ #ACC 10) cells were grown in RPMI-1640, 10% fetal calf serum, 1% penicillin/streptomycin. Dasatinib (Sprycel, BMS-354825) and nilotinib (Tasigna, AMN107) were dissolved in DMSO and used at final concentrations of 100nM and 1μM, respectively. K562 cells were mock-, dasatinib- or nilotinib - treated at the indicated concentrations for 3 hours. K562 total cell lysates for immunoprecipitation and immunoblot experiments were prepared by washing cells in ice-cold PBS and lysed in 'lysis buffer' containing 50 mM Tris-HCl pH 7.5, 150 mM NaCl, 1% NP-40, 5 mM EDTA, 5 mM EGTA, 25 mM NaF, 1mM Na_3VO_4, 1mM PMSF, 5μg/ml TLCK, 1μg/ml leupeptin, 1μg/ml aprotinin, 10μg/ml soybean trypsin inhibitor. K562 total cell lysates for tandem affinity purification and 'large-scale' immunoprecipitation were prepared in 'TAP lysis' buffer (50 mM Tris-HCl pH 7.5, 100 mM NaCl, 5% glycerol, 0.2% NP-40, 1.5 mM $MgCl_2$, 25 mM NaF, 1 mM Na_3VO_4 and protease inhibitors) (Burckstummer, Bennett et al. 2006; Hantschel, Rix et al. 2007). Insoluble material was removed by high-speed centrifugation and protein concentration was determined by Bradford-assay using γ-globulin as reference standard (Biorad). For immunoprecipitation, total cell lysates were incubated with the antibodies for 3 hrs at 4°C followed by pull-down of the immune-complexes by protein G-Sepharose^{TM} 4 Fast Flow (GE Healthcare) for 1 h at 4°C. Immunoblot assays were routinely performed by blotting proteins separated by SDS-PAGE on nitrocellulose membranes (Schleicher & Schuell) for 1 h at 1mA/cm^2. The membranes were blocked and incubated with primary antibody diluted in convenient blocking buffer (3% BSA – PBS - 0.1% Tween, 5% Milk – PBS - 0.1% Tween or Li-Cor blocking reagent). We then incubated the membranes using IRDye680- or IRDye800-coupled goat anti-rabbit or rabbit anti-mouse secondary antibodies at 1:7000 dilution in PBS-Tween (1x PBS, 0.1% Tween in H_2O) for detection using the Odyssey fluorescent imaging system (Li-Cor).

2.4   Large-scale   immunoprecipitation   of   endogenous   protein complexes of Bcr-Abl and its stoichiometric candidate 'core' interactors

For large-scale immunoprecipitation of endogenous protein complexes from K562 cells, c-Abl-, Sos-1, Ship2-, c-Cbl-, p85β-, Sts-1-, Shc1-, Grb2- and c-Crk(-I/II) antibodies were coupled to NHS-activated sepharose as follows:

c-Abl (21-24) antibody was first affinity purified on an Äkta FPLC using HiTRAP ProteinG HP 1ml sepharose columns (Amersham). c-Abl antibody aliquots were centrifuged at 14,000rpm for 15min to remove antibody aggregates, diluted at a 1:10 ratio in 'binding buffer' (20mM Na_2PO_4 pH 7.0), loaded onto the proteinG column equilibrated in 'binding buffer', washed with 'binding buffer', eluted with a pH-shift by applying 'elution buffer' (0.1M glycine-HCl pH 2.7) and collected in 250μl fractions. Elution fractions were collected in a 96-well plate with 25μl 'neutralization buffer' (1M Tris-HCl pH 9.0) provided per well. Elution fractions corresponding to high protein content were pooled and checked by immunoblotting. Ship2 antibodies were purified from the antiserum kindly provided by David Wisniewski by adding 100μl bed-volume Protein G Sepharose^{TM} (4 Fast Flow, GE Healthcare) (PGS), pre-washed in 'binding buffer', to 600μl serum and incubation for 2hrs at 4°C. The beads were transferred to MoBiCon columns and washed twice with 1ml 'binding buffer', followed by elution with 200μl 'elution buffer' and neutralization with 20μl 'neutralization buffer. Shc1 and c-Crk antibodies (BD Biosciences) were depleted from BSA as described for fluorescent labelling with IRDye800CW, prior to NHS-sepharose coupling (see section 3.2). c-Abl, Ship2, c-Cbl, Sts-1, Shc1 and c-Crk antibodies were then dialyzed twice in 2ltrs 1x PBS at 4°C. Grb2 (C-23, Santa Cruz), p85β, c-Cbl and Sos-1 (A-9, Santa Cruz) antibodies were directly used for coupling, without prior purification nor dialysis. Prior to coupling, 500μl bed-volume NHS-sepharose beads were activated by addition of an excess (about 15ml) of 1mM HCl pH3.0 and protonization of the NHS ester groups. The HCl was removed by centrifugation and the beads were mixed with about 100μg antibody and incubated on a rotary incubator for 2hrs at room temperature. Upon completion of the coupling, the antibody beads were

recovered by centrifugation and un-reated ester-groups were saturated with an excess (10ml) 100mM Tris pH8.0 over night at 4°C. The next morning, the Tris was removed by centrifugation and ion-bonded interactors were washed off the antibody beads by three consecutive washing steps, alternating between 100mM Tris pH8.0 and 100mM Acetate pH4.0. The covalently coupled antibody beads were then stored as 50% slurry in 1x PBS containing 0.03% NaN_3 until use.

For immunoprecipitation, $1*10^9$ K562-cells were harvested and lysed in TAP lysis buffer (see section 3.5) (Burckstummer, Bennett et al. 2006), cleared by high-speed centrifugation at 27,500rpm for 1h and incubated with respective antibodies covalently coupled to NHS-Sepharose beads at 4 °C for 6 hrs. For purification of Bcr-Abl / c-Abl complexes we used 250μl bed-volume and for purification of Bcr-Abl interactors we used 75μl bed-volume of antibody beads. Bcr-Abl large-scale immunoprecipitations were performed in triplicates from mock- and dasatinib-treated cells. Bcr-Abl large-scale immunoprecipitations for analysis by iTRAQ quantification were perfomed once, from mock- and dasatinib- and from mock- and nilotinib treated cells, each. Large-scale immunoprecipitations of Grb2 for iTRAQ quantification and of Bcr-Abl interactors were performed once from mock- and nilotinib treated cells, each. We washed bound proteins with TAP lysis buffer. Bcr-Abl / c-Abl protein complexes for analysis by gel-base LC-MSMS were eluted several times with one column volume 1% SDS. Bcr-Abl / c-Abl protein complexes and protein complexes of the candidate Bcr-Abl 'core complex' interactors Ship2, c-Cbl, p85β, Sts-1, Shc1, Grb2 and Crk-I for analysis by 1D-shotgun LC-MSMS and for relative iTRAQ quantification by MALDI-TOFTOF MS, protein complexes were transferred to a buffer free of amines and detergent (50mM HEPES NaOH pH 7.5, 5% Glycerol, 150mM NaCl and 1.5mM $MgCl_2$) via a second washing step. These protein complexes were then eluted several times with one column volume of 150mM HCl and neutralized with triethylammonium bicarbonate at a final concentration of 200mM. To assess the efficiency of the elution, we boiled the remaining antibody-beads in SDS sample buffer. We assessed performance

of the large-scale immunoprecipitations and final yield of protein complexes by immunoblot analysis of the respective purification fractions.

2.5 Generation of stable transgenic cell lines and Tandem Affinity Purification (TAP)

K562 cells stably expressing NTAP- or CTAP-fusion entry point proteins were generated by stable transduction by retroviral gene transfer (Bouwmeester, Bauch et al. 2004). Tandem affinity purifications were performed as described earlier (Burckstummer, Bennett et al. 2006) (for details see section 1.12).

2.6 Mass Spectrometry and Bioinformatics

All mass-spectrometric analysis described in sections 3.6.1, 3.6.2 and 3.6.5 was performed by our mass spectrometry group at CeMM, headed by Keiryn Bennett with the valuable assistance of Gregor Schütze, Melanie Planyavsky and André Müller. André Müller was critically involved in the processing of the 1D-shotgun samples (section 3.6.5). Relative quantification studies by iTRAQ mass-spectrometry were performed by Thomas Köcher and Karl Mechtler at the IMP, Vienna (see section 3.6.6). All bioinformatics analysis described in sections 3.6.3 and 3.6.4 was performed by our bioinformatics team at CeMM, headed by Jacques Colinge.

In brief, proteins were separated by SDS-PAGE, visualized by silver- or Coomassie staining, entire gel lanes were sliced into pieces, digested in situ with trypsin, purified, concentrated and analyzed by nano-LC-MSMS. Tryptic digests were analyzed by data-dependent nanocapillary reversed-phase LC-MSMS and proteins were identified by automated database searching. Proteins significantly enriched in the large-scale immunoprecipitations were identified by statistical analysis that resulted in a list of 18 candidate Bcr-Abl 'core complex' components. Of these 18, nine representative components were used for TAP experiments. Using a different statistical analysis, proteins significantly

identified in the TAP experiments were determined and network modeling resulted in the generation of the Bcr-Abl signaling network.

2.6.1 Sample preparation for mass spectrometry and in situ tryptic digestion

Tandem affinity purification (TAP), large-scale immunoprecipitate (IP) samples and the total cell lysate of wild-type K562 cells (50 mg total protein) in 4× Laemmli buffer (containing 10% b-mercaptoethanol) were boiled for 3 min, cooled to room temperature and alkylated by incubation with iodoacetamide (final concentration, 13 μg/μL) for 20 minutes in the dark. Reduced and alkylated samples were separated by 1D SDS-PAGE on a 4 – 12% bis-Tris gel (NuPAGE, Invitrogen, CA). After visualisation of the proteins by silver staining (TAP) (Shevchenko, Wilm et al. 1996), or Coomassie Brilliant Blue G Colloidal (Sigma) (K562 total cell lysate and large-scale IP), entire gel lanes were sliced into 20 equal pieces (TAP and large-scale IP's) or 48 equal pieces (K562 total cell lysate).

Proteins in the gel slices were reduced with dithiothreitol, alkylated by incubation with iodoacetamide and digested in situ with modified porcine trypsin (Promega Corp., Madison, WI) (Shevchenko, Wilm et al. 1996). The resultant peptide mixture was extracted from the gel slices and desalted with customised reversed-phase stage tips (Rappsilber, Ishihama et al. 2003). The volume of the eluted sample was reduced to approximately 2 μL in a vacuum centrifuge and reconstituted to 10 μL with LC Phase A (see below). Depending on the intensity of the protein band staining, additional multiples of 8 μL LC Phase A were added to specific samples prior to analysis by LCMS.

2.6.2 Gel-based LC-MSMS and data analysis of protein complexes obtained by Bcr-Abl large-scale immunoprecipitation and TAP

Mass spectrometry was performed on a quadrupole time-of-flight (QTOF) mass spectrometer (QTOF Ultima, Waters, Manchester, UK) equipped with a nanoelectrospray ion source coupled to a high-performance liquid

chromatography Agilent 1100 nanoflow system (Agilent, Palo Alto, CA). The HPLC system was comprised of a solvent degasser, a binary pump and a nanoflow pump. Phase A consisted of 0.4 percent acetic acid, 0.005% heptafluorobutyric acid (HFBA) in water and Phase B consisted of 0.4 percent acetic acid, 0.005% heptafluorobutyric acid (HFBA) in 90 percent acetonitrile. From the thermostatted micro-autosampler, 8 μL of the tryptic peptide mixture was automatically loaded onto a trap column (Zorbax 5 mm, Agilent Technologies, Palo Alto, CA) with the binary pump at a flow rate of 50 μL/min (3% Phase B). After the trap column was washed with 3% Phase B, the peptides were back-flushed onto a customised eight cm fused silica analytical column (inner diameter 75 μm) packed with C18 3 μm diameter Reprosil beads (Maisch, Germany). The peptides were eluted from the analytical column with a 25 minute gradient ranging from 13 to 35 percent Phase B, followed by a 3 minute gradient from 35 to 50 percent Phase B and a 4 minute gradient from 50 to 100 percent Phase B at a constant flow rate of 250 nL/min. The analysis was performed in a data-dependent acquisition mode using one MS channel for every three MSMS channels and a dynamic exclusion for selected ions of 60 s (MassLynx, Waters, Manchester, UK).

The acquired data were processed with ProteinLynx Global Server 2.2.1 (Waters, Manchester, UK) and searched against an internally curated version of the International Protein Index protein sequence database (human IPI version 3.32, European Bioinformatics Institute, www.ebi.ac.uk/IPI/) with the search engine MASCOT. This compilation of entries from Swiss-Prot, TrEMBL, RefSeq, and Ensembl was appended with frequently observed non-human contaminants (e.g., TEV protease). Submission to MASCOT was via a Perl script that performs an initial search with broad mass tolerances on both the precursor and fragment ions (200 ppm and 0.15 Da, respectively). High confidence peptide identifications are used to recalibrate all precursor and fragment ion masses prior to a second search with narrower mass tolerances (15 ppm and 0.05 Da). One missed tryptic cleavage site was allowed. Carbamidomethyl cysteine was set as a fixed modification, and oxidised methionine was set as a variable modification. A false-discovery detection rate (FDR) of less than 0.25 percent

was estimated by searching the data set against a reversed database. Criterion for a positive protein identification was identification of a minimum of 2 peptides with a Mascot peptide score of ≥ 20. Protein identifications were grouped according to shared peptides and only one protein per group, having all the peptides, is reported as identified.

2.6.3 Identification of Bcr-Abl 'core' complex candidates

The total cell lysate of wild-type K562 cells ('core proteome') was analysed by LC-MSMS as technical duplicates, and the large-scale Bcr-Abl immunoprecipitates were analysed as technical triplicates. Results obtained from each of the five gel lanes were merged to give five data files. Comparison of the IP samples with the 'core proteome' was based on peptide counts (PC), i.e., the total number of unique peptides. This approach has been used before by our laboratory and other groups to report protein abundance in a semi-quantitative manner (Colinge, Chiappe et al. 2005; Liu, Sadygov et al. 2004; Rix, Hantschel et al. 2007). Analysis of the data using a Perl script enabled the association of each protein identified in one of the samples with the corresponding identified peptides. This resulted not only in a peptide count for each sample, but also reduced the number of proteins identified to groups of proteins distinguishable by MS (Nesvizhskii and Aebersold 2005). The resultant table of peptide counts was processed using an R script to perform statistical analysis and flag the proteins that were significantly more abundant in the IP samples versus the 'core proteome' samples. A test based on 'significance analysis of microarrays' (SAM) (Tusher, Tibshirani et al. 2001) was used and imposed a 'false discovery rate' (FDR) of 5% (Zaykin, Young et al. 2000).

2.6.4 Identification of confident binders in TAP experiments and statistical analysis of the protein-protein interaction network

Each TAP experiment was analyzed by LC-MSMS as technical duplicates. The statistical method outlined above for the large-scale immunoprecipitates, however, could not be applied in these experiments. Thus

empirical criteria were used: a protein identified from a TAP sample was considered a confident binder provided the protein was identified in each of the duplicate TAP samples, with a minimum peptide count (PC) of 3, or in only one TAP sample with a minimum PC of 4, but was not identified in the 'core proteome'. Alternatively, if the ratio of the minimum TAP PC by the maximum core proteome PC was greater than 3, then the protein was also considered as a confident interactor.

To identify the group of proteins significantly related to BCR-ABL, which we postulated as the 'core complex' around the latter, the topology of the network, represented as an 'undirected graph' obtained by linking each complex candidate to confident binders, was exploited. We then applied random network simulations and generated 100,000 random graphs by shuffling edges and searched each for the largest k with a non-empty k-core (Tong, Drees et al. 2002). Thereby we learned the null distribution of the largest k, which is significant at the 10^{-5} level for values equal or larger than 4 and not significant under 4. We then considered the real network and found the 4- and 5-cores (no 6-core).

2.6.5 1D-shotgun LC-MSMS analysis of protein complexes obtained by large-scale immunoprecipitation

HCl elution fractions of large-scale immunoprecipitated protein complexes were assessed by immunoblotting for recovery of bait protein and known interactors, fractions enriched in the protein complexes were pooled and $30\mu l$ were analyzed in by 1D-shotgun LC-MSMS analysis in technical duplicates. Samples were resuspended in 100mM triethylammonium bicarbonate buffer, pH8.53, reduced with 10mM dithiothreitol for 30 minutes at 56°C, free cystein residues blocked with 55 mM iodacetamide and digested by adding $2.5\mu g$ trypsin (Promega, Madison, USA). Digestion was carried out at 37°C overnight and subsequently quenched by the addition of TFA to final concentration of 1%. Peptides were extracted using in-house fabricated stage-tips utilizing C18 embedded mesh material (Empore C18 extraction discs, 3M

Centre, Minnesota, USA) and used for a total of two injections onto a NanoLC system.

Analysis was performed on a Thermo LTQ Orbitrap XL (Thermo Fisher Scientific Inc.) coupled to a split NanoLC system (Agilent Technologies) operated with a trap-column setup. Peptides were separated on in-house fabricated 16 cm x 50 μm reversed-phase-columns (Reprosil pur, Maisch, Germany) at a constant flow rate of 100 nl/min with a gradient time of 175 min from 3 to 50%, then ramped up to 100% acetonitrile within 15min, in 0.4% acetic acid with 0.005% heptafluorobutyric acid as ion pairing agent. The LTQ Orbitrap XL mass analyzer was operated using Excalibur 2.0.6 software. For internal calibration of the mass spectrometer, the signals of the following background ions were used as lock masses: [Si(CH3)2O]5H+, (Si(CH3)2O)6H+, [Si(CH3)2O]6H+ + NH3, [Si(CH3)2O]7H+ + NH3, and [Si(CH3)2O]8H+ + NH3 at m/z 371.101233, m/z 445.120025, m/z 462.146573, m/z 536.165365 and m/z 610.184156, respectively. The analyses were performed in a data-dependent acquisition mode using a top 10 collision-induced dissociation (CID) method (up to 10 CID spectra were acquired following each MS scan) and a dynamic exclusion for selected ions of 60 seconds. Maximal ion accumulation time allowed on the LTQ Orbitrap in CID mode was 150 ms for MSn in the LTQ and 1000 ms in the C-trap. Automatic gain control was used to prevent overfilling of the ion traps and was set to 5000 ions in MSn mode for the LTQ and 1 million ions for a full FTMS scan. Intact peptides were detected in the Orbitrap at 60,000 resolution. For statistical purposes, samples were analysed by LCMSMS as technical duplicates.

The acquired data were processed with Bioworks V3.3.1 SP1 (ThermoFisher, Manchester, UK), data files merged with an internally-developed program, and searched against the human IPI database version v3.41 with the search engine MASCOT (Matrix Sciences). Submission to MASCOT was executed via a Perl script that performs an initial search with relatively broad mass tolerances on both the precursor and fragment ions (±10 ppm and ±0.6 Da, respectively). High-confidence peptide identifications are used to recalibrate all precursor and fragment ion masses prior to a second

search with narrower mass tolerances (±4 ppm and ±0.3 Da, respectively). One missed tryptic cleavage site was allowed. Carbamidomethyl cysteine was set as a fixed modification, and oxidised methionine was set as a variable modification. For unambiguous protein identification at least two unique peptides with a MASCOT peptide ion score greater than, or equal to, 20 were required. A false-positive detection rate of less than 1 percent was estimated by searching the data set against a reversed database.

2.6.6 Quantitative iTRAQ mass spectrometry analysis of Bcr-Abl- and Grb2-protein complexes obtained by large-scale immunoprecipitation in the presence of tyrosine kinase inhibitors

Bcr-Abl- and Grb2-complexes were immunoprecipitated from mock-, dasatinib- or nilotinib-treated K562 cells, washed in detergent- and amine-free HEPES-buffer, eluted with 150mM HCl and neutralized with 0.5M triethylammonium bicarbonate (TEAB). Elution fractions were pooled, reduced, alkylated and digested with trypsin. Each sample was split into two aliquots and labeled with the respective iTRAQ reagents (two channels per sample after splitting). The peptide mixture was separated with reversed phase HPLC, spotted onto a MALDI plate and analyzed by MALDI-TOF/TOF tandem mass spectrometry (4800 MALDI TOF/TOF, Applied Biosystems, Toronto, Canada). Data interpretation was performed by computing the median of all 4 iTRAQ ratios (116:114, 117:114, 116:115, 117:115) for each protein and assuming they are dominated by proteins whose abundance is not modulated by nilotinib or dasatinib treatment. Therefore we fit a Gamma distribution to capture the random ratios by using robust estimates, where the average is replaced by the median and standard deviation is replaced by the median absolute deviation (MAD), and we set a threshold corresponding to a P-value < 0.005.

2.7 Quantitative characterization of the Bcr-Abl 'core' complex

2.7.1 Expression and purification of recombinant epitope protein standards

Mouse c-Abl-1b recombinant kinase domain (residues 248-534) was expressed in Sf9 cells and purified as described previously (Nagar, Bornmann et al. 2002). Recombinant F-actin binding domain of Bcr-Abl/c-Abl (FABD) was generated by cloning the coding region (residues 1026 – 1149, human c-Abl spliceform 1b numbering) into the pETM30 vector, providing an N-hexa-His-GST-tag, as described before (Hantschel, Wiesner et al. 2005). The constructs spanning the epitopes recognized by each of the antibodies for Ship2, c-Cbl, p85β, Sts-1, Shc1, Grb2 and Crk-I were cloned in pETM30 and pETM41 vectors for expression of recombinant protein as C-terminal fusions to 6xHis-GST or 6xHis-MBP (mannose binding peptide), respectively, including a Tobacco Etch Virus protease cleavage site. Initially all epitopes were cloned as 6xHis-GST fusion proteins and purified from *E.coli*. In consequence, different amounts of recombinant protein were analyzed by immunoblotting next to recombinant GST for antibody cross-reaction with GST alone. Recombinant epitope proteins, whose antibodies displayed cross-reactivity with GST alone were replaced by 6xHis-MBP fusion proteins in order to exclude cross-reactivity with GST as an error source during quantitative immunoblotting using the Odyssey imaging system (Li-Cor Biosciences, Lincoln, NE, USA). The following table shows details and fusion-type of the recombinant epitope protein standard used in this study:

Protein	Epitope	Residues	Vector	Fusion tag	MW (kDa)
c-Abl / Bcr-Abl	Kinase - domain	S248 - T534	-	-	34
c-Abl / Bcr-Abl	FABD	S1026 - R1149	pETM-30	N-6-His-GST	43
Ship2	SAM - domain	E1184 - K1258	pETM-41	N-6-His-MBP	53
c-Cbl	UBA - domain	A853 - T906	pETM-41	N-6-His-MBP	50
p85β	RhoGAP - domain	D102 - P307	pETM-30	N-6-His-GST	55
Sts-1	C' peptide	P636 - E649	pETM-30	N-6-His-GST	31
Shc1	SH2 - domain	A358 - L474	pETM-30	N-6-His-GST	42
Grb2	full length	M1 - V217	pETM-30	N-6-His-GST	54
Crk-I	full length	M1 - N204	pETM-30	N-6-His-GST	52

The recombinant plasmids were transformed into BL21(DE3) and protein expression was induced by addition of 1mM IPTG followed by incubation at room temperature. 3h post induction cells were harvested and resuspended in 'nickel-wash buffer' (50mM Tris-HCl pH 7.5, 20mM imidazole, 500mM NaCl, 5% Glycerol, 5mM β-mercaptoethanol, 1mM PMSF) and flash frozen in liquid N_2. Cells were lysed using a French press (Avestin Emulsiflex-C3 high pressure homogenizer) and a cell-free extract was obtained by high-speed centrifugation. The extract was loaded onto a 1ml Ni-NTA column (Qiagen) equilibrated in 'nickel-wash buffer'. Recombinant fusion protein was eluted as 0.5ml fractions with 'nickel-elution buffer' (50mM Tris-HCl pH 7.5, 250mM imidazole, 500mM NaCl, 5% Glycerol, 5mM β-mercaptoethanol) applying a linear imidazole gradient (20mM – 250mM) and fractions containing the recombinant protein (as determined by SDS-PAGE and Coomassie staining) were pooled. Pooled protein was re-buffered with 'nickel wash buffer' using Amicon® Ultra centrifugal filter devices (Millipore). In individual cases, gel filtration on a Superdex75 (XK16/60 column) in 'gel filtration buffer' (20mM Tris-HCl pH7.5, 300mM NaCl, 3mM dithiothreitol (DTT)) resulted in increased homogeneity of the protein preparation. Protein concentration was determined by measuring a UV absorbance-spectrum (250-350nM) of an adequate dilution in 50mM Na_2PO_4-buffer (pH 7.0). Protein concentration was determined by multiplying the absorption at 280nm with the dilution factor and dividing by the extinction coefficient of the purified protein construct. Extinction coefficients were determined using the ExPASy ProtParam tool (http://www.expasy.ch/tools/protparam.html). Based on these protein concentration values, 1:1.5 dilution series were generated for each recombinant epitope protein standard, starting at appropriate amount (according to detection by immunoblot).

2.7.2 Absolute quantification of total cellular protein copy numbers

We used 50, 100, 150 and 200 μg K562 total cell lysate of known cell count (9,903*10^5 viable cells/ml), known protein concentration (27,2 μg/μl) and known lysis volume (8 ml) to quantify absolute cellular protein copy numbers of

each of the 8 Bcr-Abl 'core complex' members. Following SDS-PAGE and immunoblotting relative quantification was performed using the Odyssey imaging system (Li-Cor Biosciences, Lincoln, NE, USA). Knowing cell count, protein concentration and lysis volume allowed calculation of protein amount per K562 cell **P(cell)**. Each quantification was performed in technical triplicates. Per quantification experiment internal triplicates of K562 total cell lysate quantifications (50, 100, 150, 200μg each) were performed in parallel. Primary antibodies were detected with AlexaFluor-680 labeled goat anti-mouse or goat anti-rabbit secondary antibodies, detected using the Odyssey imaging system (Li-Cor Biosciences, Lincoln, NE, USA) and quantified. Integrated pixel intensities per band were quantified for the 50, 100, 150 and 200μg and quantified at hands of a standard curve generated using recombinant epitope protein standards.

For absolute quantification, recombinant protein standards corresponding to the respective antibody epitopes were expressed in *E. coli*, purified to homogeneity and immunoblotted as internal reference standard as 1:1,5 serial - dilutions in each quantification experiment along with the total cell extracts. The concentration ranges of these recombinant epitope standard dilution series was adjusted to the detection intensity of the respective endogenous reference proteins as follows:

Protein	Recombinant epitope standard	Dilution series from (ng)
c-Abl / Bcr-Abl	Kinase - domain	22.7
c-Abl / Bcr-Abl	FABD	8.6
Ship2	SAM - domain	57.4
c-Cbl	UBA - domain	8.1
p85β	RhoGAP - domain	10.2
Sts-1	C' peptide	9.7
Shc1	SH2 - domain	19.9
Grb2	full length	18.2
Crk-I	full length	7.0

The seven recombinant epitope standard curve bands were quantified as described above and blotted against the amount of input (ng). Following quantification, values corresponding to the 50, 100 and 150μg samples were

normalized to the value corresponding to the 200µg sample. The 4 values of each triplicate were averaged and we finally determined the median of the three average values. For some quantifications, more than three average values were generated in order to reduce the error of the median. This "median of the averages" - value **M(ng)** was used to calculate total protein copy numbers per cell (**c(x)/cell**) considering the molecular weight (Da) of the respective recombinant protein epitope standard as well as Avogadro's number as follows:

Protein/K562-cell = **P(cell)** = $4{,}395 * 10^{-4}$ µg protein/cell

Li-Cor "median of the averages" = **M(ng):**

1. Bcr-Abl: 7.74; 4.92; 10.75; 6.21
2. Ship2: 13.25; 17.33; 26.83
3. c-Cbl: 15.35; 11.86; 14.68
4. p85β: 5.23; 6.78; 9.4; 11.08
5. Sts-1: 4.37; 3.65; 2.24; 2.51; 5.56; 5.36; 5.22
6. Shc1: 16.08; 9.46; 8.37; 14.46
7. Grb2: 8.2; 6.6; 11.4; 11.06; 6.61; 7.81
8. Crk-I: 1.5; 0.9; 0.8

Core interactor protein (g) / µg total cell lysate = **g(x)/µg** = $\dfrac{M(ng) \times 10^{-9} g}{200}$

Core interactor protein (%) / cell = **%(x)/cell** = $(g(x)/\mu g) \times (1 \times 10^{8})$

Core interactor protein (g) / cell = **g(x)/cell** = $\dfrac{(\%(x)/cell) \times P(cell)}{100}$

<u>Absolute protein copy number / cell</u> = **c (x)/cell** = $\dfrac{(6{,}02 \times 10^{23} \times (g(x)/\text{cell}))}{\text{MW}(\text{standard}_x)(Da)}$

Following quantification of the total copy number per cell of each of the proteins, the error was calculated as % standard deviation (% STDEV).

2.7.3 Quantification of the Bcr-Abl 'core' complex interaction stoichiometry and overall Bcr-Abl – associated proportions of each protein

For stoichiometry calculation, we immunoprecipitated Bcr-Abl complexes from 150 mg K562 total cell lysate using 24-21 anti-Abl antibody covalently coupled to NHS-Sepharose beads. Protein complexes were eluted from the beads by boiling in Lämmli SDS-PAGE sample buffer (containing β-mercaptoethanol). Following quantitative immunoblotting using the Odyssey system (Li-Cor), protein copy numbers of Bcr-Abl and each of the seven Bcr-Abl 'core complex' candidate proteins per 2% immunoprecipitate were quantified. Quantifications were performed by including the corresponding recombinant epitope protein standard in each quantification experiment, as described in the previous section. The interaction stoichiometry within the Bcr-Abl core complex was determined by calculating the ratios of each core interactor's copy numbers over the Bcr-Abl copy numbers in the IP-fraction. Each quantification was performed at least in triplicates and the average values and standard deviations were determined. In addition, taking the total cellular protein copy numbers into account, quantification of the band intensities in the input- and supernatant samples of the IP allowed calculation of the proportion of depleted versus undepleted protein corresponding to distribution of each core interactor as Bcr-Abl-associated (%) versus "free" cellular protein (%) (free or in different protein complexes).

2.8 Biophysical characterization of the Bcr-Abl 'core' complex

2.8.1 1-step TAP of *Saccharomyces cerevisiae* Pwp2 complexes

Pwp2 (pre-ribosomal complex) protein complexes were purified from *Saccharomyces cerevisiae* under the courtesy of Anne-Claude Gavin at the European Molecular Biology Laboratory (EMBL) in order to serve as size-standards for 'sizing' of the Bcr-Abl 'core complex' by density gradient centrifugation. Eight liters of Pwp2$^+$ yeast culture were grown to an OD of 3.5 - 3.8 in YPD medium and harvested at 4,000rpm for 15min. The supernatant was

discarded, the pellets were washed with 1x PBS containing 0.5mM PMSF and the centrifugation was repeated in 50ml tubes (Falcon). The supernatant was removed and the pellets were flash-frozen in liquid nitrogen. Pellets were thawed in a wather bath at 37°C, transferred to room temperature and lysed in lysis buffer containing 50mM Tris-HCl pH7.5, 100mM NaCl, 0.15% Igepal, 1.5mM MgCl$_2$, 0.5mM DTT, 1mM PMSF and 1x self-made protease inhibitor cocktail. Yeast cells were further lysed 3 x 4min at 350rpm in a planetary ball mill containing 25ml glass beads at 0.5mm diameter per beaker. Lysate of each strain was split in four equal parts. For each strain, three technical repeats of one-step TAP was performed using 250µl bed-volume IgG-sepharose (Amersham). After 1h incubation, beads were sedimented by 3min centrifugation at 1,200rpm, supernatant was recovered and kept as IgG-supernatant fraction for immunoblot analysis. The beads were transferred to 0.8ml MoBiTech columns and washed with 10ml 'yeast lysis' buffer containing 1mM DTT. Aliquots of the wash fraction were kept for immunoblot analysis. TEV-cleavage was then performed by adding 250µl lysis buffer and 16µl TEV protease (1mg/ml) and incubated 1h at 16°C in a thermo shaker at 750rpm. After elution of the TEV-cleaved protein complexes from the columns, glycerol was added to a final concentration of 5%, aliquots were flash frozen and stored at -80°C. Input, IgG-supernatant and TEV-eluate fractions were then analyzed by immunoblotting.

2.8.2 Glycerol density gradient centrifugation of *Saccharomyces cerevisiae* Pwp2 complexes and K562 Bcr-Abl / c-Abl complexes

20 – 80% gradients of glycerol (in 10mM Tris-HCl pH 7.5, 100mM NaCl 0.5mM EDTA, 0.2% NP40) were generated using a gradient maker (model #GM-20: C.B.S. Scientific Co., Del Mar, CA, USA) in 2ml polyallomer centrifuge tubes (11x34mm, No.: 347357,Beckman). Gradients were loaded with 50µl Pwp2 complex TEV eluate for calibration of gradient conditions or with 3mg of mock- and dasatinib-treated K562 cell lysate and ultra-centrifuged at 54,000rpm for 7hrs (Beckman Coulter Optima^{TM} Max-E ultracentrifuge). 16 gradient fractions à 125µl were collected with a pipette from top to bottome.

2.8.3   Analysis of K562 cell lysates in the presence of tyrosine kinase inhibitors by fluid phase liquid chromatography gel filtration

Mock-, dasatinib- and nilotinib-treated K562 cell lysate was analyzed by fluid phase liquid chromatography (FPLC) gel filtration in order to study changes in co-migration of Bcr-Abl and its seven 'core' interactor proteins. A Superose™ 6 (10/300 GL, Pharmacia Biotech) gel filtration column was calibrated by analyzing a run of a mixture of gel filtration standards (Bio-Rad Laboratories; catalog: 151-1901) containing a lyophilized mixture of the molecular weight markers ranging from 1350 to 670000 Da, thyroglobulin (bovine) 670000 Da, γ-globulin (bovine) 158000 Da, ovalbumin (chicken) 44000 Da, myoglobulin (horse) 17000 Da and vitamin b12 1350 Da. Next, 500μl of mock-, dasatinib- and nilotinib-treated K562 cell lysate were run, fractions were collected within the MW-range of the smallest Bcr-Abl interactor (Crk-I: 23kDa) up to the MDa MW-range compatible with high molecular weight tetrameric Bcr-Abl multi-protein complexes between 1 and 4MDa and the fractions were analyzed by immunoblotting.

2.9   siRNA perturbation of protein expression

Small interfering RNA (siRNA) knock-down was performed by transfecting K562 cells with Smartpool™ (Dharmacon RNAi Technologies, Inc., Chicago, IL, USA) siRNA duplexes targeting c-Abl, Ship2, c-Cbl, p85α, p85β, Sts-1, Shc1, Grb2 and Crk-I or a control siRNA using HiPerFect® transfection reagent (QIAGEN Inc., Valencia, CA, USA). The day before transfection, cells were diluted at a density of $3*10^5$ / ml in RPMI medium containing 10% fetal calf serum (FCS) and 1% antibiotics (penicillin/streptomycin) and incubated at standard conditions (37°C, 5% CO_2). On the day of transfection 10^6 K562 cells in logarithmic growth phase were each plated in a well of a 6-well plate in 500μl RPMI culture medium (10% fetal calf serum (FCS) and 1% penicillin/streptomycin). 1.5μg of the respective siRNAs (5μl) and 18μl HiPerFect® were diluted in 500μl culture medium without FCS and mixed by vortexing. Samples were incubated for 5-10min at room temperature in order to allow formation of transfection complexes. These were then drop-wise added to

the cells while gently swirling the culture dish to ensure uniform distribution of the transfection complexes. Cells were then incubated under standard conditions and, after 6hrs, 2ml RPMI culture medium (10% fetal calf serum (FCS) and 1% penicillin/streptomycin) were added and cells were incubated for 24 hours, harvested and analyzed for gene silencing by immunoblotting. For 48h and 72h gene-silencing experiments, K562 cells were re-transfected after 24h, adding fresh medium, harvested after 48h or 72h and analyzed for protein knock-down by immunoblotting.

RESULTS

3   RESULTS

3.1   Epitope mapping of the 24-21 Abl antibody

K562-cells endogenously express both Bcr-Abl and, from the other allele, the c-Abl protein. In order to identify endogenous Bcr-Abl interactors, we chose to isolate endogenous Bcr-Abl / c-Abl protein complexes from cell lysates of the CML cell line K562 by immunoprecipitation with the monoclonal Abl antibody 24-21 (Schiff-Maker, Burns et al. 1986), of which we had sufficient amounts in the lab. The antibody recognizes the very C-terminal F-actin binding domain of Bcr-Abl / c-Abl (residues 1026 – 1149 of h-Abl1b). A comprehensive set of recombinant proteins of a series of mutants of surface-exposed residues of the c-Abl F-actin binding domain from earlier work on the structure of the C-terminal F-actin binding domain (FABD) of Bcr-Abl by Oliver Hantschel (Hantschel, Wiesner et al. 2005) opened the possibility to precisely map the epitope of this antibody from the beginning of the project. The epitope of the Abl 24-21 antibody was mapped by quantitative immunoblotting of these recombinant mutant proteins using the Odyssey system (Li-Cor). These mutants were expressed in *E. coli* as recombinant GST-fusion proteins, purified to homogeneity and 5µg of each mutant recombinant fusion protein was immunoblotted against Abl FABD using the 24-21 antibody and against the GST-tag, including glutathione-S-transferase (GST) only as a control (recombinant proteins kindly provided by Oliver Hantschel). Protein levels were quantified and FABD-construct recognition by the 24-21 antiserum was monitored as the ratio of 24-21- over GST-signal, normalized to the ratio of wild-type FABD over GST. Mapping of the epitope of this antibody showed that only the construct containing mutations of the residues Q1094, Q1095 and M1096 within the FABD displayed reduced binding of the antibody (Figure 3.1). The epitope Q1094, Q1095, M1096 is located within the αII-αIII loop of the FABD (PDB entry 1ZZP; (Hantschel, Wiesner et al. 2005);Figure 3.1). While residues 1097, 1099, 1100, 1104 and 1108 within helix αIII have been shown to be critical for F-actin binding and cytosceletal association (Hantschel, Wiesner et al. 2005) and hence to be a critical determinant of Bcr-Abl / c-Abl localization,

the epitope Q1094, Q1095, M1096 is not involved in F-actin binding or any other known protein-protein interaction (Hantschel, Wiesner et al. 2005).
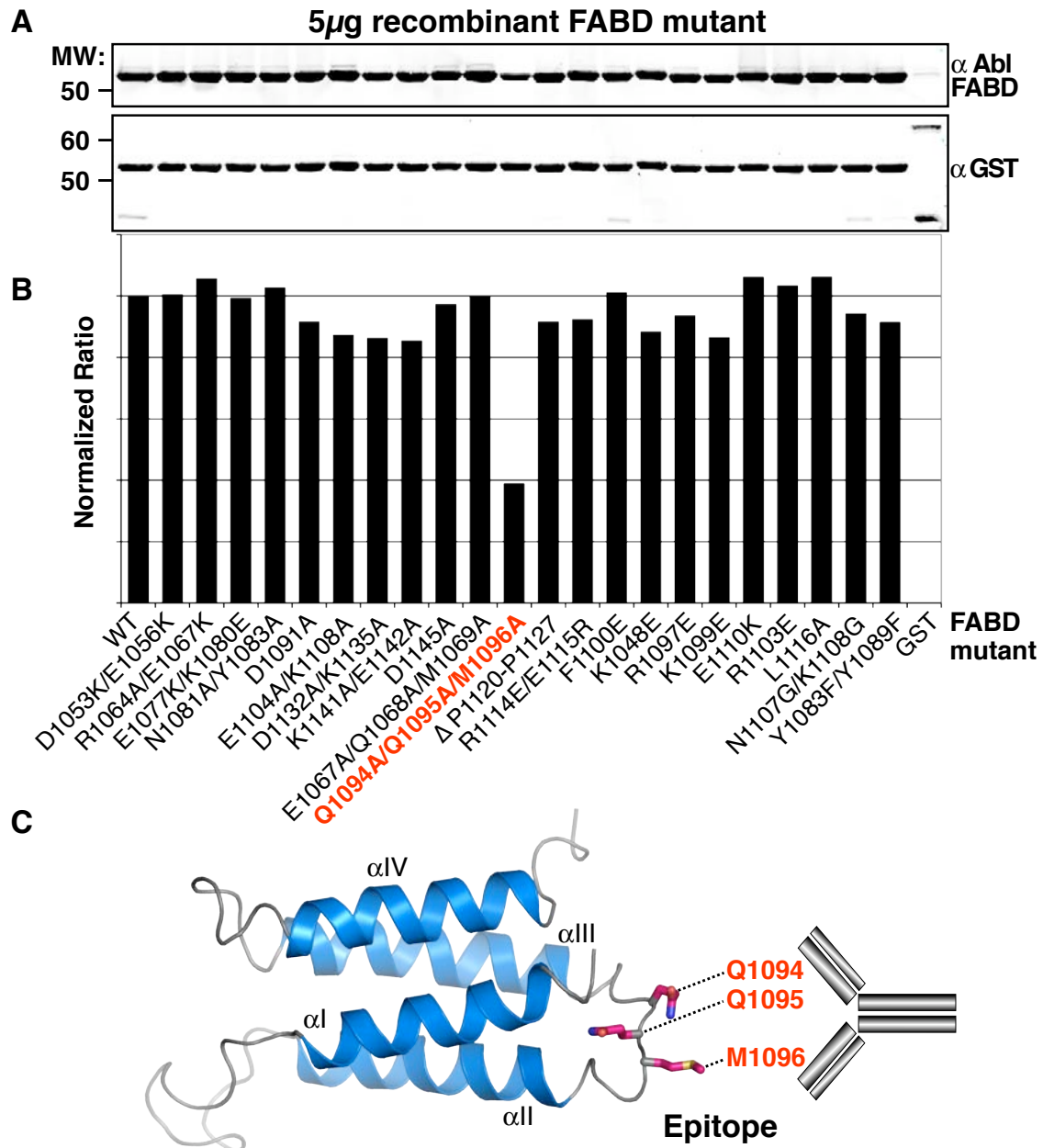
Figure 3.1 Epitope mapping of the Abl antibody 24-21 (Ab-3)
(A) The epitope of the Abl 24-21 antibody was mapped by immunoblotting recombinant proteins of Abl F-actin binding domain mutants (kindly provided by Oliver Hantschel). The mutants were expressed in E. coli as recombinant GST-fusion proteins, purified to homogeneity and 5µg of each mutant recombinant fusion protein were immunoblotted against Abl FABD (24-21) and GST.
(B) Protein levels were quantified and protein recognition was monitored as ratio of 24-21- over GST-signal, normalized to the ratio of wild-type FABD over GST. Only mutation of residues Q1094, Q1095 and M1096 within the αII-αIII loop showed reduced binding of the antibody.
(C) The epitope Q1094, Q1095 and M1096 is highlighted on the NMR-structure of the Abl F-actin binding domain (PDB entry 1ZZP) (Hantschel, Wiesner et al. 2005).

Therefore, the elucidation of the precise location of this antibodies epitope at the very beginning represented a vital control, as we could now exclude the interference of the antibody with protein-protein interactions to the best of our knowledge. Furthermore, knowing the epitope, we could is it together with recombinant FABD protein as recombinant epitope protein standard, besides recombinant Abl kinase domain, for absolute quantification of endogenous Bcr-Abl / c-Abl proteins by quantitative immunoblotting, as will be discussed later (see section 3.6).

3.2 Proteomic identification of the endogenous Bcr-Abl multi-protein complex

In order to identify endogenous interactors of Bcr-Abl, we immunoprecipitated Bcr-Abl/c-Abl protein complexes from cell lysates of the CML cell line K562 using the monoclonal Abl antibody 24-21 (Schiff-Maker, Burns et al. 1986). Bcr-Abl/c-Abl and interacting proteins were isolated using the Abl antibody covalently coupled to sepharose beads and, after washing the protein complexes with TAP lysis buffer (Burckstummer, Bennett et al. 2006), protein complexes were eluted using detergent (1% SDS). The efficiency of the purifications was checked by immunoblotting the input, wash and eluate fractions for Bcr-Abl/c-Abl and, as a control, the known Bcr-Abl interactor Shc1 (Tauchi, Boswell et al. 1994). Both Bcr-Abl and c-Abl were depleted completely from the extract and enriched in the elution fractions and Shc-1 co-eluted with Bcr-Abl/c-Abl (Figure 3.2B). Elution fractions that contained most Bcr-Abl (elution fractions 2-4,Figure 3.2) were pooled, separated by 1D-SDS-PAGE, stained with coomassie and analyzed by mass spectrometry (Figure 3.2C,D). Searching the mass spectrometry data against the human IPI protein database yielded a primary dataset of 427 proteins (Kersey, Duarte et al. 2004). In parallel, by analyzing 50μl of crude K562 cell lysate by LC-MSMS in a technical duplicate, we identified the 708 proteins most prevalent in K562 cells, representing the 'K562 core proteome' (Figure 3.2A). This set of the 708 most abundant proteins is likely to primarily reflect the cellular repertoire of abundant housekeeping and structural proteins (Schirle, Heurtier et al. 2003). Based on

these data sets, specific proteins were identified by comparing pull-down versus 'core proteome' datasets applying the 'significance analysis of microarrays' (SAM) statistical test (Tusher, Tibshirani et al. 2001). This process greatly improved the signal-to-noise ratio and even allowed the selection of abundant proteins (present in the K562 core proteome) based on their enrichment in the purifications. However, the cellular abundance of some proteins, e.g. HSP90 that is known to be complexed with Bcr-Abl and potentially of therapeutic interest (Shiotsu, Soga et al. 2002; Wu, Xu et al. 2008), precludes significant detection in a pull-down, because the enrichment does not yield a ratio sufficiently high to allow protein selection according to SAM criteria. This statistical procedure, gauged at 5% false discovery rate, yielded 18 high confidence interactors of Bcr-Abl/c-Abl with an average sequence coverage of 31% that is within the range of the observed sequence coverage for Bcr-Abl and would be compatible with a high stoichiometry interaction (Figure 3.2D). A number of these 18 Bcr-Abl/c-Abl complex component candidates were known interactors of Bcr-Abl and are well-described signalling proteins (Figure 3.2D). Grb2, Shc-1 and Crk-I are adaptor proteins containing SH3, SH2 and PTB domains that serve as adaptor interfaces in tyrosine kinase signaling (Pawson 2007). p85α and β are two of five regulatory subunits, that associate with the catalytic subunits (p110α,β, or δ) of the dimeric enzyme phosphatidylinositol-3-kinase (PI3K) that is playing a prominent role in oncogenesis as one of its components, PIK3CA (encoding p110α), is frequently found mutated in common human cancers such as breast, prostate and colon carcinoma (Geering, Cutillas et al. 2007; Zhao and Vogt 2008). The E3-ubiquitin ligases c-Cbl and Cbl-B typically bind and ubiquitinate activated tyrosine kinases and negatively regulate their activity (Thien and Langdon 2001). Ship2 is a SH2 domain-containing phosphatidylinositol-5-phosphatase known to bind the Abl SH3 domain and also, via its PTB domain, Shc1, with yet unknown function in Bcr-Abl signaling (Wisniewski, Strife et al. 1999).

Protein	Entrez gene name	Unique peptide count			Sequence coverage	MW (kDa)	Protein function	SMART-domains
		MS1	MS2	MS3	Average (%)			
Bcr	BCR	38	38	34	34	224	Rho-GAP	CC, RhoGEF, PH, C2, RhoGAP
Abl1	ABL	50	43	40	45		Tyrosine kinase	SH3, SH2, TyrKc, FABD
Ship-2	INPPL1	45	40	42	41	139	5-Inositol phosphatase	SH2, IPPc, SAM
Bike	BMP2K	10	19	15	17	129	Serine/threonine kinase	Pkinase
Cbl-B	CBLB	3	4	5	7	109	E3 ubiquitin ligase	Cbl_N, Cbl_N2, SH2, Ring
AP2β1	AP2B1	28	25	28	34	106	Adaptor protein complex subunit	Adaptin_N, Alpha adaptin C2, B2-adapt-app_C
AP2α1	AP2A1	32	25	29	38	105	Adaptor protein complex subunit	Adaptin_N, Alpha adaptin C2, Alpha adaptin_C
c-Cbl	CBL	15	19	17	25	100	E3 ubiquitin ligase	TKB (SH2-like), RING, UBA
Eps15	EPS15	9	13	10	16	99	Adaptor protein	EH, EFh, UIM (multiple)
p85α	PIK3R1	5	5	4	7	84	PI3K regulatory subunit	SH3, RhoGAP, SH2, SH2
p85β	PIK3R2	8	8	10	14	82	PI3K regulatory subunit	SH3, RhoGAP, SH2, SH2
Reps1	REPS1	7	7	7	12	81	Adaptor protein	EH
Stn2	STON2	6	8	7	11	80	Adaptor protein	Adap_comp_sub
Sts-1	UBASH3B	20	16	15	31	73	Atypical tyrosine phosphatase	UBA, SH3, PGAM
Shc-1	SHC1	15	14	13	31	63	Adaptor protein	PTB, SH2
Shc-1	SHC1	16	13	13	31	52	Adaptor protein	PTB, SH2
AP-2μ1	AP2M1	16	13	11	36	49	Adaptor protein complex subunit	Adap_comp_sub
Grb2	GRB2	15	13	15	68	25	Adapter protein	SH3, SH2, SH3
Crk-I	CRK	9	13	9	58	23	Adaptor protein	SH2, SH3

Figure 3.2 Proteomic identification of endogenous Bcr-Abl interactors

(A) Large-scale immunoprecipitation purification of endogenous Bcr-Abl/c-Abl protein complexes were performed in a technical triplicate from $1*10^9$ K562 cells, each, using an anti-Abl antibody (24-21) recognizing the c-terminal F-actin binding domain (FABD) of Bcr-Abl/c-Abl (see B,C) coupled to sepharose beads. Also, 50μg of K562 cell lysate were analyzed by LC-MSMS in a technical duplicate and resulted in the K562 'core proteome' of the 708 most abundant proteins.

(B) Immunoblot analysis of the purification of endogenous Bcr-Abl/c-Abl complexes showing efficient purification of Bcr-Abl/c-Abl and the known Abl interactor Shc1. 100μg of the total cell lysate, equivalent volumes of the flow-through and wash fraction and 5% of the elution fractions were loaded. Of the three technical repeats, one representative immunoblot is shown here.

(C) Of each triplicate immunoprecipitation, elution fractions 2, 3 and 4 were pooled, separated by SDS-PAGE and analysed by mass spectrometry.

(D) Table of the 18 high confidence interactors of Bcr-Abl/c-Abl at 5% false discovery rate identified by mass spectrometry. The table shows the protein name, the Entrez gene name, the number of unique peptides identified by mass spectrometry in three

technical repeats, the average sequence coverage, protein function and the domain composition. Proteins are ranked by molecular weight (kDa) in a decreasing order.

Sts-1 (suppressor of T-cell receptor signaling 1) was initially identified as a JAK2 interactor containing an SH3 domain. Subsequently, Sts-1 was described as a negative regulator of the EGF receptor, ZAP70 and Syk, which can be attributed to the presence of a non-canonical tyrosine phosphatase domain in the C-terminus of the protein (Carpino, Kobayashi et al. 2002; Mikhailik, Ford et al. 2007). Sts-1 is a hitherto not described interactor of Bcr-Abl and may be a novel regulator or antagonist of Bcr-Abl action. In line with our observations, Sts-1 was recently found to co-elute with a similar kinetic than Bcr-Abl in drug binding and competition experiments further corroborating its possible partnership in a protein complex with Bcr-Abl (Bantscheff, Eberhard et al. 2007). Besides these, the remaining interactors within the list of top-18 candidate Bcr-Abl interactors belong mainly to the clathrin-mediated endocytic machinery, including the adaptor protein 2 (AP2) complex subunits AP2α1, AP2β1 and AP2μ1, or are known to be tightly associated with the latter, here represented by the epidermal growth factor receptor substrate 15 (Eps15), Stonin-2 (STN2), BMP-2-inducible protein kinase (BMP2K/BIKE) and RALBP1-associated EPS domain-containing protein (REPS1) (Figure 3.2D) (Pearse, Smith et al. 2000). These AP2 adaptor protein complex components will be described in more detail in section 3.5. In addition to the 18 interactors compatible with stoichiometric interactions (Figure 3.2D), we identified many additional previously characterized Bcr-Abl/c-Abl interacting proteins, such as Abi-1, Abi-2, DNA-PK, WAVE-2, SHP-2 and Crk-L, but with lower peptide counts (Pendergast 2002). As the Abl immunoprecipitation experiment of endogenous complexes did not allow to distinguish between interactors of Bcr-Abl and c-Abl, we engineered K562 cell lines expressing Bcr-Abl and versions of wild-type c-Abl (autoinhibited) and the constitutively active c-Abl PP variant (Barilá and Superti-Furga 1998) fused to a tandem affinity purification (TAP-) tag (Burckstummer, Bennett et al. 2006) and performed duplicate TAP purifications. TAP-tagged Bcr-Abl showed only a very low degree of

overexpression in K562 cells that also decreased rapidly over only a few passages. Nevertheless, TAP purifications with N- and C-terminally tagged Bcr-Abl were performed and despite only a low yield of purified bait protein, the few interactors coincided with proteins identified most significantly in the purifications of endogenous c-Abl/Bcr-Abl, e.g. SHIP-2, Cbl and Grb2 (data not shown). In contrast, both c-Abl and c-Abl PP TAP purifications from K562 cells yielded large amounts of the c-Abl bait protein, but none of the 18 interactors described above. Furthermore, an additional technical triplicate set of large-scale immunoprecipitations of endogenous Bcr-Abl/c-Abl protein complexes was performed using dasatinib-treated K562 cells and the same protocol. Convincingly, the majority of the 18 proteins described above were either completely absent upon dasatinib treatment or retrieved levels (peptide count) were significantly reduced (Figure 3.3).
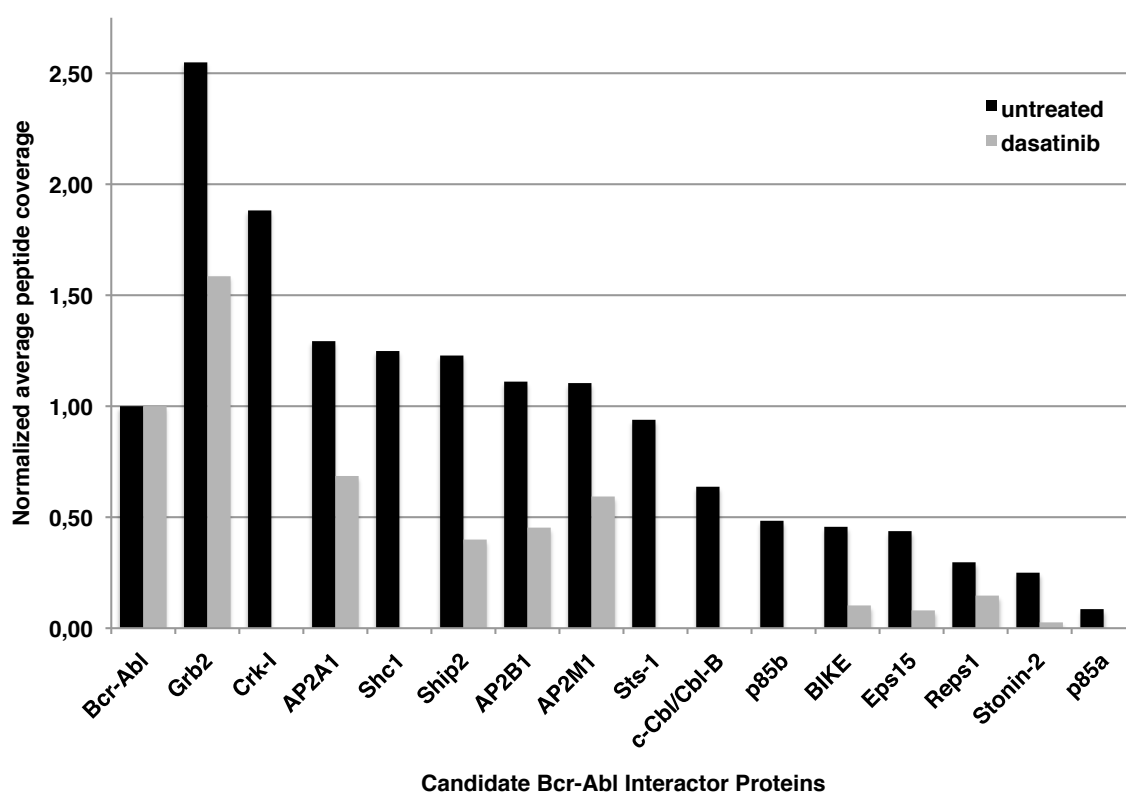
Figure 3.3 All 18 high confidence Bcr-Abl complex member candidates are either absent or present at significantly reduced levels upon dasatinib treatment
Graph displaying the average peptide coverage of the triplicate large-scale Bcr-Abl/c-Abl immunoprecipitations from mock- (black bars) or dasatinib-treated (grey bars) K562

cells for each of the 18 candidate Bcr-Abl interactor proteins. Average peptide count was normalized to the molecular weight of each protein and assuming that 2/3 of all Bcr-Abl/c-Abl peptides identified by LC-MSMS can be attributed to Bcr-Abl. Bcr-Abl is set to 1,00, the other 17 protein are ordered by decreasing normalized average peptide coverage. (AP2A1 = AP2α1, AP2B1 = AP2β1, AP2M1 = AP2μ1, Shc1 = p52Shc1 and p62Shc1, p85a = p85α, p85b = p85β)

This underlines that these interactors are specific for constitutively active Bcr-Abl kinase, that the majority of them might use SH2-phosphotyrosine dependent interaction modes and that they are not interacting with endogenous c-Abl. This strongly argues that the candidate proteins identified in our immunoprecipitation approach are *bona fide* interactors of Bcr-Abl, but not of c-Abl.

3.3 Duplicate tandem affinity purification of 9 candidate interactors yields high co-occurrence and numerous known and novel interacting proteins

We performed medium-scale TAP complex purifications of nine Bcr-Abl interacting proteins from K562 cells with a two-fold aim: (i) to obtain reciprocal confirmatory data on the interaction with Bcr-Abl of the individual proteins and (ii) to perform a topological analysis of the enlarged network obtained from the entire analysis. Of the 18 putative Bcr-Abl complex members, we chose Shc-1, SHIP-2, Crk-I, Grb2, Sts-1 and one member each of the Cbl and p85 families (c-Cbl and p85β, respectively). Of all the proteins thought to be involved in the AP2 adaptor complex (AP2α1, AP2β1, AP2μ1, Eps15, Stn2, Bike, Reps1), we chose to analyze two representative members (Eps15 and AP2μ1) taking amenability and size into account. All nine TAP purifications were performed as biological duplicates, following the same protocol used for the c-Abl and c-Abl PP TAP purifications (see 3.2), and statistically significant interactors were identified using core proteome enrichment (Figure 3.5,Figure 3.6). In all cases the bait protein was identified abundantly in the final TAP eluate by immunoblotting and LC-MSMS analysis (Figure 3.4).
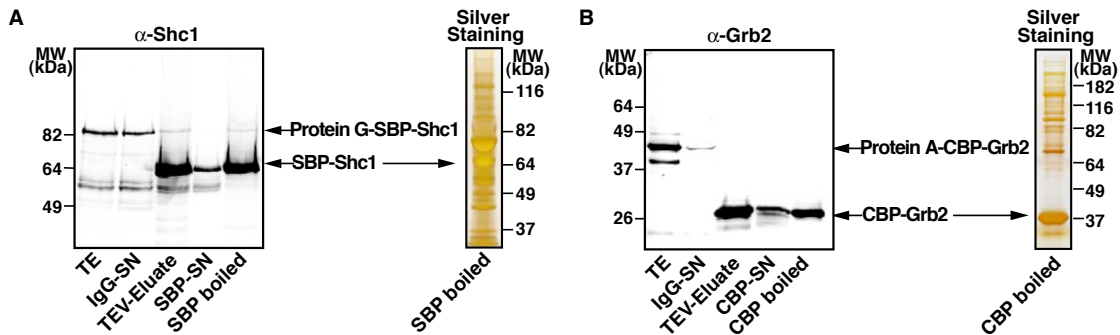
Figure 3.4 Shc1- and Grb2-NTAP tandem affinity purification
Following all TAP purifications, total extract (TE), IgG-beads supernatant (IgG-SN), streptavidin-beads supernatant (SBP-SN) or calmodulin-beads supernatant (CBP-SN) and the boiled beads (SBP/CBP boiled) fractions were analyzed by 1D SDS-PAGE and immunoblotting against the bait protein to monitor protein complex purification yield in each respective TAP purification. The assessment of the TAP purifications Shc1 and Grb2 (A: Shc1-NTAP, B: Grb2-NTAP) are shown here as representative examples. A fraction of each boiled beads sample was separated by 1D-SDS-PAGE and silver stained. Entire gel lanes were sliced into 16 equal pieces, digested with trypsin and analyzed by LC-MSMS.

Rewardingly, with the exception of Eps15 and AP2μ1, all remaining bait proteins (Ship2, c-Cbl, p85β, Sts-1, Shc1, Grb2 and Crk-I) interacted with at least half of the other bait proteins, including Bcr-Abl at a high level of co-occurrence and reproducibility (Figure 3.5). All reverse TAP purifications, except Ship2, Eps15 and AP2*μ*1, recovered Bcr-Abl peptides. For unknown reasons, Ship2 was found to perform poor in TAP as far as reciprocal recovery of the other candidate Bcr-Abl complex members and Bcr-Abl is concerned (Figure 3.5). In the Eps15 and AP2*μ*1 TAP purifications the bait protein and the other partner were identified abundantly. No other core interactor of the postulated Bcr-Abl core complex was identified except for 3 and 5 Crk-I peptides in the Eps15- and AP2*μ*1 TAP purifications, respectively, and 4 peptides Bcr-Abl in the AP2*μ*1 TAP purification. This suggests that Eps15 and AP2*μ*1 are not part of a stoichiometric Bcr-Abl complex but that they may be indirectly associated with Bcr-Abl as members of a distinct more remotely Bcr-Abl associated complex. Overall, the TAP experiments show a high level of reciprocal co-occurrence between Bcr-Abl, c-Cbl, Shc1, Grb2, Crk-I, Ship2 and p85β. In contrast, Sts-1 was only observed in the Crk-I TAP-purification and recovers only two other core complex members (Ship2 and Crk-I) besides Bcr-Abl, when

used as bait. However, in contrast to Eps15, Bcr-Abl peptides are retrieved abundantly. Therefore it can be hypothesized that six proteins are highly interconnected in a Bcr-Abl-centered 'core' protein complex while Sts-1 is either more transiently bound or member of a separate Bcr-Abl protein sub-complex (Figure 3.5). Out of 56 possible pairwise interactions among the seven candidate Bcr-Abl complex members, 30 were experimentally observed, of which 21 were detected in both directions (Figure 3.5).

	Ship2-CTAP	c-Cbl-NTAP	p85β-NTAP	Sts-1-NTAP	Shc1-NTAP	Crk-I-CTAP	Grb2-NTAP	Eps15-NTAP	AP2μ1-NTAP
Ship2	55	18	14	7	27	18	5		
c-Cbl	x	32	17		x	14	7		
p85β	4	20	44		4	43	16		
Sts-1	x			26		11			
Shc1	10	5	11		28	x	6		x
Crk-I	x	9	4	10	5	26	x	3	5
Grb2	x		x		16	12	19		
Eps15						8		50	23
AP2μ1					4	4		19	21
Bcr-Abl	x	11	3	12	5	48	4	x	4

Figure 3.5 High level of reciprocal co-occurrence between seven of the nine TAP baits and Bcr-Abl
Cross-matrix displaying the numbers of unique peptides identified for each protein, identified in each of the nine duplicate TAP purifications. The heat map color-coding shows bait proteins in dark red, proteins reciprocally and bi-directionally identified in red and proteins reciprocally but only uni-directionally identified in light red.

In CML, Bcr-Abl mimics an activated tyrosine kinase signalling setting that physiologically only occurs upon stimulation with a cognate biological trigger. Five of our seven Bcr-Abl core complex candidates, Cbl, Shc, Grb2, p85 and Crk, are known to generally co-occur in activated TK signalling, such as

EGF receptor signalling (Fukazawa, Miyake et al. 1996), and Cbl, Shc, Grb2 and p85 have also been described to co-occur in the same protein complex in activated B-cell receptor signalling (Panchamoorthy, Fukazawa et al. 1996). Besides the Bcr-Abl 'core' complex candidates, we identified numerous additional signalling proteins, including kinases, phosphatases and GTPases (Figure 3.6). In addition to the kinases BMP2K, PKCδ, TTBK2, AAK1 and Btk we identified Csk in three TAP purifications (Cbl, Sts-1 and Shc1 baits). Phosphatases identified include PTPN11, PTPN12, PPP1R9B and PTPRA. In addition to the regulatory PI3-kinase subunits p85α/β we repeatedly identified the catalytic PI3K subunits PIK3CA, PIK3CB, PIK3CD and also PIK3C2B. Additionally, we identified the phosphatidylinositol 4,5-bisphosphate-dependent Arf1GAP DDEF1. Other GTPase activating proteins (GAPs) identified are DNM2 isoforms 1, 2 and 4. We also identified the guanine nucleotide exchange factors (GEFs) Sos1, Sos2 and RapGEF1. Adaptor proteins identified are Gab1, Gab2, Traf2 and NCKIPSD. Besides AP2α1, AP2β1 and AP2μ1, we additionally identified the AP2 adaptor protein complex components AP2α2 and AP2σ1. We also found the Sts-1 homologue Sts-2 (TULA) (Figure 3.6). Overall, each of the nine bait proteins identified a number of known interactors, validating the experimental approach, whereas about 2/3 of all interactors may be considered as novel according to the HPRD or IntAct databases (Figure 3.6). Not unexpectedly, the small SH2/SH3/PTB domain containing adaptor proteins Grb2, Shc-1 and Crk-I displayed most interactors, many of which link to important downstream signaling pathways (Figure 3.6).

Figure 3.6 TAP purifications with nine Bcr-Abl interactors recover the majority of known and numerous novel protein-protein interactions
Schematic representation of the domains and known tyrosine phosphorylation sites of the nine Bcr-Abl interactors that were tagged on their N- or C-terminus and subjected to TAP. Identified interactors are represented as 'star'-diagram with the respective bait protein in the middle. Interactors that had been annotated in HPRD or IntAct are shown as white circles, whereas black circles represent potential novel interactions.

This dataset enriches the still scanty database of human mass spectrometry-analyzed protein-protein interactions and the accumulation of interesting signalling proteins as members of the Bcr-Abl core complex candidates' protein complexes prompted us to further analyze the physical protein-protein interaction network around the Bcr-Abl 'core' complex.

3.4 Bcr-Abl protein network analysis identifies a 4- and 5-core Bcr-Abl 'core' complex

The combination of the datasets from the nine TAP purifications resulted in a single coherent protein-protein interaction network around the nine bait proteins embedding Bcr-Abl in its center. Analysis of the network topology revealed a high level of interconnectivity (Figure 3.7). To monitor the significance and degree of interconnectivity, we considered 'k-cores' in the network (Tong, Drees et al. 2002), which were first used by Christopher Hogue and Charlie Boone. A 'k-core' is a sub-network of proteins (nodes) containing at least k nodes, where each node is linked to at least k other nodes. For example, in a 4-core (i.e. k=4) each node is connected to at least four other members of the protein network constituting the 4-core network. If, according to our hypothesis, the candidate members of endogenous Bcr-Abl 'core' complexes were indeed more intimately associated with Bcr-Abl than any other protein identified in the enlarged TAP protein-protein interaction network, then they should cluster around Bcr-Abl by having many more links amongst each other. Indeed, the eight proteins (nodes) Bcr-Abl, Ship2, c-Cbl, p85α/β, Sts-1, Shc-1, Grb2 and Crk-I form a 4-core. Interestingly, if Sts-1 is excluded, the closer Bcr-Abl interactors form an even more connected 5-core (Figure 3.7,Figure 3.9). To assess the significance of our finding of a 4- and 5-core Bcr-Abl 'core' complex, we performed randomized network simulations. Generating 10^5 different randomized networks resulted only in 2- and 3-cores in approximately equal proportion (Figure 3.8, grey histogram), but no k-cores with k larger than 3. Therefore, the observed 4- and 5-core networks are statistically highly significant ($P<10^{-5}$, Figure 3.8, red and blue line graph). In other words, no 4- and 5-cores were found in 100,000 randomly simulated networks of the size (number of nodes = 91) of our experimentally generated network (Figure 3.7). The two TAP baits of the AP2 adaptor protein complex (Eps15 and AP2μ1) display three (AP2μ1) and only one edge (Eps15) to the members of the 5-core and are therefore positioned more distantly in the network (Figure 3.7,Figure 3.10).

74
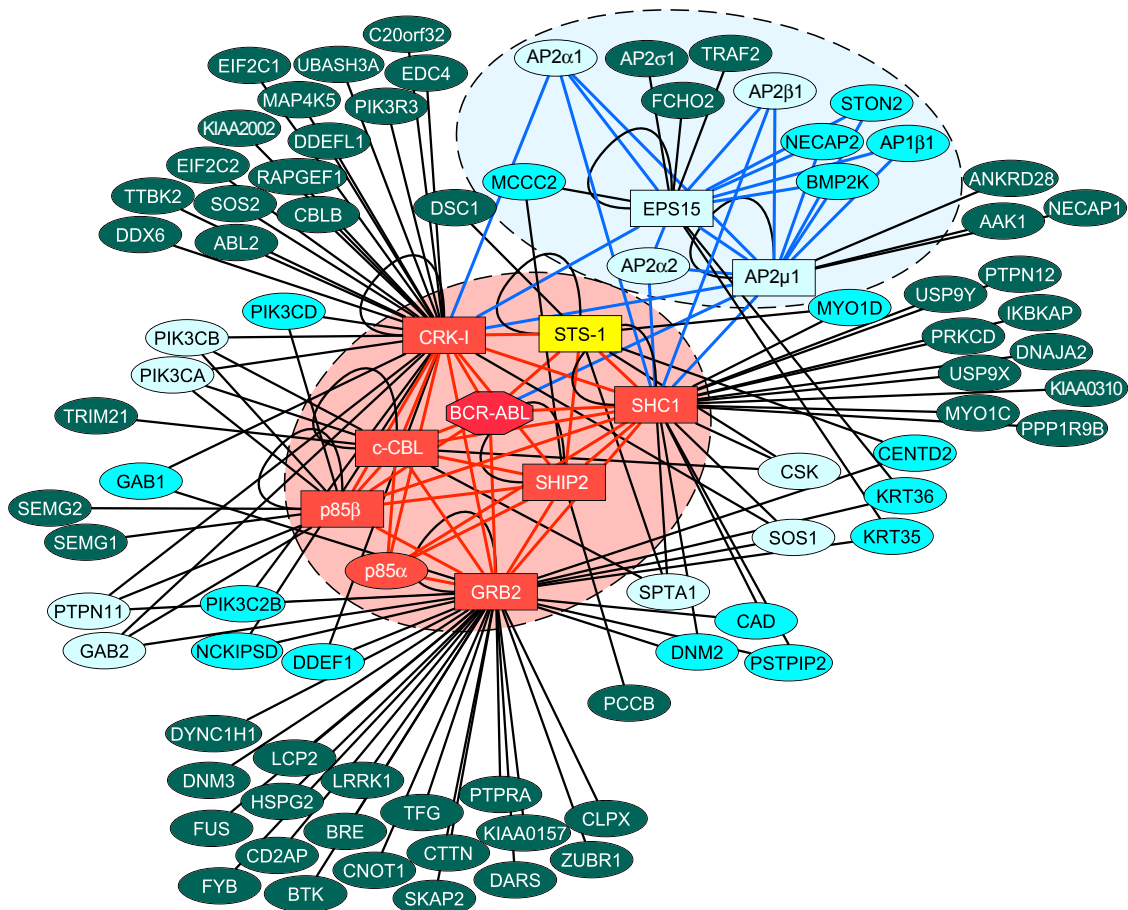
Figure 3.7 The Bcr-Abl protein-protein interaction network
Combination of the nine TAP purification datasets results in a single protein-protein interaction network. The nine TAP bait proteins are shown as rectangles, Bcr-Abl as diamond-shape and all other identified interactors as ellipses. The 4-core Bcr-Abl 'core complex' is highlighted in red, the associated AP2 adaptor complex is highlighted in blue. Interactors with three, two or one edge(s) to the Bcr-Abl core network are shown in light blue, turquoise and dark green, respectively. Sts-1 is shown in yellow, as its removal from the 4-core Bcr-Abl 'core complex' results in a 5-core complex. The figure was created using Cytoscape.

To limit the possible bias introduced by the *a priori* selection of the nine bait proteins, where a protein that was not initially selected as Bcr-Abl interactor could have a reduced connectivity with the complex around Bcr-Abl, we represent the TAP-MS results as an undirected graph, meaning that the edges between the nodes in the network do not contain directionality information on the interactions. Therefore, a link created from a bait protein is also valid starting from its prey (Figure 3.7).
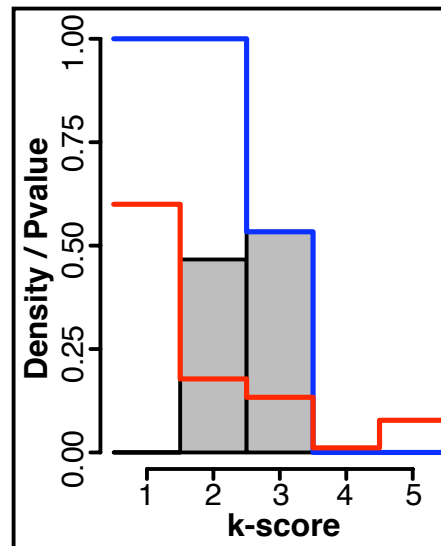
Figure 3.8 Randomized network simulations yield only 2- or 3-cores.
The grey histogram shows the proportion (density) of random networks that contain a k-core with highest possible k. The blue line graph shows the P-value of a k-core deduced from the histogram. The red line graph represents the proportion (density) of proteins in the network that are found in a k-core with highest possible k for k=1,2,3,4,5. Therefore, the experimentally observed 4-core and 5-core networks are statistically highly significant.

Clearly, Bcr-Abl is most intimately interconnected with Ship2, c-Cbl, p85α/β, Shc1, Sts-1, Grb2 and Crk-I, that we define as the eight member Bcr-Abl 'core' complex (Gavin, Aloy et al. 2006). From all that is known about the biology of p85α and p85β, it is unlikely that both p85 isoforms may have a different binding mode nor be present simultaneously in the Bcr-Abl core complex (Geering, Cutillas et al. 2007; Zhao and Vogt 2008). Therefore, both isoforms are treated equally throughout this thesis. The network analysis also revealed some proteins interacting with three different Bcr-Abl core interactors, each (Figure 3.7, light blue nodes). These included Spectrin-α, two of the catalytic subunits of PI3K (p110α and p110β), the SH2-domain containing tyrosine phosphatase Shp-2, the tyrosine kinase Csk, the Grb2 adaptor binding protein Gab2 and the guanine nucleotide exchange factor Sos1. Many of these proteins are proto-oncogenes and have been described to form critical links to downstream signaling pathways (p110α/β for the PI3K/Akt pathway, Sos1, Gab2 and SHP-2 for the Ras/MAPK pathway) and were shown to be necessary for Bcr-Abl dependent transformation, e.g. SHP-2 and Gab2 (Chen, Yu et al. 2007), (Sattler, Mohi et al. 2002).
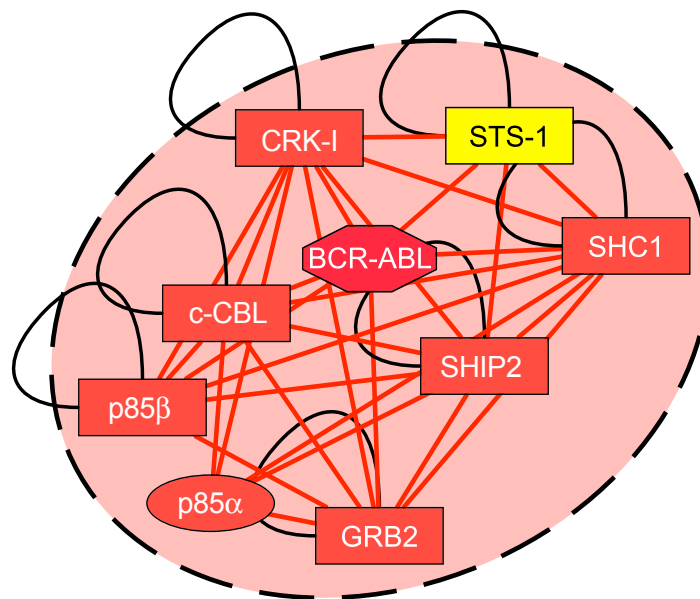
Figure 3.9 The Bcr-Abl multi-protein complex is a '4-core' complex
A representation of the Bcr-Abl protein interaction network in the absence of interactors with less than four edges to other nodes (k ≥ 4), highlighting the 4-core Bcr-Abl 'core complex'.

3.5 Identification of a 3-core AP2 adaptor protein complex associated with the Bcr-Abl 'core' complex

Interestingly, the network analysis of the TAP dataset showed that Eps15 and AP2μ1 are part of an 11 member 2-core complex (AP2α1, AP2α2, AP2β1, AP2μ1, AP1β1, Bike, Eps15, NECAP2, Stn-2) that included Shc-1 and Crk-I (Figure 3.7, blue halo). Within this complex, AP2μ1, Eps15, AP2α1, AP2α2 and AP2β1 even form a 3-core complex, again including Shc-1 and Crk-I. Only AP2μ1 is directly linked to Bcr-Abl (Figure 3.10). However, as Crk-I has three edges to AP2α1, Eps15 and AP2μ1 and Shc1 has four edges to AP2α1, AP2α2, AP2β1 and AP2μ1, these can clearly be considered as the interface of the Bcr-Abl 'core' complex to the AP2 adaptor protein complex. Eps15 is an interactor of AP2 subunit AP2α1 (Benmerah, Gagnon et al. 1995; Benmerah, Lamaze et al. 1998). Stn-2 (Stonin-2), but not Stn-1, was shown to be associated with Eps15 via an NPF signature in its proline rich domain and the EH-domain (Eps15-homology domain) of Eps15 (Martina, Bonangelino et al. 2001). This evidence was additionally confirmed by the recent description of the

structure of the Eps15-Stonin-2 complex confirming this interaction mode between the endocytic sorting adaptor Stonin-2 and the clathrin accessory protein Eps15 (Rumpf, Simon et al. 2008). Reps1 has been shown to form complexes with the SH3 domains of c-Crk and Grb2, which may link Reps1 to AP2 containing endocytic protein complexes in receptor tyrosine kinase trafficking (Yamaguchi, Urano et al. 1997). Eps15 also binds c-Crk in an SH3-domain dependent manner (Schumacher, Knudsen et al. 1995), just as REPS1, underlining our finding that the AP2 adaptor protein complex is linked to the Bcr-Abl 'core' complex via Crk-I and Shc1.
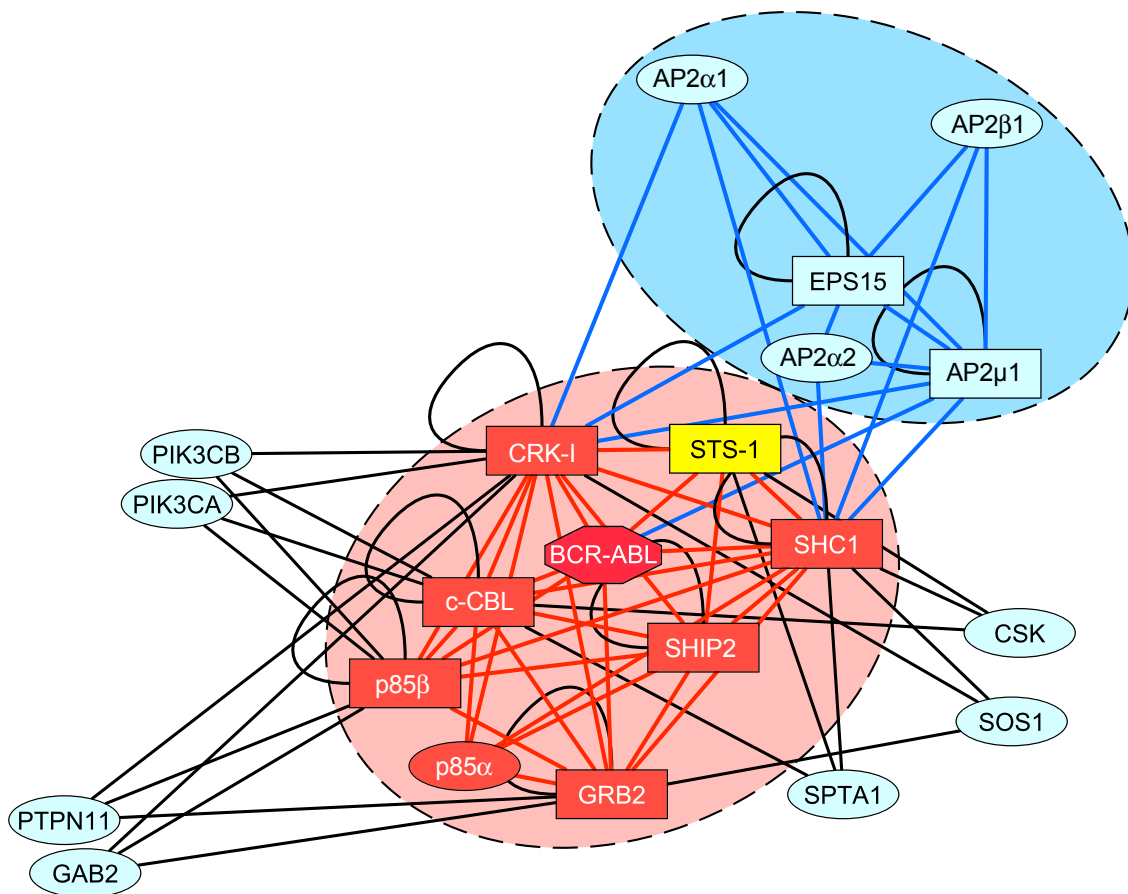
Figure 3.10 The Bcr-Abl 'core' complex complex is linked to the AP2 adaptor protein complex
A representation of the Bcr-Abl protein-protein interaction network in the absence of interactors with less than three edges to other nodes (k ≥ 3), highlighting the associated 3-core AP2-adaptor protein complex.

This raised the possibility that AP2 adaptor complex mediated intracellular trafficking is functionally linked to the Bcr-Abl complex in analogy to the function of the AP2 adaptor complex in receptor tyrosine kinase trafficking via clathrin-coated pits (Beattie, Howe et al. 2000). Interestingly, the small adaptor protein Grb2, which is also part of the Bcr-Abl 'core' complex, has been shown to be involved in this process (Johannessen, Pedersen et al. 2006).

3.6 Quantitative characterization of the Bcr-Abl 'core' complex

All modern systems-biological approaches require quantitative information in addition to physical and functional descriptions (Ong and Mann 2005; Papin, Hunter et al. 2005) and the tools for the comprehensive identification and relative quantification of the cellular abundance of entire proteomes have already been established (Cox and Mann 2008; de Godoy, Olsen et al. 2008). Both the semi-quantitative analysis of the endogenous Bcr-Abl interactors by mass spectrometry (section 3.2), as well as the ensuing network analysis (section 3.4) are compatible with the existence of an eight protein Bcr-Abl 'core' complex, making the effort worthwhile to determine the absolute cellular protein copy numbers as well as the interaction stoichiometry of the proteins involved in the Bcr-Abl 'core' complex.

3.6.1 Cellular protein copy number quantification of the Bcr-Abl 'core' complex components

First, we expressed and purified one recombinant protein of each of the Bcr-Abl core complex members containing the epitopes for the respective antibodies (Figure 3.11). We used dilutions of these recombinant 'epitope standards' and compared them to four dilutions of K562 total cell lysate (50, 100, 150 and 200µg total protein) by semi-quantitative immunoblotting (see Materials and Methods). Knowing the precise cell count, volume and protein concentration of the cell lysate, this enabled us to infer the apparent absolute protein copy number per K562 cell of Bcr-Abl and the seven core interactors (Figure 3.12).
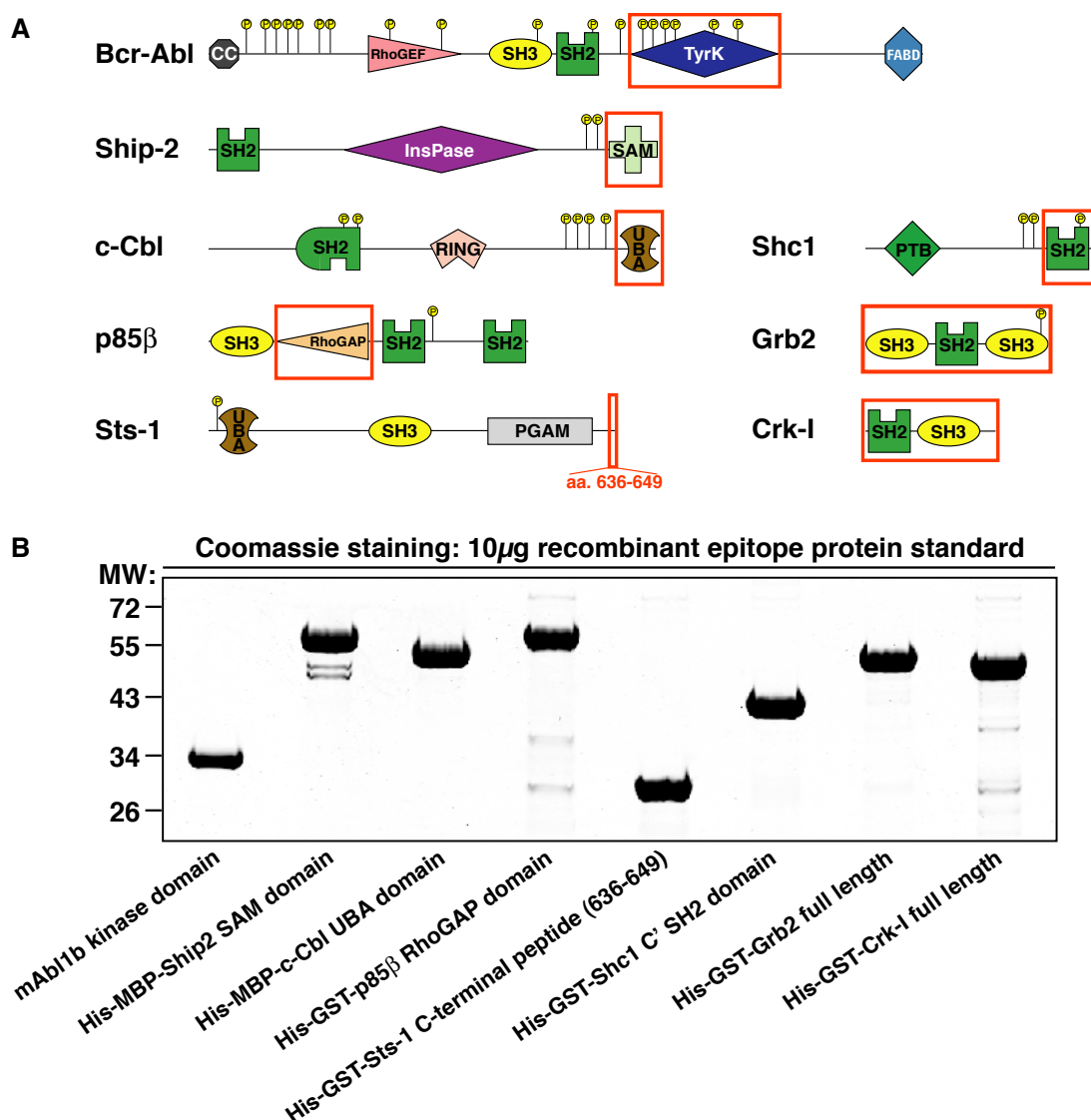
Figure 3.11 Recombinant epitope protein standards
(A) Schematic representation of recombinant protein standards corresponding to the epitopes of the antibodies used to detect Bcr-Abl and the seven core interactors. The position of the recombinant epitope standard with respect to the full-length protein is highlighted (red box).
(B) Recombinant epitope standards were expressed as GST- or MBP-fusion proteins and purified to homogeneity. 10µg of each purified recombinant protein were resolved by SDS-PAGE and stained with coomassie to confirm protein size, purity and protein concentration.

All eight proteins, except for Crk-I, are expressed within one order of magnitude of each other. Bcr-Abl is present at about 300,000 copies per cell. This number was generated using recombinant Abl kinase domain (Abl KD) as 'epitope standard'. Quantification of total cellular protein copy numbers of Bcr-Abl using recombinant FABD as 'epitope standard' led to a lower number of

about 200,000 copies Bcr-Abl per K562 cell. However, given the possibility that Bcr-Abl may degrade from its C-terminal end in the total K562 cell lysates used for the absolute quantification, thereby losing the epitope for the 24-21 antibody, we focused on quantifications using Abl KD as 'epitope standard' in order to exclude this potential error source. Interestingly, c-Abl was found to be expressed at about equal protein copy numbers as Bcr-Abl (data not shown). p85β, Sts-1 and Grb2 had similar expression levels at approximately 200,000 copies per cell. Ship2 (~500,000), c-Cbl and Shc1 (~350,000) were found to be most abundant among the Bcr-Abl core members (Figure 3.12). These measurements were performed at least as technical triplicates and at an overall average error of 30% standard deviation (% STDEV) (Figure 3.12). Determination of the copy number of the adaptor protein Crk-I was hampered by unsolvable ambiguity problems mainly with Crk-II, but also with CrkL, at the mass spectrometry and antibody level, so that the derived copy number of approximately 25,000 should be considered with caution, particularly as it is poorly compatible with the proposed Bcr-Abl stoichiometry (seeFigure 3.3). Assuming that all seven proteins interact with Bcr-Abl at stoichiometric levels, each K562 cell potentially contains a theoretical number of about 200,000 to 300,000 Bcr-Abl protein complexes.
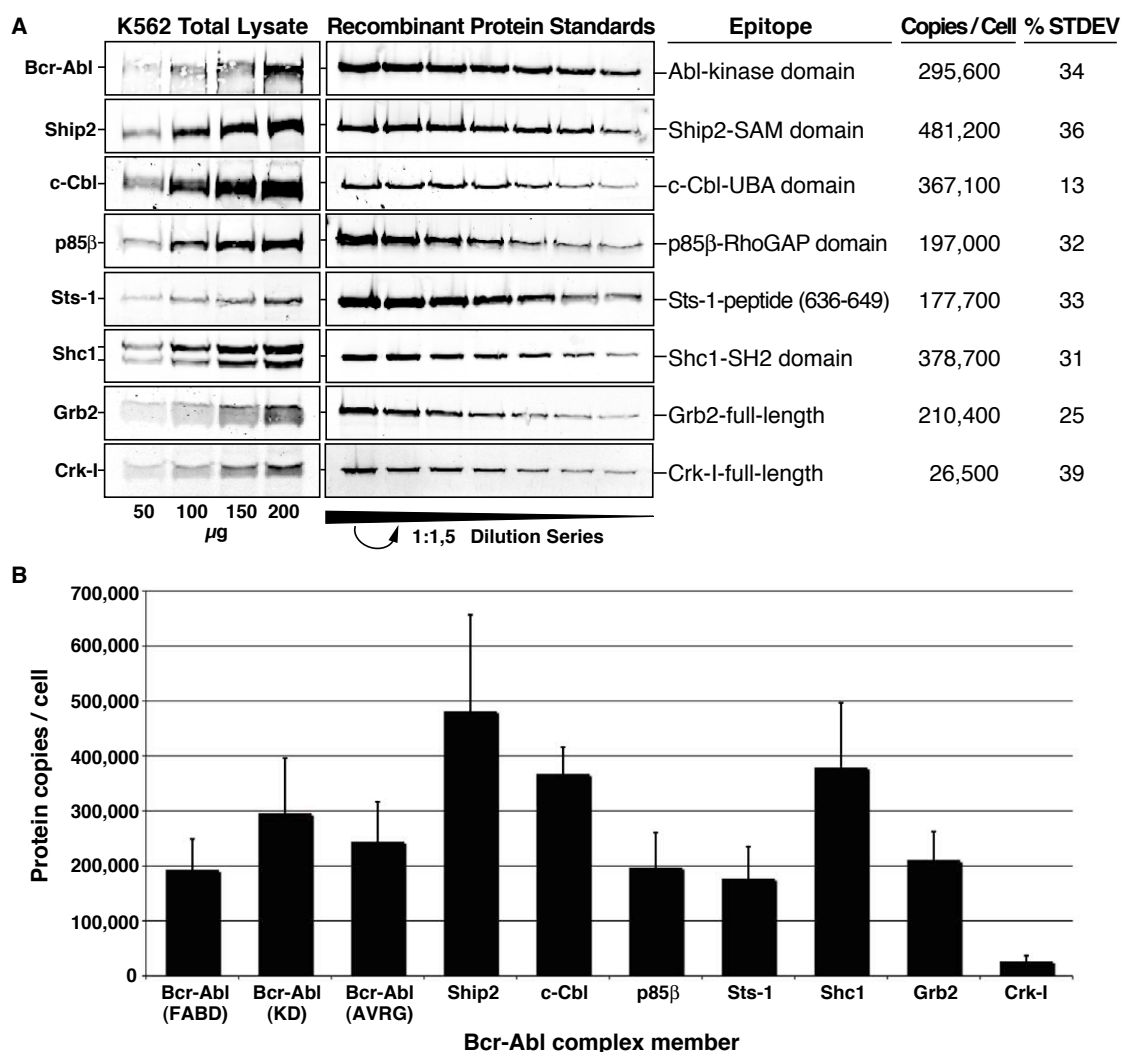
Figure 3.12 Absolute quantification of total cellular protein copy numbers
(A) Serial dilutions of K562 total cell lysate were analyzed next to serial dilutions of the indicated recombinant epitope standard by immunoblot against Bcr-Abl and the seven core complex members. The protein copy number per K562 cell was calculated by determining the molarity of the respective protein in the extract using the epitope standard dilution series to obtain a partial regression line and the concentration and total cell number of protein extract used. The average copy number per cell was obtained from at least three independent experiments.
(B) Bar graph displaying the total cellular protein copy number of Bcr-Abl and the seven Bcr-Abl complex comonents. Error bars show the standard deviation, which was derived from at least three technical repeats.

This, however, would imply the unlikely scenario that all protein copies of the seven interactors are complexed with Bcr-Abl and that no 'free' copies remain available in the K562 cell for participation in other protein complexes and signal transduction pathways. Furthermore, we observed that, albeit surprising, the interaction stoichiometry for the majority of the interactors is

rather sub-stoichiometric and that, indeed, only proportions of a maximum of 30% of the total cellular copies of the Bcr-Abl interacting proteins are associated with Bcr-Abl upon co-immunoprecipitation (see section 3.6.2,Figure 3.13). Therefore, lower actual interaction stoichiometries should be taken into account and the absolute protein copy numbers should be treated with caution.

3.6.2 Quantification of the Bcr-Abl 'core' complex interaction stoichiometry and cellular Bcr-Abl – associated proportions of each protein

Following the quantification of the total protein copy numbers per K562 cell we quantified the amount of copies of each Bcr-Abl core interactor co-immunoprecipitating with Bcr-Abl and the interaction stoichiometry between Bcr-Abl and its 'core' complex interactors. From a single medium-scale Bcr-Abl/c-Abl immunoprecipitation we quantified the absolute copies of Bcr-Abl and the co-immunoprecipitated Bcr-Abl interactors using the recombinant 'epitope standards' (Figure 3.13A). We were able to derive the Bcr-Abl 'core' complex interaction stoichiometry by calculating the ratio of copies of each core complex member over Bcr-Abl copies (Figure 3.13A,B). The molarity of immunoprecipitated Bcr-Abl was quantified using recombinant Abl KD as 'epitope standard'. To our surprise, only Ship2 had a stoichiometry around 1 (1.3) with Bcr-Abl. Sts-1, Shc1 and Grb2 were found with a lower stoichiometry of around 0.5 (0.4, 0.4 and 0.3, respectively) (Figure 3.13B). The sub-stoichiometric ratios obtained for p85β (0.04) and Crk-I (0.01) are clearly in contradiction with our 'semi-quantitative' evidence for stoichiometric interaction of these two proteins with Bcr-Abl by mass spectrometry (peptide coverage) (Figure 3.2, Figure 3.3). As already suggested for the low absolute cellular copy number of the Crk-I protein, also in this case detection ambiguity issues with the Crk-I antibody are likely to influence the result.

We furthermore determined, which fraction of total cellular protein of each core complex member was sequestered into Bcr-Abl complexes as compared to how much was associated with different complexes that do not contain Bcr-Abl. Therefore, we quantified the input- and supernatant bands for each core interactor in order to monitor the depletion (equals Bcr-Abl association) of each from the cell lysate following c-Abl/Bcr-Abl-immunoprecipitation (Figure 3.13A). We calculated the fraction of Bcr-Abl associated core interactor (%) by subtracting the band intensity of the supernatant-sample from the band intensity of the input-sample and subsequently deduced the proportion of "Bcr-Abl associated" protein (Figure 3.13A,C). Bcr-Abl was depleted by about 83%. While ~40% of total Ship2 and 30% of Sts-1 were found to be Bcr-Abl-associated, ~20% c-Cbl and Shc1 and ~10% of cellular p85β and Grb2 were Bcr-Abl associated. In contrast again, very little of the total Crk-I protein seemed to be bound in Bcr-Abl complexes. Protein co-depletion upon Bcr-Abl immunoprecipitation is supposed to be in correlation with the total cellular copy numbers and the interaction stoichiometry within the complex. We found this correlation by large confirmed upon comparison of our stoichiometry and 'Bcr-Abl-association' data (Figure 3.12,Figure 3.13).

					Epitope	Quantification			
Bcr-Abl					Abl-kinase domain	1.00	-	83	5
Ship2					Ship2-SAM domain	1.30	0.64	41	4
c-Cbl					c-Cbl-UBAdomain	0.13	0.04	16	4
p85β					p85β-RhoGAP domain	0.04	0.02	10	10
Sts-1					Sts-1-peptide (636-649)	0.36	0.20	27	3
Shc1					Shc1-SH2 domain	0.37	0.20	18	6
Grb2					Grb2-full-length	0.29	0.06	11	5
Crk-I					Crk-I-full-length	0.01	0.01	1	0
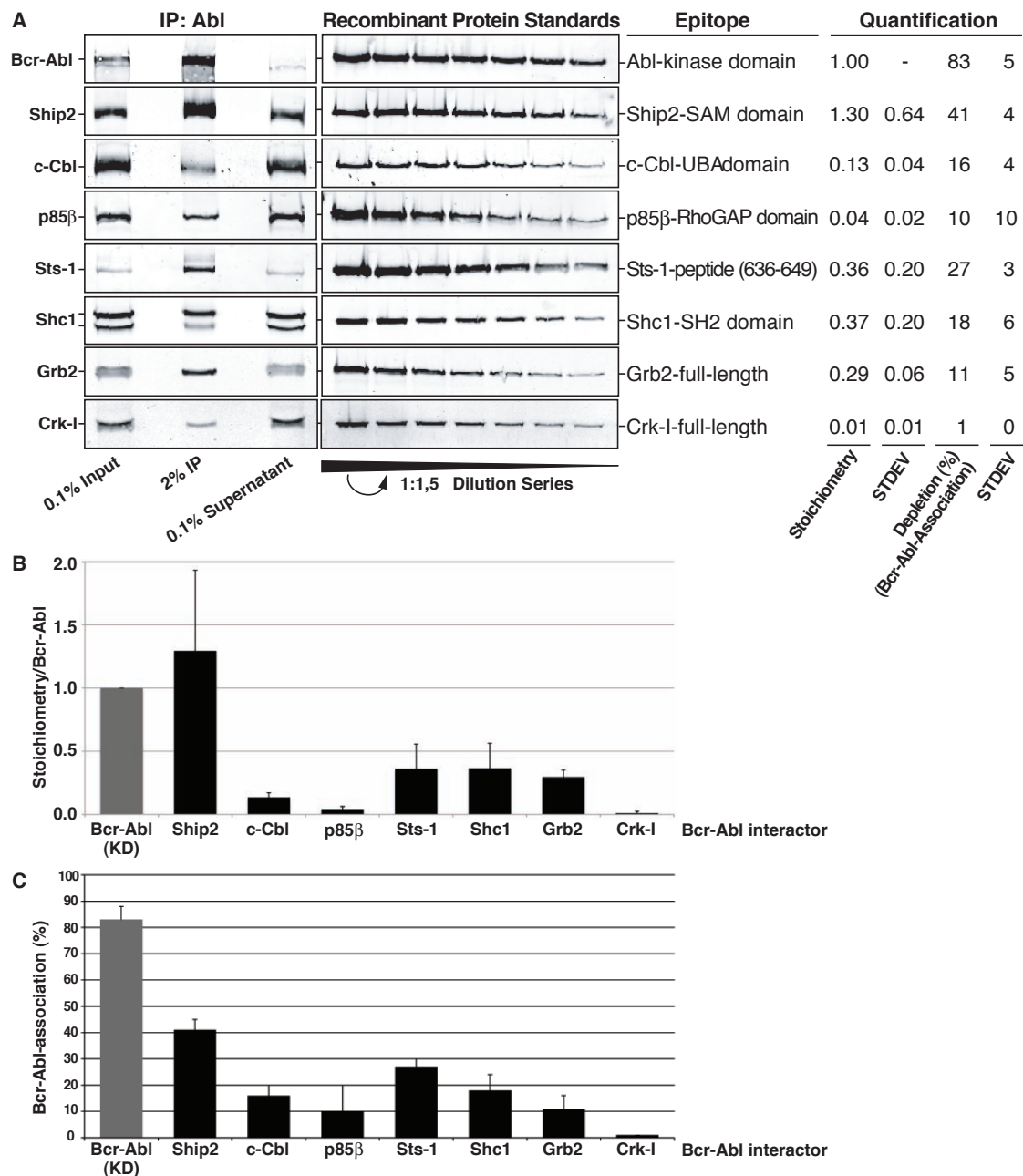
Figure 3.13 Absolute quantification of the Bcr-Abl 'core' complex stoichiometry and cellular Bcr-Abl-association

(A) Input, immunoprecipitation and supernatant fractions of one Abl-immunoprecipitation were analyzed next to serial dilutions of the indicated recombinant epitope standard by immunoblot against Bcr-Abl and the seven core complex members.

(B) The interaction stoichiometry of the complex was calculated by determining the molarity of the respective protein in the immunoprecipitate using the epitope standard dilution series to obtain a partial regression line and by calculating the ratios over Bcr-Abl. The average stoichiometry and standard deviation was obtained from at least three independent experiments.

(C) Bcr-Abl associated versus 'free' protein fractions were determined by quantification of the input and supernatant bands and calculation of the respective protein's depletion (%).

Ship2 is expressed at about two-fold the number of Bcr-Abl protein copies and was found at highest stoichiometry of about 1:1 with Bcr-Abl. Accordingly, about 50% of total Ship2 protein were depleted. Similarly, we found roughly twice as much c-Cbl protein depleted (20%) as compared to p85β (10%). This is in line with the about three-fold higher stoichiometry measure of c-Cbl (0.13) than that of p85β (0.04) and roughly twice as much c-Cbl copies expressed (370,000) compared to p85β (200,000). Strikingly, also the measurements for Sts-1 and Shc1 nicely correlate. Both were found at the same stoichiometry (0.4). With twice as much Shc1 copies (400,000) expressed compared to Sts-1 (200,000), accordingly much less total Shc1 is depleted from the lysate. Both p85β and Grb2 are present at about 200,000 copies per cell. According to their stoichiometries, depletion upon Bcr-Abl immunoprecipitation does not correlate. Shc1 and c-Cbl are both present at about 370,000 copies per cell. Despite of the higher stoichiometry of Shc1, however, about equal levels of c-Cbl and Shc1 were found depleted. Overall however, proteins with the highest stoichiometries, Ship2, Sts-1 and Shc1 show the highest degree of Bcr-Abl association in this depletion measurement (Figure 3.12,Figure 3.13).

Overall, taking these results into account, the initially deduced stoichiometric interaction of all seven proteins with Bcr-Abl has to be treated with caution, because the semi-quantitative measures peptide count and sequence coverage might have been biased by the fact that not all peptides in a protein have equal chances to be detected by the mass spectrometer due to their different physico-chemical properties. Accepting lower stoichiometries for the 'core' interactors in light of the observed total cellular protein copy numbers would consequently match the observed proportions of Bcr-Abl-associated versus 'free' proteins. This would imply an overall lower number of Bcr-Abl 'core' complexes containing all seven interactors and also suggest the possibility of the existence of various Bcr-Abl sub-'core'-complexes that contain only some of the 'core' interactors at a time and are not obvious from the network analysis (see Discussion, section 4.6, Figure 4.3, Figure 3.7,Figure 3.9).

3.7 Biophysical characterization of the Bcr-Abl 'core' complex

Assuming a stoichiometric interaction of 1:1 of all seven 'core' complex components with tetrameric Bcr-Abl we postulated a macromolecular Bcr-Abl molecular machine of about 3MDa (mega-dalton). In order to confirm this concept, we set out to determine the overall size of the complex by glycerol density gradient centrifugation and gel-filtration chromatography in mock- and tyrosine kinase inhibitor (TKI) - treated K562 cells. According to our preliminary evidence, TKI action inhibits Bcr-Abl and, as a consequence, also abrogates binding of the interactors significantly (Figure 3.3).

3.7.1 Purification of the *Saccharomyces cerevisiae* Pwp2 high molecular weight pre-ribosomal complex as a size standard

In order to adjust the gradient conditions to the postulated MDa size-range, we chose to purify a stable and abundant high molecular weight complex from *Saccharomyces cerevisiae (S. cerevisiae)*. Under the courtesy of Anne-Claude Gavin at the EMBL, Heidelberg, we purified high molecular weight *S. cerevisiae* pre-ribosomal protein complexes to 40S ribosome subunits by 1-step TAP using Pwp2 as bait (from here on referred to as 'Pwp2 complex') (Figure 3.14A) (Grandi, Rybin et al. 2002). The bait protein Pwp2 was recovered abundantly alongside with its stoichiometric interactors (Figure 3.14A,B).
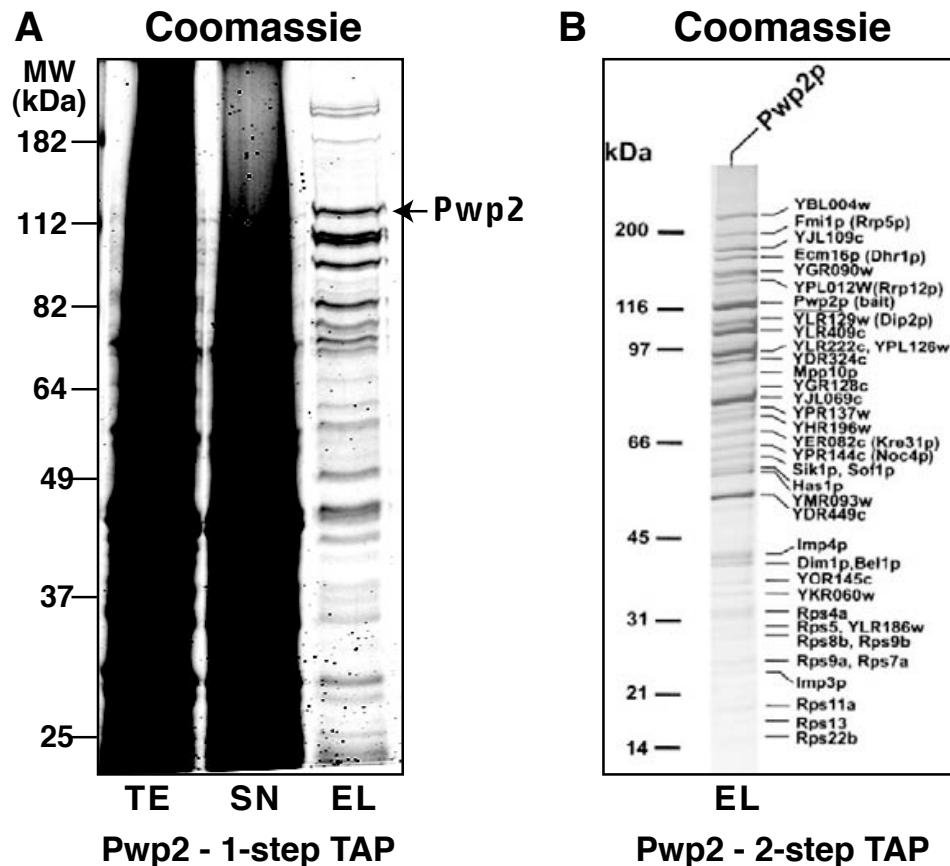
Figure 3.14 One-step TAP of the *Saccharomyces cerevisiae* Pwp2 complex
(A) Pwp2 complexes were purified from eight litres yeast culture by one-step TAP. 5µl of input material, equal volume of IgG-supernatant and 20µl of TEV-eluted Pwp2 complex were separated by 10% SDS-PAGE and visualized by coomassie staining.
(B) Pwp2 complexes purified by two-step TAP. Protein complexes were eluted from calmodulin beads using EGTA and visualized on a 4%-12% gradient gel by coomassie staining. Proteins annotated on the right were identified by mass spectrometry (MALDI-TOF) (Figure (B) taken from (Grandi, Rybin et al. 2002)).

This protein complex has been described in detail by density gradient centrifugation and gel-filtration chromatography before and features the inherent advantage that it has about 4-6MDa size and also contains a highly stable 600kDa sub-complex (Grandi, Rybin et al. 2002). As tetrameric Bcr-Abl without protein interactors has a molecular weight of about 840kDa and, within our postulated 'core' complex, around 3MDa, the Pwp2 complexes were chosen to adjust the gradients for this size-range.

3.7.2 'Sizing' the Bcr-Abl 'core' complex by density gradient centrifugation

Our aim was to identify Bcr-Abl in high-molecular weight fractions of 20-80% glycerol density gradients corresponding to about 3MDa size together with all of the seven 'core' complex interactors, as well as to, eventually, identify smaller sub-complexes. 20-80% glycerol density gradients were able to resolve the 600kDa Pwp2 sub-complex (fraction 4, Figure 3.15A) from the high-molecular weight (4-6MDa) Pwp2 complexes (fractions 7-9, Figure 3.15A). We then analyzed mock- and dasatinib-treated K562 cell lysate by density gradient centrifugation on 20-80% glycerol, following the same conditions. Interestingly, following immunoblot analysis for Bcr-Abl, c-Abl and its 'core' interactors Ship2, c-Cbl, Sts-1, Shc1 and Grb2, we found the strongest signal for Bcr-Abl starting from fraction 5. Stable Pwp2 600kDa complexes were observed at fraction 4. Therefore Bcr-Abl appearing primarily in fractions 5, 6 and 7 was in line with its primary presence as a tetramer of about 840kDa size (Figure 3.15B,C), however without protein interactors bound. c-Abl, however, which lacks the N-terminal coiled-coil domain responsible for tetramerization of Bcr-Abl, was shifted left-wards relative to Bcr-Abl and was detectable already in fraction 2, while it was basically absent in fractions 6 and 7. Overall, the majority of the Bcr-Abl ineractors migrated in the early fractions 1-5, corresponding to their lower molecular weight (Grb2 peak in fraction 1). Interestingly, however, Bcr-Abl and Ship2 were both prominently detectable in fractions 7-9, corresponding to higher molecular weight complexes (Figure 3.15B), as 4-6MDa Pwp2 complexes were found in fractions 7-9, too (Figure 3.15A). The other interactors were also detectable in these fractions, albeit much more faintly. This profile surprisingly mirrors the interaction stoichiometry observed from the Bcr-Abl co-immunoprecipitation, where Ship2 showed the highest interaction stoichiometry as compared to the other proteins.
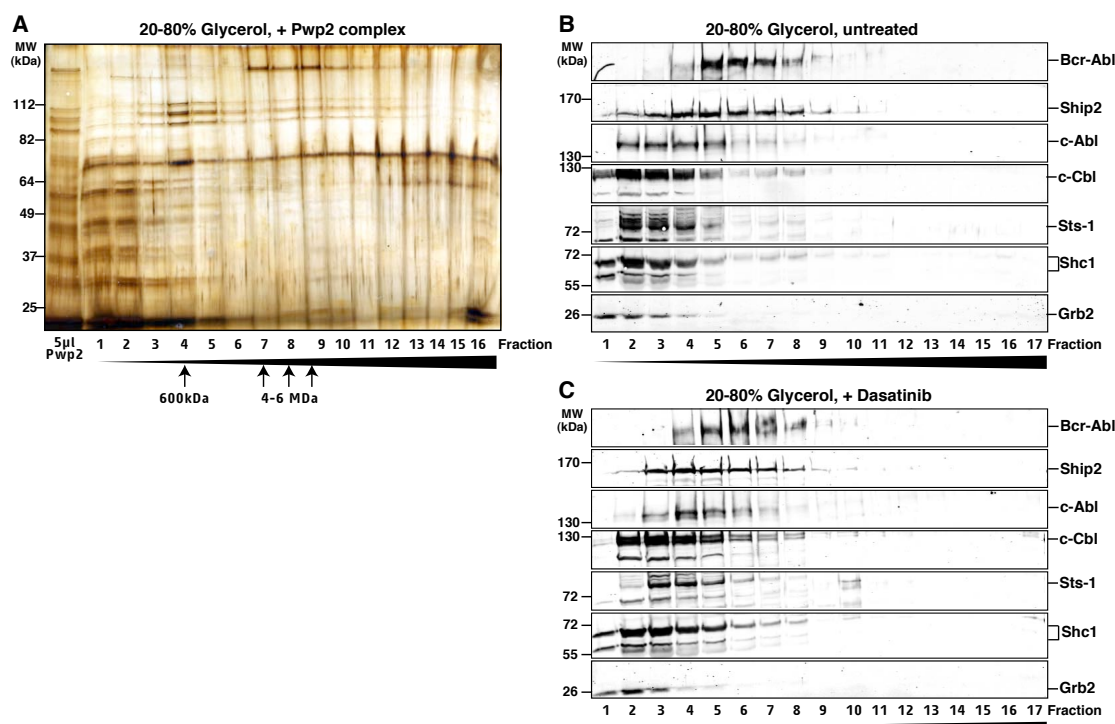
Figure 3.15 Glycerol density gradient centrifugation of the *S. cerevisiae* Pwp2 complex and mock- and dasatinib-treated K562 total cell lysate

50μl of purified *S.cerevisiae* Pwp2 complex (A) and 3mg mock- (B) and dasatinib-treated (C) K562 cell lysate were separated on 2ml 20-80% glycerol density gradients at 54,000rpm for seven hours. Fractions à 125μl were collected with a pipette from top to bottom.

(A) 50μl of each fraction were separated on a 10% SDS-gel and Pwp2 complexes were visualized by silver-staining.

(B,C) 50μl of each fraction were separated on a 6% and 10% gel and Bcr-Abl and candidate 'core' interactors were analyzed by immunoblotting.

However, we were not able to observe a clear left-shift of Bcr-Abl and its interactors towards lower molecular weight upon treatment with dasatinib (Figure 3.15C). Differences observed between the two samples were too subtle to explain the disruption of a MDa protein complex and most likely resulted from variation in the gradient or fraction harvesting. It is possible, that the high-molecular weight complexes did not resist the long high-speed centrifugation procedure and that the picture above reflects a mixture of monomeric protein components and a variety of subcomplexes between Bcr-Abl and its interactors as well as between the interactors themselves, not involving Bcr-Abl.

3.7.3 Bcr-Abl 'core' complex members are found in MDa high molecular weight fractions together with Bcr-Abl only in the absence of tyrosine kinase inhibitors

Given the possibility that the high molecular-weight Bcr-Abl 'core' complexes are destroyed during long-term high-speed density gradient centrifugation (see 3.7.2), we applied 500μl of mock- and dasatinib-treated K562 cell lysate at equal protein concentration on a FPLC Superose 6 gel-filtration column. Before, we calibrated the column using molecular weight standard proteins and analyzed fractions within a range of 10kDa and several MDa molecular weight, in order to capture proteins starting from the smallest Bcr-Abl 'core' complex component Crk-I up to MDa multi-protein complexes around Bcr-Abl. In this experiment we included CrkL as a control, a well-known Bcr-Abl interactor that was not found significantly involved within the Bcr-Abl multi-protein complex in our TAP-LC-MSMS network analysis. The major proportion of the proteins were found distributed in low molecular weight fractions with a peak corresponding to their respective molecular weigth, which resulted in a right-shifted diagonale pattern with decreasing size of the monomeric proteins (Figure 3.16). However, comparing the two FPLC runs performed either with untreated or dasatinib-treated K562 cell lysate directly next to each other revealed that Bcr-Abl and a proportion of its 'core' interactors are found together in high molecular weight fractions compatible with a MDa multi-protein complex only in the untreated sample. CrkL, on the other hand, is completely absent from these fractions and only found in fractions D1-D3 (Figure 3.16).
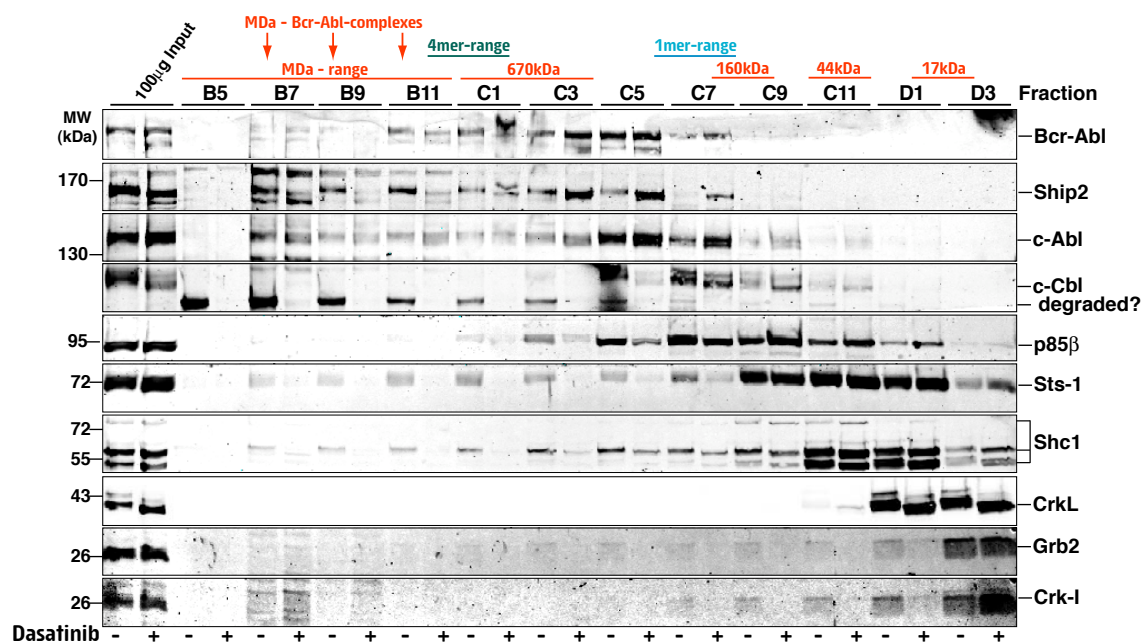
Figure 3.16 Superose 6 gel-filtration analysis of mock- and dasatinib-treated K562 total cell lysate
500µl of mock- and dasatinib-treated K562 total cell lysate were applied on a FPLC Superose 6 gel-filtration column. Fractions were analyzed by SDS-PAGE and immunoblotting. The Superose 6 column was calibrated with gel-filtration standard proteins of 600, 158, 44 and 17kDa molecular weight.

In the dasatinib-treated samples, proteins shift right towards low-molecular weight fractions according to their molecular weight. In the untreated sample, however, the small proteins Grb2 and Crk-I, but not Crk-L can faintly but clearly be seen up to higher molecular weight fractions (fraction C1) (Figure 3.16). Ship2, p85β and Shc1 are clearly co-eluting with Bcr-Abl within the MDa-range (fractions B7-C1) in the untreated but not in the treated sample. c-Cbl also shows this pattern, however down-shifted between fractions B5 and C5 probably due to degradation, so that this effect has to be treated with caution (Figure 3.16). A slight down-shift can be observed for Ship2 upon treatment, which is in line with its loss of tyrosine phosphorylation. Strikingly, however, residual levels of Ship2 protein were found at high molecular weight fractions even in the treated samples, which would be in line with residual SH3-domain mediated interaction of Ship2 with Bcr-Abl after treatment with tyrosine kinase inhibitors (Figure 3.16 fractions B7-C1, Figure 3.3). Unfortunately, detection of Bcr-Abl was difficult given the dilution of the material upon gel-filtration and did

not allow to nicely visualize a shift towards lower molecular weight upon dasatinib-treatment. However, the shift becomes obvious, when Bcr-Abl levels are compared between fractions B11 to C5, where monomeric Bcr-Abl is present at equal amounts. Increased levels of Bcr-Abl are present in the untreated sample in fractions B9 and B11. c-Abl, which also appears to be present in higher molecular weight complexes, does not show the dasatinib-dependent pattern described for Bcr-Abl and its interactors, and serves as a control (Figure 3.16). Similar results could also be obtained upon nilotinib-treatment, whereas the differences were less pronounced (data not shown). As this analysis is based on total cell lysate, however, and as dasatinib and nilotinib both inhibit the major driver of tyrosine-phosphorylation in K562 cells (Bcr-Abl), treatment might consequently have affected tyrosine phosphorylation - dependent interactions of many other protein complexes involving these proteins, besides Bcr-Abl 'core' complexes.

3.8 siRNA perturbation of Bcr-Abl 'core' interactors neither affects K562 cell proliferation nor other known signal transduction markers

In order to assess the functional relevance of the identified Bcr-Abl interactors, we performed siRNA knockdown experiments of the 7 core complex components including Bcr-Abl/c-Abl itself and reduced the levels of the target proteins by at least 75% for all core interactors (Figure 3.17A, data kindly provided by Agnes Gstöttenbauer and Ines Kaupe). However, the knockdowns of the individual core interactors did not have an effect on Bcr-Abl autophosphorylation levels (Figure 3.17B) or K562 proliferation rate or viability (data not shown). Furthermore, none of the known signal transduction markers, such as phospho-Stat5 (Harir, Pecquet et al. 2007) or phospho-Akt (Steelman, Pohnert et al. 2004; Yang, Cron et al. 2002, Chu, 2007 #1233), showed conclusive changes in immunoblot analysis of K562 siRNA-knock-down samples (data not shown).
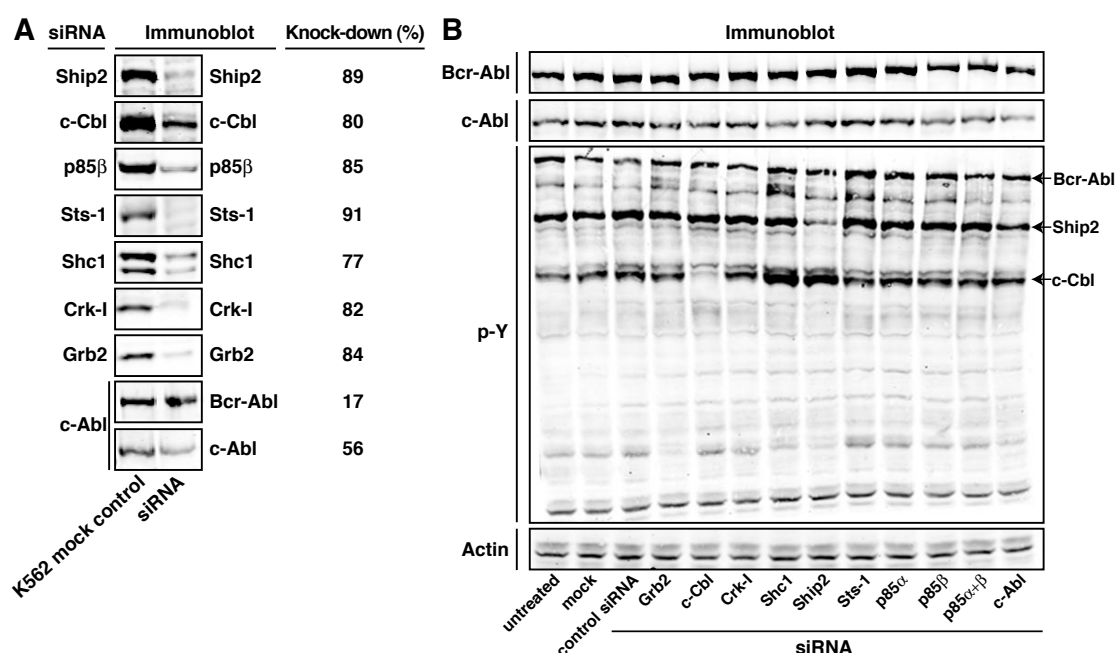
Figure 3.17 siRNA perturbation of seven Bcr-Abl 'core' complex members
(A) K562 cells were transiently transfected with Smartpool™ siRNAs targeting c-Abl, Ship2, c-Cbl, p85α, p85β, Sts-1, Shc1, Grb2 and Crk-I or a control siRNA and retransfected after 24h. 72 h after the first transfection 100µg of total cell lysate was analyzed by quantitative immunoblotting for assessment of protein knockdown efficiency.
(B) K562 cell lysates from wildtype, mock-, control- siRNA and Smartpool™ siRNA-transfected cells were analyzed by immunoblotting for total Bcr-Abl, c-Abl, total p-Y and Actin protein levels. Actin served as control for uniform sample loading.

Even multiple attempts knocking down pairwise combinations of interactors or all seven interactors at a time did not affect K562 viability. In contrast, K562 cells rapidly stopped proliferating and underwent apoptosis when Bcr-Abl protein levels were reduced using an Abl or Bcr-Abl breakpoint-specific siRNA (Figure 3.17A and data not shown). This may be in line with the severe addiction of K562 cells to their oncogene Bcr-Abl that may be able to override many different, even severe perturbations in its downstream signal transduction network and may uncover unexpected redundancy in signalling pathways exerting Bcr-Abl's oncogenicity.

3.9 Tyrosine kinase inhibitors disrupt and remodel the Bcr-Abl 'core' complex

The tyrosine kinase inhibitors nilotinib and dasatinib are very potent inhibitors of Bcr-Abl and successfully used to treat CML patients (Quintas-Cardama, Kantarjian et al. 2007). Dasatinib has a markedly broader specificity compared to the highly selective nilotinib (Hantschel, Rix et al. 2008), (Rix, Hantschel et al. 2007). In order to monitor the impact of these tyrosine kinase inhibitors on the integrity and composition of the Bcr-Abl complex, we treated K562 cells with dasatinib and nilotinib for 3 hours at concentrations approximately 10 times higher than their respective IC_{50} values for Bcr-Abl. Under these conditions, no Bcr-Abl autophosphorylation or tyrosine phosphorylation of other proteins in K562 cell lysates was detectable by immunoblotting, suggesting effective suppression of Bcr-Abl kinase activity and Bcr-Abl dependent signal transduction (data not shown). In contrast, cell viability, total cell numbers and protein content was not decreased after 3 hours of inhibitor treatment when compared to mock-treated control cells (data not shown). We immunoprecipitated Bcr-Abl complexes from mock- and drug-treated cells and analyzed the samples by immunoblotting against the Bcr-Abl interactors (Figure 3.18A). In addition, we performed relative quantification by mass spectrometry using iTRAQ labelling (Ross, Huang et al. 2004) in cooperation with the lab of Karl Mechtler at the IMP in Vienna. The outline of the iTRAQ workflow is shown in Figure 3.18C. While Bcr-Abl immunoprecipitated with equal efficiency from mock-, dasatinib- and nilotinib-treated K562 cells, a strong decrease in the interaction of all seven 'core' interactors was observed in the presence of the drugs (Figure 3.18A). Interaction of Bcr-Abl with c-Cbl, Sts-1, Shc1 and Crk-I were undetectable upon drug treatment, whereas residual binding of Ship2, p85β and Grb2 to Bcr-Abl could be detected in the presence of both drugs (Figure 3.18A). In line with these results, interaction of all seven 'core' members with Bcr-Abl was significantly reduced by dasatinib using relative iTRAQ quantification by mass spectrometry (Figure 3.18B). In another iTRAQ experiment we compared mock- and nilotinib-treated samples. Here, Crk-I, Sts-1 and Shc-1 showed reduced binding to Bcr-Abl (Figure 3.18B).

Interestingly, Crk-I, Sts-1 and Shc-1, which were undetectable in Abl immunoprecpitates from drug-treated cells, also showed the strongest reduction in binding to Bcr-Abl (>5-fold) in both quantitative mass spectrometry experiments (Figure 3.18A,B). Notably, Ship2 showed the mildest reduction (2.5-fold) in binding by dasatinib in the mass spectrometry experiment. In line with this, residual interaction with Bcr-Abl could be detected by immunoblotting (Figure 3.18A,B).
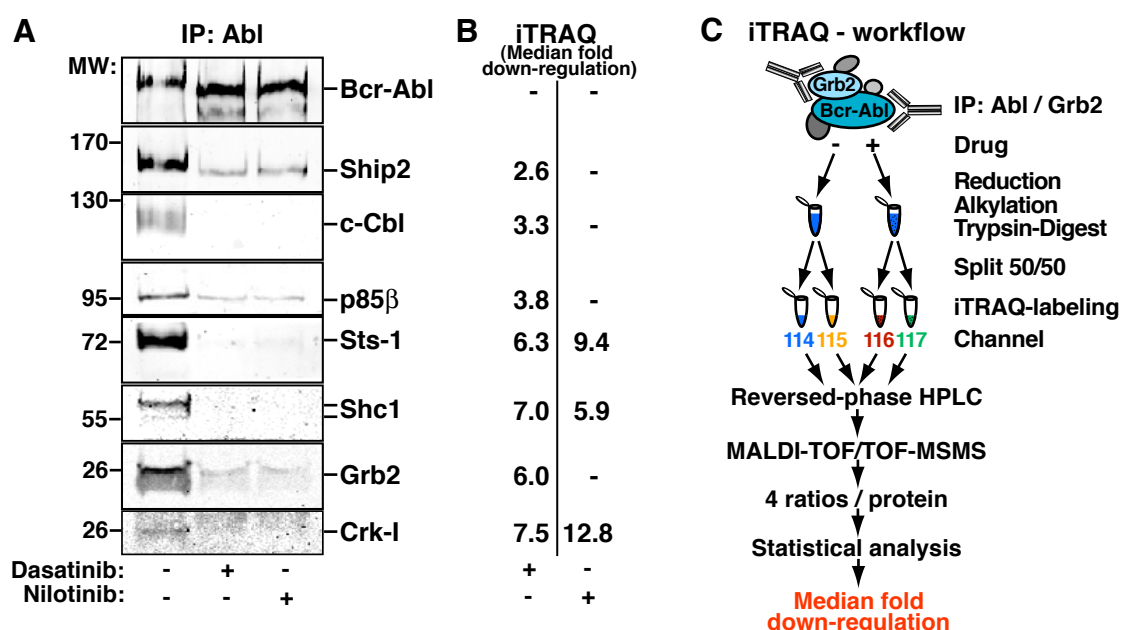
Figure 3.18 Nilotinib and dasatinib disrupt and remodel the Bcr-Abl 'core' complex
(A) Bcr-Abl protein complexes were immunoprecipitated from mock-, dasatinib- and nilotinib-treated K562 cells and immunoblotted against Bcr-Abl and the seven core interactors.
(B) Quantitative mass spectrometry analysis using iTRAQ labelling comparing dasatinib- versus mock-treated and nilotinib- versus mock-treated Bcr-Abl immunoprecipitates. Numbers indicate the medians of the four fold down-regulation ratios.
(C) Workflow outlining the iTRAQ labelling strategy employed for this study. Bcr-Abl or Grb2 protein complexes were immunoprecipitated and eluted with HCl. Eluates were reduced, alkylated, digested with trypsin, split in half and labelled with two different isobaric tags, each.

In order to analyze changes in protein complex composition of a specific Bcr-Abl interactor, we immunoprecipitated Grb2 (Figure 3.18C), probed for Bcr-Abl and the selected core interactors and performed relative quantification using iTRAQ in the presence and absence of nilotinib. Reduced

binding of Bcr-Abl, Ship2 and Shc-1 to Grb-2 was detected by iTRAQ and immunoblotting (Figure 3.19A,B).
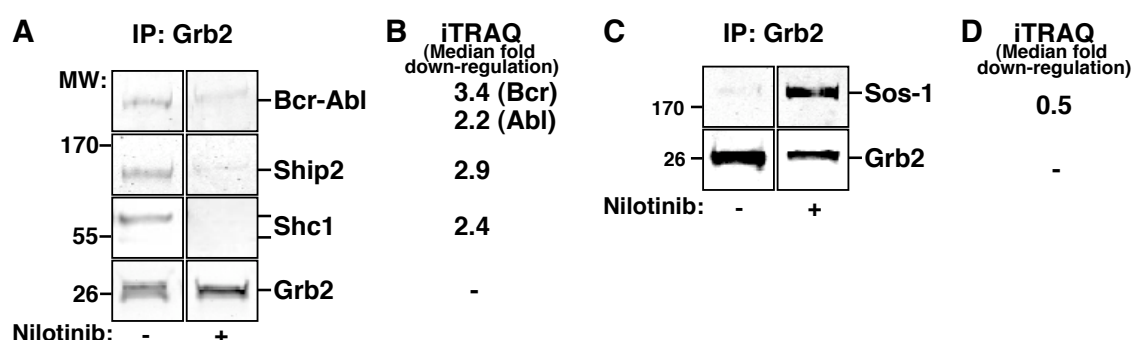
Figure 3.19 Nilotinib disrupts and remodels the Bcr-Abl - Grb2 protein complex (A,C). Grb2 protein complexes were immunoprecipitated from mock- and nilotinib-treated K562 cells and immunoblotted against Grb2, Bcr-Abl, SHIP2, Shc-1 and Sos1. (B,D). Quantitative mass spectrometry analysis using iTRAQ labelling comparing nilotinib- versus mock-treated Grb2 immunoprecipitates. Each of the two conditions was labeled with two different isobaric tags.

Interestingly, we detected an increase in binding of Sos1 to Grb-2 by both iTRAQ (0.5-fold) and immunoblotting (Figure 3.19C,D). Altogether, this shows that the entire Bcr-Abl complex is severely affected by the drug treatment, but at the same time that individual interactions are affected differentially, so that one can still detect a post-drug protein complex. In order to confirm that the Bcr-Abl 'core' complex *per se* is the target of tyrosine kinase inhibitors such as dasatinib and nilotinib, we immobilized dasatinib on sepharose beads with the help of Uwe Rix in the lab, and used the drug beads as an affinity reagent for a pull-down experiment from untreated with K562 cells or the Bcr-Abl negative lymphoblast cell line U937 (Hantschel, Rix et al. 2007), (Rix, Hantschel et al. 2007) (samples provided by Tilmann Bürckstümmer and Oliver Hantschel). Bound proteins were analyzed by immunoblotting for Bcr-Abl, Ship2, Sts-1, Shc1 and Grb2 (Figure 3.20). From K562 cells, Bcr-Abl and four core interactors could be identified by immunoblotting, whereas none of the core interactors were identified from U937 cells (Figure 3.20).

Pull-down: Dasatinib
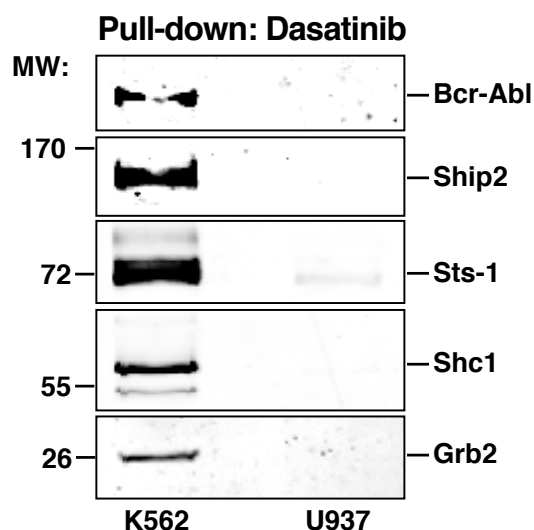
Figure 3.20 The Bcr-Abl 'core' complex is the target of tyrosine kinase inhibitors
Immobilized dasatinib was incubated with K562 or U937 total cell extracts and bound proteins eluted by boiling in SDS sample buffer. The eluates were immunoblotted for Bcr-Abl, Ship2, Sts-1, Shc1 and Grb2.

This may indicate that the core interactors may be precipitated along with Bcr-Abl and not with another dasatinib target common between K562 and U937 cells.

The increased Sos-1 association with Grb2 upon drug treatment was furthermore confirmed by analysis of the same samples by 1D-shotgun LC-MSMS (data not shown). This result motivated the large-scale immunoprecipitation of the remaining six Bcr-Abl interactors Ship2, c-Cbl, p85β, Sts-1, Shc1 and Crk-I from mock- and nilotinib-treated K562 cells (Figure 3.21) with a two-fold aim; (i) to reciprocally confirm the disruption and remodelling of the Bcr-Abl 'core' complex by nilotinib action following 1D-shotgun LC-MSMS analysis of all remaining 12 samples and (ii) to seek for more effects such as the increased Grb2-Sos-1 interaction, observed upon immunoprecipitation of Grb2 (Figure 3.19A-D).
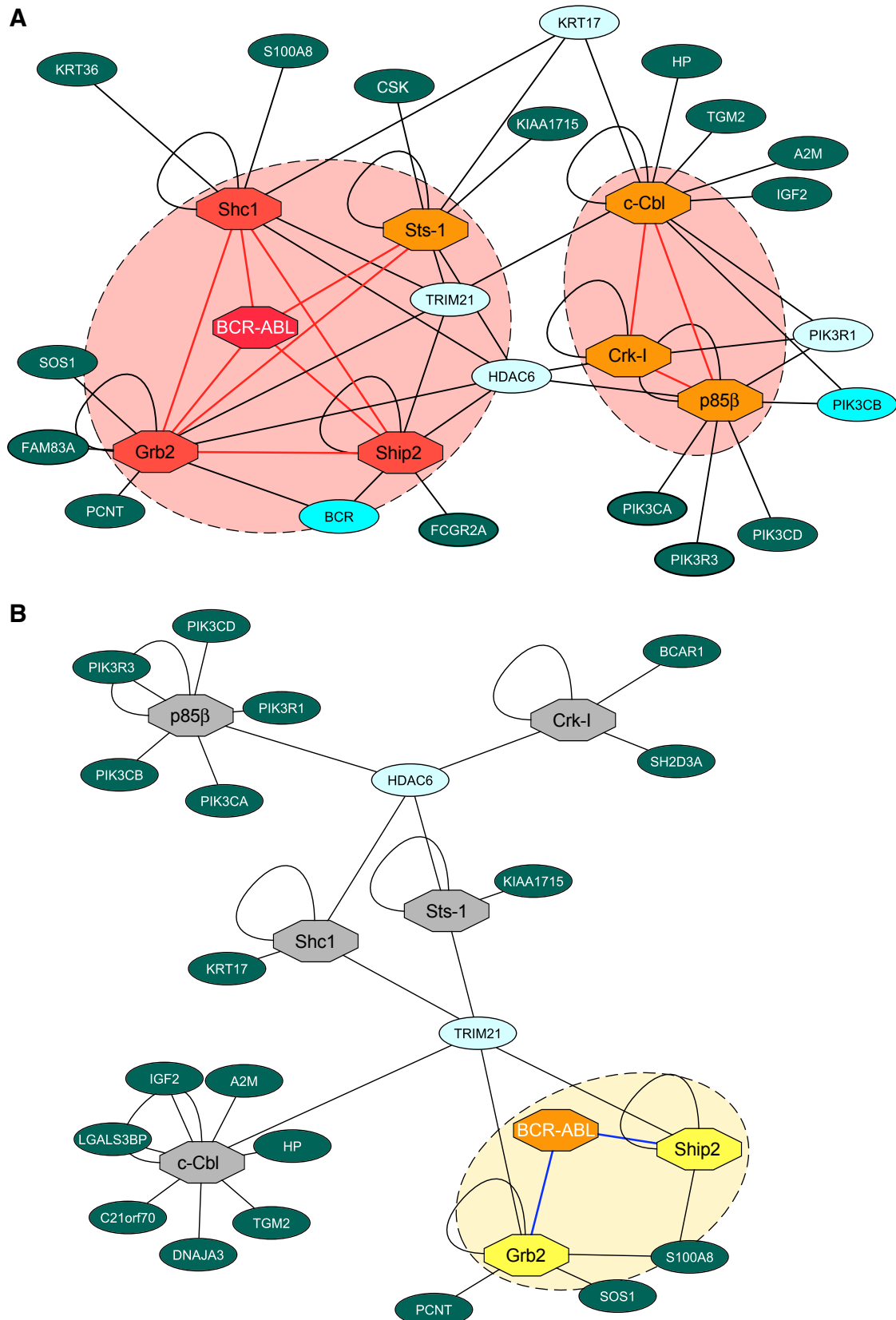
Figure 3.21 Disruption of the Bcr-Abl 'core' complex network is confirmed by reciprocal immunoprecipitation in the presence of the tyrosine kinase inhibitor nilotinib

Protein complexes of Bcr-Abl and each of its seven 'core' complex members were purified from mock- (A) and nilotinib-treated (B) K562 cells by large-scale immunoprecipitations using antibodies coupled to sepharose beads.
(A,B) Bound proteins were identified by 1D-shotgun LC-MSMS analysis and statistically analyzed as describe before. The eight proteins used as bait in the large-scale immunoprecipitations are shown as diamond-shapes and all identified interactors as ellipses. In (A and B), complexed Bcr-Abl 'core' complex members are highlighted by red and yellow halos. Baits with three or more edges are shown in red, bait proteins with two or one edge amongst each other are shown in orange. Interactors with three, two or one edge(s) to the Bcr-Abl 'core' complex components are shown in light blue, turquoise and dark green, respectively. The figures were generated using Cytoscape and modified using Illustrator.

Large-scale immunoprecipitation of Bcr-Abl and all of its seven 'core' interactors from untreated K562 cells followed by 1D-shotgun mass spectrometry and network analysis confirms, that the core interactors are strongly inter-connected amongst each other and that Grb2, Ship2, Shc1 and Sts-1 cluster around Bcr-Abl (Figure 3.21A, large red halo). As observed before, amongst these, Sts-1 has a lower degree of connections to Bcr-Abl, here only two edges to Bcr-Abl and Grb2, while Bcr-Abl, Grb2, Ship2 and Shc1 form a 3-core (Figure 3.21A, large red halo). c-Cbl, Crk-I and p85β are connected amongst each other, however, edges to Bcr-Abl as well as Grb2, Ship2 and Shc1 were not observed (Figure 3.21A, small red halo). This shows that the gel-based large-scale immunoprecipitation/TAP approach to protein complex and signalling network mapping was superior to this medium-scale immunoprecipitation 1D-shotgun-MSMS approach. Many proteins (nodes) and protein-protein connections (edges) observed in the Bcr-Abl large-scale immunoprecipitation experiments as well as in the TAP network are missing from this analysis, which might be a consequence of the reduced amounts of starting material in these reciprocal immunoprecipitations as well as a shortcoming of gel-free 1D-shotgun-MSMS detection (Figure 3.7). Many proteins identified in these experiments, but not in the initial TAP experiments, however, might be proteins brought down by the individual antibodies unspecifically.

Despite of these technical differences, however, large-scale immunoprecipitation of Bcr-Abl and its seven interactors from nilotinib-treated K562 cells independently confirm that the Bcr-Abl 'core' complex is profoundly

disrupted and remodelled by the action of tyrosine kinase inhibitors. c-Cbl, p85β, Sts-1, Shc1 and Crk-I lose their edges to Bcr-Abl and amongst each other, while Bcr-Abl, Ship2 and Grb2 remain associated in the 'post-drug' complex. This is in line with the observed residual interaction of Ship2 and Grb2 with Bcr-Abl upon dasatinib and nilotinib treatment observed by immunoblotting and iTRAQ analysis before (Figure 3.18).

Overall, these experiments suggest the conclusion that Bcr-Abl tyrosine kinase inhibitors are targeting the Bcr-Abl 'core' complex leading to its re-modeling rather than 'just' binding to the Bcr-Abl kinase domain.

DISCUSSION

4 DISCUSSION

4.1 General conclusions

In order to study the composition of endogenous Bcr-Abl protein complexes we have performed two independent, but connected lines of experiments that lead to the characterization of what we would like to call the Bcr-Abl 'core' complex in CML cells. In order to start out with the identification of the native endogenous Bcr-Abl complex we precisely mapped the epitope of the 24-21 Abl antibody within the C-terminal FABD of Bcr-Abl/c-Abl to exclude disturbance of protein interactor binding by the antibody, prepared an antibody resin and performed a comprehensive triplicate set of large-scale IPs (Figure 3.1,Figure 3.2). In parallel we constructed cell lines expressing wildtype Abl and the activated form Abl PP and performed duplicate TAP purifications with each in order to profile endogenous interactors of c-Abl (167 proteins) (Figure 4.1). In addition, profiling of crude K562 cell lysate for the most abundant proteins in K562 cells (K562 'core proteome', 708 proteins) allowed us to determine significant interactors out of the 427 proteins identified in the large-scale IPs (Figure 4.1). Statistical analysis of these data-sets lead to a concise list of 18 candidate interactor proteins for which the semi-quantitative parameter 'sequence coverage' by mass spectrometry was compatible with their association being stoichiometric in nature (Figure 3.2, Figure 3.3 black bars, Figure 4.1). While the identity of the individual components is statistically certain (high peptide counts, three experimental repeats), the stoichiometry itself is less certain, because of the fact that not all peptides in a protein have equal chances to be detected by the mass spectrometer due to their different physico-chemical properties. Therefore, we determined the protein interaction network of nine of the candidates (excluding Bcr-Abl as bait) using a TAP-LC-MSMS approach to enable a statistical analysis of the resulting protein network topology (Figure 3.7, Figure 4.1) and found eight proteins (Ship2, c-Cbl, p85, Sts-1, Shc1, Grb2, Crk-I and Bcr-Abl) significantly clustering around Bcr-Abl in a highly inter-connected sub-network (Figures 3.7, 3.8 and 3.9).
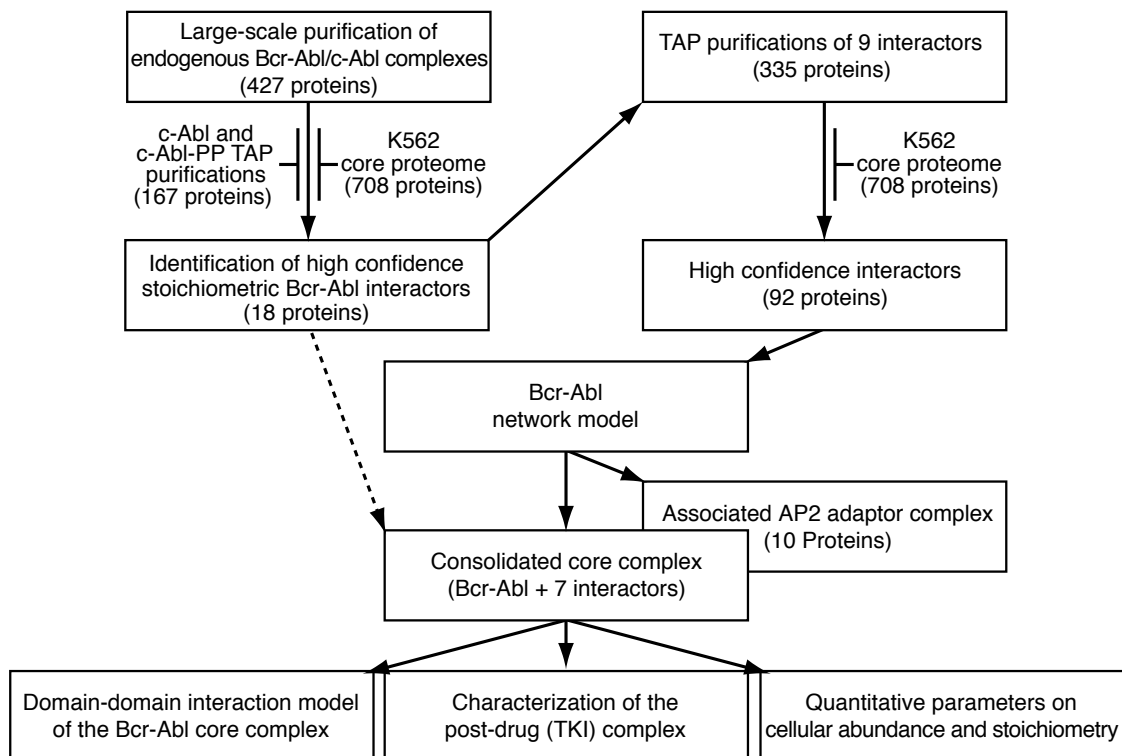
Figure 4.1 Workflow diagram and key findings of the presented study
The dataset of the purification of endogenous Bcr-Abl/c-Abl complexes from K562 cells and the K562 'core proteome' identified 18 candidate interactors compatible with high stoichiometric interactions. TAP purifications of c-Abl and nine selected interactor candidates were performed and ensuing network analysis suggested a highly interconnected Bcr-Abl core complex (sub-network). Quantification of total cellular copy numbers and quantitative analysis of the Bcr-Abl core complex composition in the presence of tyrosine kinase inhibitors was performed. A domain-domain interaction model of the Bcr-Abl core complex was built.

TAP and other two-step affinity purification strategies have proven a robust technology for the characterization of protein complexes (Gavin, Bosche et al. 2002; Gavin and Superti-Furga 2003; Rigaut, Shevchenko et al. 1999) and are known to reliably identify rather sturdy protein-protein interactions of either high affinity and/or favourable kinetic parameters (e.g. low k_{off} rates) (Gingras, Gstaiger et al. 2007; Kocher and Superti-Furga 2007). Therefore, many interactions that had been described in the literature, of which some are critical for Bcr-Abl function, may have evaded detection by TAP as they may be less sturdy, less stoichiometric or confined to other particular cells or conditions. The Src family kinase hematopoietic cell kinase (Hck), for instance, has been shown to be activated upon formation of complexes with Bcr-Abl and to be the effector for the activation of the Jak-Stat pathway by Bcr-Abl (Klejman, Schreiner et al.

2002), but has not been identified as a part of our network around the stoichiometric interactors of Bcr-Abl (Figure 3.7). A large group of Bcr-Abl interactors described in the literature are likely to include Bcr-Abl substrate proteins that are 'just' phosphorylated by Bcr-Abl without engaging in an interaction intimate enough to survive two affinity purification steps, such as the Jak and Stat proteins (Ilaria and Van Etten 1996) (Figure 4.5, Figure 4.6). In this study, we have therefore focused on the seven 'core' interactors of Bcr-Abl that are thought to form a signalling scaffold that links the Bcr-Abl 'core' complex to different signal transduction pathways and that is embedded within a wider signal transduction network, including major downstream transcriptional targets, such as Stat5 or c-Myc (Ren 2005) (Figure 4.5,Figure 4.6).

4.2   A limited set of seven stoichiometric interactors associates with Bcr-Abl in a 'core' complex

The significant identification of 18 candidate Bcr-Abl protein interactors at high sequence coverage similar to that of Bcr-Abl itself, following purification of endogenous Bcr-Abl protein complexes from K562 cells, suggested a stoichiometric level of interaction with Bcr-Abl. Eight of these proteins were hypothesized to represent modules related to the AP2 adaptor protein complex, exerting cellular housekeeping functions and presumably forming different sub-networks more loosely connected to Bcr-Abl. Out of the remaining 10 candidate proteins, eight (c-Cbl, Cbl-B, p85α/β, p52Shc1, p62Shc1, Grb2, Crk-I) were well-described *bona fide* interactors of Bcr-Abl, while Ship2 is of unknown function in Bcr-Abl signaling and Sts-1 represents a novel interactor of Bcr-Abl. Following TAP purifications with 9 representative proteins (Figure 3.6), we obtained a protein-protein interaction network consisting of 91 nodes connected by 157 edges in total. Rewardingly, within the centre of the network, the seven proteins (Ship2, c-Cbl, p85, Sts-1, Shc1, Grb2 and Crk-I) clustered around Bcr-Abl and were significantly more inter-connected with each other than with any other of the about hundred proteins in the analysis by a total of 29 edges. Accordingly, within themselves these eight proteins formed a 4-core sub-network and, without Sts-1, even a 5-core, where each of the eight or seven

proteins has at least 4- or 5 connections to each of the other proteins, respectively. Strikingly, neither 4- nor 5-cores were found in 10^5 randomly simulated control networks, underlining the significance of the 4- and 5-core protein cluster (Figure 3.7,Figure 3.8). This inter-connection becomes nicely apparent from a different representation of the reciprocal TAP matrix displaying the proteins co-occurring in each of the TAP purifications as 'building blocks' of the complex (Figure 4.2).
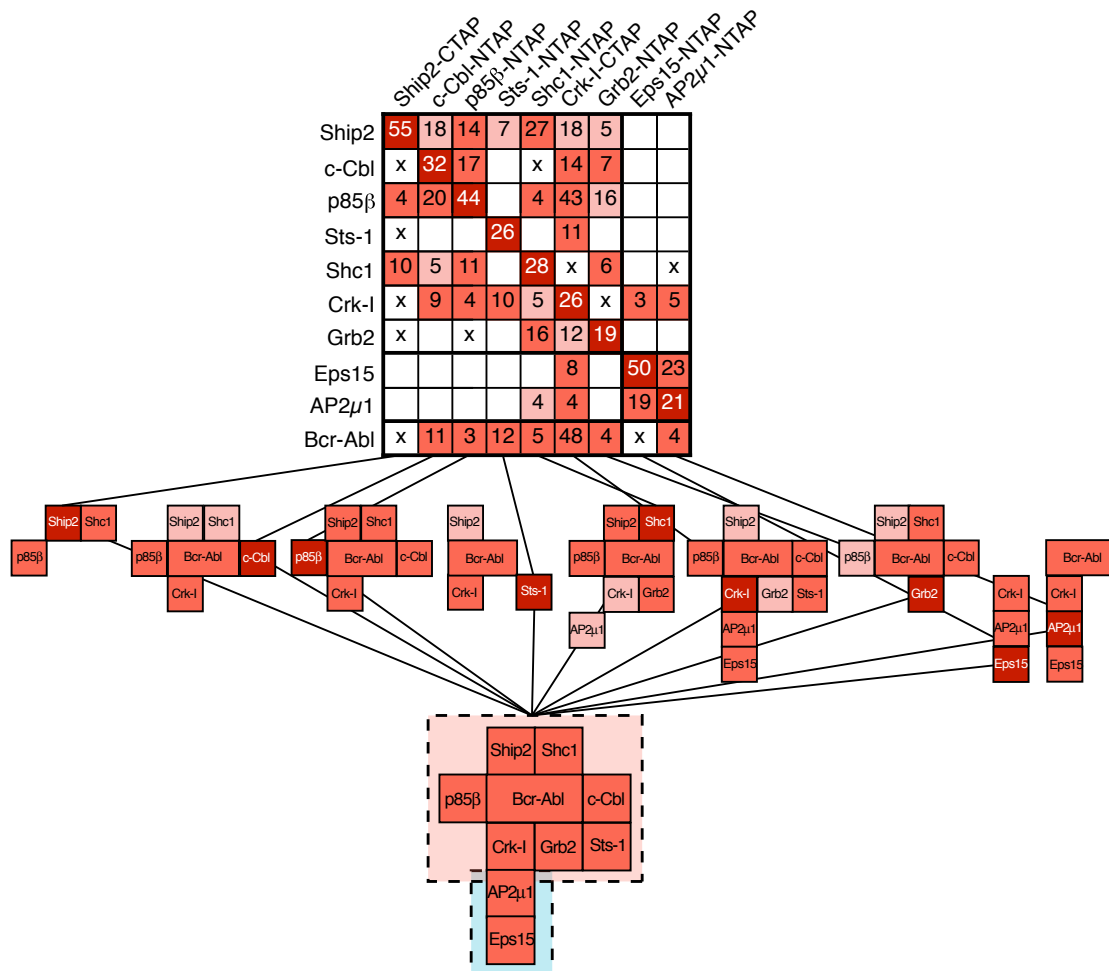
Figure 4.2 Redundant reciprocal recovery of Bcr-Abl complex components
Representation of the reciprocal co-occurrence within the nine TAP purifications (Figure 3.5) visualizes (i) the performance of the individual TAP purifications, (ii) points out putative sub-complexes and (iii) identifies Eps15 and AP2μ1 as members of an associated protein complex. Bait proteins are shown in dark red, proteins reciprocally and bi-directionally or only uni-directionally identified are shown in red and light red, respectively.

Besides the overall high level of co-occurrence, it is obvious that the individual TAP purifications yielded different results. While only two interactors

were found in the Ship2-TAP, the Crk-I TAP purification, being the smallest bait, identified basically the entire candidate Bcr-Abl 'core' complex (except Shc1). Furthermore, these results suggest the possibility of sub-complexes within the Bcr-Abl 'core' complex, such as a complex involving Bcr-Abl, Crk-I and Sts-1, and clearly position Eps15 and AP2μ1 within a more loosely associated protein complex (Figure 3.10). The clustering in Figure 4.3 takes an underlying model into account, where each of the seven candidates might be able to directly interact with Bcr-Abl. Besides differences in the performance of the individual bait proteins in the purifications, these results might point out possible architectural characteristics of the complex, such as the strength of individual protein-protein interactions or a sub-module architecture. For instance, Bcr-Abl and the known protein pair Ship2/Shc1 were co-purified in four out of nine cases (Wisniewski, Strife et al. 1999), while for the Ship2-TAP we have to assume that Bcr-Abl was not identified for technical reasons related to the size of the bait. Both c-Cbl and p85β TAP purifications identified the same set of proteins, Bcr-Abl, Crk-I, p85β, Ship2, Shc1 and c-Cbl. Only the bait Crk-I identifies the components Eps15 and AP2μ1, while when these were used as baits, Crk-I was always identified. All interactions observed bi-directionally (red blocks) provide the building blocks for an eight component multi-protein complex around Bcr-Abl (Figure 4.2).

Overall, the results obtained by this two-pronged approach presented above (see section 4.1) offer convincing evidence for the existence of an eight-component Bcr-Abl multi-protein complex of high stoichiometry. Such a complex, taking Bcr-Abl tetramerization into account, is calculated to exceed 2.5 megadalton molecular weight. However, all attempts to confirm the size of the intact complex by sucrose density gradients (section 3.7.2), gel filtration (section 3.7.3) or native gel electrophoresis (data not shown), even when combined with chemical cross-linking (data not shown), were frustrated by the failure to yield homogenous results. This is likely to reflect the general difficulty to measure protein assemblies in solution that are close to the size limits of these technologies, as well as the relatively low affinity by which the mainly SH2/SH3 domain dependent interactions of this particular complex appear to depend on

(Figure 4.3). Nevertheless, we continued to characterize this eight component Bcr-Abl complex in further detail with respect to (i) the functional relevance of the seven interactors (siRNA perturbation, see section 4.5.2), (ii) their domain-domain interaction architecture (see section 4.6) and (iii) their quantitative contribution to the complex. We were able to knock down protein expression of each of the eight complex components by siRNA efficiently, however, only knock-down of Bcr-Abl itself had an effect on the proliferation and viability of K562 cells whereas knock-down of the individual 'core' complex components had no effect (Figure 3.17). While protein knockdown of the individual complex components did not seem to affect Bcr-Abl activity, targeted inhibition of Bcr-Abl had a severe effect not only on the activity of Bcr-Abl but also on the composition of the complex. We could show that the action of tyrosine kinase inhibitors such as dasatinib and nilotinib severely disrupts the complex integrity and that it leads to a remodelled post-drug composition of the complex (Figure 3.18, Figure 3.19 and section 4.5). Taking known binary protein-protein interactions and binding preferences of individual protein-protein interaction domains into account, we built domain-domain interaction models for the untreated and drug-treated Bcr-Abl complex that are in line with our experimental observations (Figure 4.3). In the future, it could be interesting to assess if and how the composition of the complex is affected upon siRNA knockdown of each of its individual components.

Finally, we were able to quantify the absolute cellular protein copy number of each of the eight protein complex components as well as the interaction stoichiometry within the complex (Figure 3.12,Figure 3.13). We found Bcr-Abl to be expressed at about 300,000 protein copies per cell and all of its seven 'core' interactors within one order of magnitude (Figure 3.12). The quantification of 25,000 Crk-I copies per cell, however, appears too low to be in line with our semi-quantitative MS data and could be due to detection ambiguity problems. Furthermore, the overall interaction stoichiometry measured from one Abl immunoprecipitation yielded unexpected results. While only Ship2 seemed to interact with Bcr-Abl at a stoichiometry of around 1:1, all the other components were found at a ratio of 0.4:1 or lower (Figure 3.13). These results

are in clear contradiction to the abundance of these interactors in our MS analysis, which indicated significant stoichiometric interaction of the seven components with Bcr-Abl. Given the expression of these seven proteins at total cellular copy numbers within one order of magnitude, this would have implied that the majority of the cellular copies is associated with Bcr-Abl, which may be considered unlikely. By measuring the degree of co-depletion of each of the seven interactors following immunoprecipitation of Bcr-Abl complexes, we could confirm that this is indeed not the case and that at most, 30% of total cellular protein (Sts-1) are Bcr-Abl associated. This inconsistency could be due to errors in (i) the quantification of total cellular protein copy numbers or (ii) the interaction stoichiometry. Furthermore, the semi-quantitative MS data might be misleading as different proteins display different detection efficiency depending on their physico-chemical properties (Ong and Mann 2005).

Rewardingly, however, we were able to confirm the disruption and remodelling of the eight-component Bcr-Abl machine observed by immunoprecipitation and immunoblotting (i) by iTRAQ relative quantification (Figure 3.18,Figure 3.19) and (ii) reciprocal immunoprecipitation of each interactor from mock- and nilotinib-treated cells followed by 1D-shotgun-MSMS and network analysis (Figure 3.21) (see section 4.5).

4.3 Discovery of Sts-1 as a novel stoichiometric interactor of Bcr-Abl

Sts-1 (suppressor of T-cell receptor signaling 1) (TULA-2), is an SH3 domain containing protein that is ubiquitously expressed, whereas expression of its homolog Sts-2 (TULA) is restricted to lymphocytes (Wattenhofer, Shibuya et al. 2001). Both, Sts-1 and Sts-2 possess an N-terminal ubiquitin-association (UBA) domain, an SH3 domain and a C-terminal region highly similar to the phosphoglycerate mutase (PGM) enzyme family. Sts-1 was initially identified as an interactor of Jak2 (Carpino, Kobayashi et al. 2002) although the role in Jak2 signaling could not be confirmed. The paralogues Sts-1 and Sts-2 differ in their biological properties, such as the distinct binding properties of their UBA domains (Hoeller, Crosetto et al. 2006) or the reduced phosphatase activity of Sts-2 despite the conservation of crucial catalytic residues (Chen, Jakoncic et

al. 2009). These differences point towards different target profiles of the two proteins and only Sts-1/2$^{-/-}$ double knockout mice show a phenotype in their T-cells (Carpino, Turner et al. 2004). Sts proteins were found to control the levels of Zap-70 phosphorylation and thereby to be involved in regulation of signaling downstream of the TCR (Carpino, Turner et al. 2004; Mikhailik, Ford et al. 2007). Sts proteins bind c-Cbl via their SH3 domain and mono-ubiquitin via their UBA domain and consequently negatively regulate the ubiquitin ligase c-Cbl, a critical attenuator of receptor tyrosine kinase signaling, resulting in an inhibitory effect on receptor endocytosis (EGFR, PDGFR) (Kowanetz, Crosetto et al. 2004). The crystal structure of the PGM domain was solved and showed that it possesses tyrosine phosphatase activity (Mikhailik, Ford et al. 2007). Recently, also the structure of the Sts-2 PGM domain was solved and showed that Sts-2 might function as an acid-dependent phosphatase (Chen, Jakoncic et al. 2009). Furthermore, while Sts-2 utilized its UBA- and SH3 domains for mono-ubiquitin and c-Cbl binding in order to achieve this effect, Sts-1 was shown to differ in this regard, as it used its tyrosine phosphatase activity to dephosphorylate the EGFR and to attenuate its signaling without an obvious implication of its UBA domain (Raguz, Wagner et al. 2007). Phosphorylation of c-Cbl can be mediated by Src, Fyn, Yes, Syk and Abl and overexpression of Sts-1 was shown to dephosphorylate endogenous c-Cbl potently (Raguz, Wagner et al. 2007). In line with this, Sts-1 was also described as a negative regulator of Syk, a protein tyrosine kinase with a key role in lymphoid signalling, and the effect was shown to require an intact PGM domain (Agrawal, Carpino et al. 2008).

To date, Sts-1 was mentioned twice in the context of Bcr-Abl. A gene expression screening of adult patients with acute lymphoblastic leukemia (ALL) followed by network analysis of gene expression data between Bcr-Abl-positive patient subgroups revealed Sts-1 to be overexpressed in p185Bcr-Abl-positive ALL relative to p210Bcr-Abl-positive ALL (Juric, Lacayo et al. 2007). Shortly thereafter, Sts-1 was identified in a chemical proteomics approach (Bantscheff, Eberhard et al. 2007), which suggested that Grb2, Shc1, Ship2 as well as the adaptor protein Sts-1 are in a complex with the drug target Bcr-Abl (Figure 3.9).

Sts-1 is a hitherto not described interactor of Bcr-Abl and, supported by the evidence presented above, may be a novel regulator or antagonist of Bcr-Abl action.

4.4 The role of the phosphatases Sts-1 and Ship2 within the Bcr-Abl 'core' complex

The prominent identification of the 5-inositol phosphatase Ship2 and the protein tyrosine phosphatase Sts-1 as a novel Bcr-Abl interactor were interesting as both proteins have been described as negative regulators in different signal transduction pathways (Taylor, Wong et al. 2000), (Mikhailik, Ford et al. 2007). Ship2 was shown to exert a crucial anti-proliferative function by causing protein kinase B (PKB/Akt) inactivation and cell cycle arrest in glioblastoma cells (Taylor, Wong et al. 2000). Like PTEN, Ship2 regulates the levels of the PI3K product PIP3 (PtdIns(3,4,5)P3), but, unlike PTEN, not the levels of PIP2 (PtdIns(3,4)P2). Ship2 was a prime target in drug discovery as it was suggested to be a negative regulator of insulin signalling, however, the mechanism could not be elucidated to date (Sleeman, Wortley et al. 2005; Vinciguerra and Foti 2006). Ship2 is tyrosine phosphorylated in K562 cells (Goss, Lee, Moritz, Nardone, Spek, Macneill et al. 2006; Mishra, Suresh et al. 2006; Salomon, Ficarro et al. 2003) (Figure 3.17B) and it is reduced upon TKI treatment (data not shown). However, it was shown that tyrosine phosphorylation of Ship2 upon growth factor stimulation did not influence its phosphatase activity (Taylor, Wong et al. 2000). It is therefore not clear, whether Bcr-Abl activity influences Ship2 activity and if the PI3K-PKB pathway is affected. Foci of Bcr-Abl protein complexes with Grb2, c-Cbl and CrkL (which is not part of our complex) have been shown to localize in proximity to the membrane in primary CML cells (Patel, Marley et al. 2006). Localization of Bcr-Abl complexes to the cell membrane would support a membrane-proximal interaction of Ship2 with its substrate even in complex with Bcr-Abl. Furthermore, the observed association with the AP2 adaptor protein complex supports the membrane-proximal location of Bcr-Abl complexes (Figure 3.10). The presence of the 5-inositol phosphatase, Ship2, in complex with adaptor

proteins like Grb2 and Bcr-Abl represents similarity to other AP2 adaptor protein-associated complexes between activated receptor tyrosine kinases, Grb2 and the 5-inositol-phosphatase synaptojanin (SYNJ1) (Figure 4.4D) (Haffner, Takei et al. 1997; Praefcke, Ford et al. 2004). This raises the possibility that the Bcr-Abl 'core' complex potentially mimics the mode of action of activated receptor tyrosine kinase protein complexes in order to exert its downstream signalling effects.

Sts-1 and Ship2 display tumor-suppressor characteristics and it could be hypothesized that Bcr-Abl exerts parts of its oncogenic effects by modulating Sts-1 and Ship2 activity. I observed an apparent increase in total cellular Sts-1 protein levels (about 2-fold) upon treatment of K562 cell lysate with nilotinib (data not shown), an effect that has not been described. Given the increase in protein levels upon inhibition of Bcr-Abl with the specific tyrosine kinase inhibitor nilotinib, Bcr-Abl signalling might possibly lead to reduced overall Sts-1 protein levels. Oliver Hantschel and Ines Kaupe, in our lab, have already obtained preliminary evidence (i) on the ability of Sts-1 to dephosphorylate Bcr-Abl on tyrosine residues and (ii) on the dependence on the SH2 domain of Bcr-Abl for interaction with Sts-1 on the other hand (unpublished results). Further elucidation of the molecular and functional details of this fascinating Sts-1-Bcr-Abl interaction promises to shed new light on a putative negative regulation of Bcr-Abl function and will be the object of future studies.

4.5 The Bcr-Abl multi-protein complex is the therapeutic target of tyrosine kinase inhibitors

Arguably, one of the most interesting findings of our study is the fact that not Bcr-Abl alone, but rather a multi-component Bcr-Abl 'core' complex is the target of tyrosine kinase inhibitors, which consequently alter the integrity of this complex. This became apparent from the observations that (i) the tyrosine kinase inhibitor dasatinib, used as an affinity reagent, binds to Bcr-Abl and the four 'core' complex members we tested for (Ship2, Sts-1, Shc1 and Grb2) upon incubation with K562 cell lysate but not with lysate from Bcr-Abl negative U937 cells (Figure 3.20); (ii) that the tyrosine kinase inhibitors dasatinib and nilotinib

disrupt the complex integrity and lead to loss or severe reduction of all seven interactors (Figure 3.3,Figure 3.18) and (iii) that, reciprocally confirmatory, the protein complex composition of one of Bcr-Abl's prominent interactors, Grb2, is altered accordingly (Figure 3.19). Inhibition of Bcr-Abl kinase activity with dasatinib or nilotinib led to a severe reduction in the interactions of four (c-Cbl, Sts-1,Shc1 and Crk-I) out of seven core interactors with Bcr-Abl, likely to be caused by the inhibition of Bcr-Abl tyrosine kinase activity and the resulting loss of autophosphorylation sites on tyrosine residues. As a consequence, SH2- and PTB-domain mediated interactions were abolished, whereas interactions that are independent of tyrosine phosphorylation, such as SH3-domain mediated interactions, could be maintained (Figure 4.3). Furthermore, as tyrosine phosphorylation may also allosterically change domain conformations or intramolecular interactions, protein-protein interactions may remodel in the presence of tyrosine kinase inhibitors. Indeed, we observed that certain interactions (Ship2, p85β and Grb2) were only reduced, but not completely abolished (Figure 3.3, Figure 3.18, Figure 3.19) and that few interactions, exemplified by the Grb2-Sos1 interaction, are even enhanced in the presence of drug (Figure 3.19). Therefore, we propose a 'post drug complex' that may be assembled differently, as residually bound Bcr-Abl interactors may have switched their molecular interaction mode and that may still contain some enzymatic activity (e.g. Ship2 5-inositol phosphatase activity). These insights led us to a novel post-genomic view of a drug-target.

4.5.1   A novel post-genomic view of a drug-target

The small molecule tyrosine kinase inhibitor imatinib served as a paradigmatic case for modern targeted cancer therapy at hands of Bcr-Abl in CML (Druker 2008). As for imatinib and Bcr-Abl, drug targets in general are typically regarded as single proteins or even protein fragments. This traditional view is based on the fact that high-throughput screening of large compound libraries - that is still the most commonly used approach to identify lead compounds in drug discovery - mainly assay binding or inhibition of proteins or protein fragments (Bleicher, Bohm et al. 2003; Brown and Superti-Furga 2003).

In line with this, also the action of drugs in a cellular context is commonly envisaged as the interaction of the drug with a single or very limited number of cellular proteins. In stark strong contrast to this reductionist view, modern post-genomic technologies, in particular large-scale interaction proteomics and drug/chemical proteomics approaches have dramatically changed our view of the organization of the human proteome and drug action. Proteins very rarely act in isolation, but are organized as part of large multi-protein complexes/molecular machines that may dynamically change their spatial and temporal organization (Bouwmeester, Bauch et al. 2004; Gavin, Aloy et al. 2006; Kuriyan and Eisenberg 2007). Along this line, unbiased proteomics approaches for drug targets have shown that even drugs that were considered highly specific often interact with a much larger number of previously unidentified target proteins that themselves are also even part of larger protein complexes (Bantscheff, Eberhard et al. 2007; Daub 2005; Rix, Hantschel et al. 2007). In line with this, pharmacogenomic and microarray profiling studies suggest that dozens, if not hundreds of gene products affect the efficacy of drugs in individuals (Evans and McLeod 2003; Hantschel, Gstoettenbauer et al. 2008). Furthermore, drugs often have undesired side effects by impinging on different pathways that, in turn, may be shared by different diseases (Yildirim, Goh et al. 2007), (Campillos, Kuhn et al. 2008). These insights have changed our view of drug action. Instead of considering the alteration of the activity of a single protein by a drug, in a more post-genomic view, 'drug' action may have pleiotropic effects on a number of different proteins leading to a perturbation of molecular networks at different levels, including changes in gene expression, metabolite levels and turn-over, protein-protein interactions and post-translational modifications.

4.5.2 Oncogene addiction but not 'oncogene protein complex' addiction

Apart from the role as stoichiometric interactors of Bcr-Abl, we have also tried to address their functional relevance by reducing protein levels using siRNAs. We were able to knock-down the protein expression of each of the core interactors by at least 75% in K562 cells, but unexpectedly were unable to detect changes in the viability or proliferation rate, whereas K562 cells rapidly stopped proliferating and underwent apoptosis when Bcr-Abl protein levels were reduced using an Abl or Bcr-Abl breakpoint-specific siRNA (data not shown). Although drug action clearly seems to target the entire protein complex rather than just inhibiting Bcr-Abl, removal of the complex components alone, had no effect on Bcr-Abl action. It is not clear to us why none of the individual knockdown experiments had an effect on K562 cell proliferation. For the p85α subunit of PI3K, for instance, a clear functional relationship between binding to fusion tyrosine kinases (FTK) such as Bcr-Abl, as part of a protein network involving proteins like Shc, c-Cbl and Gab2, and constitutive activation of the p110 catalytic subunit of PI3K and its downstream effector Akt kinase has been shown (Ren, Bolton et al. 2005). Here, point mutations of the domains critical for the protein-protein interaction with the FTK, the N- and C-terminal SH2 and the SH3 domains of p85α, disrupted phosphotyrosine and proline-rich motif binding and, as a consequence, abrogated interaction with Bcr-Abl, Shc, c-Cbl and Gab2, whereas binding to the catalytic subunit of PI3K remained intact, and resulted in reduced activation of PI3K and Akt (Ren, Bolton et al. 2005). Both siRNA knockdown of p85α, p85β and simultaneous knockdown of both subunits had no effect on the viability of K562 cells (Figure 3.17 and data not shown). On one hand, residual protein levels upon knock-down might still be sufficient to mediate leukemogenic signalling from Bcr-Abl, on the other hand, this may be in line with the severe Bcr-Abl addiction of K562 cells to their oncogene Bcr-Abl that may be able to override many different, even severe perturbations in its downstream signal transduction network and may uncover unexpected redundancy in signalling pathways exerting Bcr-Abl's oncogenicity. Furthermore, a recent large-scale effort by the RNAi consortium to map the

functional basis of cancer at hands of the identification of the essential genes in cancer cells by genome-scale pooled short hairpin RNA (shRNA) screens in several cancer cell lines, including K562, by large confirms our data (Luo, Cheung et al. 2008). In K562 cells, ABL1 and BCR genes ranked amongst the five top-scoring genes out of about 9,500, clearly identifying Bcr-Abl as selectively highly required gene in the K562 cell line (Luo, Cheung et al. 2008).

4.6 Towards a domain-domain interaction map of the Bcr-Abl 'core' complex

At this point I would like to mention that I am especially grateful for the valuable assistance and the insights provided by Oliver Hantschel in the lab who has a long-standing background and superior experience in c-Abl/Bcr-Abl structure-function analysis as well as the role of the phospho-tyrosine residues of these proteins in the regulation of Abl kinase activity as well as their function in protein-protein interactions.

The identification of the stoichiometric interactors of Bcr-Abl by mass spectrometry, the ensuing TAP network analysis and the insights from the effects of tyrosine kinase inhibitors on the integrity of the complex enabled the attempt to build putative Bcr-Abl 'core' complex domain-domain interaction models based on the domain composition and the tyrosine phosphorylation sites of Bcr-Abl and its interactors available from the literature. As all proteins included in the analysis, except for Crk-I, are tyrosine-phosphorylated in K562 cells (Liang, Hajivandi et al. 2006; Steen, Fernandez et al. 2003) (Superti-Furga laboratory, unpublished results) and as most contain SH2 domains (7x), SH3 domains (5x) and/or PxxP motifs (4x), there is a very large number of theoretically possible combinations for these eight proteins in a domain-domain interaction model. However, the number of possible combinations can be reduced by taking information on the molecular interaction mode of known binary protein-protein interaction pairs and binding preferences for SH2- and SH3 domains into account (Mayer 2001; Pawson 1994; Pawson, Gish et al. 2001). In the models presented below, for simplicity reasons, formation of Bcr-Abl tetramers via its N-terminal coiled-coil domain is not considered (Figure

4.3). The SH2 domain of Grb2 bound to pTyr-177 in Bcr-Abl (Pendergast, Quilliam et al. 1993), as well as the PTB domain interaction of Shc-1 with a C-terminal tyrosine phosphorylation site in SHIP-2 were built to form the innermost interactions with Bcr-Abl (Tauchi, Boswell et al. 1994; Wisniewski, Strife et al. 1999) (Figure 4.3A,B,C). In addition to its interaction via Shc-1, a PxxP motif in Ship2 was also shown to bind the Bcr-Abl SH3 domain (Wisniewski, Strife et al. 1999). c-Cbl and p85 may interact by one of their PxxP motifs with the C-terminal SH3 domain of Grb2 (Gaston, Johnson et al. 2004; Skorski, Kanakaraj et al. 1995)(Figure 4.3 A,B,C). Alternatively, interactions of the Cbl TKB (SH2-like) domain or one of the p85 SH2 domains with one of the numerous tyrosine-phosphorylated residues of Bcr-Abl can be envisaged (Figure 4.3A,B,C). Crk-I may also interact with its SH2- or SH3-domain either directly with Bcr-Abl or with one of the other core interactors (Sattler and Salgia 1998) (Uemura, Salgia et al. 1997)(Figure 4.3A,B,C). Finally, Sts-1 may interact with its SH3-domain directly with Bcr-Abl, e.g. binding to one of the proline-rich motifs in the last exon region downstream of the kinase domain (Figure 4.3A), or the Abl SH2 domain may bind to a tyrosine-phosphorylated residue in Sts-1 (Figure 4.3D,E). In an alternative model, Sts-1 may be indirectly associated with Bcr-Abl by using its SH3 domain to bind the PxxP motif in c-Cbl (Figure 4.3B). The lower k-core for Sts-1 in the Bcr-Abl core network may be indicative for this indirect interaction mode but also suggests the formation of an alternative complex with Bcr-Abl that is lacking other core interactors, besides Ship2, which might be involved in this alternative complex (Figure 4.3D,E)(Figure 3.5).
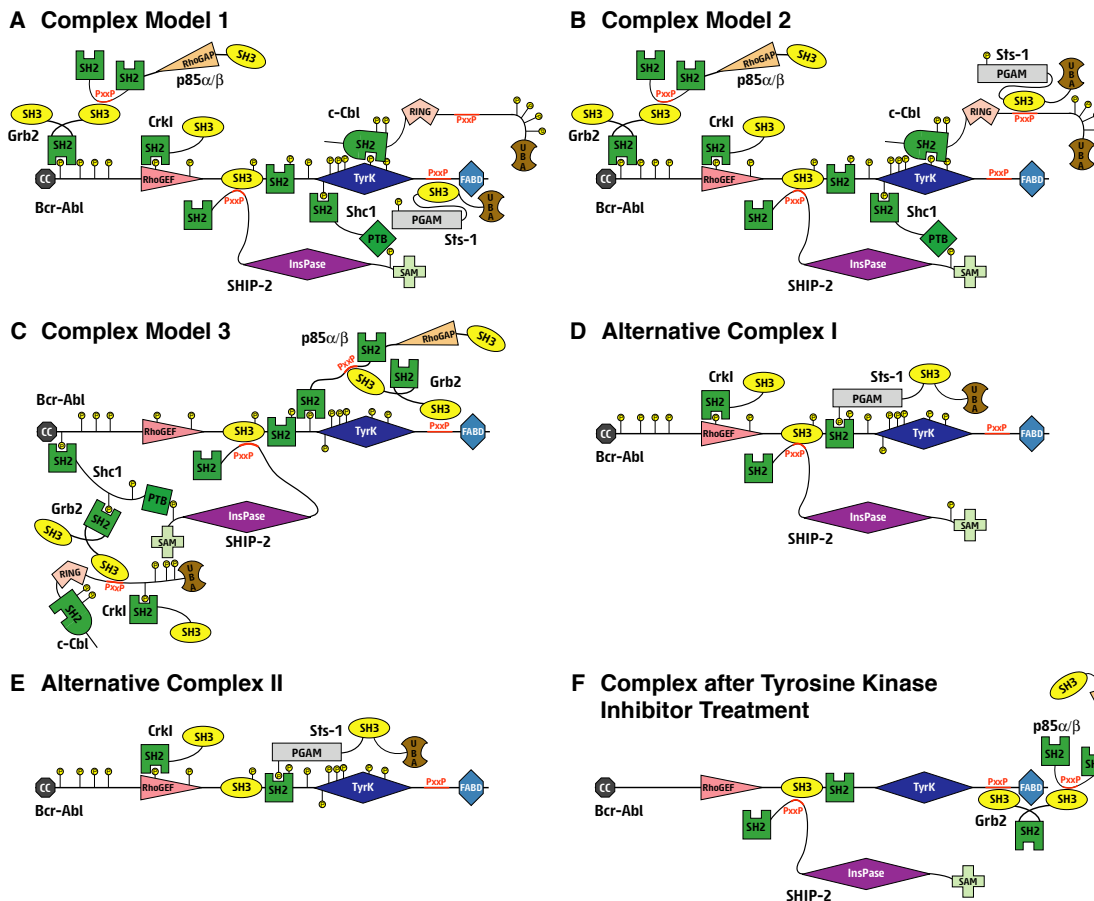
Figure 4.3 Domain-domain interaction model of the Bcr-Abl 'core' complex in the absence and presence of nilotinib or dasatinib

Schematic representation of possible domain interactions within the Bcr-Abl core complex. Tyrosine phosphorylation sites are indicated. Different scenarios are shown.

(A) p85 bound to the C-terminal SH3 domain of Grb2. c-Cbl interacting with unknown phosphotyrosine on Bcr-Abl with its TKB (SH2-like) domain.

(B) Alternatively to (A), Sts-1 may interact with the PxxP motif of c-Cbl via its SH3 domain.

(C) c-Cbl bound to the C-terminal SH3 domain of Grb2. p85 interacting with unknown phosphotyrosine on Bcr-Abl with one of its SH2 domains. In addition, an alternative binding of the Grb2 SH2 domain to a phosphotyrosine residue in Shc-1 is shown. Sts-1 may not be involved in these complexes ('5-core')

(D,E) Potential alternative Bcr-Abl complexes with dominant contribution of Sts-1 that may bind the Bcr-Abl SH2 domain. Ship2 may be involved in these complexes (D).

(F) Bcr-Abl complex in the presence of nilotinib or dasatinib. Note the absence of tyrosine-phosphorylated residues. Residual interactions of Bcr-Abl with Ship2, Grb2 and p85 are mediated by SH3 domain-PxxP motif interactions.

As we have observed the complete loss of the interactions of Bcr-Abl with c-Cbl, Sts-1, Shc1 and Crk-I upon drug treatment, it is likely that these interactions are mainly phosphotyrosine-SH2 domain dependent. In contrast, Ship2, p85β and Grb2 still show residual interaction with Bcr-Abl in the presence of the drugs. As under these conditions, Bcr-Abl is not tyrosine-

phosphorylated anymore, the remaining interactions must be SH2 domain-independent. For Ship2, the interaction with Bcr-Abl via Shc-1 is lost and may only be maintained by interaction with the Bcr-Abl SH3 domain. Also for Grb2 and p85, SH3 domains binding to proline-rich motifs may mediate residual binding, replacing SH2 domains binding to phosphotyrosine residues (Figure 4.3F).

4.7 A novel link between Bcr-Abl and the AP2 adaptor protein complex

Within the 2-core AP2 complex that we found associated to the Bcr-Abl 'core' complex (Figure 3.7), AP2α1, AP2α2, AP2β1, AP2μ1 and Eps15 even formed a 3-core complex (Figure 3.10). While only AP2μ1 is directly linked to Bcr-Abl, Crk-I has three edges to AP2α1, Eps15 and AP2μ1 and Shc1 has four edges to AP2α1, AP2α2, AP2β1 and AP2μ1, hereby hypothesized as the interface to the Bcr-Abl 'core' complex. The interactions between Eps15 and AP2α1 (Benmerah, Gagnon et al. 1995; Benmerah, Lamaze et al. 1998) and between Stonin-2 and Eps15 (Martina, Bonangelino et al. 2001; Rumpf, Simon et al. 2008) are known (Figure 4.4A). Also interactions between Eps15 and the N-terminal SH3 domain c-Crk (Schumacher, Knudsen et al. 1995) as well as the binding of Shc1 to AP2α have been reported in the literature (Sakaguchi, Okabayashi et al. 2001), which corroborates our model (Figure 4.4A). In this model, we show only Bcr-Abl, Shc1 and Crk-I and omit the other components of the Bcr-Abl complex for graphical simplicity. The AP2 complex may be recruited by binding the signature FDMKPF within the collagen homology region of Shc1 (Sakaguchi, Okabayashi et al. 2001).

The AP2 complex brings along Eps15, which is simultaneously bound to the α-adaptin appendages of either AP2α or β. This interaction might be mediated via DPF-repeats in Eps15 (Iannolo, Salcini et al. 1997; Praefcke, Ford et al. 2004). Eps15, in turn, uses its proline-rich motif (PALPPK) to bind the N-terminal SH3 domain of c-Crk (here Crk-I) (Schumacher, Knudsen et al. 1995).
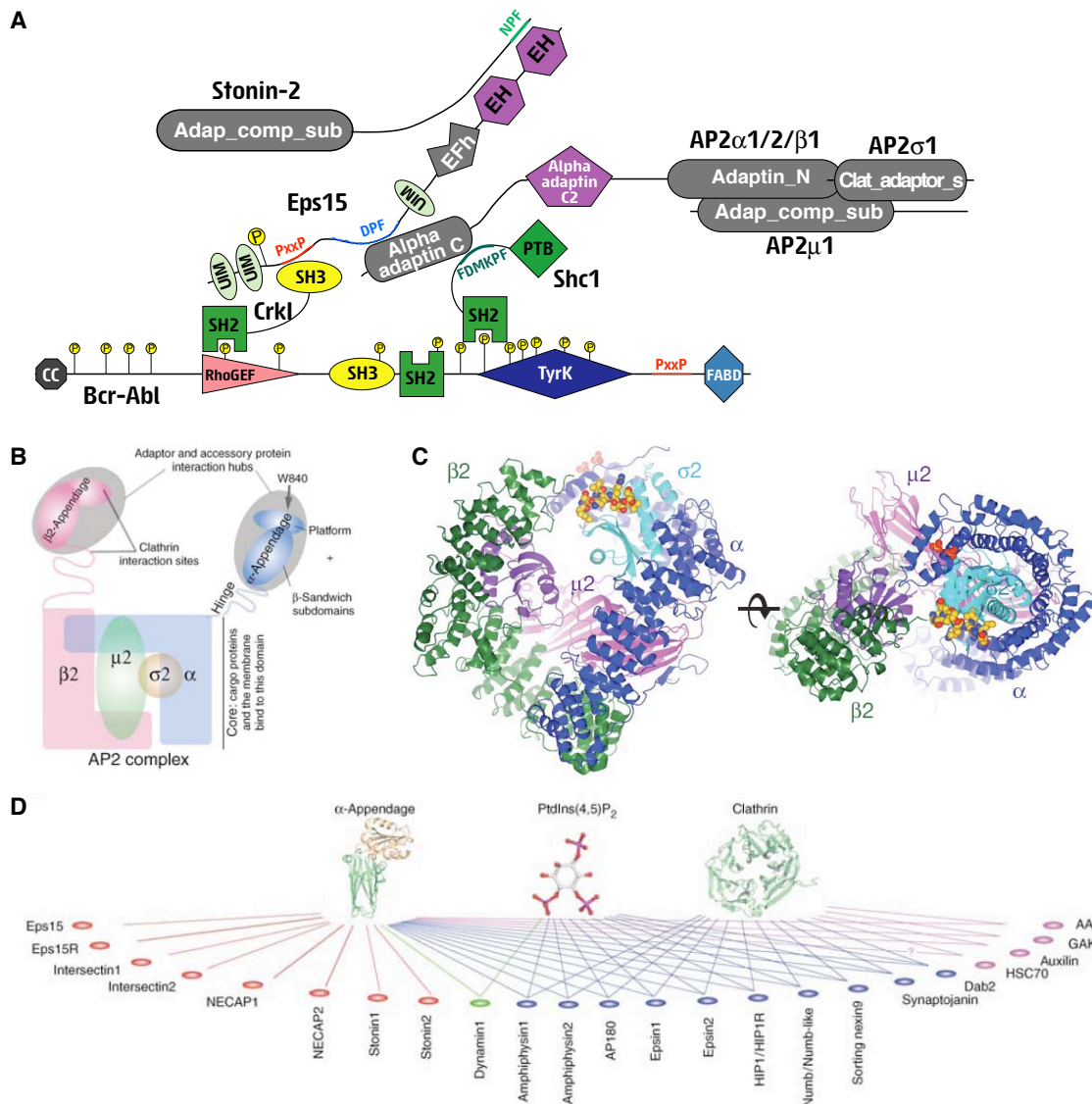
Figure 4.4 Domain-domain interaction model of the Bcr-Abl 'core' complex and its associated AP2 adaptor protein complex

(A) Domain-domain interaction model of the accessory AP2-complex with its connections to Crk-I and Shc1 within the Bcr-Abl core complex. Only one domain-structure is shown representative for AP2α and AP2β for simplicity. The other Bcr-Abl complex components are omitted for simplicity.

(B) Cartoon of an AP2 adaptor complex, consisting of AP2α, AP2β, AP2μ and AP2σ. The appendages of AP2α and AP2β are the major protein interaction hubs.

(C) Structure of the AP2 adaptor core in complex with dileucine peptide of CD4 (orthogonal views) in ribbon surface representation.

(D) Proteomic analysis of AP2α-appendage interactions by GST-AP2α-appendage pulldown and MS-analysis. Also shown are proteins interacting with the two other interaction hubs in clathrin-mediated endocytosis, Clathrin and PtdIns(4,5)P₂. (B, D) taken from (Praefcke, Ford et al. 2004), (C) taken from (Kelly, McCoy et al. 2008)

Finally, the EH (Eps15 homology) domain of Eps15 interacts with two NPF motifs (only one shown for simplicity) within the proline-rich domain of Stonin-2 (Martina, Bonangelino et al. 2001; Rumpf, Simon et al. 2008) (Figure

4.4A). It is known that, within the AP2-complex, the adaptin-appendage regions ('ear') act as the primary hubs for protein protein interaction (Praefcke, Ford et al. 2004) (Figure 4.4B). Accordingly, within our network, using AP2μ1 as a bait, AP2α1, AP2α2 and AP2β1 are recovered in an interconnected network with AP2μ2, Shc1 and Crk-I. Just recently, the structure of the AP2 complex has been solved in complex with the endocytic dileucine motif of the ligand CD4 (Figure 4.4C) (Kelly, McCoy et al. 2008). Acidic dileucine motifs ([ED]xxxL[LI]) and the YxxΦ motif are the two major recognition motifs of endocytic cargo ligands of AP2 (Kelly, McCoy et al. 2008; Owen and Evans 1998). Furthermore, a proteomic analysis of AP2α-appendage interactions furthermore confirms many of the proteins that we identify in our network, such as Eps15, Necap2 and Stonin-2 (Figure 4.4D). The requirement for the interaction between Eps15 and the AP2-complex in receptor-mediated endocytosis has been shown and therefore the Bcr-Abl 'core' complex seems linked to this process (Benmerah, Lamaze et al. 1998). However, direct interactions between any of the components of the AP2 components and Bcr-Abl directly have not been described to date. Phosphorylation of proteins involved in receptor-mediated endocytosis by Bcr-Abl could have effects on the activity of these proteins as well as the composition of endocytic protein complexes and consequently lead to altered rates of endocytosis of certain receptors. This process could contribute to the oncogenic properties of Bcr-Abl expressing cells, such as K562.

4.8 Putative cellular redistribution of signaling components upon therapeutic disruption of the Bcr-Abl 'core' complex

The observation that the Bcr-Abl 'core' complex is remodelled by the action of tyrosine kinase inhibitors, where binding of most of the interactors to Bcr-Abl was disrupted (Figure 3.18), raised the question whether the dissociated signalling molecules might redistribute to other signalling complexes, thereby altering the activity of the associated signalling pathways. While screening for this effect, we indeed found an increased association of Sos-1 with Grb2 upon tyrosine kinase inhibitor treatment (Figure 3.19). This

effect, however, rather than being the consequence of a redistribution of Grb2 molecules from Bcr-Abl protein complexes into Sos-1 protein complexes, might be due to the loss of tyrosine phosphorylation within the Grb2 SH3 domain upon TKI treatment. It was shown that phosphorylation of Grb2 by Bcr-Abl reduces its SH3-dependent binding to Sos-1 *in vivo*, but not its SH2-dependent binding to Bcr-Abl (Li, Couvillon et al. 2001). Tyrosine 209 in the C-terminal SH3 domain of Grb2 was shown to by phosphorylated and phosphorylated Y209 abolished the binding of the C-terminal SH3 domain of Grb2 to a proline-rich Sos-1 peptide *in vitro* (Li, Couvillon et al. 2001). Expression of a Y209F mutant lead to increased Grb2-mediated activation of Ras and Erk (Li, Couvillon et al. 2001; Pendergast, Quilliam et al. 1993). However, as significant amounts of Grb2 are lost from Bcr-Abl complexes, it might still be of relevance that these molecules become available to redistribute into complexes with Sos-1 so that both mechanisms actually contribute to the observed effect. Interestingly it was shown that reduction of Bcr-Abl activity by imatinib treatment leads to a growth factor-dependent compensatory increase in activity of the important Bcr-Abl effector p42/44 mitogen-activated protein kinase (MAPK) and that, concordantly, combined treatment with MAPK inhibitors lead to an increased elimination of CML progenitors by imatinib (Chu, Holtz et al. 2004).

Taken together, these observations raise the possibility of a 'gain-of-function' role for kinase inhibitors, where, as opposed to a simple 'loss-of-function', the molecular mode-of-action of nilotinib and dasatinib can be described as a 'system perturbation' that leads to a dynamic remodelling of the protein-protein interaction space. This may represent a new paradigm for the characterization of drug targets in the post-genomic era, but needs further experimental support beyond the Bcr-Abl core complex.

4.9   Towards an enlarged physical, functional and quantitative network of Bcr-Abl signaling

The TAP-MS approach with the nine selected baits proteins confirmed numerous previously identified interactors of most bait proteins through unbiased protein identification by mass spectrometry, in particular of the intensively studied SH2-containing adaptor proteins Shc1, Grb2 and Crk-I. In addition, the approach resulted in the identification of a large number of novel protein-protein interactions, taking the human protein reference database (HPRD) and the IntAct database as a reference (Figure 3.6) (Hermjakob, Montecchi-Palazzi et al. 2004; Mishra, Suresh et al. 2006). The IntAct database was screened for human experimentally observed physical associations. Out of a total of 161 identified binary protein interactions for the nine bait proteins (including reciprocal pairs), 53 were known (annotated in the HPRD and/or IntAct databases) while 108 novel interactions were observed (Figure 3.6). None of the eight interactors found for Sts-1 was previously annotated, and only one (AP2β1) out of 13 interactors found for AP2μ1 was known. For Ship2, four interactions were novel in addition to the known interactor Shc1. A large number of novel interactions were found for the well-described small adaptor proteins Shc1 (11 known/16 new), Grb2 (10 known/22 new) and Crk-I (17 known/21 new). This dataset significantly increases the existing protein-protein interactions of the bait proteins and will be a valuable resource for the scientific community.

The data contained in the Bcr-Abl protein-protein interaction network presented here (Figure 3.7) contains only interactors associated with the seven Bcr-Abl 'core' complex members as well as with Eps15 and AP2μ1, that were identified as candidates from initial large-scale immunoprecipitations of Bcr-Abl/c-Abl protein complexes followed by TAP purifications using these proteins as bait. It is within the long-term interest of the lab to generate a comprehensive large-scale protein-protein interaction network around Bcr-Abl in K562 cells by using more bait proteins in order to reconcile the vast amounts of fragmented knowledge on Bcr-Abl signalling in a unified picture. During this study, known interactors and putative or known pathway components were already generated

as additional 'entry point' proteins for ensuing TAP-MS analysis, such as Paxillin, Dok2, Fes, Hck, Shp2, Fak, Myc, Nck, Crk-II, PKCδ or PSTPIP1 of which the TAP purifications for Dok2 and Crk-II were already performed and further entry points, such as Stat1, Stat5, PTP1B, PTPN11 (Shp2), Src, Yes and Fyn are planned (Cong, Spencer et al. 2000; Frank and Varticovski 1996; Hu, Liu et al. 2004; Kin, Shibuya et al. 2001; LaMontagne, Flint et al. 1998; LaMontagne, Hannon et al. 1998; Shuai, Halpern et al. 1996; Smith, Katz et al. 1999; Tauchi, Feng et al. 1994). The extension of the present network will create a more precise picture of the protein-protein interaction network more remote from Bcr-Abl and be a valuable data-set to identify components that could be exploited pharmocalogically. Furthermore, functional studies such as siRNA knockdown of its components as well as large-scale relative quantification by mass spectrometry of all network nodes in the presence of TKIs might add important information about candidate effector proteins.

In an attempt to simulate such an enlarged protein-protein interaction network, Jacques Colinge complemented our present network (Figure 3.7) with all protein-protein interactions annotated in the HPRD database for each of the 91 nodes. This resulted in a hybrid model network consisting of 1130 nodes and 2574 edges (Figure 4.5). Again, 10^3 random simulations of a network of this size yielded no k-core > 3, corroborating the significance of the Bcr-Abl 'core' complex. However, this model network suffers from the severe limitation that many protein-protein interactions, that might have no relevance in K562 cells, were added. Many of these proteins might not be expressed in K562 cells and many of the interactions might occur only in different cell types or represent 'false positive' interactions from Y2H (yeast-two-hybrid) studies. Accordingly, in this model, Bcr-Abl is part of an 8-core with numerous additional members (red nodes).
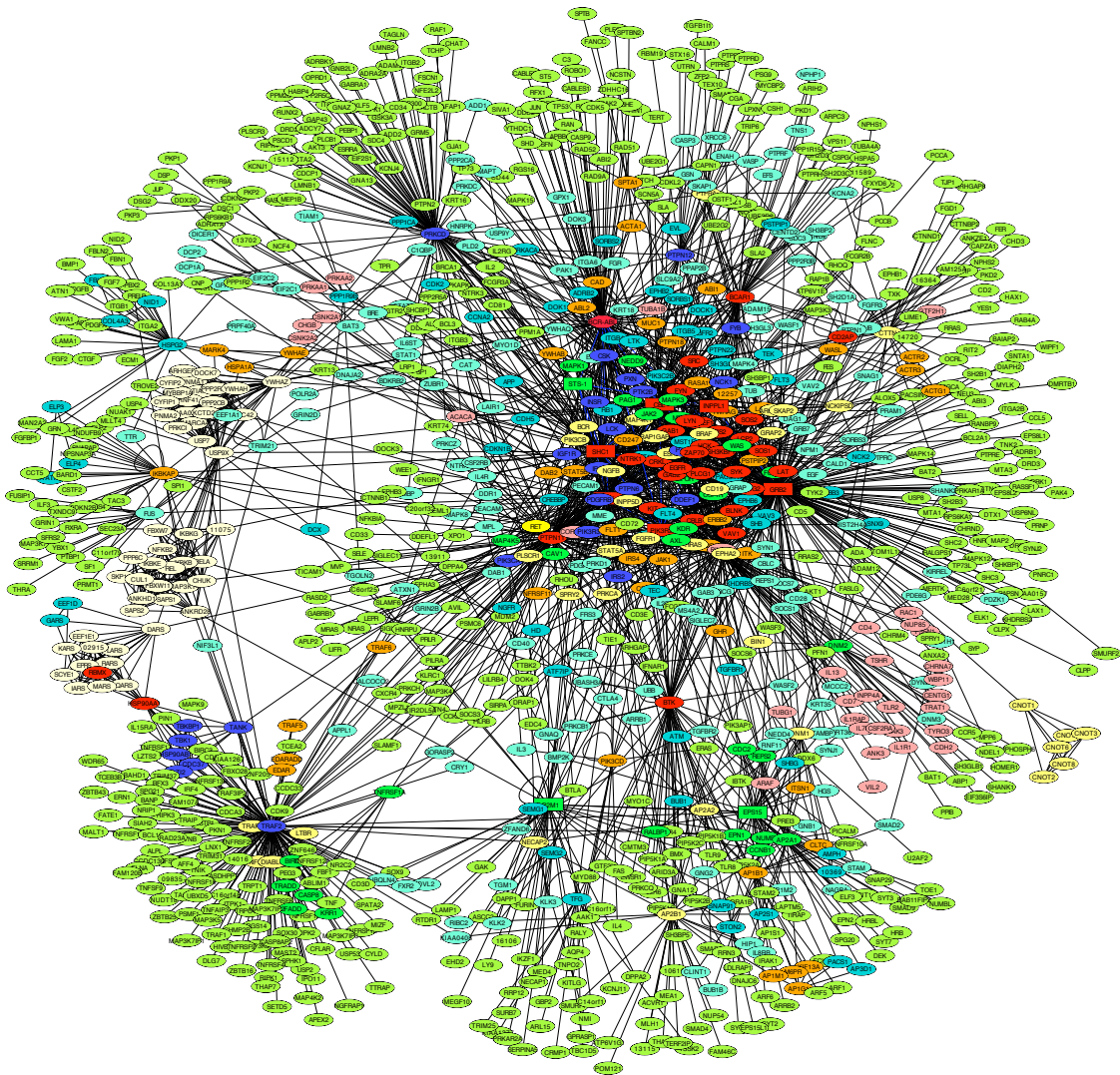
Figure 4.5 The Bcr-Abl 'core' complex and its signaling network enlarged by all HPRD - interactions

The Bcr-Abl protein-protein interaction network experimentally observed by TAP-LC-MSMS (Figure 3.7) computationally complemented with all interactions stored in the human protein reference database (HPRD). The network contains 1130 nodes and 2574 edges. 10^3 randomizations of the network give no k-core with k > 3 and hence support the significance of the Bcr-Abl core complex. However, within this network, the Bcr-Abl 'core' complex is an 8-core with numerous additional members. Furthermore, more disjoint 9-core sub-complexes (white nodes) are found.

Furthermore, more disjoint 9-core sub-complexes (white nodes) are found. Therefore, the network model has to be treated with caution, as it suggests the existence of a much bigger Bcr-Abl 'core' complex (Figure 4.5). However, this representation can serve as an example for the 'focus' that the Bcr-Abl network generated in this study generates by highlighting only the 91 nodes of the network (Figure 3.7) amongst all connected HPRD annotations (Figure 4.6).
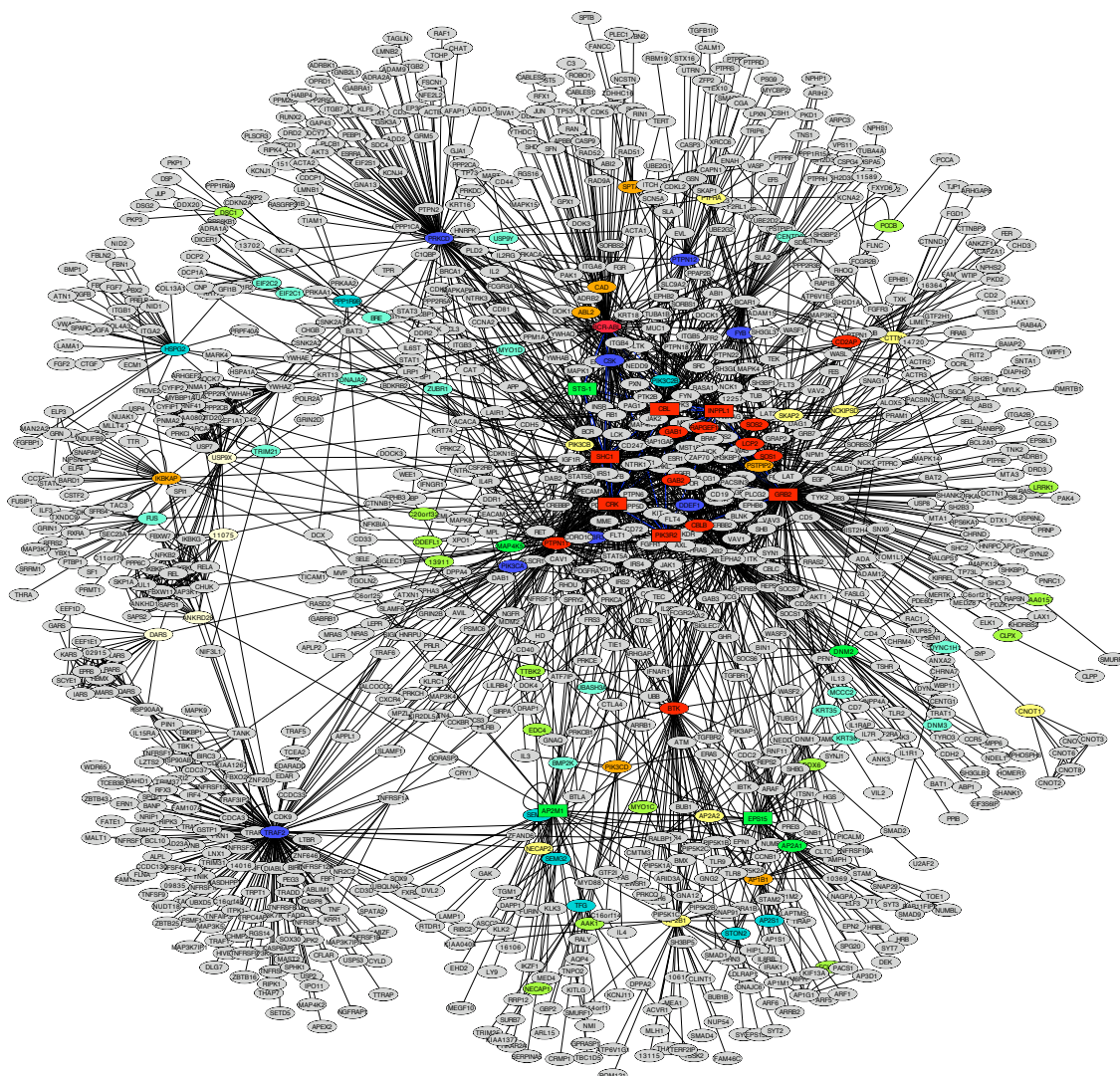
Figure 4.6 The Bcr-Abl 'core' complex and its signaling network within an enlarged network of HPRD - interactions

The Bcr-Abl protein-protein interaction network experimentally observed by TAP-LC-MSMS (Figure 3.7) computationally complemented with all interactions stored in the human protein reference database (HPRD). Only the 91 nodes present in the Bcr-Abl 'core' network are highlighted, all other nodes are shown in grey.

From this simulation it becomes obvious that our Bcr-Abl network contains protein-protein interaction hubs such as Traf2, Btk and PRKCD (PKCδ) that could represent interesting pharmacological targets for alternative or combination CML therapy and it remains to be determined if these exist in K562 cells (Calderwood, Venkatesan et al. 2007) (Figure 4.6). These data in conjunction with recently generated human drug target networks might help to select candidate targets and might even allow to assess known compounds targeting these candidates for synergistic effects with TKIs in CML (Goh, Cusick et al. 2007; Yildirim, Goh et al. 2007). Bruton's tyrosine kinase (Btk) has already

been shown to be a major target of dasatinib and it might contribute to the potent effect of dasatinib on the inhibition of Bcr-Abl signaling (Hantschel, Rix et al. 2007). However, it was shown that it is not an essential target for Bcr-Abl-mediated transformation of lymphoid or myeloid cells (MacPartlin, Smith et al. 2008). Interestingly, synergistic effects of the anti-cancer drugs arsenic trioxide (ATO) and the proteasome inhibitor bortezomib on K562 cells showed that cotreatment synergistically induced apoptosis in K562 cells and that they synergistically induced proteolytic activation of protein kinase C delta (PKCδ), while the effect was reversed by the PKCδ specific inhibitor rottlerin (Yan, Wang et al. 2007). Finally, Traf2 is a mediator of antiapoptotic signaling and might therefore also represent an attractive co-target (Natoli, Costanzo et al. 1998). These examples provide evidence that hub proteins within the Bcr-Abl signaling network might represent attractive alternative pharmacological targets. However, this hypothetical approach is overshadowed by the lack of functional consequence of knockdowns of the seven individual 'core' interactors (Figure 3.17), that this network is built on, and might at best give insights on potential target combinations to overcome the obvious signaling redundancy in Bcr-Abl-'addicted' cells. A recent genome-scale pooled shRNA screen of 12 cancer cell lines for essential cancer genes, including K562, identified four genes, PTPN1, NF1, SMARCB1 and SMARCE1 to be required for the response of CML cells to imatinib treatment (Luo, Cheung et al. 2008). Out of these, we find PTPN1, a negative regulator of Bcr-Abl signaling (Koyama, Koschmieder et al. 2006; LaMontagne, Flint et al. 1998), present in our simulated enlarged hybrid network (Figure 4.5) but not with the Bcr-Abl 'core' complex network (Figure 3.7, Figure 4.6).

Clearly, the presented network displays a focus on the interactions in the closest proximity to Bcr-Abl in K562 cells and may represent a starting point resource for further Bcr-Abl signaling studies in K562 cells.

4.10   Future perspectives

The protein-protein interaction network around the Bcr-Abl 'core' complex presented in this study represents a concise overview of the Bcr-Abl-proximal connection points to cellular signaling in K562 cells and a valuable resource of Bcr-Abl signaling (Figure 3.7). A large-scale extension of this signaling network, however, will be crucial for a refined picture of the more remote protein-protein interaction network around Bcr-Abl. The comprehensive functional analysis of these Bcr-Abl signaling networks and their components hold the potential to identify the crucial signal transduction pathways involved in Bcr-Abl mediated transformation. One of the major remaining challenges will then be the identification of key proteins within these pathways that are suitable for pharmacological targeting in synergy with Bcr-Abl, in order to tackle resistance complications associated with tyrosine kinase inhibitor therapy) (Azam, Latek et al. 2003; Cowan-Jacob, Fendrich et al. 2007; Daub, Specht et al. 2004; Druker 2006; Mohi, Boulton et al. 2004).

The identification of an eight component multi-protein complex around Bcr-Abl and the observation of its sensitivity to tyrosine kinase inhibitors led to the understanding that not just the polypeptide Bcr-Abl but also its 'first shell' of stoichiometric protein interactors is affected by the action of the drugs. This new concept, however, poses numerous novel challenges. Further experimental approaches are required to elucidate and refine our current models of the interaction architecture within this complex, the interaction stoichiometry as well as the overall size and macromolecular structure of the complex as an entity. Furthermore, while for some components, such as Grb2, the molecular interaction mode and the link to downstream signaling pathways are well described (Pendergast, Quilliam et al. 1993), the functional role of many of its individual components as a part of the complex, such as Ship2 and Sts-1, still remains elusive (Bantscheff, Eberhard et al. 2007). We were challenged by the fact that none of the siRNA perturbations of these complex components affected the fitness of K562 cells and it seems that 'oncogene addiction' of this model cell line is strictly limited to its oncogene, not to the oncogene protein complex. It will be rewarding to explore alternative targets that could be

harnessed to overcome Bcr-Abl 'addiction' and resistance to current tyrosine kinase inhibitors.

Finally, it remains to be shown, if this complex can also be identified in other Bcr-Abl positive model cell lines, in primary and patient cells and whether its composition is static or dynamic in nature with a differential composition between different patients and disease stages.

4.11   Final conclusions

Our study enables a novel view of the tyrosine kinase Bcr-Abl as the cognate target of tyrosine kinase inhibitors representing the current front-line therapy for chronic myelogenous leukemia. A two-pronged approach featuring the purification of endogenous complexes of Bcr-Abl from K562 cells and TAP-LC-MSMS analysis of its candidate stoichiometric interactors resulted in the quantitative identification of a highly significant and interconnected eight-component Bcr-Abl 'core' complex that is embedded in an interaction network of 90 proteins and links Bcr-Abl to different key signaling pathways. Furthermore, the network analysis reveals a new link to the endocytic AP2 adaptor protein complex. The components Bcr-Abl, Ship2, c-Cbl, p85, Shc1, Grb2, Crk-I and the novel Bcr-Abl interactor Sts-1 assemble into around 200,000 to 300,000 stoichiometric complexes per K562 cell. Quantitative proteomics analysis uncovered that tyrosine kinase inhibitors dramatically disrupt and remodel this complex, changing the view of the paradigmatic drug target Bcr-Abl as a single polypeptide to a multi-protein macromolecular machine. These data and the associated paradigm shift underline the importance of the functional understanding of drug targets for the elucidation of drug action in a proteomic and cellular context.

REFERENCES

5 REFERENCES

Adrian, F. J., Q. Ding, T. Sim, A. Velentza, C. Sloan, Y. Liu, G. Zhang, W. Hur, S. Ding, P. Manley, J. Mestan, D. Fabbro and N. S. Gray (2006). "Allosteric inhibitors of Bcr-abl-dependent cell proliferation." Nat Chem Biol 2(2): 95-102.

Advani, A. S. and A. M. Pendergast (2002). "Bcr-Abl variants: biological and clinical aspects." Leuk Res 26(8): 713-20.

Aebersold, R. (2003). "Constellations in a cellular universe." Nature 422(6928): 115-6.

Aebersold, R. and M. Mann (2003). "Mass spectrometry-based proteomics." Nature 422(6928): 198-207.

Agrawal, R., N. Carpino and A. Tsygankov (2008). "TULA proteins regulate activity of the protein tyrosine kinase Syk." J Cell Biochem 104(3): 953-64.

Amanchy, R., D. E. Kalume and A. Pandey (2005). "Stable isotope labeling with amino acids in cell culture (SILAC) for studying dynamics of protein abundance and posttranslational modifications." Sci STKE 2005(267): pl2.

Andersen, J. S., C. J. Wilkinson, T. Mayor, P. Mortensen, E. A. Nigg and M. Mann (2003). "Proteomic characterization of the human centrosome by protein correlation profiling." Nature 426(6966): 570-4.

Arlinghaus, R. B. (2002). "Bcr: a negative regulator of the Bcr-Abl oncoprotein in leukemia." Oncogene 21(56): 8560-7.

Arnold, K. (2001). "After 30 years of laboratory work, a quick approval for STI571." J Natl Cancer Inst 93(13): 972.

Azam, M., R. R. Latek and G. Q. Daley (2003). "Mechanisms of Autoinhibition and STI-571/Imatinib Resistance Revealed by Mutagenesis of BCR-ABL." Cell 112(6): 831-43.

Azam, M., T. Raz, V. Nardi, S. L. Opitz and G. Q. Daley (2003). "A screen to identify drug resistant variants to target-directed anti-cancer agents." Biol Proced Online 5: 204-210.

Bai, R. Y., T. Jahn, S. Schrem, G. Munzert, K. M. Weidner, J. Y. Wang and J. Duyster (1998). "The SH2-containing adapter protein GRB10 interacts with BCR-ABL." Oncogene 17(8): 941-8.

Bandyopadhyay, G., T. Biswas, K. C. Roy, S. Mandal, C. Mandal, B. C. Pal, S. Bhattacharya, S. Rakshit, D. K. Bhattacharya, U. Chaudhuri, A. Konar and S. Bandyopadhyay (2004). "Chlorogenic acid inhibits Bcr-Abl tyrosine kinase and triggers p38 mitogen-activated protein kinase-dependent apoptosis in chronic myelogenous leukemic cells." Blood 104(8): 2514-22.

Bantscheff, M., D. Eberhard, Y. Abraham, S. Bastuck, M. Boesche, S. Hobson, T. Mathieson, J. Perrin, M. Raida, C. Rau, V. Reader, G. Sweetman, A. Bauer, T. Bouwmeester, C. Hopf, U. Kruse, G. Neubauer, N. Ramsden, J. Rick, B. Kuster and G. Drewes (2007). "Quantitative chemical proteomics reveals mechanisms of action of clinical ABL kinase inhibitors." Nat Biotechnol 25(9): 1035-44.

Barilá, D. and G. Superti-Furga (1998). "An intramolecular SH3-domain interaction regulates c-Abl activity." Nature Genet. 18: 280-282.

Barnes, D. J., D. Palaiologou, E. Panousopoulou, B. Schultheis, A. S. Yong, A. Wong, L. Pattacini, J. M. Goldman and J. V. Melo (2005). "Bcr-Abl expression levels determine the rate of development of resistance to imatinib mesylate in chronic myeloid leukemia." Cancer Res 65(19): 8912-9.

Bartram, C. R., A. de Klein, A. Hagemeijer, T. van Agthoven, A. Geurts van Kessel, D. Bootsma, G. Grosveld, M. A. Ferguson-Smith, T. Davies, M. Stone and et al. (1983). "Translocation of c-abl oncogene correlates with the presence of a Philadelphia chromosome in chronic myelocytic leukaemia." Nature 306(5940): 277-80.

Bassermann, F., T. Jahn, C. Miething, P. Seipel, R. Y. Bai, S. Coutinho, V. L. Tybulewicz, C. Peschel and J. Duyster (2002). "Association of Bcr-Abl with the proto-oncogene Vav is implicated in activation of the Rac-1 pathway." J Biol Chem 277(14): 12437-45.

Beattie, E. C., C. L. Howe, A. Wilde, F. M. Brodsky and W. C. Mobley (2000). "NGF signals through TrkA to increase clathrin at the plasma membrane and enhance clathrin-mediated membrane trafficking." J Neurosci 20(19): 7325-33.

Beissert, T., E. Puccetti, A. Bianchini, S. Guller, S. Boehrer, D. Hoelzer, O. G. Ottmann, C. Nervi and M. Ruthardt (2003). "Targeting of the N-terminal coiled coil oligomerization interface of BCR interferes with the transformation potential of BCR-ABL and increases sensitivity to STI571." Blood 102(8): 2985-93.

Ben-Neriah, Y., G. Q. Daley, A. M. Mes-Masson, O. N. Witte and D. Baltimore (1986). "The chronic myelogenous leukemia-specific P210 protein is the product of the bcr/abl hybrid gene." Science 233(4760): 212-4.

Benmerah, A., J. Gagnon, B. Begue, B. Megarbane, A. Dautry-Varsat and N. Cerf-Bensussan (1995). "The tyrosine kinase substrate eps15 is constitutively associated with the plasma membrane adaptor AP-2." J Cell Biol 131(6 Pt 2): 1831-8.

Benmerah, A., C. Lamaze, B. Begue, S. L. Schmid, A. Dautry-Varsat and N. Cerf-Bensussan (1998). "AP-2/Eps15 interaction is required for receptor-mediated endocytosis." J Cell Biol 140(5): 1055-62.

Bennett, J. (1845). "Case of hypertrophy of the spleen liver, in which death took place from suppuration of the blood." Edinb. Med. Surg. J. 64: 413-23.

Beynon, R. J., M. K. Doherty, J. M. Pratt and S. J. Gaskell (2005). "Multiplexed absolute quantification in proteomics using artificial QCAT proteins of concatenated signature peptides." Nat Methods 2(8): 587-9.

Bleicher, K. H., H. J. Bohm, K. Muller and A. I. Alanine (2003). "Hit and lead generation: beyond high-throughput screening." Nat Rev Drug Discov 2(5): 369-78.

Booker, G. W., A. L. Breeze, A. K. Downing, G. Panayotou, I. Gout, M. D. Waterfield and I. D. Campbell (1992). "Structure of an SH2 domain of the p85 alpha subunit of phosphatidylinositol-3-OH kinase." Nature 358(6388): 684-7.

Bouwmeester, T., A. Bauch, H. Ruffner, P. O. Angrand, G. Bergamini, K. Croughton, C. Cruciat, D. Eberhard, J. Gagneur, S. Ghidelli, C. Hopf, B. Huhse, R. Mangano, A. M. Michon, M. Schirle, J. Schlegl, M. Schwab, M. A. Stein, A. Bauer, G. Casari, G. Drewes, A. C. Gavin, D. B. Jackson, G. Joberty, G. Neubauer, J. Rick, B. Kuster and G. Superti-Furga (2004). "A physical and functional map of the human TNF-alpha/NF-kappa B signal transduction pathway." Nat Cell Biol 6(2): 97-105.

Brajenovic, M., G. Joberty, B. Kuster, T. Bouwmeester and G. Drewes (2004). "Comprehensive proteomic analysis of human Par protein complexes reveals an interconnected protein network." J Biol Chem 279(13): 12804-11.

Brasher, B. B. and R. A. Van Etten (2000). "c-Abl has high intrinsic tyrosine kinase activity that is stimulated by mutation of the src homology 3 domain and by autophosphorylation at two distinct regulatory tyrosines." J Biol Chem 275(45): 35631-7.

Brown, D. and G. Superti-Furga (2003). "Rediscovering the sweet spot in drug discovery." Drug Discov Today 8(23): 1067-77.

Buchdunger, E., C. L. Cioffi, N. Law, D. Stover, S. Ohno-Jones, B. J. Druker and N. B. Lydon (2000). "Abl protein-tyrosine kinase inhibitor STI571 inhibits in vitro signal transduction mediated by c-kit and platelet-derived growth factor receptors." J Pharmacol Exp Ther 295(1): 139-45.

Buchdunger, E., J. Zimmermann, H. Mett, T. Meyer, M. Muller, B. J. Druker and N. B. Lydon (1996). "Inhibition of the Abl protein-tyrosine kinase in vitro and in vivo by a 2-phenylaminopyrimidine derivative." Cancer Res 56(1): 100-4.

Buchdunger, E., J. Zimmermann, H. Mett, T. Meyer, M. Muller, U. Regenass and N. B. Lydon (1995). "Selective inhibition of the platelet-derived growth factor signal transduction pathway by a protein-tyrosine kinase inhibitor of the 2-phenylaminopyrimidine class." Proc Natl Acad Sci U S A 92(7): 2558-62.

Burckstummer, T., K. L. Bennett, A. Preradovic, G. Schutze, O. Hantschel, G. Superti-Furga and A. Bauch (2006). "An efficient tandem affinity purification procedure for interaction proteomics in mammalian cells." Nat Methods 3(12): 1013-9.

Calabretta, B. and D. Perrotti (2004). "The biology of CML blast crisis." Blood 103(11): 4010-22.

Calderwood, M. A., K. Venkatesan, L. Xing, M. R. Chase, A. Vazquez, A. M. Holthaus, A. E. Ewence, N. Li, T. Hirozane-Kishikawa, D. E. Hill, M. Vidal, E. Kieff and E. Johannsen (2007). "Epstein-Barr virus and virus human protein interaction maps." Proc Natl Acad Sci U S A 104(18): 7606-11.

Campillos, M., M. Kuhn, A. C. Gavin, L. J. Jensen and P. Bork (2008). "Drug target identification using side-effect similarity." Science 321(5886): 263-6.

Capdeville, R., E. Buchdunger, J. Zimmermann and A. Matter (2002). "Glivec (STI571, imatinib), a rationally developed, targeted anticancer drug." Nat Rev Drug Discov 1(7): 493-502.

Carpino, N., R. Kobayashi, H. Zang, Y. Takahashi, S. T. Jou, J. Feng, H. Nakajima and J. N. Ihle (2002). "Identification, cDNA cloning, and targeted deletion of p70, a novel, ubiquitously expressed SH3 domain-containing protein." Mol Cell Biol 22(21): 7491-500.

Carpino, N., S. Turner, D. Mekala, Y. Takahashi, H. Zang, T. L. Geiger, P. Doherty and J. N. Ihle (2004). "Regulation of ZAP-70 activation and TCR signaling by two related proteins, Sts-1 and Sts-2." Immunity 20(1): 37-46.

Chen, J., W. M. Yu, H. Daino, H. E. Broxmeyer, B. J. Druker and C. K. Qu (2007). "SHP-2 phosphatase is required for hematopoietic cell transformation by Bcr-Abl." Blood 109(2): 778-85.

Chen, R., V. Gandhi and W. Plunkett (2006). "A sequential blockade strategy for the design of combination therapies to overcome oncogene addiction in chronic myelogenous leukemia." Cancer Res 66(22): 10959-66.

Chen, Y., J. Jakoncic, N. Carpino and N. Nassar (2009). "Structural and Functional Characterization of the 2H-Phosphatase Domain of Sts-2 Reveals an Acid-Dependent Phosphatase Activity (dagger)." Biochemistry.

Chu, S., M. Holtz, M. Gupta and R. Bhatia (2004). "BCR/ABL kinase inhibition by imatinib mesylate enhances MAP kinase activity in chronic myelogenous leukemia CD34+ cells." Blood 103(8): 3167-74.

Chu, S., L. Li, H. Singh and R. Bhatia (2007). "BCR-tyrosine 177 plays an essential role in Ras and Akt activation and in human hematopoietic progenitor transformation in chronic myelogenous leukemia." Cancer Res 67(14): 7045-53.

Cicchetti, P., B. J. Mayer, G. Thiel and D. Baltimore (1992). "Identification of a protein that binds to the SH3 region of Abl and is similar to Bcr and GAP-rho." Science 257: 803-806.

Clarkson, B., A. Strife, D. Wisniewski, C. L. Lambek and C. Liu (2003). "Chronic myelogenous leukemia as a paradigm of early cancer and possible curative strategies." Leukemia 17(7): 1211-62.

Colinge, J., D. Chiappe, S. Lagache, M. Moniatte and L. Bougueleret (2005). "Differential proteomics via probabilistic peptide identification scores." Anal Chem 77(2): 596-606.

Collins, S. J. and M. T. Groudine (1983). "Rearrangement and amplification of c-abl sequences in the human chronic myelogenous leukemia cell line K-562." Proc Natl Acad Sci U S A 80(15): 4813-7.

Cong, F., S. Spencer, J. F. Cote, Y. Wu, M. L. Tremblay, L. A. Lasky and S. P. Goff (2000). "Cytoskeletal protein PSTPIP1 directs the PEST-type protein tyrosine phosphatase to the c-Abl kinase to mediate Abl dephosphorylation." Mol Cell 6(6): 1413-23.

Coutinho, S., T. Jahn, M. Lewitzky, S. Feller, P. Hutzler, C. Peschel and J. Duyster (2000). "Characterization of Ggrb4, an adapter protein interacting with Bcr-Abl." Blood 96(2): 618-24.

Cowan-Jacob, S. W., G. Fendrich, A. Floersheimer, P. Furet, J. Liebetanz, G. Rummel, P. Rheinberger, M. Centeleghe, D. Fabbro and P. W. Manley (2007). "Structural biology contributions to the discovery of drugs to treat chronic myelogenous leukaemia." Acta Crystallogr D Biol Crystallogr 63(Pt 1): 80-93.

Cox, J. and M. Mann (2008). "MaxQuant enables high peptide identification rates, individualized p.p.b.-range mass accuracies and proteome-wide protein quantification." Nat Biotechnol 26(12): 1367-72.

Craigie, D. (1845). "Case of disease of the spleen, in which death took place in consequence of the presence of purulent matter in the blood." Edinb. Med. Surg. J. 64: 400-13.

Dai, Z. and A. M. Pendergast (1995). "Abi-2, a novel SH3-containing protein interacts with the c-Abl tyrosine kinase and modulates c-Abl transforming activity." Genes & Dev 9: 2596-2582.

Daley, G. Q., R. A. Van Etten and D. Baltimore (1990). "Induction of chronic myelogenous leukemia in mice by the P210bcr/abl gene of the Philadelphia chromosome." Science 247(4944): 824-30.

Danial, N. N., A. Pernis and P. B. Rothman (1995). "Jak-STAT signaling induced by the v-abl oncogene." Science 269(5232): 1875-7.

Danial, N. N. and P. Rothman (2000). "JAK-STAT signaling activated by Abl oncogenes." Oncogene 19(21): 2523-31.

Daub, H. (2005). "Characterisation of kinase-selective inhibitors by chemical proteomics." Biochim Biophys Acta 1754(1-2): 183-90.

Daub, H., K. Specht and A. Ullrich (2004). "Strategies to overcome resistance to targeted protein kinase inhibitors." Nat Rev Drug Discov 3(12): 1001-10.

de Godoy, L. M., J. V. Olsen, J. Cox, M. L. Nielsen, N. C. Hubner, F. Frohlich, T. C. Walther and M. Mann (2008). "Comprehensive mass-spectrometry-based proteome quantification of haploid versus diploid yeast." Nature 455(7217): 1251-4.

de Klein, A., A. G. van Kessel, G. Grosveld, C. R. Bartram, A. Hagemeijer, D. Bootsma, N. K. Spurr, N. Heisterkamp, J. Groffen and J. R. Stephenson (1982). "A cellular oncogene is translocated to the Philadelphia chromosome in chronic myelocytic leukaemia." Nature 300(5894): 765-7.

Deininger, M., E. Buchdunger and B. J. Druker (2005). "The development of imatinib as a therapeutic agent for chronic myeloid leukemia." Blood 105(7): 2640-53.

Deininger, M. W., J. M. Goldman, N. Lydon and J. V. Melo (1997). "The tyrosine kinase inhibitor CGP57148B selectively inhibits the growth of BCR-ABL-positive cells." Blood 90(9): 3691-8.

Deininger, M. W., J. M. Goldman and J. V. Melo (2000). "The molecular biology of chronic myeloid leukemia." Blood 96(10): 3343-56.

Deutsch, E., A. Dugray, B. AbdulKarim, E. Marangoni, L. Maggiorella, S. Vaganay, R. M'Kacher, S. D. Rasy, F. Eschwege, W. Vainchenker, A. G. Turhan and J. Bourhis (2001). "BCR-ABL down-regulates the DNA repair protein DNA-PKcs." Blood 97(7): 2084-90.

Diekmann, D., S. Brill, M. D. Garrett, N. Totty, J. Hsuan, C. Monfries, C. Hall, L. Lim and A. Hall (1991). "Bcr encodes a GTPase-activating protein for p21rac." Nature 351(6325): 400-2.

Dimery, I. W., D. D. Ross, J. R. Testa, S. K. Gupta, R. L. Felsted, A. Pollak and N. R. Bachur (1983). "Variation amongst K562 cell cultures." Exp Hematol 11(7): 601-10.

Donato, N. J., J. Y. Wu, J. Stapley, G. Gallick, H. Lin, R. Arlinghaus and M. Talpaz (2003). "BCR-ABL independence and LYN kinase overexpression in chronic myelogenous leukemia cells selected for resistance to STI571." Blood 101(2): 690-8.

Dorey, K., J. R. Engen, J. Kretzschmar, M. Wilm, G. Neubauer, T. Schindler and G. Superti-Furga (2001). "Phosphorylation and structure-based functional studies reveal a positive and a negative role for the activation loop of the c-Abl tyrosine kinase." Oncogene 20(56): 8075-84.

Drewes, G. and T. Bouwmeester (2003). "Global approaches to protein-protein interactions." Curr Opin Cell Biol 15(2): 199-205.

Druker, B. J. (2006). "Circumventing resistance to kinase-inhibitor therapy." N Engl J Med 354(24): 2594-6.

Druker, B. J. (2004). "Imatinib as a paradigm of targeted therapies." Adv Cancer Res 91: 1-30.

Druker, B. J. (2008). "Translation of the Philadelphia chromosome into therapy for CML." Blood 112(13): 4808-17.

Druker, B. J., S. G. O'Brien, J. Cortes and J. Radich (2002). "Chronic myelogenous leukemia." Hematology Am Soc Hematol Educ Program: 111-35.

Druker, B. J., C. L. Sawyers, R. Capdeville, J. M. Ford, M. Baccarani and J. M. Goldman (2001). "Chronic myelogenous leukemia." Hematology (Am Soc Hematol Educ Program): 87-112.

Druker, B. J., C. L. Sawyers, H. Kantarjian, D. J. Resta, S. F. Reese, J. M. Ford, R. Capdeville and M. Talpaz (2001). "Activity of a specific inhibitor of the BCR-ABL tyrosine kinase in the blast crisis of chronic myeloid leukemia and acute lymphoblastic leukemia with the Philadelphia chromosome." N Engl J Med 344(14): 1038-42.

Druker, B. J., M. Talpaz, D. J. Resta, B. Peng, E. Buchdunger, J. M. Ford, N. B. Lydon, H. Kantarjian, R. Capdeville, S. Ohno-Jones and C. L. Sawyers (2001). "Efficacy and safety of a specific inhibitor of the BCR-ABL tyrosine kinase in chronic myeloid leukemia." N Engl J Med 344(14): 1031-7.

Druker, B. J., S. Tamura, E. Buchdunger, S. Ohno, G. M. Segal, S. Fanning, J. Zimmermann and N. B. Lydon (1996). "Effects of a selective inhibitor of the Abl tyrosine kinase on the growth of Bcr-Abl positive cells." Nat Med 2(5): 561-6.

Evans, W. E. and H. L. McLeod (2003). "Pharmacogenomics--drug disposition, drug targets, and side effects." N Engl J Med 348(6): 538-49.

Ezaki, K. (2000). "Interferon-alpha and cytosine arabinoside therapy in chronic myeloid leukemia." Gan To Kagaku Ryoho 27 Suppl 2: 279-84.

Fan, P. D., F. Cong and S. P. Goff (2003). "Homo- and hetero-oligomerization of the c-Abl kinase and Abelson-interactor-1." Cancer Res 63(4): 873-7.

Feller, S. M., B. Knudsen and H. Hanafusa (1994). "c-Abl kinase regulates the protein binding activity of c-Crk." EMBO J. 13: 2341-2351.

Feller, S. M., G. Posern, J. Voss, C. Kardinal, D. Sakkab, J. Zheng and B. S. Knudsen (1998). "Physiological signals and oncogenesis mediated through Crk family adapter proteins." J Cell Physiol 177(4): 535-52.

Felsher, D. W. and J. M. Bishop (1999). "Reversible tumorigenesis by MYC in hematopoietic lineages." Mol Cell 4(2): 199-207.

Ferrajoli, A., A. M. Liberati, P. Caricchi, E. Donti, E. Morra, M. Lazzarino, A. R. Betti, P. Bernasconi and G. Saglio (1995). "Interferon-alpha plus low-dose cytosine arabinoside in advanced phase chronic myelogenous leukaemia patients." Eur J Haematol 55(3): 184-8.

Frank, D. A. and L. Varticovski (1996). "BCR/abl leads to the constitutive activation of Stat proteins, and shares an epitope with tyrosine phosphorylated Stats." Leukemia 10(11): 1724-30.

Fukazawa, T., S. Miyake, V. Band and H. Band (1996). "Tyrosine phosphorylation of Cbl upon epidermal growth factor (EGF) stimulation and its association with EGF receptor and downstream signaling proteins." J Biol Chem 271(24): 14554-9.

Gaston, I., K. J. Johnson, T. Oda, A. Bhat, M. Reis, W. Langdon, L. Shen, M. W. Deininger and B. J. Druker (2004). "Coexistence of phosphotyrosine-dependent and -independent interactions between Cbl and Bcr-Abl." Exp Hematol 32(1): 113-21.

Gavin, A. C., P. Aloy, P. Grandi, R. Krause, M. Boesche, M. Marzioch, C. Rau, L. J. Jensen, S. Bastuck, B. Dumpelfeld, A. Edelmann, M. A. Heurtier, V. Hoffman, C. Hoefert, K. Klein, M. Hudak, A. M. Michon, M. Schelder, M. Schirle, M. Remor, T. Rudi, S. Hooper, A. Bauer, T. Bouwmeester, G. Casari, G. Drewes, G. Neubauer, J. M. Rick, B. Kuster, P. Bork, R. B. Russell and G. Superti-Furga (2006). "Proteome survey reveals modularity of the yeast cell machinery." Nature.

Gavin, A. C., M. Bosche, R. Krause, P. Grandi, M. Marzioch, A. Bauer, J. Schultz, J. M. Rick, A. M. Michon, C. M. Cruciat, M. Remor, C. Hofert, M. Schelder, M. Brajenovic, H. Ruffner, A. Merino, K. Klein, M. Hudak, D. Dickson, T. Rudi, V. Gnau, A. Bauch, S. Bastuck, B. Huhse, C. Leutwein, M. A. Heurtier, R. R. Copley, A. Edelmann, E. Querfurth, V. Rybin, G. Drewes, M. Raida, T. Bouwmeester, P. Bork, B. Seraphin, B. Kuster, G. Neubauer and G. Superti-Furga (2002). "Functional organization of the yeast proteome by systematic analysis of protein complexes." Nature 415(6868): 141-7.

Gavin, A. C. and G. Superti-Furga (2003). "Protein complexes and proteome organization from yeast to man." Current Opinion in Chemical Biology 7(1): 21-27.

Geering, B., P. R. Cutillas, G. Nock, S. I. Gharbi and B. Vanhaesebroeck (2007). "Class IA phosphoinositide 3-kinases are obligate p85-p110 heterodimers." Proc Natl Acad Sci U S A 104(19): 7809-14.

Gerber, S. A., J. Rush, O. Stemman, M. W. Kirschner and S. P. Gygi (2003). "Absolute quantification of proteins and phosphoproteins from cell lysates by tandem MS." Proc Natl Acad Sci U S A 100(12): 6940-5.

Gingras, A. C., M. Gstaiger, B. Raught and R. Aebersold (2007). "Analysis of protein complexes using mass spectrometry." Nat Rev Mol Cell Biol 8(8): 645-54.

Goga, A., J. McLaughlin, D. E. Afar, D. C. Saffran and O. N. Witte (1995). "Alternative signals to RAS for hematopoietic transformation by the BCR-ABL oncogene." Cell 82(6): 981-8.

Goh, K. I., M. E. Cusick, D. Valle, B. Childs, M. Vidal and A. L. Barabasi (2007). "The human disease network." Proc Natl Acad Sci U S A 104(21): 8685-90.

Golas, J. M., K. Arndt, C. Etienne, J. Lucas, D. Nardin, J. Gibbons, P. Frost, F. Ye, D. H. Boschelli and F. Boschelli (2003). "SKI-606, a 4-anilino-3-quinolinecarbonitrile dual inhibitor of Src and Abl kinases, is a potent antiproliferative agent against chronic myelogenous leukemia cells in culture and causes regression of K562 xenografts in nude mice." Cancer Res 63(2): 375-81.

Goldman, J. M. (2004). "Chronic myeloid leukemia-still a few questions." Exp Hematol 32(1): 2-10.

Goldman, J. M. and J. V. Melo (2003). "Chronic myeloid leukemia--advances in biology and new approaches to treatment." N Engl J Med 349(15): 1451-64.

Gorre, M. E., M. Mohammed, K. Ellwood, N. Hsu, R. Paquette, P. N. Rao and C. L. Sawyers (2001). "Clinical resistance to STI-571 cancer therapy caused by BCR-ABL gene mutation or amplification." Science 293(5531): 876-80.

Goss, V. L., K. A. Lee, A. Moritz, J. Nardone, E. J. Spek, J. Macneill, J. Rush, M. J. Comb and R. D. Polakiewicz (2006). "A common phosphotyrosine signature for the Bcr-Abl kinase." Blood.

Goss, V. L., K. A. Lee, A. Moritz, J. Nardone, E. J. Spek, J. MacNeill, J. Rush, M. J. Comb and R. D. Polakiewicz (2006). "A common phosphotyrosine signature for the Bcr-Abl kinase." Blood 107(12): 4888-97.

Grandi, P., V. Rybin, J. Bassler, E. Petfalski, D. Strauss, M. Marzioch, T. Schafer, B. Kuster, H. Tschochner, D. Tollervey, A. C. Gavin and E. Hurt (2002). "90S pre-ribosomes include the 35S pre-rRNA, the U3 snoRNP, and 40S subunit processing factors but predominantly lack 60S synthesis factors." Mol Cell 10(1): 105-15.

Griswold, I. J., M. MacPartlin, T. Bumm, V. L. Goss, T. O'Hare, K. A. Lee, A. S. Corbin, E. P. Stoffregen, C. Smith, K. Johnson, E. M. Moseson, L. J. Wood, R. D. Polakiewicz, B. J. Druker and M. W. Deininger (2006). "Kinase domain mutants of Bcr-Abl exhibit altered transformation potency, kinase activity, and substrate utilization, irrespective of sensitivity to imatinib." Mol Cell Biol 26(16): 6082-93.

Groffen, J., J. R. Stephenson, N. Heisterkamp, A. de Klein, C. R. Bartram and G. Grosveld (1984). "Philadelphia chromosomal breakpoints are clustered within a limited region, bcr, on chromosome 22." Cell 36(1): 93-9.

Guilhot, F., J. Apperley, D. W. Kim, E. O. Bullorsky, M. Baccarani, G. J. Roboz, S. Amadori, C. A. de Souza, J. H. Lipton, A. Hochhaus, D. Heim, R. A. Larson, S. Branford, M. C. Muller, P. Agarwal, A. Gollerkeri and M. Talpaz (2007). "Dasatinib induces significant hematologic and cytogenetic responses in patients with imatinib-resistant or -intolerant chronic myeloid leukemia in accelerated phase." Blood 109(10): 4143-50.

Gumireddy, K., S. J. Baker, S. C. Cosenza, P. John, A. D. Kang, K. A. Robell, M. V. Reddy and E. P. Reddy (2005). "A non-ATP-competitive inhibitor of BCR-ABL overrides imatinib resistance." Proc Natl Acad Sci U S A 102(6): 1992-7.

Gygi, S. P., B. Rist, S. A. Gerber, F. Turecek, M. H. Gelb and R. Aebersold (1999). "Quantitative analysis of complex protein mixtures using isotope-coded affinity tags." Nat Biotechnol 17(10): 994-9.

Haffner, C., K. Takei, H. Chen, N. Ringstad, A. Hudson, M. H. Butler, A. E. Salcini, P. P. Di Fiore and P. De Camilli (1997). "Synaptojanin 1: localization on coated endocytic intermediates in nerve terminals and interaction of its 170 kDa isoform with Eps15." FEBS Lett 419(2-3): 175-80.

Hanahan, D. and R. A. Weinberg (2000). "The hallmarks of cancer." Cell 100(1): 57-70.

Hantschel, O., A. Gstoettenbauer, J. Colinge, I. Kaupe, M. Bilban, T. R. Burkard, P. Valent and G. Superti-Furga (2008). "The chemokine interleukin-8 and the surface activation protein CD69 are markers for Bcr-Abl activity in chronic myeloid leukemia." Mol Onc 2(3): 272-281.

Hantschel, O., B. Nagar, S. Guettler, J. Kretzschmar, K. Dorey, J. Kuriyan and G. Superti-Furga (2003). "A Myristoyl/Phosphotyrosine Switch Regulates c-Abl." Cell 112(6): 845-57.

Hantschel, O., U. Rix, U. Schmidt, T. Burckstummer, M. Kneidinger, G. Schutze, J. Colinge, K. L. Bennett, W. Ellmeier, P. Valent and G. Superti-Furga (2007). "The Btk tyrosine kinase is a major target of the Bcr-Abl inhibitor dasatinib." Proc Natl Acad Sci U S A 104(33): 13283-8.

Hantschel, O., U. Rix and G. Superti-Furga (2008). "Target spectrum of the Bcr-Abl inhibitors imatinib, nilotinib and dasatinib." Leuk Lymphoma in press.

Hantschel, O. and G. Superti-Furga (2004). "Regulation of the c-Abl and Bcr-Abl Tyrosine Kinases." Nat Rev Mol Cell Biol 5(1): 33-44.

Hantschel, O., S. Wiesner, T. Guttler, C. D. Mackereth, L. L. Rix, Z. Mikes, J. Dehne, D. Gorlich, M. Sattler and G. Superti-Furga (2005). "Structural basis for the cytoskeletal association of Bcr-Abl/c-Abl." Mol Cell 19(4): 461-73.

Harir, N., C. Pecquet, M. Kerenyi, K. Sonneck, B. Kovacic, R. Nyga, M. Brevet, I. Dhennin, V. Gouilleux-Gruart, H. Beug, P. Valent, K. Lassoued, R. Moriggl and F. Gouilleux (2007). "Constitutive activation of Stat5 promotes its cytoplasmic localization and association with PI3-kinase in myeloid leukemias." Blood 109(4): 1678-86.

Harnois, T., B. Constantin, A. Rioux, E. Grenioux, A. Kitzis and N. Bourmeyster (2003). "Differential interaction and activation of Rho family GTPases by p210bcr-abl and p190bcr-abl." Oncogene 22(41): 6445-54.

Harrison, S. C. (2003). "Variation on an Src-like Theme." Cell 112(6): 737-40.

Hermjakob, H., L. Montecchi-Palazzi, C. Lewington, S. Mudali, S. Kerrien, S. Orchard, M. Vingron, B. Roechert, P. Roepstorff, A. Valencia, H. Margalit, J. Armstrong, A. Bairoch, G. Cesareni, D. Sherman and R. Apweiler (2004). "IntAct: an open source molecular interaction database." Nucleic Acids Res 32(Database issue): D452-5.

Hoeller, D., N. Crosetto, B. Blagoev, C. Raiborg, R. Tikkanen, S. Wagner, K. Kowanetz, R. Breitling, M. Mann, H. Stenmark and I. Dikic (2006). "Regulation of ubiquitin-binding proteins by monoubiquitination." Nat Cell Biol 8(2): 163-9.

Hoover, R. R., F. X. Mahon, J. V. Melo and G. Q. Daley (2002). "Overcoming STI571 resistance with the farnesyl transferase inhibitor SCH66336." Blood 100(3): 1068-71.

Hornbeck, P. V., I. Chabra, J. M. Kornhauser, E. Skrzypek and B. Zhang (2004). "PhosphoSite: A bioinformatics resource dedicated to physiological protein phosphorylation." Proteomics 4(6): 1551-61.

Hu, Y., Y. Liu, S. Pelletier, E. Buchdunger, M. Warmuth, D. Fabbro, M. Hallek, R. A. Van Etten and S. Li (2004). "Requirement of Src kinases Lyn, Hck and Fgr for BCR-ABL1-induced B-lymphoblastic leukemia but not chronic myeloid leukemia." Nat Genet 36(5): 453-61.

Huang, Y., E. O. Comiskey, R. S. Dupree, S. Li, A. J. Koleske and J. K. Burkhardt (2008). "The c-Abl tyrosine kinase regulates actin remodeling at the immune synapse." Blood 112(1): 111-9.

Huettner, C. S., P. Zhang, R. A. Van Etten and D. G. Tenen (2000). "Reversibility of acute B-cell leukaemia induced by BCR-ABL1." Nat Genet 24(1): 57-60.

Iannolo, G., A. E. Salcini, I. Gaidarov, O. B. Goodman, Jr., J. Baulida, G. Carpenter, P. G. Pelicci, P. P. Di Fiore and J. H. Keen (1997). "Mapping of the molecular determinants involved in the interaction between eps15 and AP-2." Cancer Res 57(2): 240-5.

Ilaria, R. L., Jr. and R. A. Van Etten (1996). "P210 and P190(BCR/ABL) induce the tyrosine phosphorylation and DNA binding activity of multiple specific STAT family members." J Biol Chem 271(49): 31704-10.

Jain, M., C. Arvanitis, K. Chu, W. Dewey, E. Leonhardt, M. Trinh, C. D. Sundberg, J. M. Bishop and D. W. Felsher (2002). "Sustained loss of a neoplastic phenotype by brief inactivation of MYC." Science 297(5578): 102-4.

Jennings, B. A. and K. I. Mills (1998). "c-myc locus amplification and the acquisition of trisomy 8 in the evolution of chronic myeloid leukaemia." Leuk Res 22(10): 899-903.

Johannessen, L. E., N. M. Pedersen, K. W. Pedersen, I. H. Madshus and E. Stang (2006). "Activation of the epidermal growth factor (EGF) receptor induces formation of EGF receptor- and Grb2-containing clathrin-coated pits." Mol Cell Biol 26(2): 389-401.

Juric, D., N. J. Lacayo, M. C. Ramsey, J. Racevskis, P. H. Wiernik, J. M. Rowe, A. H. Goldstone, P. J. O'Dwyer, E. Paietta and B. I. Sikic (2007). "Differential gene expression patterns and interaction networks in BCR-ABL-positive and -negative adult acute lymphoblastic leukemias." J Clin Oncol 25(11): 1341-9.

Kantarjian, H., F. Giles, L. Wunderle, K. Bhalla, S. O'Brien, B. Wassmann, C. Tanaka, P. Manley, P. Rae, W. Mietlowski, K. Bochinski, A. Hochhaus, J. D. Griffin, D. Hoelzer, M. Albitar, M. Dugan, J. Cortes, L. Alland and O. G. Ottmann (2006). "Nilotinib in imatinib-resistant CML and Philadelphia chromosome-positive ALL." N Engl J Med 354(24): 2542-51.

Kantarjian, H., C. Sawyers, A. Hochhaus, F. Guilhot, C. Schiffer, C. Gambacorti-Passerini, D. Niederwieser, D. Resta, R. Capdeville, U. Zoellner, M. Talpaz, B. Druker, J. Goldman, S. G. O'Brien, N. Russell, T. Fischer, O. Ottmann, P. Cony-Makhoul, T. Facon, R. Stone, C. Miller, M. Tallman, R. Brown, M. Schuster, T. Loughran, A. Gratwohl, F. Mandelli, G. Saglio, M. Lazzarino, D. Russo, M. Baccarani and E. Morra (2002). "Hematologic and cytogenetic responses to imatinib mesylate in chronic myelogenous leukemia." N Engl J Med 346(9): 645-52.

Kantarjian, H. M., S. O'Brien, J. E. Cortes, J. Shan, F. J. Giles, M. B. Rios, S. H. Faderl, W. G. Wierda, A. Ferrajoli, S. Verstovsek, M. J. Keating, E. J. Freireich and M. Talpaz (2003). "Complete cytogenetic and molecular responses to interferon-alpha-based therapy for chronic myelogenous leukemia are associated with excellent long-term prognosis." Cancer 97(4): 1033-41.

Kantarjian, H. M., M. Talpaz, S. O'Brien, F. Giles, G. Garcia-Manero, S. Faderl, D. Thomas, J. Shan, M. B. Rios and J. Cortes (2003). "Dose escalation of imatinib mesylate can overcome resistance to standard-dose therapy in patients with chronic myelogenous leukemia." Blood 101(2): 473-5.

Kelly, B. T., A. J. McCoy, K. Spate, S. E. Miller, P. R. Evans, S. Honing and D. J. Owen (2008). "A structural explanation for the binding of endocytic dileucine motifs by the AP2 complex." Nature 456(7224): 976-979.

Kersey, P. J., J. Duarte, A. Williams, Y. Karavidopoulou, E. Birney and R. Apweiler (2004). "The International Protein Index: an integrated database for proteomics experiments." Proteomics 4(7): 1985-8.

Kin, Y., M. Shibuya and Y. Maru (2001). "Inhibition of protein kinase C delta has negative effect on anchorage-independent growth of BCR-ABL-transformed Rat1 cells." Leuk Res 25(9): 821-5.

Kipreos, E. T. and J. Y. Wang (1992). "Cell cycle-regulated binding of c-Abl tyrosine kinase to DNA." Science 256(5055): 382-5.

Klein, E., H. Ben-Bassat, H. Neumann, P. Ralph, J. Zeuthen, A. Polliack and F. Vanky (1976). "Properties of the K562 cell line, derived from a patient with chronic myeloid leukemia." Int J Cancer 18(4): 421-31.

Klejman, A., L. Rushen, A. Morrione, A. Slupianek and T. Skorski (2002). "Phosphatidylinositol-3 kinase inhibitors enhance the anti-leukemia effect of STI571." Oncogene 21(38): 5868-76.

Klejman, A., S. J. Schreiner, M. Nieborowska-Skorska, A. Slupianek, M. Wilson, T. E. Smithgall and T. Skorski (2002). "The Src family kinase Hck couples BCR/ABL to STAT5 activation in myeloid leukemia cells." Embo J 21(21): 5766-74.

Kocher, T. and G. Superti-Furga (2007). "Mass spectrometry-based functional proteomics: from molecular machines to protein networks." Nat Methods 4(10): 807-15.

Kolch, W., M. Calder and D. Gilbert (2005). "When kinases meet mathematics: the systems biology of MAPK signalling." FEBS Lett 579(8): 1891-5.

Konopka, J. B., S. M. Watanabe and O. N. Witte (1984). "An alteration of the human c-abl protein in K562 leukemia cells unmasks associated tyrosine kinase activity." Cell 37(3): 1035-42.

Kowanetz, K., N. Crosetto, K. Haglund, M. H. Schmidt, C. H. Heldin and I. Dikic (2004). "Suppressors of T-cell receptor signaling Sts-1 and Sts-2 bind to Cbl and inhibit endocytosis of receptor tyrosine kinases." J Biol Chem 279(31): 32786-95.

Koyama, N., S. Koschmieder, S. Tyagi, I. Portero-Robles, J. Chromic, S. Myloch, H. Nurnberger, T. Rossmanith, W. K. Hofmann, D. Hoelzer and O. G. Ottmann (2006). "Inhibition of phosphotyrosine phosphatase 1B causes resistance in BCR-ABL-positive leukemia cells to the ABL kinase inhibitor STI571." Clin Cancer Res 12(7 Pt 1): 2025-31.

Kuhn, E., J. Wu, J. Karl, H. Liao, W. Zolg and B. Guild (2004). "Quantification of C-reactive protein in the serum of patients with rheumatoid arthritis using multiple reaction monitoring mass spectrometry and 13C-labeled peptide standards." Proteomics 4(4): 1175-86.

Kuriyan, J. and D. Eisenberg (2007). "The origin of protein interactions and allostery in colocalization." Nature 450(7172): 983-90.

Kusmierz, J. J., R. Sumrada and D. M. Desiderio (1990). "Fast atom bombardment mass spectrometric quantitative analysis of methionine-enkephalin in human pituitary tissues." Anal Chem 62(21): 2395-400.

LaMontagne, K. R., Jr., A. J. Flint, B. R. Franza, Jr., A. M. Pandergast and N. K. Tonks (1998). "Protein tyrosine phosphatase 1B antagonizes signalling by oncoprotein tyrosine kinase p210 bcr-abl in vivo." Mol Cell Biol 18(5): 2965-75.

LaMontagne, K. R., Jr., G. Hannon and N. K. Tonks (1998). "Protein tyrosine phosphatase PTP1B suppresses p210 bcr-abl-induced transformation of rat-1 fibroblasts and promotes differentiation of K562 cells " Proc Natl Acad Sci U S A 95(24): 14094-9.

Laneuville, P. (1995). "Abl tyrosine protein kinase." Semin Immunol 7(4): 255-66.

le Coutre, P., O. G. Ottmann, F. Giles, D. W. Kim, J. Cortes, N. Gattermann, J. F. Apperley, R. A. Larson, E. Abruzzese, S. G. O'Brien, K. Kuliczkowski, A. Hochhaus, F. X. Mahon, G. Saglio, M. Gobbi, Y. L. Kwong, M. Baccarani, T. Hughes, G. Martinelli, J. P. Radich, M. Zheng, Y. Shou and H. Kantarjian (2007). "Nilotinib (formerly AMN107), a highly selective BCR-ABL tyrosine kinase inhibitor, is active in patients with imatinib-resistant or -intolerant accelerated phase chronic myelogenous leukemia." Blood.

Leguay, T., V. Desplat, V. Lagarde, G. Marit, J. Reiffers and F. X. Mahon (2005). "An amino-acid switch in the BCR-ABL kinase domain modifies sensitivity to imatinib mesylate." Leukemia 19(9): 1671-3.

Li, B., S. Boast, K. de los Santos, I. Schieren, M. Quiroz, S. L. Teitelbaum, M. M. Tondravi and S. P. Goff (2000). "Mice deficient in Abl are osteoporotic and have defects in osteoblast maturation." Nat Genet 24(3): 304-8.

Li, S., A. D. Couvillon, B. B. Brasher and R. A. Van Etten (2001). "Tyrosine phosphorylation of Grb2 by Bcr/Abl and epidermal growth factor receptor: a novel regulatory mechanism for tyrosine kinase signaling." Embo J 20(23): 6793-804.

Li, S., R. L. Ilaria, Jr., R. P. Million, G. Q. Daley and R. A. Van Etten (1999). "The P190, P210, and P230 forms of the BCR/ABL oncogene induce a similar chronic myeloid leukemia-like syndrome in mice but have different lymphoid leukemogenic activity." J Exp Med 189(9): 1399-412.

Liang, X., M. Hajivandi, D. Veach, D. Wisniewski, B. Clarkson, M. D. Resh and R. M. Pope (2006). "Quantification of change in phosphorylation of BCR-ABL kinase and its substrates in response to Imatinib treatment in human chronic myelogenous leukemia cells." Proteomics 6(16): 4554-4564.

Lilly, M., C. Tompkins, C. Brown, G. Pettit and A. Kraft (1990). "Differentiation and growth modulation of chronic myelogenous leukemia cells by bryostatin." Cancer Res 50(17): 5520-5.

Liu, H., R. G. Sadygov and J. R. Yates, 3rd (2004). "A model for random sampling and estimation of relative protein abundance in shotgun proteomics." Anal Chem 76(14): 4193-201.

Liu, J., M. Campbell, J. Q. Guo, D. Lu, Y. M. Xian, B. S. Andersson and R. B. Arlinghaus (1993). "BCR-ABL tyrosine kinase is autophosphorylated or transphosphorylates P160 BCR on tyrosine predominantly within the first BCR exon [published erratum appears in Oncogene 1993 Jul;8(7):2021]." Oncogene 8(1): 101-9.

Liu, J., Y. Wu, G. Z. Ma, D. Lu, L. Haataja, N. Heisterkamp, J. Groffen and R. B. Arlinghaus (1996). "Inhibition of Bcr serine kinase by tyrosine phosphorylation." Mol Cell Biol 16(3): 998-1005.

Lombardo, L. J., F. Y. Lee, P. Chen, D. Norris, J. C. Barrish, K. Behnia, S. Castaneda, L. A. Cornelius, J. Das, A. M. Doweyko, C. Fairchild, J. T. Hunt, I. Inigo, K. Johnston, A. Kamath, D. Kan, H. Klei, P. Marathe, S. Pang, R. Peterson, S. Pitt, G. L. Schieven, R. J. Schmidt, J. Tokarski, M. L. Wen, J. Wityak and R. M. Borzilleri (2004). "Discovery of N-(2-chloro-6-methyl- phenyl)-2-(6-(4-(2-hydroxyethyl)- piperazin-1-yl)-2-methylpyrimidin-4- ylamino)thiazole-5-carboxamide (BMS-354825), a dual Src/Abl kinase inhibitor with potent antitumor activity in preclinical assays." J Med Chem 47(27): 6658-61.

Lozzio, C. B. and B. B. Lozzio (1975). "Human chronic myelogenous leukemia cell-line with positive Philadelphia chromosome." Blood 45(3): 321-34.

Luo, B., H. W. Cheung, A. Subramanian, T. Sharifnia, M. Okamoto, X. Yang, G. Hinkle, J. S. Boehm, R. Beroukhim, B. A. Weir, C. Mermel, D. A. Barbie, T. Awad, X. Zhou, T. Nguyen, B. Piqani, C. Li, T. R. Golub, M. Meyerson, N. Hacohen, W. C. Hahn, E. S. Lander, D. M. Sabatini and D. E. Root (2008). "Highly parallel identification of essential genes in cancer cells." Proc Natl Acad Sci U S A 105(51): 20380-5.

MacPartlin, M., A. M. Smith, B. J. Druker, L. A. Honigberg and M. W. Deininger (2008). "Bruton's tyrosine kinase is not essential for Bcr-Abl-mediated transformation of lymphoid or myeloid cells." Leukemia 22(7): 1354-60.

Mahlmann, S., J. McLaughlin, D. E. Afar, R. Mohr, R. J. Kay and O. N. Witte (1998). "Dissection of signaling pathways and cloning of new signal transducers

in tyrosine kinase-induced pathways by genetic selection." <u>Leukemia</u> 12(12): 1858-65.

Martina, J. A., C. J. Bonangelino, R. C. Aguilar and J. S. Bonifacino (2001). "Stonin 2: an adaptor-like protein that interacts with components of the endocytic machinery." <u>J Cell Biol</u> 153(5): 1111-20.

Maru, Y. and O. N. Witte (1991). "The BCR gene encodes a novel serine/threonine kinase activity within a single exon." <u>Cell</u> 67(3): 459-68.

Mayer, B. J. (2001). "SH3 domains: complexity in moderation." <u>J Cell Sci</u> 114(Pt 7): 1253-63.

Mayer, B. J., P. K. Jackson and D. Baltimore (1991). "The noncatalytic src homology region 2 segment of abl tyrosine kinase binds to tyrosine-phosphorylated cellular proteins with high affinity." <u>Proc Natl Acad Sci U S A</u> 88(2): 627-31.

Mayer, B. J., P. K. Jackson, R. A. Van Etten and D. Baltimore (1992). "Point mutations in the abl SH2 domain coordinately impair phosphotyrosine binding in vitro and transforming activity in vivo." <u>Mol. Cell. Biol.</u> 12: 609-618.

Mayer, J. P. and R. D. Dimarchi (2005). "Drugging the undruggable." <u>Chem Biol</u> 12(8): 860-1.

Mayerhofer, M., K. J. Aichberger, S. Florian, M. T. Krauth, A. W. Hauswirth, S. Derdak, W. R. Sperr, H. Esterbauer, O. Wagner, C. Marosi, W. F. Pickl, M. Deininger, E. Weisberg, B. J. Druker, J. D. Griffin, C. Sillaber and P. Valent (2005). "Identification of mTOR as a novel bifunctional target in chronic myeloid leukemia: dissection of growth-inhibitory and VEGF-suppressive effects of rapamycin in leukemic cells." <u>Faseb J</u> 19(8): 960-2.

McWhirter, J. R., D. L. Galasso and J. Y. Wang (1993). "A coiled-coil oligomerization domain of Bcr is essential for the transforming function of Bcr-Abl oncoproteins." <u>Mol Cell Biol</u> 13(12): 7587-95.

McWhirter, J. R. and J. Y. Wang (1993). "An actin-binding function contributes to transformation by the Bcr-Abl oncoprotein of Philadelphia chromosome-positive human leukemias." <u>Embo J</u> 12(4): 1533-46.

Melo, J. V. and D. J. Barnes (2007). "Chronic myeloid leukaemia as a model of disease evolution in human cancer." <u>Nat Rev Cancer</u> 7(6): 441-53.

Melo, J. V., D. E. Gordon, N. C. Cross and J. M. Goldman (1993). "The ABL-BCR fusion gene is expressed in chronic myeloid leukemia." <u>Blood</u> 81(1): 158-65.

Melo, J. V., D. E. Gordon, A. Tuszynski, S. Dhut, B. D. Young and J. M. Goldman (1993). "Expression of the ABL-BCR fusion gene in Philadelphia-positive acute lymphoblastic leukemia." <u>Blood</u> 81(10): 2488-91.

Melo, J. V., H. Myint, D. A. Galton and J. M. Goldman (1994). "P190BCR-ABL chronic myeloid leukaemia: the missing link with chronic myelomonocytic leukaemia?" Leukemia 8(1): 208-11.

Meyn, M. A., 3rd, M. B. Wilson, F. A. Abdi, N. Fahey, A. P. Schiavone, J. Wu, J. M. Hochrein, J. R. Engen and T. E. Smithgall (2006). "Src family kinases phosphorylate the Bcr-Abl SH3-SH2 region and modulate Bcr-Abl transforming activity." J Biol Chem 281(41): 30907-16.

Michor, F., T. P. Hughes, Y. Iwasa, S. Branford, N. P. Shah, C. L. Sawyers and M. A. Nowak (2005). "Dynamics of chronic myeloid leukaemia." Nature 435(7046): 1267-70.

Mikhailik, A., B. Ford, J. Keller, Y. Chen, N. Nassar and N. Carpino (2007). "A phosphatase activity of Sts-1 contributes to the suppression of TCR signaling." Mol Cell 27(3): 486-97.

Mishra, G. R., M. Suresh, K. Kumaran, N. Kannabiran, S. Suresh, P. Bala, K. Shivakumar, N. Anuradha, R. Reddy, T. M. Raghavan, S. Menon, G. Hanumanthu, M. Gupta, S. Upendran, S. Gupta, M. Mahesh, B. Jacob, P. Mathew, P. Chatterjee, K. S. Arun, S. Sharma, K. N. Chandrika, N. Deshpande, K. Palvankar, R. Raghavnath, R. Krishnakanth, H. Karathia, B. Rekha, R. Nayak, G. Vishnupriya, H. G. Kumar, M. Nagini, G. S. Kumar, R. Jose, P. Deepthi, S. S. Mohan, T. K. Gandhi, H. C. Harsha, K. S. Deshpande, M. Sarker, T. S. Prasad and A. Pandey (2006). "Human protein reference database--2006 update." Nucleic Acids Res 34(Database issue): D411-4.

Mitelman, F. (1993). "The cytogenetic scenario of chronic myeloid leukemia." Leuk Lymphoma 11 Suppl 1: 11-5.

Miyoshi-Akiyama, T., L. M. Aleman, J. M. Smith, C. E. Adler and B. J. Mayer (2001). "Regulation of Cbl phosphorylation by the Abl tyrosine kinase and the Nck SH2/SH3 adaptor." Oncogene 20(30): 4058-69.

Mizuchi, D., T. Kurosu, A. Kida, Z. H. Jin, A. Jin, A. Arai and O. Miura (2005). "BCR/ABL activates Rap1 and B-Raf to stimulate the MEK/Erk signaling pathway in hematopoietic cells." Biochem Biophys Res Commun 326(3): 645-51.

Mohi, M. G., C. Boulton, T. L. Gu, D. W. Sternberg, D. Neuberg, J. D. Griffin, D. G. Gilliland and B. G. Neel (2004). "Combination of rapamycin and protein tyrosine kinase (PTK) inhibitors for the treatment of leukemias caused by oncogenic PTKs." Proc Natl Acad Sci U S A 101(9): 3130-5.

Musacchio, A., M. Noble, R. Pauptit, R. Wierenga and M. Saraste (1992). "Crystal structure of a Src-homology 3 (SH3) domain." Nature 359(6398): 851-5.

Musacchio, A., M. Saraste and M. Wilmanns (1994). "High-resolution crystal structures of tyrosine kinase SH3 domains complexed with proline-rich peptides." Nat. Struct. Biol. 1: 546.

Musacchio, A., M. Wilmanns and M. Saraste (1994). "Structure and function of the SH3 domain." Prog Biophys Mol Biol 61(3): 283-97.

Nagar, B., W. G. Bornmann, P. Pellicena, T. Schindler, D. R. Veach, W. T. Miller, B. Clarkson and J. Kuriyan (2002). "Crystal Structures of the Kinase Domain of c-Abl in Complex with the Small Molecule Inhibitors PD173955 and Imatinib (STI-571)." Cancer Res 62(15): 4236-43.

Nagar, B., O. Hantschel, M. Seeliger, J. M. Davies, W. I. Weis, G. Superti-Furga and J. Kuriyan (2006). "Organization of the SH3-SH2 Unit in Active and Inactive Forms of the c-Abl Tyrosine Kinase." Mol Cell 21(6): 787-98.

Nagar, B., O. Hantschel, M. A. Young, K. Scheffzek, D. Veach, W. Bornmann, B. Clarkson, G. Superti-Furga and J. Kuriyan (2003). "Structural Basis for the Autoinhibition of c-Abl Tyrosine Kinase." Cell 112(6): 859-71.

Nakajima, A., T. Tauchi, M. Sumi, W. R. Bishop and K. Ohyashiki (2003). "Efficacy of SCH66336, a farnesyl transferase inhibitor, in conjunction with imatinib against BCR-ABL-positive cells." Mol Cancer Ther 2(3): 219-24.

Natoli, G., A. Costanzo, F. Guido, F. Moretti, A. Bernardo, V. L. Burgio, C. Agresti and M. Levrero (1998). "Nuclear factor kB-independent cytoprotective pathways originating at tumor necrosis factor receptor-associated factor 2." J Biol Chem 273(47): 31262-72.

Naumann, S., D. Reutzel, M. Speicher and H. J. Decker (2001). "Complete karyotype characterization of the K562 cell line by combined application of G-banding, multiplex-fluorescence in situ hybridization, fluorescence in situ hybridization, and comparative genomic hybridization." Leuk Res 25(4): 313-22.

Neshat, M. S., A. B. Raitano, H. G. Wang, J. C. Reed and C. L. Sawyers (2000). "The survival function of the Bcr-Abl oncogene is mediated by Bad-dependent and -independent pathways: roles for phosphatidylinositol 3-kinase and Raf." Mol Cell Biol 20(4): 1179-86.

Nesvizhskii, A. I. and R. Aebersold (2005). "Interpretation of shotgun proteomic data: the protein inference problem." Mol Cell Proteomics 4(10): 1419-40.

Nowell, P. C. and D. A. Hungerford (1960). "A minute chromosome in human chronic granulocytic leukemia." Science 132: 1497.

O'Hare, T., A. S. Corbin and B. J. Druker (2006). "Targeted CML therapy: controlling drug resistance, seeking cure." Curr Opin Genet Dev 16(1): 92-9.

O'Hare, T. and B. J. Druker (2005). "BIRB-796 is not an effective ABL(T315I) inhibitor." Nat Biotechnol 23(10): 1209-10; author reply 1210-1.

O'Hare, T., C. A. Eide and M. W. Deininger (2007). "Bcr-Abl kinase domain mutations, drug resistance, and the road to a cure for chronic myeloid leukemia." Blood 110(7): 2242-9.

O'Hare, T., D. K. Walters, E. P. Stoffregen, T. Jia, P. W. Manley, J. Mestan, S. W. Cowan-Jacob, F. Y. Lee, M. C. Heinrich, M. W. Deininger and B. J. Druker (2005). "In vitro activity of Bcr-Abl inhibitors AMN107 and BMS-354825 against clinically relevant imatinib-resistant Abl kinase domain mutants." Cancer Res 65(11): 4500-5.

O'Hare, T., D. K. Walters, E. P. Stoffregen, D. W. Sherbenou, M. C. Heinrich, M. W. Deininger and B. J. Druker (2005). "Combined Abl inhibitor therapy for minimizing drug resistance in chronic myeloid leukemia: Src/Abl inhibitors are compatible with imatinib." Clin Cancer Res 11(19 Pt 1): 6987-93.

Ohren, J. F. and J. S. Sebolt-Leopold (2006). "Inhibitors of Bcr-abl... breaking new ground again." Nat Chem Biol 2(2): 63-4.

Okuda, K., E. Weisberg, D. G. Gilliland and J. D. Griffin (2001). "ARG tyrosine kinase activity is inhibited by STI571." Blood 97(8): 2440-8.

Ong, S. E., B. Blagoev, I. Kratchmarova, D. B. Kristensen, H. Steen, A. Pandey and M. Mann (2002). "Stable isotope labeling by amino acids in cell culture, SILAC, as a simple and accurate approach to expression proteomics." Mol Cell Proteomics 1(5): 376-86.

Ong, S. E. and M. Mann (2005). "Mass spectrometry-based proteomics turns quantitative." Nat Chem Biol 1(5): 252-62.

Owen, D. J. and P. R. Evans (1998). "A structural explanation for the recognition of tyrosine-based endocytotic signals." Science 282(5392): 1327-32.

Panchamoorthy, G., T. Fukazawa, S. Miyake, S. Soltoff, K. Reedquist, B. Druker, S. Shoelson, L. Cantley and H. Band (1996). "p120cbl is a major substrate of tyrosine phosphorylation upon B cell antigen receptor stimulation and interacts in vivo with Fyn and Syk tyrosine kinases, Grb2 and Shc adaptors, and the p85 subunit of phosphatidylinositol 3-kinase." J Biol Chem 271(6): 3187-94.

Papin, J. A., T. Hunter, B. O. Palsson and S. Subramaniam (2005). "Reconstruction of cellular signalling networks and analysis of their properties." Nat Rev Mol Cell Biol 6(2): 99-111.

Parmar, S., E. Katsoulidis, A. Verma, Y. Li, A. Sassano, L. Lal, B. Majchrzak, F. Ravandi, M. S. Tallman, E. N. Fish and L. C. Platanias (2004). "Role of the p38 mitogen-activated protein kinase pathway in the generation of the effects of imatinib mesylate (STI571) in BCR-ABL-expressing cells." J Biol Chem 279(24): 25345-52.

Patel, H., S. B. Marley and M. Y. Gordon (2006). "Detection in primary chronic myeloid leukaemia cells of p210BCR-ABL1 in complexes with adaptor proteins CBL, CRKL, and GRB2." Genes Chromosomes Cancer 45(12): 1121-9.

Pawson, T. (2007). "Dynamic control of signaling by modular adaptor proteins." Curr Opin Cell Biol 19(2): 112-6.

Pawson, T. (1994). "SH2 and SH3 domains in signal transduction." Adv Cancer Res 64: 87-110.

Pawson, T., G. D. Gish and P. Nash (2001). "SH2 domains, interaction modules and cellular wiring." Trends Cell Biol 11(12): 504-11.

Pearse, B. M., C. J. Smith and D. J. Owen (2000). "Clathrin coat construction in endocytosis." Curr Opin Struct Biol 10(2): 220-8.

Peck, J., G. t. Douglas, C. H. Wu and P. D. Burbelo (2002). "Human RhoGAP domain-containing proteins: structure, function and evolutionary relationships." FEBS Lett 528(1-3): 27-34.

Pendergast, A. M. (2002). "The Abl family kinases: mechanisms of regulation and signaling." Adv Cancer Res 85: 51-100.

Pendergast, A. M., L. A. Quilliam, L. D. Cripe, C. H. Bassing, Z. Dai, N. Li, A. Batzer, K. M. Rabun, C. J. Der, J. Schlessinger and M. L. Gishizky (1993). "BCR-ABL-induced oncogenesis is mediated by direct interaction with the SH2 domain of the GRB-2 adaptor protein." Cell 75: 175-185.

Pierce, A., R. D. Unwin, C. A. Evans, S. Griffiths, L. Carney, L. Zhang, E. Jaworska, C. F. Lee, D. Blinco, M. J. Okoniewski, C. J. Miller, D. A. Bitton, E. Spooncer and A. D. Whetton (2008). "Eight-channel iTRAQ enables comparison of the activity of six leukemogenic tyrosine kinases." Mol Cell Proteomics 7(5): 853-63.

Plattner, R., L. Kadlec, K. A. DeMali, A. Kazlauskas and A. M. Pendergast (1999). "c-Abl is activated by growth factors and src family kinases and has a role in the cellular response to PDGF." Genes Dev 13(18): 2400-11.

Pluk, H., K. Dorey and G. Superti-Furga (2002). "Autoinhibition of c-Abl." Cell 108(2): 247-59.

Praefcke, G. J., M. G. Ford, E. M. Schmid, L. E. Olesen, J. L. Gallop, S. Y. Peak-Chew, Y. Vallis, M. M. Babu, I. G. Mills and H. T. McMahon (2004). "Evolving nature of the AP2 alpha-appendage hub during clathrin-coated vesicle endocytosis." Embo J 23(22): 4371-83.

Puig, O., F. Caspary, G. Rigaut, B. Rutz, E. Bouveret, E. Bragado-Nilsson, M. Wilm and B. Seraphin (2001). "The tandem affinity purification (TAP) method: a general procedure of protein complex purification." Methods 24(3): 218-29.

Puil, L., J. Liu, G. Gish, G. Mbamalu, D. Bowtell, P. G. Pelicci, R. Arlinghaus and T. Pawson (1994). "Bcr-Abl oncoproteins bind directly to activators of the Ras signalling pathway." Embo J 13(4): 764-73.

Quintas-Cardama, A., H. Kantarjian and J. Cortes (2007). "Flying under the radar: the new wave of BCR-ABL inhibitors." Nat Rev Drug Discov 6(10): 834-48.

Raguz, J., S. Wagner, I. Dikic and D. Hoeller (2007). "Suppressor of T-cell receptor signalling 1 and 2 differentially regulate endocytosis and signalling of receptor tyrosine kinases." FEBS Lett 581(24): 4767-72.

Raitano, A. B., J. R. Halpern, T. M. Hambuch and C. L. Sawyers (1995). "The Bcr-Abl leukemia oncogene activates Jun kinase and requires Jun for transformation." Proc Natl Acad Sci U S A 92(25): 11746-50.

Raitano, A. B., Y. E. Whang and C. L. Sawyers (1997). "Signal transduction by wild-type and leukemogenic Abl proteins." Biochim. Biophys. Acta 1333: F201-F216.

Rappsilber, J., Y. Ishihama and M. Mann (2003). "Stop and go extraction tips for matrix-assisted laser desorption/ionization, nanoelectrospray, and LC/MS sample pretreatment in proteomics." Anal Chem 75(3): 663-70.

Redaelli, S., R. Piazza, R. Rostagno, V. Magistroni, P. Perini, M. Marega, C. Gambacorti-Passerini and F. Boschelli (2008). "Activity of Bosutinib, Dasatinib, and Nilotinib Against 18 Imatinib-Resistant BCR/ABL Mutants." J Clin Oncol.

Remsing Rix, L. L., U. Rix, J. Colinge, O. Hantschel, K. L. Bennett, T. Stranzl, A. Muller, C. Baumgartner, P. Valent, M. Augustin, J. H. Till and G. Superti-Furga (2008). "Global target profile of the kinase inhibitor bosutinib in primary chronic myeloid leukemia cells." Leukemia.

Ren, R. (2005). "Mechanisms of BCR-ABL in the pathogenesis of chronic myelogenous leukaemia." Nat Rev Cancer 5(3): 172-183.

Ren, S. Y., E. Bolton, M. G. Mohi, A. Morrione, B. G. Neel and T. Skorski (2005). "Phosphatidylinositol 3-kinase p85{alpha} subunit-dependent interaction with BCR/ABL-related fusion tyrosine kinases: molecular mechanisms and biological consequences." Mol Cell Biol 25(18): 8001-8.

Reuther, G. W., H. Fu, L. D. Cripe, R. J. Collier and A. M. Pendergast (1994). "Association of the protein kinases c-Bcr and Bcr-Abl with proteins of the 14-3-3 family." Science 266(5182): 129-33.

Rigaut, G., A. Shevchenko, B. Rutz, M. Wilm, M. Mann and B. Seraphin (1999). "A generic protein purification method for protein complex characterization and proteome exploration." Nat Biotechnol 17(10): 1030-2.

Rittinger, K., P. A. Walker, J. F. Eccleston, K. Nurmahomed, D. Owen, E. Laue, S. J. Gamblin and S. J. Smerdon (1997). "Crystal structure of a small G protein in complex with the GTPase-activating protein rhoGAP." Nature 388(6643): 693-7.

Rix, U., O. Hantschel, G. Durnberger, L. L. Remsing Rix, M. Planyavsky, N. V. Fernbach, I. Kaupe, K. L. Bennett, P. Valent, J. Colinge, T. Kocher and G. Superti-Furga (2007). "Chemical proteomic profiles of the BCR-ABL inhibitors imatinib, nilotinib and dasatinib reveal novel kinase and non-kinase targets." Blood 110(12): 4055-63.

Ross, P. L., Y. N. Huang, J. N. Marchese, B. Williamson, K. Parker, S. Hattan, N. Khainovski, S. Pillai, S. Dey, S. Daniels, S. Purkayastha, P. Juhasz, S. Martin, M. Bartlet-Jones, F. He, A. Jacobson and D. J. Pappin (2004). "Multiplexed protein quantitation in Saccharomyces cerevisiae using amine-reactive isobaric tagging reagents." Mol Cell Proteomics 3(12): 1154-69.

Roumiantsev, S., N. P. Shah, M. E. Gorre, J. Nicoll, B. B. Brasher, C. L. Sawyers and R. A. Van Etten (2002). "Clinical resistance to the kinase inhibitor STI-571 in chronic myeloid leukemia by mutation of Tyr-253 in the Abl kinase domain P-loop." Proc Natl Acad Sci U S A 99(16): 10700-5.

Rowley, J. D. (1973). "Identificaton of a translocation with quinacrine fluorescence in a patient with acute leukemia." Ann Genet 16(2): 109-12.

Rumpf, J., B. Simon, N. Jung, T. Maritzen, V. Haucke, M. Sattler and Y. Groemping (2008). "Structure of the Eps15-stonin2 complex provides a molecular explanation for EH-domain ligand specificity." Embo J 27(3): 558-69.

Sadowski, I., J. C. Stone and T. Pawson (1986). "A noncatalytic domain conserved among cytoplasmic protein-tyrosine kinases modifies the kinase function and transforming activity of Fujinami sarcoma virus P130gag-fps." Mol Cell Biol 6(12): 4396-408.

Sahay, S., N. L. Pannucci, G. M. Mahon, P. L. Rodriguez, N. J. Megjugorac, E. V. Kostenko, H. L. Ozer and I. P. Whitehead (2007). "The RhoGEF domain of p210 Bcr-Abl activates RhoA and is required for transformation." Oncogene.

Sakaguchi, K., Y. Okabayashi and M. Kasuga (2001). "Shc mediates ligand-induced internalization of epidermal growth factor receptors." Biochem Biophys Res Commun 282(5): 1154-60.

Salgia, R., E. Pisick, M. Sattler, J. L. Li, N. Uemura, W. K. Wong, S. A. Burky, H. Hirai, L. B. Chen and J. D. Griffin (1996). "p130CAS forms a signaling complex with the adapter protein CRKL in hematopoietic cells transformed by the BCR/ABL oncogene." J Biol Chem 271(41): 25198-203.

Salomon, A. R., S. B. Ficarro, L. M. Brill, A. Brinker, Q. T. Phung, C. Ericson, K. Sauer, A. Brock, D. M. Horn, P. G. Schultz and E. C. Peters (2003). "Profiling of tyrosine phosphorylation pathways in human cells using mass spectrometry." Proc Natl Acad Sci U S A 100(2): 443-8.

Sattler, M. and J. D. Griffin (2003). "Molecular mechanisms of transformation by the BCR-ABL oncogene." Semin Hematol 40(2 Suppl 2): 4-10.

Sattler, M., M. G. Mohi, Y. B. Pride, L. R. Quinnan, N. A. Malouf, K. Podar, F. Gesbert, H. Iwasaki, S. Li, R. A. Van Etten, H. Gu, J. D. Griffin and B. G. Neel (2002). "Critical role for Gab2 in transformation by BCR/ABL." <u>Cancer Cell</u> 1(5): 479-92.

Sattler, M. and R. Salgia (1998). "Role of the adapter protein CRKL in signal transduction of normal hematopoietic and BCR/ABL-transformed cells." <u>Leukemia</u> 12(5): 637-44.

Sattler, M., S. Verma, C. H. Byrne, G. Shrikhande, T. Winkler, P. A. Algate, L. R. Rohrschneider and J. D. Griffin (1999). "BCR/ABL directly inhibits expression of SHIP, an SH2-containing polyinositol-5-phosphatase involved in the regulation of hematopoiesis." <u>Mol Cell Biol</u> 19(11): 7473-80.

Sawyers, C. L. (1999). "Chronic myeloid leukemia." <u>N Engl J Med</u> 340(17): 1330-40.

Schiff-Maker, L., M. C. Burns, J. B. Konopka, S. Clark, O. N. Witte and N. Rosenberg (1986). "Monoclonal antibodies specific for v-abl- and c-abl-encoded molecules." <u>J Virol</u> 57(3): 1182-6.

Schiffer, C. A. (2007). "BCR-ABL tyrosine kinase inhibitors for chronic myelogenous leukemia." <u>N Engl J Med</u> 357(3): 258-65.

Schindler, T., W. Bornmann, P. Pellicena, W. T. Miller, B. Clarkson and J. Kuriyan (2000). "Structural mechanism for STI-571 inhibition of abelson tyrosine kinase." <u>Science</u> 289(5486): 1938-42.

Schirle, M., M. A. Heurtier and B. Kuster (2003). "Profiling core proteomes of human cell lines by one-dimensional PAGE and liquid chromatography-tandem mass spectrometry." <u>Mol Cell Proteomics</u> 2(12): 1297-305.

Schumacher, C., B. S. Knudsen, T. Ohuchi, P. P. Di Fiore, R. H. Glassman and H. Hanafusa (1995). "The SH3 domain of Crk binds specifically to a conserved proline-rich motif in Eps15 and Eps15R." <u>J Biol Chem</u> 270(25): 15341-7.

Shah, N., J. Nicoll, B. Nagar, M. Gorre, R. Paquette, J. Kuriyan and C. Sawyers (2002). "Multiple BCR-ABL kinase domain mutations confer polyclonal resistance to the tyrosine kinase inhibitor imatinib (STI571) in chronic phase and blast crisis chronic myeloid leukemia." <u>Cancer Cell</u> 2(2): 117-125.

Shah, N. P. and C. L. Sawyers (2003). "Mechanisms of resistance to STI571 in Philadelphia chromosome-associated leukemias." <u>Oncogene</u> 22(47): 7389-95.

Shah, N. P., C. Tran, F. Y. Lee, P. Chen, D. Norris and C. L. Sawyers (2004). "Overriding imatinib resistance with a novel ABL kinase inhibitor." <u>Science</u> 305(5682): 399-401.

Sharma, S. V., P. Gajowniczek, I. P. Way, D. Y. Lee, J. Jiang, Y. Yuza, M. Classon, D. A. Haber and J. Settleman (2006). "A common signaling cascade

may underlie "addiction" to the Src, BCR-ABL, and EGF receptor oncogenes." Cancer Cell 10(5): 425-35.

Shevchenko, A., M. Wilm, O. Vorm and M. Mann (1996). "Mass spectrometric sequencing of proteins silver-stained polyacrylamide gels." Anal Chem 68(5): 850-8.

Shi, Y., K. Alin and S. P. Goff (1995). "Abl-interactor-1, a novel SH3 protein binding to the carboxy-terminal portion of the Abl protein, suppresses v-abl transforming activity." Genes Dev 9(21): 2583-97.

Shiotsu, Y., S. Soga and S. Akinaga (2002). "Heat shock protein 90-antagonist destabilizes Bcr-Abl/HSP90 chaperone complex." Leuk Lymphoma 43(5): 961-8.

Shteper, P. J. and D. Ben-Yehuda (2001). "Molecular evolution of chronic myeloid leukaemia." Semin Cancer Biol 11(4): 313-23.

Shuai, K., J. Halpern, J. ten Hoeve, X. Rao and C. L. Sawyers (1996). "Constitutive activation of STAT5 by the BCR-ABL oncogene in chronic myelogenous leukemia." Oncogene 13(2): 247-54.

Skaggs, B. J., M. E. Gorre, A. Ryvkin, M. R. Burgess, Y. Xie, Y. Han, E. Komisopoulou, L. M. Brown, J. A. Loo, E. M. Landaw, C. L. Sawyers and T. G. Graeber (2006). "Phosphorylation of the ATP-binding loop directs oncogenicity of drug-resistant BCR-ABL mutants." Proc Natl Acad Sci U S A 103(51): 19466-71.

Skorski, T., P. Kanakaraj, M. Nieborowska-Skorska, M. Z. Ratajczak, S. C. Wen, G. Zon, A. M. Gewirtz, B. Perussia and B. Calabretta (1995). "Phosphatidylinositol-3 kinase activity is regulated by BCR/ABL and is required for the growth of Philadelphia chromosome-positive cells." Blood 86(2): 726-36.

Sleeman, M. W., K. E. Wortley, K. M. Lai, L. C. Gowen, J. Kintner, W. O. Kline, K. Garcia, T. N. Stitt, G. D. Yancopoulos, S. J. Wiegand and D. J. Glass (2005). "Absence of the lipid phosphatase SHIP2 confers resistance to dietary obesity." Nat Med 11(2): 199-205.

Smith, J. M., S. Katz and B. J. Mayer (1999). "Activation of the abl tyrosine kinase in vivo by src homology 3 domains from the src homology 2/Src homology 3 adaptor Nck " J Biol Chem 274(39): 27956-62.

Smith, K. M., R. Yacobi and R. A. Van Etten (2003). "Autoinhibition of Bcr-Abl through Its SH3 Domain." Mol Cell 12(1): 27-37.

Somia, N. V., H. Miyoshi, M. J. Schmitt and I. M. Verma (2000). "Retroviral vector targeting to human immunodeficiency virus type 1-infected cells by receptor pseudotyping." J Virol 74(9): 4420-4.

Stanglmaier, M., M. Warmuth, I. Kleinlein, S. Reis and M. Hallek (2003). "The interaction of the Bcr-Abl tyrosine kinase with the Src kinase Hck is mediated by multiple binding domains." <u>Leukemia</u> 17(2): 283-9.

Steelman, L. S., S. C. Pohnert, J. G. Shelton, R. A. Franklin, F. E. Bertrand and J. A. McCubrey (2004). "JAK/STAT, Raf/MEK/ERK, PI3K/Akt and BCR-ABL in cell cycle progression and leukemogenesis." <u>Leukemia</u> 18(2): 189-218.

Steen, H., M. Fernandez, S. Ghaffari, A. Pandey and M. Mann (2003). "Phosphotyrosine Mapping in Bcr/Abl Oncoprotein Using Phosphotyrosine-specific Immonium Ion Scanning." <u>Mol Cell Proteomics</u> 2(3): 138-45.

Taagepera, S., D. McDonald, J. E. Loeb, L. L. Whitaker, A. K. McElroy, J. Y. Wang and T. J. Hope (1998). "Nuclear-cytoplasmic shuttling of C-ABL tyrosine kinase." <u>Proc Natl Acad Sci U S A</u> 95(13): 7457-62.

Talpaz, M., R. T. Silver, B. J. Druker, J. M. Goldman, C. Gambacorti-Passerini, F. Guilhot, C. A. Schiffer, T. Fischer, M. W. Deininger, A. L. Lennard, A. Hochhaus, O. G. Ottmann, A. Gratwohl, M. Baccarani, R. Stone, S. Tura, F. X. Mahon, S. Fernandes-Reese, I. Gathmann, R. Capdeville, H. M. Kantarjian and C. L. Sawyers (2002). "Imatinib induces durable hematologic and cytogenetic responses in patients with accelerated phase chronic myeloid leukemia: results of a phase 2 study." <u>Blood</u> 99(6): 1928-37.

Tanaka, M., R. Gupta and B. J. Mayer (1995). "Differential inhibition of signaling pathways by dominant-negative SH2/SH3 adapter proteins." <u>Mol Cell Biol</u> 15(12): 6829-37.

Tanaka, R. and S. Kimura (2008). "Abl tyrosine kinase inhibitors for overriding Bcr-Abl/T315I: from the second to third generation." <u>Expert Rev Anticancer Ther</u> 8(9): 1387-98.

Tauchi, T., H. S. Boswell, D. Leibowitz and H. E. Broxmeyer (1994). "Coupling between p210bcr-abl and Shc and Grb2 adaptor proteins in hematopoietic cells permits growth factor receptor-independent link to ras activation pathway." <u>J Exp Med</u> 179(1): 167-75.

Tauchi, T., G. S. Feng, R. Shen, H. Y. Song, D. Donner, T. Pawson and H. E. Broxmeyer (1994). "SH2-containing phosphotyrosine phosphatase Syp is a target of p210bcr-abl tyrosine kinase." <u>J Biol Chem</u> 269(21): 15381-7.

Tauchi, T., K. Miyazawa, G. S. Feng, H. E. Broxmeyer and K. Toyama (1997). "A coiled-coil tetramerization domain of BCR-ABL is essential for the interactions of SH2-containing signal transduction molecules." <u>J Biol Chem</u> 272(2): 1389-94.

Taylor, C. M. and A. E. Keating (2005). "Orientation and oligomerization specificity of the Bcr coiled-coil oligomerization domain." <u>Biochemistry</u> 44(49): 16246-56.

Taylor, V., M. Wong, C. Brandts, L. Reilly, N. M. Dean, L. M. Cowsert, S. Moodie and D. Stokoe (2000). "5' phospholipid phosphatase SHIP-2 causes protein kinase B inactivation and cell cycle arrest in glioblastoma cells." Mol Cell Biol 20(18): 6860-71.

Thien, C. B. and W. Y. Langdon (2001). "Cbl: many adaptations to regulate protein tyrosine kinases." Nat Rev Mol Cell Biol 2(4): 294-307.

Thiesing, J. T., S. Ohno-Jones, K. S. Kolibaba and B. J. Druker (2000). "Efficacy of STI571, an abl tyrosine kinase inhibitor, in conjunction with other antileukemic agents against bcr-abl-positive cells." Blood 96(9): 3195-9.

Thomas, E. K., J. A. Cancelas, Y. Zheng and D. A. Williams (2008). "Rac GTPases as key regulators of p210-BCR-ABL-dependent leukemogenesis." Leukemia.

Tokarski, J. S., J. A. Newitt, C. Y. Chang, J. D. Cheng, M. Wittekind, S. E. Kiefer, K. Kish, F. Y. Lee, R. Borzillerri, L. J. Lombardo, D. Xie, Y. Zhang and H. E. Klei (2006). "The structure of Dasatinib (BMS-354825) bound to activated ABL kinase domain elucidates its inhibitory activity against imatinib-resistant ABL mutants." Cancer Res 66(11): 5790-7.

Tong, A. H., B. Drees, G. Nardelli, G. D. Bader, B. Brannetti, L. Castagnoli, M. Evangelista, S. Ferracuti, B. Nelson, S. Paoluzi, M. Quondam, A. Zucconi, C. W. Hogue, S. Fields, C. Boone and G. Cesareni (2002). "A combined experimental and computational strategy to define protein interaction networks for peptide recognition modules." Science 295(5553): 321-4.

Traxler, P., G. Bold, E. Buchdunger, G. Caravatti, P. Furet, P. Manley, T. O'Reilly, J. Wood and J. Zimmermann (2001). "Tyrosine kinase inhibitors: from rational design to clinical trials." Med Res Rev 21(6): 499-512.

Tusher, V. G., R. Tibshirani and G. Chu (2001). "Significance analysis of microarrays applied to the ionizing radiation response." Proc Natl Acad Sci U S A 98(9): 5116-21.

Uemura, N., R. Salgia, J. L. Li, E. Pisick, M. Sattler and J. D. Griffin (1997). "The BCR/ABL oncogene alters interaction of the adapter proteins CRKL and CRK with cellular proteins." Leukemia 11(3): 376-85.

Unwin, R. D., A. Pierce, R. B. Watson, D. W. Sternberg and A. D. Whetton (2005). "Quantitative proteomic analysis using isobaric protein tags enables rapid comparison of changes in transcript and protein levels in transformed cells." Mol Cell Proteomics 4(7): 924-35.

Van Etten, R. A. (2007). "Oncogenic signaling: new insights and controversies from chronic myeloid leukemia." J Exp Med 204(3): 461-5.

Van Etten, R. A., J. Debnath, H. Zhou and J. M. Casasnovas (1995). "Introduction of a loss-of-function point mutation from the SH3 region of the

Caenorhabditis elegans sem-5 gene activates the transforming ability of c-abl in vivo and abolishes binding of proline-rich ligands in vitro." <u>Oncogene</u> 10(10): 1977-88.

Veraksa, A., A. Bauer and S. Artavanis-Tsakonas (2005). "Analyzing protein complexes in Drosophila with tandem affinity purification-mass spectrometry." <u>Dev Dyn</u> 232(3): 827-34.

Vinciguerra, M. and M. Foti (2006). "PTEN and SHIP2 phosphoinositide phosphatases as negative regulators of insulin signalling." <u>Arch Physiol Biochem</u> 112(2): 89-104.

Virchow, R. (1845). "Weisses Blut. Froriep's Neue Notizen aus dem Gebiet der Natur- und Heilkunde." <u>Weimer</u> 36: 151-55.

von Bubnoff, N., S. Barwisch, M. R. Speicher, C. Peschel and J. Duyster (2005). "A cell-based screening strategy that predicts mutations in oncogenic tyrosine kinases: implications for clinical resistance in targeted cancer treatment." <u>Cell Cycle</u> 4(3): 400-6.

von Bubnoff, N., D. R. Veach, H. van der Kuip, W. E. Aulitzky, J. Sanger, P. Seipel, W. G. Bornmann, C. Peschel, B. Clarkson and J. Duyster (2005). "A cell-based screen for resistance of Bcr-Abl-positive leukemia identifies the mutation pattern for PD166326, an alternative Abl kinase inhibitor." <u>Blood</u> 105(4): 1652-9.

Voncken, J. W., H. van Schaick, V. Kaartinen, K. Deemer, T. Coates, B. Landing, P. Pattengale, O. Dorseuil, G. M. Bokoch, J. Groffen and et al. (1995). "Increased neutrophil respiratory burst in bcr-null mutants." <u>Cell</u> 80(5): 719-28.

Waksman, G., D. Kominos, S. C. Robertson, N. Pant, D. Baltimore, R. B. Birge, D. Cowburn, H. Hanafusa, B. J. Mayer, M. Overduin and et al. (1992). "Crystal structure of the phosphotyrosine recognition domain SH2 of v-src complexed with tyrosine-phosphorylated peptides." <u>Nature</u> 358(6388): 646-53.

Waksman, G. and J. Kuriyan (2004). "Structure and specificity of the SH2 domain." <u>Cell</u> 116(2 Suppl): S45-8, 3 p following S48.

Waksman, G., S. E. Shoelson, N. Pant, D. Cowburn and J. Kuriyan (1993). "Binding of a high affinity phosphotyrosyl peptide to the Src SH2 domain: crystal structures of the complexed and peptide-free forms." <u>Cell</u> 72(5): 779-90.

Walhout, A. J., G. F. Temple, M. A. Brasch, J. L. Hartley, M. A. Lorson, S. van den Heuvel and M. Vidal (2000). "GATEWAY recombinational cloning: application to the cloning of large numbers of open reading frames or ORFeomes." <u>Methods Enzymol</u> 328: 575-92.

Wattenhofer, M., K. Shibuya, J. Kudoh, R. Lyle, J. Michaud, C. Rossier, K. Kawasaki, S. Asakawa, S. Minoshima, A. Berry, B. Bonne-Tamir, N. Shimizu, S. E. Antonarakis and H. S. Scott (2001). "Isolation and characterization of the

UBASH3A gene on 21q22.3 encoding a potential nuclear protein with a novel combination of domains." <u>Hum Genet</u> 108(2): 140-7.

Weinstein, I. B. (2002). "Cancer. Addiction to oncogenes--the Achilles heal of cancer." <u>Science</u> 297(5578): 63-4.

Weinstein, I. B. and A. Joe (2008). "Oncogene addiction." <u>Cancer Res</u> 68(9): 3077-80; discussion 3080.

Weinstein, I. B. and A. K. Joe (2006). "Mechanisms of disease: Oncogene addiction--a rationale for molecular targeting in cancer therapy." <u>Nat Clin Pract Oncol</u> 3(8): 448-57.

Weisberg, E., P. Manley, J. Mestan, S. Cowan-Jacob, A. Ray and J. D. Griffin (2006). "AMN107 (nilotinib): a novel and selective inhibitor of BCR-ABL." <u>Br J Cancer</u> 94(12): 1765-9.

Weisberg, E., P. W. Manley, W. Breitenstein, J. Bruggen, S. W. Cowan-Jacob, A. Ray, B. Huntly, D. Fabbro, G. Fendrich, E. Hall-Meyers, A. L. Kung, J. Mestan, G. Q. Daley, L. Callahan, L. Catley, C. Cavazza, A. Mohammed, D. Neuberg, R. D. Wright, D. G. Gilliland and J. D. Griffin (2005). "Characterization of AMN107, a selective inhibitor of native and mutant Bcr-Abl." <u>Cancer Cell</u> 7(2): 129-41.

Westermarck, J., C. Weiss, R. Saffrich, J. Kast, A. M. Musti, M. Wessely, W. Ansorge, B. Seraphin, M. Wilm, B. C. Valdez and D. Bohmann (2002). "The DEXD/H-box RNA helicase RHII/Gu is a co-factor for c-Jun-activated transcription." <u>Embo J</u> 21(3): 451-60.

Wiese, S., K. A. Reidegeld, H. E. Meyer and B. Warscheid (2007). "Protein labeling by iTRAQ: a new tool for quantitative mass spectrometry in proteome research." <u>Proteomics</u> 7(3): 340-50.

Wiesner, S., O. Hantschel, C. D. Mackereth, G. Superti-Furga and M. Sattler (2005). "NMR Assignment Reveals an alpha-Helical Fold for the F-Actin Binding Domain of Human Bcr-Abl/c-Abl." <u>J Biomol NMR</u> 32(4): 335.

Wisniewski, D., A. Strife, S. Swendeman, H. Erdjument-Bromage, S. Geromanos, W. M. Kavanaugh, P. Tempst and B. Clarkson (1999). "A novel SH2-containing phosphatidylinositol 3,4,5-trisphosphate 5-phosphatase (SHIP2) is constitutively tyrosine phosphorylated and associated with src homologous and collagen gene (SHC) in chronic myelogenous leukemia progenitor cells." <u>Blood</u> 93(8): 2707-20.

Wohlbold, L., H. van der Kuip, C. Miething, H. P. Vornlocher, C. Knabbe, J. Duyster and W. E. Aulitzky (2003). "Inhibition of bcr-abl gene expression by small interfering RNA sensitizes for imatinib mesylate (STI571)." <u>Blood</u> 102(6): 2236-9.

Wong, S. and O. N. Witte (2004). "The BCR-ABL Story: Bench to Bedside and Back." Annu Rev Immunol 22: 247-306.

Workman, P. (2005). "Drugging the cancer kinome: progress and challenges in developing personalized molecular cancer therapeutics." Cold Spring Harb Symp Quant Biol 70: 499-515.

Workman, P., P. A. Clarke, S. Guillard and F. I. Raynaud (2006). "Drugging the PI3 kinome." Nat Biotechnol 24(7): 794-6.

Wu, J., F. Meng, H. Lu, L. Kong, W. Bornmann, Z. Peng, M. Talpaz and N. J. Donato (2008). "Lyn regulates BCR-ABL and Gab2 tyrosine phosphorylation and c-Cbl protein stability in imatinib resistant chronic myelogenous leukemia cells." Blood.

Wu, L. X., J. H. Xu, K. Z. Zhang, Q. Lin, X. W. Huang, C. X. Wen and Y. Z. Chen (2008). "Disruption of the Bcr-Abl/Hsp90 protein complex: a possible mechanism to inhibit Bcr-Abl-positive human leukemic blasts by novobiocin." Leukemia 22(7): 1402-9.

Wu, Y., J. Liu and R. B. Arlinghaus (1998). "Requirement of two specific tyrosine residues for the catalytic activity of Bcr serine/threonine kinase." Oncogene 16(1): 141-6.

Wu, Y., G. Ma, D. Lu, F. Lin, H. J. Xu, J. Liu and R. B. Arlinghaus (1999). "Bcr: a negative regulator of the Bcr-Abl oncoprotein." Oncogene 18(31): 4416-24.

Yamaguchi, A., T. Urano, T. Goi and L. A. Feig (1997). "An Eps homology (EH) domain protein that binds to the Ral-GTPase target, RalBP1." J Biol Chem 272(50): 31230-4.

Yamamoto, M., T. Kurosu, K. Kakihana, D. Mizuchi and O. Miura (2004). "The two major imatinib resistance mutations E255K and T315I enhance the activity of BCR/ABL fusion kinase." Biochem Biophys Res Commun 319(4): 1272-5.

Yan, H., Y. C. Wang, D. Li, Y. Wang, W. Liu, Y. L. Wu and G. Q. Chen (2007). "Arsenic trioxide and proteasome inhibitor bortezomib synergistically induce apoptosis in leukemic cells: the role of protein kinase Cdelta." Leukemia 21(7): 1488-95.

Yang, J., P. Cron, V. Thompson, V. M. Good, D. Hess, B. A. Hemmings and D. Barford (2002). "Molecular mechanism for the regulation of protein kinase B/Akt by hydrophobic motif phosphorylation." Mol Cell 9(6): 1227-40.

Yildirim, M. A., K. I. Goh, M. E. Cusick, A. L. Barabasi and M. Vidal (2007). "Drug-target network." Nat Biotechnol 25(10): 1119-26.

Yokota, A., S. Kimura, S. Masuda, E. Ashihara, J. Kuroda, K. Sato, Y. Kamitsuji, E. Kawata, Y. Deguchi, Y. Urasaki, Y. Terui, M. Ruthardt, T. Ueda, K. Hatake, K. Inui and T. Maekawa (2007). "INNO-406, a novel BCR-ABL/Lyn dual tyrosine

kinase inhibitor, suppresses the growth of Ph+ leukemia cells in the central nervous system, and cyclosporine A augments its in vivo activity." Blood 109(1): 306-14.

Yu, C., G. Krystal, P. Dent and S. Grant (2002). "Flavopiridol potentiates STI571-induced mitochondrial damage and apoptosis in BCR-ABL-positive human leukemia cells." Clin Cancer Res 8(9): 2976-84.

Zaykin, D. V., S. S. Young and P. H. Westfall (2000). "Using the false discovery rate approach in the genetic dissection of complex traits: a response to Weller et al." Genetics 154(4): 1917-8.

Zhang, R. and F. E. Regnier (2002). "Minimizing resolution of isotopically coded peptides in comparative proteomics." J Proteome Res 1(2): 139-47.

Zhang, X., R. Subrahmanyam, R. Wong, A. W. Gross and R. Ren (2001). "The NH(2)-terminal coiled-coil domain and tyrosine 177 play important roles in induction of a myeloproliferative disease in mice by Bcr-Abl." Mol Cell Biol 21(3): 840-53.

Zhao, L. and P. K. Vogt (2008). "Class I PI3K in oncogenic cellular transformation." Oncogene 27(41): 5486-96.

Zhao, X., S. Ghaffari, H. Lodish, V. N. Malashkevich and P. S. Kim (2002). "Structure of the Bcr-Abl oncoprotein oligomerization domain." Nat Struct Biol 7: 117-20.

Zheng, X., S. Guller, T. Beissert, E. Puccetti and M. Ruthardt (2006). "BCR and its mutants, the reciprocal t(9;22)-associated ABL/BCR fusion proteins, differentially regulate the cytoskeleton and cell motility." BMC Cancer 6: 262.

Zipfel, P. A., M. Grove, K. Blackburn, M. Fujimoto, T. F. Tedder and A. M. Pendergast (2000). "The c-Abl tyrosine kinase is regulated downstream of the B cell antigen receptor and interacts with CD19." J Immunol 165(12): 6872-9.

Figure references:

Figures that I did not generate myself are referenced accordingly. I contacted the authors of the respective figures in order to get their consent for use in this thesis. Should any copyright infringement emerge I request my notification.

CURRICULUM VITAE

6 CURRICULUM VITAE

Marc J. Brehme, M.Sc.

Particulars

Born:	September 28, 1978, Heidelberg, Germany
Citizenship:	German
Current position:	PhD student
Institute:	CeMM – Research Center for Molecular Medicine
	Austrian Academy of Sciences
	c/o Vienna Competence Center
	Lazarettgasse 19/3, A-1090 Vienna
E-mail:	mbrehme@cemm.oeaw.ac.at

Education and Scientific Experience

Since 01/2008   **New Biotechnology, Elsevier Ireland Ltd. / EFB**
Advisory Editorial Board Member
Official peer-reviewed journal of the European Federation of Biotechnology (EFB), covering research, industrial and commercial aspects of biotechnology

Since 05/2005   **CeMM – Research Center for Molecular Medicine, Austrian Academy of Sciences,** Vienna
PhD student
- Adviser: Prof. Dr. Giulio Superti-Furga
- Thesis: „Functional Proteomics of Bcr-Abl Signaling"
- Funding: Austrian Academy of Sciences, Austrian Science Fund

04/2005   ***Master of Science*** in Molecular Biology, Biochemistry and Cell Biology *(Final grade: 1,2)*

10/2004 – 04/2005   **European Molecular Biology Laboratory (EMBL)**, Heidelberg
Master Thesis, Laboratory of Eileen Furlong: „Identifying novel targets of the *Drosophila melanogaster* transcription factor Twist"*, (Grade: 1,0)*

04/2004 - 05/2004   Internship in the laboratory of PD Dr. **Klaus Scheffzek**, European Molecular Biology Laboratory (EMBL), Heidelberg, "Expression, Purification and Crystallization of HIV - Cycline T1 proteins"

10/2003 - 01/2004   Internship in the laboratory of PD Dr. **Stefan Wiemann**, German Cancer Research Centre (DKFZ), Molecular Genome Analysis Division, Heidelberg, "Subcellular localization of novel human cDNAs and analysis of their effect on proliferation"

10/2003 – 04/2005   **University of Heidelberg, Centre for Molecular Biology (ZMBH) / German Cancer Research Center (DKFZ)**, Heidelberg
„International Graduate Programme in Molecular & Cellular Biology"
Master student

08/2003 – 09/2003   Internship in the laboratory of Prof. Dr. **David Lydall**, University of Manchester, UK, "Synthetic lethality screen for novel genes that affect cellular responses to uncapped telomeres in budding yeast"

07/2003 – 08/2003
&
05/2002 – 09/2002   **Cellzome AG**, Heidelberg
Scientific Assistant Molecular Biology (part-time)
Assistance in large-scale human TNF-α/NF-κB signal transduction pathway mapping project (Bouwmeester et al, Nat Cell Biol 2004)

Education and Scientific Experience (cont'd)

05/2003 - 07/2003	Internship in the laboratory of Prof. Dr. **Konrad Beyreuther**, Centre for Molecular Biology (ZMBH), University of Heidelberg, "Molecular biology and genetics of Alzheimer's disease"
02/2003 - 04/2003	Internship in the laboratory of Prof. Dr. **Richard Herrmann**, Centre for Molecular Biology (ZMBH), University of Heidelberg, "Characterization of transposon mutants of *Mycoplasma pneumoniae*"
09/2002 – 02/2003	**University of Manchester, School of Biological Sciences** *Erasmus scholar*, Course Units attended: Molecular Biology Practicals, Molecular Virology, Animal Cell Biotechnology, Molecular Biology of Cancer, Bioinformatics and Protein Structure/Function *(Average grade: A, First Class)*
07/2002	***Preliminary Diploma*** in General Biology (Biochemistry/Cell Biology, Molecular Biology/Genetics/Microbiology, Botany, Zoology), Chemistry and Physics *(Average grade: 1,7)*
09/2000 – 07/2003	**University of Heidelberg, Faculty of Life Sciences**, Heidelberg Student in the Biology Diploma Programme
07/1998	**Liselotte Gymnasium**, Mannheim Graduation from high school, Majors: Biology and French (*Final grade: 1,4*)

Publications

02/2009	**Brehme, M.**, Hantschel, O., Colinge, J., Kaupe, I., Planyavsky, M., Köcher, T., Mechtler, K., Bennett, K.L., Superti-Furga, G., "Charting the molecular network of the drug target Bcr-Abl", PNAS*, under revision*
02/2009	**Brehme, M.**, "Intercell - Accelerating Innovation", Interview with Alexander von Gabain (CSO), New Biotechnology*, in press*
02/2007	Sandmann, T., Girardot, C., **Brehme, M.**, Tongprasit, W., Stolc, V., Furlong, E.M., "A core transcriptional network for early mesoderm development in *Drosophila melanogaster*", Genes & Development 21 (4), 436-449, 15 February 2007
03/2006	Downey, M.S., Houlsworth, R., Maringele, L., Rollie, A., **Brehme, M.**, Galicia, S., Guillard, S., Partington, M., Zubko, M. K., Krogan, N. J., Emili, A., Greenblatt, J. F., Harrington, L., Lydall, D., Durocher, D. "A genome-wide screen identifies the evolutionarily conserved KEOPS complex as a telomere regulator", Cell 124 (6), 1155-1168, 24 March 2006

Oral Presentations

2009	6th International Symposium of the Austrian Proteomics Platform, Seefeld, Austria, January 18 - 21 (invited speaker)
2008	EMBO Meeting on Cellular Signaling and Molecular Medicine, Dubrovnik, Croatia, May 29 – June 4 (& poster)
	4th YSA PHD Symposium, Medical University of Vienna, May 28 - 29
2007	3rd YSA PhD Symposium, Medical University of Vienna, June 21 – 22 (& poster)
2006	3rd Joint Cold Spring Harbor Laboratory/Wellcome Trust conference on "Interactome Networks", Hinxton, UK, August 30 – September 3

Poster Presentations

2008	3rd ESF Conference "Functional Genomics and Disease", Innsbruck, Austria, October 1 - 4
	EMBO Meeting on Cellular Signaling and Molecular Medicine, Dubrovnik, Croatia, May 29 – June 4
	Barcelona BioMed Conference "Targeting and Tinkering with Interaction Networks", Barcelona, Spain, April 14 – 16
2007	4th Joint Cold Spring Harbor Laboratory/Wellcome Trust conference on "Interactome Networks", Hinxton, UK, August 29 – September 1
2006	2nd YSA PHD Symposium, Medical University of Vienna, June 22 - 23
2005	1st YSA PHD Symposium, Medical University of Vienna, June 23 – 24

Scientific Courses

2007	FEBS-EMBO Advanced Lecture Course "Molecular Mechanisms in Signal Transduction and Cancer", Spetses, Greece, August 20 - 31 (& poster)
2006	EMBO Practical Course "Structural Characterization of Macromolecular Complexes", EMBL outstation Grenoble, France, May 15 - 20 (& poster)

Memberships

Since 2007	EACR - European Association for Cancer Research
Since 2005	YSA - Young Scientist Association of the Medical University of Vienna
Since 2003	EFB - European Federation of Biotechnology
Since 2003	YEBN - Young European Biotech Network
Since 2003	Biotechnologische Studenteninitiative (btS) e.V.

Fellowships and Honours

Since 11/2008	Students4excellence.at – Fellow
06/2008	Travel Bursary Award, 3rd EFS Functional Genomics Conference 2008, Innsbruck, Austria
03/2006 - 03/2009	Research Grant #P18737 of the Austrian Science Fund (FWF)
04/2005	BioVision.Nxt 'Class of 2005' Fellow, World Life Sciences Forum, Lyon, France
10/2002 - 02/2003	ERASMUS Scholarship granted by the EU for studies at the Victoria University of Manchester, UK
07/1998	Prizes for overall very good and the best graduation in Biology, Liselotte-Gymnasium, Mannheim, Germany